HUNGARIAN JOURNAL OF HYDROLOGY

HIDROLÓGIAI KÖZLÖNY

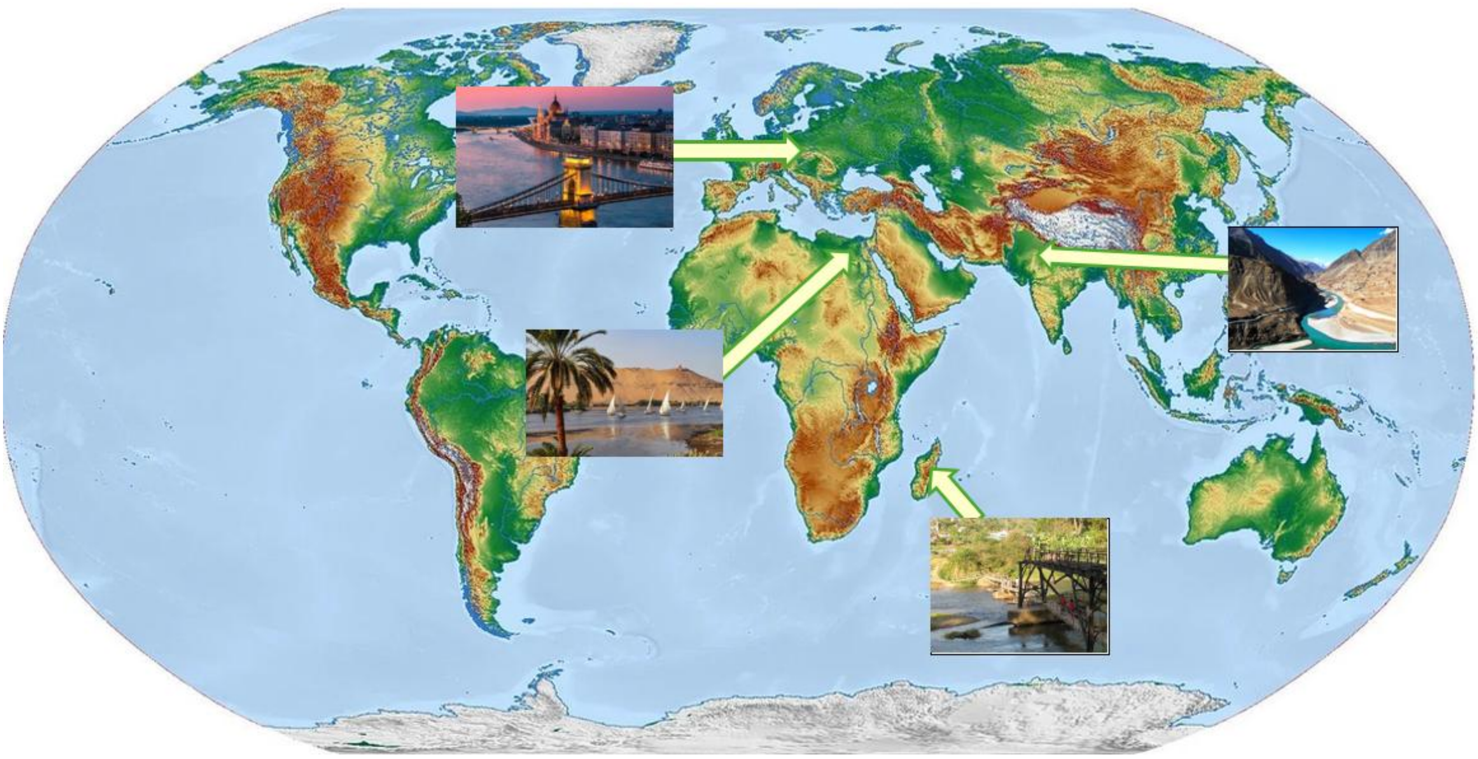

JOURNAL OF THE HUNGARIAN HYDROLOGICAL SOCIETY • VOL. 106, ISSUE 1EN • 2026
A MAGYAR HIDROLÓGIAI TÁRSASÁG LAPJA • 106. ÉVF. 1EN. SZÁM • 2026

https://doi.org/10.59258/HK

Hungarian Journal of Hydrology
Journal of the Hungarian Hydrological Society
Published quarterly

Publisher
Hungarian Hydrological Society
H-1091 Budapest, Üllői út 25., Hungary
Phone: +36-(1)-201-7655,
Fax: +36-(1)-202-7244
Email: titkarsag@hidrologia.hu
Web: www.hidrologia.hu
Represented by: József VÁRADI, Co-President of the Hungarian Hydrological Society

Indexed in
OJS, REAL, ROAD, COMPASS, MATARKA
HU ISSN 0018-1323
ISSN 2939-8495 (Online)

Contents

Cover image: Locations of scientific papers of the Hungarian Journal of Hydrology

Hidrológiai Közlöny

A Magyar Hidrológiai Társaság lapja

Megjelenik háromhavonként

Kiadó
Magyar Hidrológiai Társaság
1091 Budapest, Üllői út 25. IV. em.
Tel: +36-(1)-201-7655
Fax: +36-(1)-202-7244
E-mail: titkarsag@hidrologia.hu
Honlap: www.hidrologia.hu
A Kiadó képviselője: Váradi József, a Magyar Hidrológiai Társaság társelnöke

Indexelik
OJS, REAL, ROAD, COMPASS, MATARKA
HU ISSN 0018-1323,
ISSN 2939-8495 (Online)

Tartalomjegyzék

Címlapkép: A Hidrológiai Közlöny tudományos közleményeinek helyszínei

Foreword

We are pleased to present the 2026 English-language edition of the Hungarian Journal of Hydrology (HK), the official scientific journal of the Hungarian Hydrological Society (MHT). This is the third annual English-language edition of the journal, reflecting our commitment to sharing Hungarian and international water-related research. The papers published in this volume explore a wide range of water management issues, from the Danube Basin to the Indus River. We are confident that both our international and Hungarian readers will find these contributions informative and inspiring.

This issue presents six research articles covering diverse aspects of water science and management.

Microplastics, defined as plastic particles smaller than 5 mm, have become a major global environmental concern. In "*Riverine Microplastics in the Hungarian Danube: Distribution, Sources, and Characterisation," Pegah JAHANPEYMA and Sándor BARANYA* investigate microplastic pollution in the Hungarian section of the Danube River. Their results reveal an average microplastic concentration of 0.311 mg/m³, corresponding to 142 particles/m³. The most frequently identified polymers were polystyrene, polyethylene, and polypropylene, occurring mainly as fragments, foam, and flakes. The study also identifies the dominant colours of the particles and provides valuable information for understanding, monitoring, and mitigating microplastic pollution in freshwater ecosystems.

In "*On the Role of Bank Storage in Attenuating Lowland River Floods," Gadadhara de Figueiredo FERRAZ and Tamás KRÁMER* quantify river-aquifer exchange and evaluate the contribution of bank storage to flood attenuation in the Danube and Tisza Rivers in Hungary using a mechanistic model. Their findings highlight the importance of incorporating groundwater–surface water interactions into flood models to improve flood forecasting and flood risk assessment.

In *"Extreme Precipitation Amounts and Dry Periods in the Hungarian Great Plain (1980–2020): Four Urban Stations," Dorottya SZÁM, Kíra Erika KÁVÁSSY, Ádám BERGER, and Zsolt HETESI* examine long-term changes in precipitation-free periods across the Hungarian Great Plain, with particular attention to the implications of climate change for agriculture. Although the frequency of dry periods increased slightly at some locations, the statistical significance of these trends remained inconclusive. The study also highlights the importance of improving soil water retention, particularly in sandy and saline soils, where reduced moisture availability poses increasing challenges for agricultural productivity.

According to the World Health Organization (WHO), antibiotic resistance is among the most serious global threats to public health. In "*OxiTop Microcosm Model as a Possible Tool to Study the Effects of Antibiotic Exposure on the Microbial Community," Dongze JIANG, Yi YANG, Mátyás CSERHÁTI, Balázs KRISZT, and Edit KASZAB* investigate the relationship between wastewater load and the biological activity of microbial communities under antibiotic pressure. Their work demonstrates the potential of the OxiTop microcosm model as a valuable tool for studying the environmental impacts of antibiotic contamination.

Transboundary water cooperation has long been recognised as an important contributor to regional stability and peace, particularly for countries such as Hungary. In *"Peacebuilding Through Water Cooperation? Institutional Design and Peace-Relevant Functions in the Indus and Nile Basins," Ferenc Miklós SULLIVAN* develops a mechanism-oriented framework linking institutional design with peacebuilding functions. The study applies this approach to two internationally significant river basins: the Indus Basin, through the Permanent Indus Commission established under the 1960 Indus Waters Treaty, and the Nile Basin Initiative, established in 1999.

Madagascar's concurrent crises of energy poverty, acute food insecurity, and watershed degradation are structurally interdependent, "*The Water-Energy-Food Nexus in Madagascar: Interdependencies, Cascading Failures, and an Integrated Governance Framework*", *Rovatiana Salema ANDRIANASOLOMAHEFA* maps the Water-Energy-Food (WEF) nexus dynamics of Madagascar.

The Hungarian Journal of Hydrology is also committed to supporting the next generation of water professionals. In line with this mission, the YOUTH CORNER section provides talented secondary school students with an opportunity to publish outstanding research. We warmly invite our readers to encourage and support these young researchers. This year's featured paper, prepared for the Hungarian competition of the 2026 Stockholm Junior Water Prize, is "*Water Chestnut (Trapa natans): A Food of Ancient Times or a Bioindicator of the Modern World?" by Hanna HÁDA, Gábor KONCZ, Katalin JÁMBRIK, and Csaba BERTA.* The study investigates the accumulation of metals in water chestnut seeds collected from different locations in Lake Tisza, Hungary. Since aquatic macrophytes can absorb and accumulate pollutants from both water and sediments, they serve as valuable indicators of environmental contamination.

We extend our sincere thanks to the authors, reviewers, and members of the Editorial Board for their dedication and invaluable contributions to this English-language edition. We hope this volume will strengthen international scientific cooperation and promote the exchange of knowledge in the field of water science and management.

Welcome to the 2026 English edition of the Hungarian Journal of Hydrology.

Veronika MAJOR
Editor-in-Chief

Riverine microplastics in the Hungarian Danube: distribution, sources, and characterisation

Pegah JAHANPEYMA[1,2,3], Sándor BARANYA[1,2]

[1] Department of Hydraulic and Water Resources Engineering, Faculty of Civil Engineering, Budapest University of Technology and Economics, Műegyetem rkp. 3., H-1111 Budapest, Hungary.
(email: pegah.jahanpeyma@edu.bme.hu, baranya.sandor@emk.bme.hu)
[2] National Laboratory for Water Science and Security, Department of Hydraulic and Water Resources Engineering, Faculty of Civil Engineering, Budapest University of Technology and Economics, Műegyetem rkp. 3., H-1111 Budapest, Hungary
[3] Corresponding author: baranya.sandor@emk.bme.hu

DOI:10.59258/hk.24053

Abstract
Microplastics, defined as plastic particles smaller than 5 mm, have become a pressing global environmental issue. Ineffective recycling practices allow plastics to enter and persist in the environment, breaking down into smaller particles that travel through pathways like rivers. These microplastics can accumulate in ecosystems, where they pose significant risks to flora, fauna, and potentially human health. This study focuses on riverine microplastic pollution in the Hungarian section of the Danube River, Europe's second-largest river, as well as in its tributary system. The Danube is a vital water source for Budapest and plays a crucial role in the region's economy and ecological balance. Water samples were collected at varying river depths using a Multilevel Manta Net. Advanced laboratory techniques, including Fourier-transform infrared spectroscopy and digital microscopy, were used to identify and characterise microplastics collected. Additionally, flow measurements were conducted to estimate mass-flux rates. These findings contribute to developing practical measures for understanding, managing, and reducing microplastic pollution in freshwater systems. The findings revealed an average microplastic concentration of 0.311 mg/m³, corresponding to 142 particles/m³. The most frequently identified polymers were polystyrene, polyethylene, and polypropylene, which appeared predominantly as fragments, foam, and flakes. The microplastics exhibited a range of colours, including yellow, black, grey, and green.

Keywords
Microplastics, FTIR spectroscopy, microplastic characterisation, riverine microplastics, plastic pollution.

Mikroműanyag-szennyezés vizsgálata magyarországi folyószakaszokon

Kivonat
A mikroműanyagok, azaz az 5 mm-nél kisebb műanyag részecskék napjaink egyik legsürgetőbb globális környezeti problémájává váltak. A nem megfelelő újrahasznosítási gyakorlatok következtében a műanyagok bejutnak és hosszú ideig megmaradnak a környezetben, miközben kisebb részecskékre bomlanak. Ezek a részecskék folyók által terjedhetnek, felhalmozódhatnak az ökoszisztémákban, ahol jelentős kockázatot jelentenek a növény- és állatvilágra, valamint potenciálisan az emberi egészségre is. Ez a tanulmány a folyami mikroműanyag-szennyezést vizsgálja Európa második legnagyobb folyója, a Duna magyar szakaszán és annak mellékfolyóiban. A Duna létfontosságú vízforrást jelent Budapest számára, és kulcsfontosságú szerepet játszik a régió gazdaságában és ökológiai egyensúlyában. A vízmintákat a folyó különböző mélységeiből gyűjtöttük egy többszintes planktonháló segítségével. Korszerű laboratóriumi technikákat, köztük Fourier-transzformációs infravörös spektroszkópiát és digitális mikroszkópiát alkalmaztunk a gyűjtött mikroműanyagok azonosítására és jellemzésére. Emellett áramlásméréseket végeztünk a tömegáramok becsléséhez. Ezek az eredmények hozzájárulnak a mikroműanyag-szennyezés megértéséhez, kezeléséhez és csökkentéséhez szükséges hatékony intézkedések kidolgozásához. Az eredmények alapján az átlagos mikroműanyag-koncentráció 0,311 mg/m³ volt, ami 142 részecske/m³-nek felel meg. A leggyakrabban azonosított polimerek a polisztirol, a polietilén és a polipropilén voltak, amelyek főként törmelék, hab és pelyhek formájában fordultak elő. A mikroműanyagok színe változatos volt, többek között sárga, fekete, szürke és zöld árnyalatokat mutattak.

Kulcsszavak
Mikroműanyagok, FTIR spektroszkópia, mikroműanyag-jellemzés, folyami mikroműanyagok, műanyagszennyezés.

INTRODUCTION
Plastic pollution is a primary global concern, intensified by the steady rise in plastic production. In 2020, global output reached about 380 million tonnes and is expected to exceed 460 million tonnes by 2025 *(Plastics Europe 2024)*. Yet nearly one-third of this plastic is mismanaged and ultimately released into natural environments such as rivers, oceans, and soil (*Houssini et al. 2025, URL2, Shahira 2025, URL3*). Owing to their durability, low recycling rates, and inadequate waste treatment, plastics persist for decades, fragmenting into smaller pieces through UV radiation, abrasion, temperature changes, and microbial activity *(Andrady 2011, Barnes et al. 2009, Cole et al. 2011, Crawford and Quinn 2017, Derraik 2002, Hopewell et al. 2009, Moore 2008, Rios et al. 2010, Roy et al. 2011*).

Plastic debris is generally classified by size into mega- (>1 m), macro- (1 m to 2.5 cm), meso- (2.5 mm to 5 mm), micro- (between 1µm to 5 mm, and nanoplastics (<1 µm). Microplastics (MPs, <5 mm) are of particular concern because of their ubiquity and persistence *(Andrady 2011, Cole et al. 2011, Crawford and Quinn 2017, Hartmann et al. 2019, Jahanpeyma and Baranya 2024, Kutz 2002, Moore 2008*). They are categorized as primary MPs, produced intentionally for use in products such as cosmetics and plastic pellets, and secondary MPs, which arise from the breakdown of larger items *(Browne et al. 2011, Cole et al. 2011, NOAA-Marine Debris Program 2009*). MPs enter aquatic and terrestrial environments via wastewater, runoff, and atmospheric deposition, and rivers are the main transport route, carrying an estimated 1.15-2.41 million tonnes of plastic debris annually into marine ecosystems (*Adomat and Grischek 2021, Campanale et al. 2020, Lebreton et al. 2017, Waldschläger et al. 2020*). Key sources of MP pollution include wastewater from laundry (35%), tire wear (28%), construction activities (24%), road markings (7%), shipping and vessel coatings (3.7%), cosmetics (2%), and plastic manufacturing pellets (0.3%) (*Fadare and Okoffo 2020, Jahanpeyma and Baranya 2024*).

The ecological and health risks of MPs are increasingly evident. They have been detected in seafood, bottled water, salt, and honey, while inhalation and dermal exposure are also possible pathways for human intake *(Cook and Halden 2020)*. MPs and their additives may cause toxic effects, ranging from gastrointestinal problems to DNA damage, and they act as carriers for other pollutants and pathogens (*Cook and Halden 2020, Crawford and Quinn 2017, Geyer et al. 2017, Gouin et al. 2011, Hahladakis et al. 2018, House of Commons Environmental Audit Committee 2016, Laist 1997, Marturano et al. 2019, Mato et al. 2001, Ogata et al. 2009, Rios et al. 2007, Teuten et al. 2009, Waldschläger et al. 2020*). In aquatic systems, MPs are ingested by a wide range of species, leading to digestive blockages, reproductive impacts, and behavioral changes *(Cook and Halden 2020, Crawford and Quinn 2017, Geyer et al. 2017, Gouin et al. 2011, Hahladakis et al. 2018, House of Commons Environmental Audit Committee 2016, Laist 1997, Marturano et al. 2019, Mato et al. 2001, Ogata et al. 2009, Rios et al. 2007, Teuten et al. 2009, Waldschläger et al. 2020*). MPs also alter soil structure and microbial communities, reducing seed germination and plant growth (*Boots et al. 2019, Windsor et al. 2019*). Furthermore, plastics exhibit a complex relationship with global warming and are increasingly recognised as potential drivers of global environmental change (*Nel et al. 2018, Revell et al. 2021, Windsor et al. 2019*).

The behavior of MPs in aquatic environments is governed by their size, density, polymer type, and interactions with environmental factors such as flow velocity, salinity, and biofilm development *(Alfonso et al. 2021, Kaiser et al. 2017, Petersen and Hubbart 2021*). Polyethylene and polypropylene often remain buoyant and travel long distances, while denser polymers like PET and PA tend to settle near their sources *(Alfonso et al. 2021, Kaiser et al. 2017, Petersen and Hubbart 2021*). Hydrodynamics, turbulence, and sediment interactions further influence their transport and deposition (*Ballent et al. 2016, He et al. 2021, Nel et al. 2018, Porter et al. 2018, Waldschläger et al. 2020, Hahladakis et al. 2018, Marturano et al. 2019*).

Various sampling strategies have been developed to investigate MPs in aquatic environments, including selective, bulk, and volume-reduced sampling (*Eerkes-Medrano et al. 2015, Frias et al. 2010, Yang et al. 2021*). Net-based methods such as manta or neuston nets (60–300 µm mesh) are widely used in river and marine studies, although methodological differences often complicate cross-study comparisons *(Obbard 2018, Liu et al. 2020, Yang et al. 2021*). Standardization is therefore critical for reliable monitoring and assessment *(Hidalgo-Ruz et al. 2012, Rocchia et al. 2017, Petersen and Hubbart 2021*). The summarized workflow for sampling, preparation, and analysis of microplastic samples, as outlined in *Figure 1*, is constructed based on different methodologies reported in prior studies.

Several European studies highlight the scale of MP contamination in rivers. For instance, research in Portugal and Spain has reported concentrations ranging from a few to over 1,000 particles per cubic meter, with polyethylene and polypropylene as the dominant polymers (*Rodrigues et al. 2018, Díez-Minguito et al. 2020, Bermúdez et al. 2021*). In the Danube, surveys in Austria, Romania, and Hungary found a variety of polymers, with PE, PP, and PS the most common *(Liedermann et al. 2018, Pojar et al. 2021a, Bordos 2021, Braun et al. 2022*). These findings confirm that the Danube is one of the significant pathways for MPs in Europe.

As the continent's second-largest river and an important international waterway, the Danube plays a central role in regional ecosystems and economies. However, limited research has focused specifically on the Hungarian stretch, where urban wastewater, tributary inputs, and industrial activities are likely to intensify MP contamination. This study addresses that gap by conducting detailed sampling along the Hungarian Danube using a Manta Net device combined with Fourier-transform infrared (FTIR) spectroscopy. The aim is to provide quantitative and qualitative insights into MP distribution and composition, to advance understanding of their behavior and to support effective management strategies.

Moreover, the distribution of MPs in river systems is strongly influenced by inputs from tributaries, wastewater treatment plants (WWTPs), and urban proximity. Tributaries contribute MPs based on land use, connectivity, and local activities, particularly those draining urban, industrial, or agricultural regions. WWTPs, as significant point sources, release MPs through effluents and sludge, with smaller particles like fibres and microbeads often bypassing filtration. Urban areas exacerbate MP pollution through stormwater runoff, industrial discharges, and waste mismanagement, creating pollution hotspots near WWTP discharge points or where tributaries join main rivers. In May 2024, a longitudinal sampling campaign was conducted along the Danube River and its tributaries, including the Rába, Marcal, and Mosoni-Duna Rivers, to understand these dynamics better, offering detailed insights into MP sources and distributions.

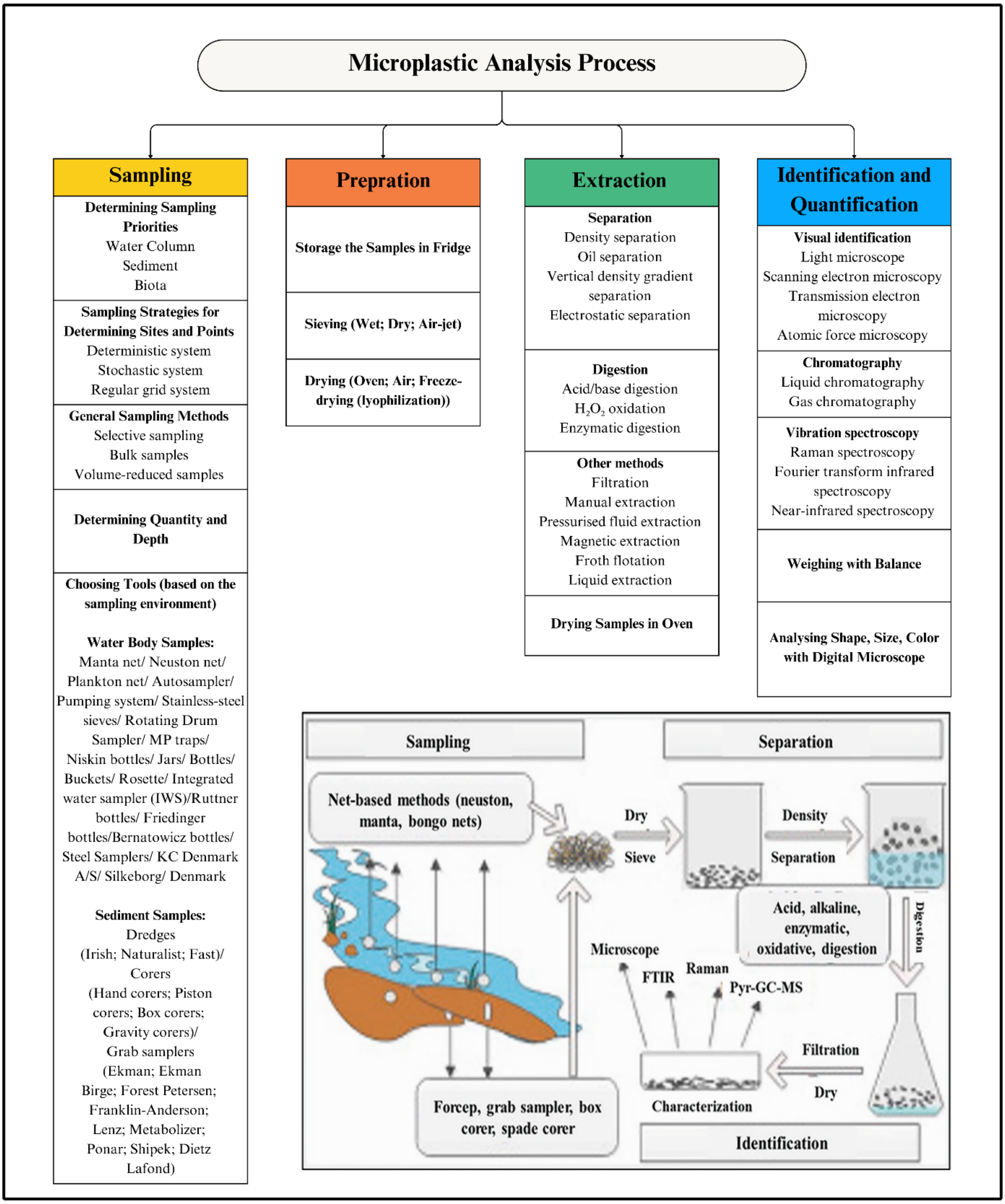

Figure 1. Microplastic sampling and analysis processes
1. ábra. Mikroműanyag mérési és elemzési eljárások

MATERIALS AND METHODS

Field sampling was conducted at two distinct river cross-sections located at 1640+000 rkm and 1642+000 rkm to study microplastic pollution in the Hungarian section of the Danube River in August 2022 and 2023, as shown in *Figure 2*. Water samples were collected from three vertical columns at each cross-section (two sampling points were positioned near the riverbanks, while the third was in the thalweg), with samples taken at three different depths within each column (one from the surface, one near the riverbed, and one at a mid-depth level). This approach ensured a comprehensive representation of the river's vertical profile. Proximity to urban areas, factories, industries, and sewage treatment systems can affect microplastic investigations. The selected cross-sections were chosen for their proximity to the Budapest Central Wastewater Treatment Plant (WWTP), which treats 80% of the city's sewage and discharges effluent into the Danube River (in the thalweg).

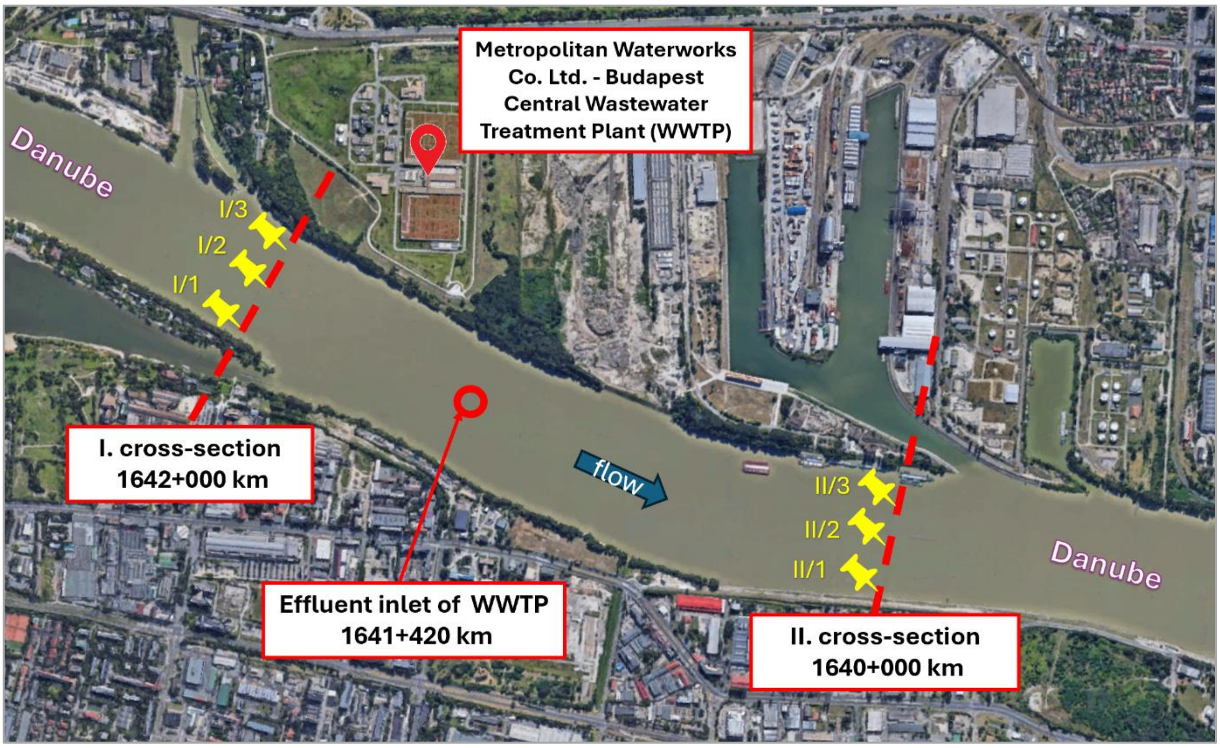

Figure 2. Sampling locations in the Danube River
2. ábra. Mintavételi helyszínek a Dunán

To collect water samples from specific depths within the water column, the Budapest University of Technology and Economics research team developed a specialised device called the Multilevel Manta Net (MLM Net), inspired by previous work conducted by *Liedermann et al. (2018)* on the Austrian stretch of the Danube River (*Liedermann et al. 2018*). The device features three nets positioned at different depths within the water column, suspended vertically using a crane mounted on a boat or a pontoon (*Figure 3*).

Each manta net was built with sturdy metal frames measuring 0.6×0.6 m^2 and featured conical polyamide (PA) nets with a mesh size of 500 µm and a length of 1.5 m. This mesh size captured MP particles ranging from 500 µm to 5 mm. Based on preliminary tests, a 500 µm mesh size was selected as the best compromise between minimizing net clogging and capturing smaller particles. At the end of each conical net, a polyvinyl chloride (PVC) container with a 0.25 m diameter was attached, fitted with a matching net to collect suspended particles from the water. The openings of the manta nets were oriented to align with and face the direction of the river's flow. The nets were fixed at the specified depth by stoppers beneath the net frames. The horizontal position of the nets was provided by blades attached to the ends of the rods attached to the frames. The nets were submerged in the water for 30 minutes. Afterwards, the nets were lifted and rinsed thoroughly using high-pressure clear water. The material and sediments gathered in the bottom container were transferred to a container, taken to the laboratory for analysis, and refrigerated until further steps.

In addition to gaining a deeper understanding of the dynamics of MPs in river systems influenced by tributaries, urban proximity, and other factors, a longitudinal sampling campaign was conducted along the Danube River and its tributaries in 2024. The study included the Rába River (7 samples collected), the Marcal River (8 samples collected), the Mosoni-Duna River (7 samples collected), and the Danube River itself (20 samples collected), providing detailed insights into MP sources and distribution patterns.

For the Rába, Marcal, and Mosoni-Duna Rivers, sampling was performed on the water surface using a portable Manta Net with a frame measuring 0.12 m × 0.35 m and a 0.70 m long conical net equipped with a 1 000 µm mesh to capture suspended particles. In contrast, the Danube samples were collected using MLM nets, as previously described. Sampling was conducted over 20 minutes, with the collected samples stored in containers and transported to the laboratory for further analysis.

A high-frequency, 1200-kHz Acoustic Doppler Current Profiler (ADCP) device from Teledyne was used to measure the water flow discharge and velocity. However, since the ADCP measurements were less accurate within 0.5 m of the riverbed, an Acoustic Doppler Velocimeter (ADV) device was attached to a net positioned close to the bed for more precise data collection.

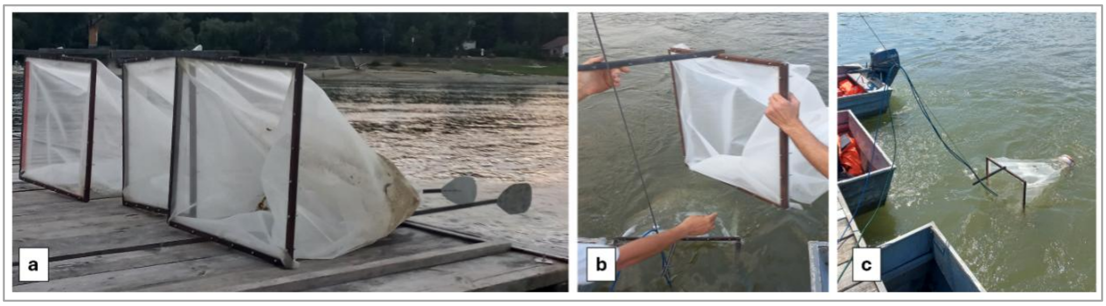

Figure 3. a) Multilevel Manta Net device. b,c) Manta nets are placed in the water column
3. ábra. a) Többszintű hálós mintavételi eszköz. b,c) Planktonhálók beeresztése a függélyben

In the laboratory, preliminary steps were taken to separate and analyse microplastic particles (*Figure 4*). The collected samples were placed in beakers containing a saturated sodium chloride (NaCl) solution and left to settle for 24 hours to separate denser materials from the samples, which were less likely to be plastics. The floating particles and possible plastic particles were carefully collected, and the samples were immersed in a 35% hydrogen peroxide (H_2O_2) solution for at least 24 hours to clean the plastic particles and remove organic materials and microorganisms. The floating particles were carefully collected and dried in an oven at 40°C for 24 hours to remove moisture. The dried samples were then sieved, isolating particles smaller than 5 mm for further analysis. Visible plastic particles were carefully removed from the samples using tweezers and transferred to Petri dishes for further study. To ensure accuracy, only visible particles were included, while fibres or particles too small to be identified by the naked eye were excluded at this stage.

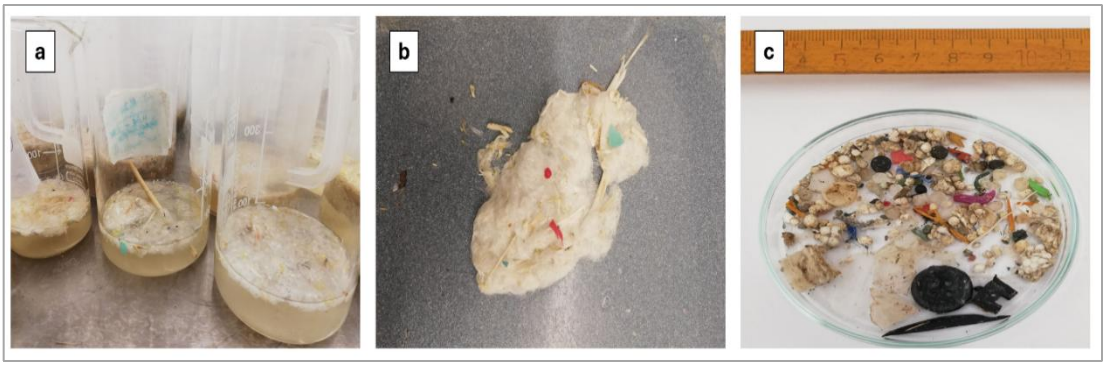

Figure 4. a) Sample purification process. The collected samples were subjected to a 24-hour immersion in a 35% H_2O_2 solution. b) Sample after laying in NaCl and H_2O_2 and drying in the oven. c) MPs extracted from one sample
4. ábra. a) Minta tisztítási folyamata. A begyűjtött mintákat 24 órán át 35%-os H_2O_2-oldatba merítették. b) A minta NaCl- és H_2O_2-kezelés, majd kemencében történő szárítás után. c) Egy mintából kivont mikroműanyagok (MP-k)

The MP polymer types were identified using a Bruker Tensor 37 FTIR spectrometer (with an attenuated total reflection attachment, 400–4000 cm^{-1} wavenumber range, 2 cm^{-1}resolution, and 16 scans per sample (*Figure 5a*). The FTIR technique works by analysing the light absorption spectrum emitted by the sample, which reveals the energy characteristics of chemical bonds within the material. Each polymer has a unique energy absorption pattern, enabling the differentiation and identification of polymer types through comparison with a spectral library stored in the instrument.

A digital microscope (Keyence VH-Z20UR, 20x-200x) was employed to measure the MPs' size, shape, and colour (*Figure 5b*). The total mass of the collected MPs was weighed and recorded by using an exact digital balance (Shimadzu AUW120D semi-micro analytical balance, with accuracy levels of ±0.01 mg for weights up to 42 g and ±0.1 mg for weights up to 120 g).

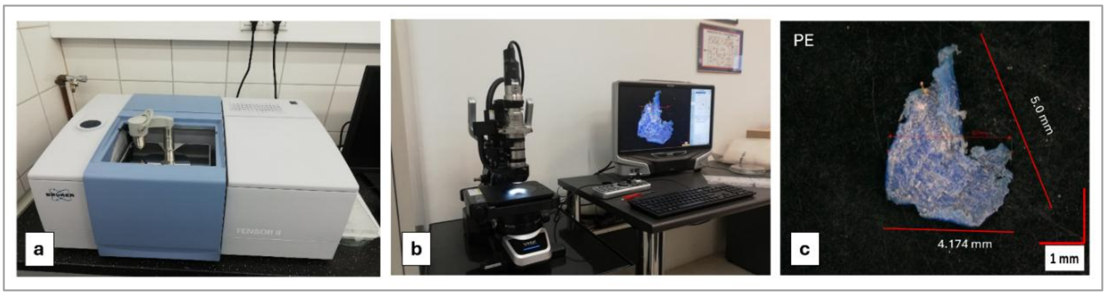

Figure 5. a) FTIR spectroscopy device. b) Digital microscope. c) MP particle under the digital microscope for shape, size, and colour analysis
5. ábra a) FTIR-spektroszkópiai eszköz. b) Digitális mikroszkóp. c) MP-részecske a digitális mikroszkóp alatt az alak, méret és szín elemzéséhez

RESULTS

The MP concentration (C_{MP}) and transport rate (q_{MP}) were determined at specific points within the study area. The C_{MP} was calculated by dividing the MP sample mass (m) in kg (or number of MP particles) by the volume of water passing through the designated sections (i.e., the volume of the filtered water, V) in m^3. V was estimated by multiplying the net entrance area (A) in m^2, flow velocity (v) in m/s, and sampling time (t) in s.

Mass-based unit methods offer a more reliable approach to quantifying C_{MP} (g/m^3) in environmental samples than particle counting alone ($particles/m^3$). By accounting for particle size, composition, and density variations, this method provides a more comprehensive and accurate assessment of the total plastic load within a sample. For instance, in two samples with an identical number of microplastics, variations in the density and size of the particles can lead to significant differences in the actual estimation of plastic pollution amounts.

The q_{MP} was calculated by multiplying the concentration of plastic material by the water flow rate, which was measured with the ADCP device during the sampling. The flow discharge was 1 500 m^3/s in 2022, and 2,126 m^3/s in 2023. The results from the experimental trials and subsequent calculations are presented in *Table 1*.

Table 1. The MP delivery rate (q_{MP}) and concentration (C_{MP}) at each sampling point (#) in two cross-sections in 2022 and 2023, (s: surface of water, m: middle level of water column, b: near bed)

1. táblázat. Az MP-szállítási sebesség (qMP) és koncentráció (CMP) az egyes mintavételi pontokon (#) két keresztmetszetben, 2022-ben és 2023-ban (s: a vízfelszín, m: a vízoszlop középső szintje, b: a mederhez közeli szint)

Year	Cross-section	# of points	Flow Velocity (m^3/s)	Filtered volume (m^3)	MP mass (g)	MP amount (particle)	CMP (µg/m^3)	qMP (mg/m^2 h)	CMP (particle/m^3)	qMP (particle/m^2 s)
2022	I	1-s	1.18	765.38	0.14897	24	195	828	31.36	37.04
		1-m	1.10	710.69	0.00204	11	3	11	15.478	16.98
		1-b	0.45	291.60	0.01366	18	27	76	61.73	27.78
		2-s	1.25	821.15	0.16471	147	201	900	179.02	223.13
		2-m	1.12	738.47	-	-	-	-	-	-
		2-b	1.06	698.33	0.02906	31	42	159	44.39	47.06
		3-s	1.23	795.75	0.08484	40	107	471	50.27	61.73
		3-m	1.11	717.34	0.03913	21	55	217	29.27	32.41
		3-b	0.70	451.35	0.05913	32	131	329	70.90	49.38
	II	1-s	1.13	743.71	0.05032	64	68	276	86.05	97.66
		1-m	1.05	688.40	0.13952	25	203	767	36.32	38.15
		1-b	0.91	596.36	0.02298	41	39	126	68.75	62.56
		2-s	1.48	980.37	0.01741	21	18	95	21.42	31.70
		2-m	1.31	865.25	0.03458	24	40	188	27.74	36.23
		2-b	1.07	708.85	0.02268	54	32	123	76.18	81.51
		3-s	1.31	846.43	0.25643	41	303	1 425	48.44	63.27
		3-m	1.20	779.17	0.09083	63	117	505	80.86	97.22
		3-b	0.75	486.00	0.22761	113	468	1 264	232.51	174.38
2023	II	1-s	1.13	735	1.03	319	1,398	1,975.1	433.79	492.28
		1-m	1.05	681	0.41	190	598	723.8	279.13	293.21
		1-b	0.79	513	0.37	193	719.9	495	376.21	297.84
		2-s	1.82	1,176	0.33	114	277.1	1,001.9	96.91	175.93
		2-m	1.69	1,097	0.26	114	234.9	738.9	103.89	175.93
		2-b	1.27	820	0.34	115	417.1	733.7	140.16	177.47
		3-s	1.56	1,009	0.12	123	114.8	305.6	121.86	189.81
		3-m	1.40	910	0.27	104	296.8	641.7	114.32	160.49
		3-b	0.87	566	0.24	167	425.1	355.4	295.23	257.72

The average C_{MP} and q_{MP} in each cross-sectional area of a specific vertical and the total cross-section Q_{MP} were calculated in 2022 and 2023 using sedimentation engineering methods. Q_{MP} was calculated by integrating the particular q_{MP} along the total cross-sectional area and summing up for a given period (e.g., g/s, t/year). The results are presented in *Table 2*.

Table 2. The average MP concentration and transport rate in two cross-sections and the overall area in 2022 and 2023 under the specified flow rate and condition
2. táblázat. Az átlagos MP-koncentráció és szállítási sebesség két keresztmetszetben és a teljes vizsgált területen 2022-ben és 2023-ban, a meghatározott vízhozam és feltételek mellett.

Year of sampling	Cross-section	Flow rate	The average MP concentration (CMP,avg)		The average MP transport rate (qMP,avg)	The total MP transport rate (QMP)		
		m^3/s	µg/ m^3	Particle/m^3	mg/s	g/s	kg/day	t/year
2022	I	1,500	104	54	156	0.2	16.2	6
	II	1,500	143	75	215			
2023	II	2,126	498	218	1,059	1.06	91.5	33.39

FTIR analysis identified the polymer types in the collected samples, providing insights into their potential sources. The findings suggest that inadequate recycling and storage practices may play a significant role in releasing these materials into surface water bodies. Those listed in *Table 3* were found in the highest concentrations among the identified polymers. Their potential sources are also outlined in the table. Among the various polymers identified, PS, PE, and PP were found to be the most abundant.

Table 3. The types of MP polymers identified in the collected samples through FTIR analysis and their potential sources
3. táblázat. Az FTIR-elemzéssel a begyűjtött mintákban azonosított MP-polimertípusok és azok lehetséges forrásai

Polymer Type	Polymer Type abbreviation	Amount (%)	Possible Source
Polystyrene	PS	37.97	In packaging and construction insulation
Polyethylene	PE	18.15	In the plastic bag and shampoo bottle production
Polypropylene	PP	10.96	Commonly used in packaging and food storage containers
other polymers		24.66	
Thermoplastic Vulcanizates	TPV	4.20	Used in automotive components, building and construction products, household appliance parts, and electrical components
Polyamide (commonly known as nylon)	PA	2.03	Used in textiles, the automotive industry, carpets, kitchen utensils, and sportswear
Styrene-Ethylene-Butylene-Styrene	SEBS	1.03	Used in items such as grips, handles, bumpers, and other requiring soft-touch and medical devices
High-Density Polyethylene	HDPE	0.85	Used in the production of plastic bottles, corrosion-resistant piping, geomembranes, and plastic lumber
Polyethylene terephthalate	PET	0.04	Used in bottle manufacturing
Thermoplastic Elastomer/Thermal Plastic Styrene	TPE/TPS	0.07	Used in toothbrushes, dashboards, and cable covers
Polyvinyl chloride	PVC	0.04	Used in pipe and floor covering production, and cable insulation

A detailed microscopic analysis was performed on the collected samples to assess MP particle size distribution. *Figure 6* illustrate the observed particle size, shape, and colour diversity. The study revealed that the predominant MP particle shapes were fragments, fibres, foams, and flakes. The most frequently identified colours among the particles were yellow, black, semi-yellow, grey, and green.

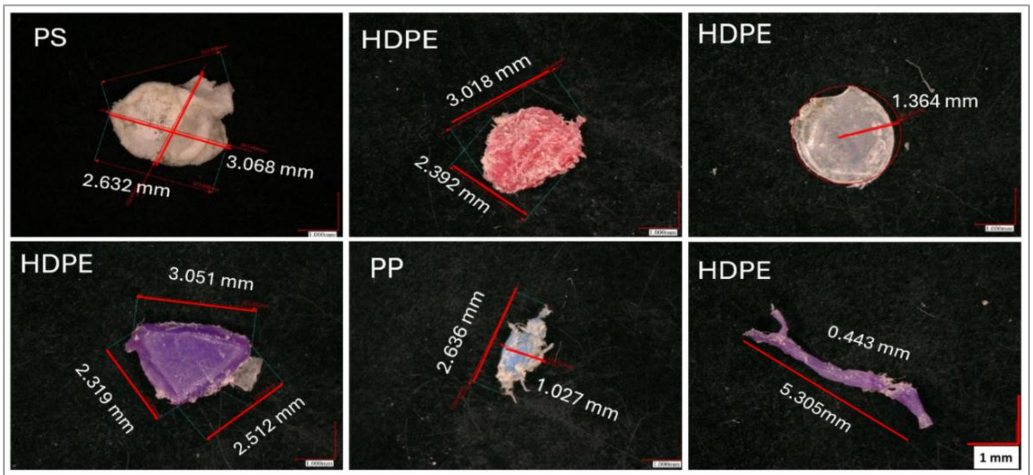

Figure 6. MP particles with different sizes, colours, and polymer types under a digital microscope
6. ábra. Különböző méretű, színű és polimer típusú MP-részecskék digitális mikroszkóp alatt

Based on the results of the longitudinal sampling campaign conducted in May 2024 along the Danube River and its tributaries, the spatial distribution of microplastic (MP) concentrations reflects distinct patterns shaped by anthropogenic pressures and hydrological features. As shown in *Figure 7*, the Danube exhibits significantly higher MP concentrations compared to its tributaries, with the most pronounced pollution hotspots located downstream of wastewater treatment plants (WWTPs) and urban areas. These regions are critical sources of MPs, mainly due to stormwater runoff, industrial discharges, and WWTP effluent, which contribute substantial MP loads to the river system. Tributaries such as the Rába and Marcal Rivers present varying MP levels, which are influenced by their land use, including agricultural activities and smaller-scale urbanisation in their catchments. The Mosoni-Duna tributary, in particular, plays a notable role, with the floodgate influencing MP transport and deposition patterns, as indicated by localised shifts in concentration levels. These findings highlight the complex interplay between tributary inflows, urban pressures, and point-source discharges in shaping MP distribution within the Danube River system. Understanding the relative contributions of these factors is crucial for developing targeted strategies to mitigate MP pollution, particularly at critical junctions where tributaries merge with the main river. This study underscores the importance of continued monitoring and tailored interventions to address the challenges posed by MP pollution in large riverine networks.

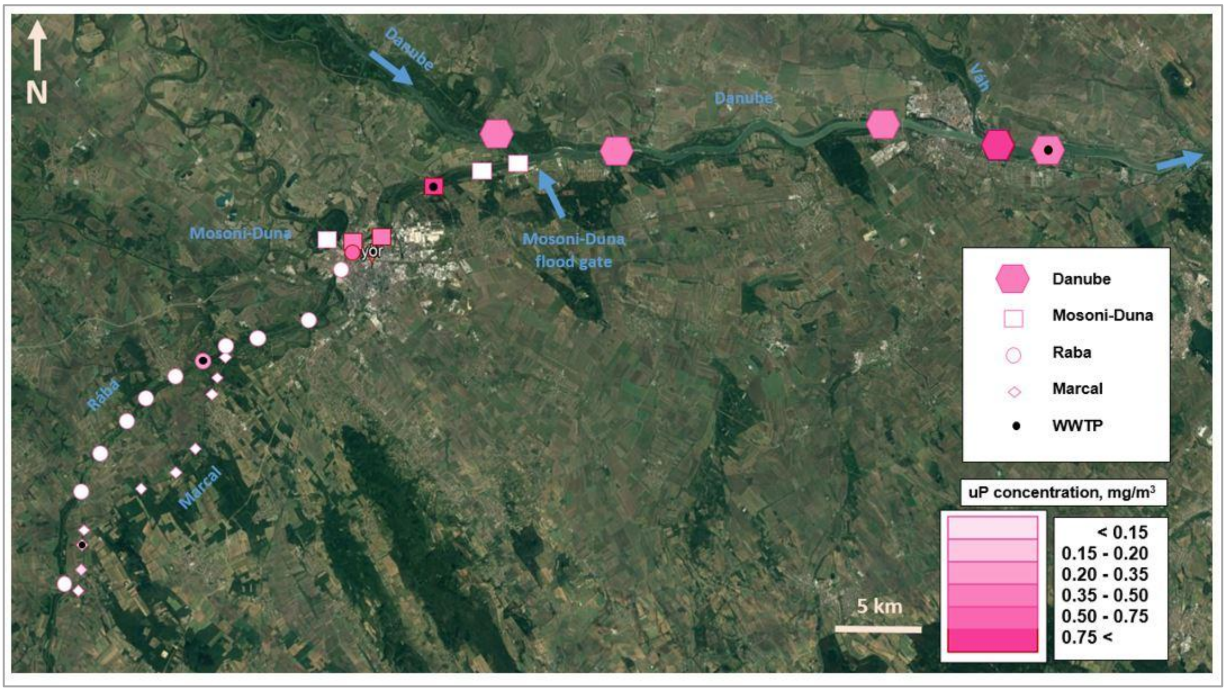

Figure 7. Spatial distribution of microplastic (MP) concentrations (mg/m³) along the Danube River and its tributaries, including the Mosoni-Duna, Rába, and Marcal rivers, based on the 2024 longitudinal sampling campaign
7. ábra: A mikroműanyag (MP) koncentrációk térbeli eloszlása (mg/m³) a Duna és mellékfolyói, köztük a Mosoni-Duna, a Rába és a Marcal folyók mentén, a 2024-es longitudinális mintavételi kampány alapján

DISCUSSION

To capture and analyse smaller MP particles, including microfibers, effectively, our findings align with prior research indicating that rivers serve as key pathways for transporting plastic pollutants to seas and oceans, contributing significantly to global plastic pollution. Studies estimate that rivers deliver between 1.15 and 4 million metric tons of plastic to the ocean annually, underscoring their critical role in this environmental issue (*Pojar et al. 2021a*). The Danube River is a major contributor to plastic pollution in the Black Sea, transporting significant amounts of MPs and other plastic debris *(Pojar et al. 2021a, Pojar et al. 2021b*). The Danube River begins in Germany and flows through Austria, Hungary, and Romania before discharging into the Black Sea. Estimates suggest that the Danube carries approximately 4.2 tons of plastic daily, amounting to an annual load of 1,533 tons delivered to the Black Sea (*Lechner et al. 2014*). Given the Danube River's critical role in Budapest as a vital waterway, a key water source, and a cornerstone of the region's tourism, economy, and ecological balance, studying plastic pollution in this river is essential.

Between 2010 and 2012, researchers from the University of Vienna and the University of Natural Resources and Life Sciences Vienna (BOKU) studied the Austrian section of the Danube River, downstream of Vienna, using the MLM Net device (*Liedermann et al. 2018*). Their analysis reported an average plastic concentration exceeding 17 particles/m³ (*Liedermann et al. 2018*). A follow-up survey in 2014 at two Austrian sampling sites estimated an annual Q_{MP} of up to 17 tonnes at Hainburg, with a total plastic load reaching 41 tonnes per year at the same location (*URL1 2019, Liedermann et al. 2018*).

Within the framework of the Tiny Plastic Puzzle project by Wessling Hungary Ltd., C_{MP} was assessed in Budapest. Measurements revealed a concentration of 45 particles/m³ at the Megyeri Bridge in the northern section of the city, which was lower than the 55 particles/m³ recorded at the Csepel Freeport in the southern part of

Budapest (*URL1 2019, Kiss et al. 2021*). These results align closely with our findings for the region. Data collected as part of our study confirm the presence of MPs in the Danube River, with notable variability in concentrations depending on sampling locations and conditions. For instance, upstream and downstream measurements near the Budapest Central WWTP in the Csepel area highlighted the influence of urban runoff and untreated effluents on MP pollution. In 2022, C_{MP} upstream of the WWTP in Budapest was recorded at approximately 54 particles/m³, increasing to 75 particles/m³ downstream. By 2023, these levels had risen substantially, reaching 218 particles/m³ downstream, likely due to increasing anthropogenic activity, changes in sampling conditions, or changes in hydrological and hydraulic factors. Our results highlight the pronounced heterogeneity of MP occurrence within the Danube. Concentrations varied strongly across cross-sections, depths, and sampling periods (*Table 1*), with surface values occasionally an order of magnitude higher or lower than mid- or bottom samples. Such variability reflects the dynamic interplay of hydrodynamic conditions, particle properties, and point-source inputs. Similar findings have been reported in other large rivers, where near-bed samples often contain more MPs due to resuspension processes (*Liedermann et al. 2018; Mani et al. 2015*). Seasonal factors such as rainfall and discharge fluctuations also contribute to irregular distribution patterns (*Moses et al. 2023, Nguyen et al. 2024*). This heterogeneity complicates both sampling and upscaling, underscoring the importance of multi-depth and multi-point approaches in future monitoring strategies.

The distribution of MPs within the water column was assessed using specialised sampling techniques. However, several factors suggest that our findings may underestimate actual C_{MP}. Limitations in sampling, such as using nets with a 500 µm mesh size, restrict the detection of smaller particles, including microfibers and transparent MPs, which are difficult to identify visually. Furthermore, purification processes and laboratory methods can inadvertently degrade or fragment MPs, affecting the accuracy of results. Regarding the laboratory procedures, the margin of error was found to be negligible. Bulk sampling methods, such as pump sampling, are highly recommended to capture and analyse smaller MP particles, including microfibers effectively. These approaches improve sensitivity and accuracy in detecting and characterising these minute particles. It is worth noting that pump sampling involves distinct methodologies, which fall beyond the scope of this article for detailed discussion. Research in this area has been conducted by our team using both the net sampling and pump sampling methods, with the results to be presented in future publications.

The composition of MPs observed in this study primarily consisted of fragmented particles, which is consistent with other studies that report fragments as the dominant form of MPs in river systems. However, fibres, which are frequently associated with textile and wastewater sources, were underrepresented, likely due to methodological constraints. Future investigations should employ alternative techniques, such as pump sampling, to better capture smaller particles and fibres. Various factors, including urban runoff, WWTPs, and geomorphological features, influence microplastic pollution in the Danube River system. The most frequently identified polymers in our study were PS (37.97%), PE (18.15%), and PP (10.96%), consistent with findings from other studies in the region. These polymers, often associated with packaging and household waste, highlight the significant role of urban centres as sources of MP pollution.

Although our study focused exclusively on MPs in the water column, sediment sampling is essential for a comprehensive understanding of MP dynamics in the Danube River system. Sediments act as sinks where MPs accumulate and are resuspended under certain conditions, influencing their transport and deposition downstream. Existing studies highlight significant MP accumulation in upstream impoundments, floodplains, and coastal sediments, particularly in areas with reduced sediment flux caused by river regulation and hydropower activities. The inclusion of sediment analysis in future studies will provide valuable insights into the interplay between MP deposition and resuspension processes.

In conclusion, our study underscores the complexity of MP pollution in riverine systems, influenced by diverse sources and environmental processes. Addressing these challenges requires methodological advancements to capture a broader spectrum of MP types and sizes. Future research should prioritise integrating water and sediment sampling to provide a more holistic view of MP transport and accumulation within the Danube River and its contribution to marine pollution in the Black Sea.

CONCLUSION

This research evaluated MP pollution in the Hungarian section of the Danube River, addressing rising concerns about MPs' environmental and health impacts. A structured sampling and analysis methodology was developed, inspired by established approaches, to obtain robust data on MP prevalence. Water samples were collected using an MLM net with a 500 µm mesh, allowing for systematic assessment of MP concentrations across varying depths. This study collected and identified microplastic particles ranging from 5 mm to 500 µm through visual inspection. Laboratory protocols facilitated the isolation and identification of MPs, followed by FTIR spectroscopy to characterise polymer types and potential sources.

Results from 2022 revealed an average MP concentration of 124 µg/m³ (65 particles/m³), equalling approximately 0.2 g/s, or 16.2 kg/day, and around 6 tons/year of MPs passing through the investigated area. In 2023, these values increased significantly, with a mean concentration of 498 µg/m³ (218 particles/m³), corresponding to 1.06 g/s, 91.5 kg/day, and approximately 33.39 tons/year. MPs detected near the riverbed might point to a potential tendency for accumulation through deposition, a hypothesis that requires confirmation in future studies. The most prevalent polymers identified were PS (37.97%), PE (18.15%), and PP (10.96%), appearing in various forms such as fragments, foam, and flakes, and in colours like yellow, black, grey, and green.

It is important to note that these estimates are conservative. Factors such as flow rate variability, sampling methods, mesh size limitations, and the inability to visually identify certain particles influence the results. For instance, smaller particles like microfibers and microbeads may not be captured. For smaller microplastic particles (<500 µm), future studies are encouraged to employ methods such as pump-based sampling to improve capture efficiency.

This study underscores the urgent need for effective mitigation strategies and policy interventions to address MP pollution. Raising awareness about MPs' pervasive nature and potential risks remains a critical step towards safeguarding aquatic ecosystems and human health.

ACKNOWLEDGEMENT

We extend our gratitude to the technician team at Budapest University of Technology and Economics, particularly Mr. Károly Tóth, Mr. István Galgóczy, and Mr. András Miklós Rehák, for their valuable technical assistance, which made this research possible. The authors would like to express their heartfelt gratitude to their esteemed colleagues, Dr. Flóra Pomázi, Dr. Alexander Anatol Ermilov, Anna Szöllősi, Dr. Dániel Gere, and Dr. Andrea Toldy, for their invaluable contributions, insightful discussions, and continuous support throughout this research. Their expertise and collaborative efforts have been instrumental in completing this study. The research presented in the article was carried out within the framework of the Széchenyi Plan Plus program with the support of the RRF 2.3.1 21 2022 00008 project. The support of the OTKA K 143623 and PD146135 projects is greatefully acknowledged.

REFERENCES

Adomat, Y., Grischek, T. (2021). Sampling and processing methods of microplastics in river sediments - A review. In Science of the Total Environment. Vol. 758. Elsevier B.V. https://doi.org/10.1016/j.scitotenv.2020.143691

Alfonso, M.B., Arias, A.H., Ronda, A.C., Piccolo, M.C. (2021). Continental microplastics: Presence, features, and environmental transport pathways. In Science of the Total Environment. Vol. 799. Elsevier B.V. https://doi.org/10.1016/j.scitotenv.2021.149447

Andrady, A.L. (2011). Microplastics in the marine environment. In Marine Pollution Bulletin.Vol. 62, Issue 8, pp. 1596-1605. https://doi.org/10.1016/j.marpolbul.2011.05.030

Ballent, A., Corcoran, P.L., Madden, O., Helm, P.A., Longstaffe, F. J. (2016). Sources and sinks of microplastics in Canadian Lake Ontario nearshore, tributary, and beach sediments. Marine Pollution Bulletin, 110(1), pp. 383-395. https://doi.org/10.1016/j.marpolbul.2016.06.037

Barnes, D.K.A., Galgani, F., Thompson, R.C., Barlaz, M. (2009). Accumulation and fragmentation of plastic debris in global environments. Philosophical Transactions of the Royal Society B: Biological Sciences, 364(1526), pp. 1985-1998. https://doi.org/10.1098/rstb.2008.0205

Bermúdez, M., Vilas, C., Quintana, R., González-Fernández, D., Cózar, A., Díez-Minguito, M. (2021). Unravelling spatio-temporal patterns of suspended microplastic concentration in the Natura 2000 Guadalquivir estuary (SW Spain): Observations and model simulations. Marine Pollution Bulletin, 170. https://doi.org/10.1016/j.marpolbul.2021.112622

Boots, B., Russell, C.W., Green, D.S. (2019). Effects of Microplastics in Soil Ecosystems: Above and below Ground. Environmental Science and Technology, 53(19), 11496-11506. https://doi.org/10.1021/acs.est.9b03304

Bordos, G. (2021). Investigation of microplastics in the environment. Hungarian University of Agriculture and Life Science.

Braun, U., Kittner, M., Kerndorff, A., Ricking, M., Bednarz, M., Obermaier, N., Lukas, M., Asenova, M., Bordós, G., Eisentraut, P., Hohenblum, P., Hudcova, H., Humer, F., István, T. G., Kirchner, M., Marushevska, O., Nemejcová, D., Oswald, P., Paunovic, M., ... G. Bannick, C. (2022). Microplastics in the Danube River Basin: A First Comprehensive Screening with a Harmonized Analytical Approach. ACS ES and T Water, 2(7), pp.174-1181. https://doi.org/10.1021/acsestwater.1c00439

Browne, M.A., Crump, P., Niven, S.J., Teuten, E., Tonkin, A., Galloway, T., Thompson, R. (2011). Accumulation of microplasticson shorelines woldwide: Sources and sinks. Environmental Science and Technology, 45(21), pp. 9175-9179. https://doi.org/10.1021/es201811s

Campanale, C., Stock, F., Massarelli, C., Kochleus, C., Bagnuolo, G., Reifferscheid, G., Uricchio, V.F. (2020). Microplastics and their possible sources: The example of Ofanto river in southeast Italy. Environmental Pollution, 258. https://doi.org/10.1016/j.envpol.2019.113284

Cole, M., Lindeque, P., Halsband, C., Galloway, T.S. (2011). Microplastics as contaminants in the marine environment: A review. In Marine Pollution Bulletin. Vol. 62, Issue 12, pp. 2588-2597. https://doi.org/10.1016/j.marpolbul.2011.09.025

Cook, C.R., Halden, R.U. (2020). Ecological and health issues of plastic waste. In Plastic Waste and Recycling, pp. 513-527. Elsevier. https://doi.org/10.1016/b978-0-12-817880-5.00020-7

Crawford, C.B., Quinn, B. (2017). Microplastic pollutants. Elsevier. https://doi.org/https://doi.org/10.1016/c2015-0-04315-5

Derraik, B. (2002). The pollution of the marine environment by plastic debris: a review. https://doi.org/https://doi.org/10.1016/s0025-326x(02)00220-5

Díez-Minguito, M., Bermúdez, M., Gago, J., Carretero, O., Viñas, L. (2020). Observations and idealised modelling of microplastic transport in estuaries: The exemplary case of an upwelling system (Ría de Vigo, NW Spain). Marine Chemistry, 222. https://doi.org/10.1016/j.marchem.2020.103780

Eerkes-Medrano, D., Thompson, R.C., Aldridge, D.C. (2015). Microplastics in freshwater systems: A review of the emerging threats, identification of knowledge gaps and prioritisation of research needs. In Water Research, Vol. 75, pp. 63-82. Elsevier Ltd. https://doi.org/10.1016/j.watres.2015.02.012

Fadare, O.O., Okoffo, E.D. (2020). Covid-19 face masks: A potential source of microplastic fibers in the environment. Science of the Total Environment, 737. https://doi.org/10.1016/j.scitotenv.2020.140279

Frias, J.P.G.L., Sobral, P., Ferreira, A.M. (2010). Organic pollutants in microplastics from two beaches of the Portuguese coast. Marine Pollution Bulletin, 60(11), pp. 1988-1992.
https://doi.org/10.1016/j.marpolbul.2010.07.030

Geyer, R., Jambeck, J.R., Law, K.L. (2017). Production, use, and fate of all plastics ever made. https://doi.org/10.1126/sciadv.1700782

Gouin, T., Roche, N., Lohmann, R., Hodges, G. (2011). A thermodynamic approach for assessing the environmental exposure of chemicals absorbed to microplastic. Environmental Science and Technology, 45(4), pp. 1466-1472. https://doi.org/10.1021/es1032025

Hahladakis, J.N., Velis, C.A., Weber, R., Iacovidou, E., Purnell, P. (2018). An overview of chemical additives present in plastics: Migration, release, fate and environmental impact during their use, disposal and recycling. In Journal of Hazardous Materials, Vol. 344, pp. 179-199. Elsevier B.V. https://doi.org/10.1016/j.jhazmat.2017.10.014

Hartmann, N.B., Hüffer, T., Thompson, R.C., Hassellöv, M., Verschoor, A., Daugaard, A.E., Rist, S., Karlsson, T., Brennholt, N., Cole, M., Herrling, M.P., Hess, M.C., Ivleva, N.P., Lusher, A.L., Wagner, M. (2019). Are We Speaking the Same Language? Recommendations for a Definition and Categorization Framework for Plastic Debris. Environmental Science and Technology, 53(3), pp. 1039-1047. https://doi.org/10.1021/acs.est.8b05297

He, B., Smith, M., Egodawatta, P., Ayoko, G.A., Rintoul, L., Goonetilleke, A. (2021). Dispersal and transport of microplastics in river sediments. Environmental Pollution, 279.
https://doi.org/10.1016/j.envpol.2021.116884

Hidalgo-Ruz, V., Gutow, L., Thompson, R.C., Thiel, M. (2012). Microplastics in the marine environment: A review of the methods used for identification and quantification. Environmental Science and Technology, 46(6), pp. 3060-3075. https://doi.org/10.1021/es2031505

Hopewell, J., Dvorak, R., Kosior, E. (2009). Plastics recycling: Challenges and opportunities. In Philosophical Transactions of the Royal Society B: Biological Sciences, Vol. 364, Issue 1526, pp. 2115-2126. Royal Society. https://doi.org/10.1098/rstb.2008.0311

House of Commons Environmental Audit Committee (2016). Environmental impact of microplastics Fourth Report of Session 2016-17.

Houssini, K., Li, J., Tan, Q. (2025). Complexities of the global plastics supply chain revealed in a trade-linked material flow analysis. Communications Earth and Environment, 6(1). https://doi.org/10.1038/s43247-025-02169-5

Jahanpeyma, P., Baranya, S. (2024). A Review of Microplastic Identification and Characterization Methods in Aquatic Environments. Periodica Polytechnica Civil Engineering. https://doi.org/10.3311/ppci.22886

Kaiser, D., Kowalski, N., Waniek, J.J. (2017). Effects of biofouling on the sinking behaviour of microplastics. Environmental Research Letters, 12(12). https://doi.org/10.1088/1748-9326/aa8e8b

Kiss, T., Fórián, S., Szatmári, G., Sipos, G. (2021). Spatial distribution of microplastics in the fluvial sediments of a transboundary river – A case study of the Tisza River in Central Europe. Science of the Total Environment, 785.
https://doi.org/10.1016/j.scitotenv.2021.147306

Kutz, M. (2002). Handbook of Materials Selection. J. Wiley.
https://doi.org/https://doi.org/10.1002/9780470172551

Laist, D.W. (1997). Impacts of Marine Debris: Entanglement of Marine Life in Marine Debris Including a Comprehensive List of Species with Entanglement and Ingestion Records. Springer Series on Environmental Management. Springer, New York, NY. https://doi.org/https://doi.org/10.1007/978-1-4613-8486-1_10

Lebreton, L.C.M., Van Der Zwet, J., Damsteeg, J.W., Slat, B., Andrady, A., Reisser, J. (2017). River plastic emissions to the world's oceans. Nature Communications, 8. https://doi.org/10.1038/ncomms15611

Lechner, A., Keckeis, H., Lumesberger-Loisl, F., Zens, B., Krusch, R., Tritthart, M., Glas, M., Schludermann, E. (2014). The Danube so colourful: A potpourri of plastic litter outnumbers fish larvae in Europe's second largest river. Environmental Pollution, 188, pp. 177-181. https://doi.org/10.1016/j.envpol.2014.02.006

Liedermann, M., Gmeiner, P., Pessenlehner, S., Haimann, M., Hohenblum, P., Habersack, H. (2018). A methodology for measuring microplastic transport in large or medium rivers. Water (Switzerland), 10(4). https://doi.org/10.3390/w10040414

Liu, K., Courtene-Jones, W., Wang, X., Song, Z., Wei, N., Li, D. (2020). Elucidating the vertical transport of microplastics in the water column: A review of sampling methodologies and distributions. In Water Research, Vol. 186. Elsevier Ltd.
https://doi.org/10.1016/j.watres.2020.116403

Mani, T., Hauk, A., Walter, U., Burkhardt-Holm, P. (2015). Microplastics profile along the Rhine River. Scientific Reports, 5. https://doi.org/10.1038/srep17988

Marturano, V., Cerruti, P., Ambrogi, V. (2019). Polymer additives. Physical Sciences Reviews, 2(6). https://doi.org/10.1515/psr-2016-0130

Mato, Y., Isobe, T., Takada, H., Kanehiro, H., Ohtake, C., Kaminuma, T. (2001). Plastic resin pellets as a transport medium for toxic chemicals in the marine environment. Environmental Science and Technology, 35(2), p. 318-324. https://doi.org/10.1021/es0010498

Moore, C.J. (2008). Synthetic polymers in the marine environment: A rapidly increasing, long-term threat. Environmental Research, 108(2), pp. 131-139. https://doi.org/10.1016/j.envres.2008.07.025

Moses, S.R., Löder, M.G.J., Herrmann, F., Laforsch, C. (2023). Seasonal variations of microplastic pollution in the German River Weser. Science of the Total Environ-ment, 902. https://doi.org/10.1016/j.scitotenv.2023.166463

Nel, H.A., Dalu, T., Wasserman, R.J. (2018). Sinks and sources: Assessing microplastic abundance in river sediment and deposit feeders in an Austral temperate urban river system. Science of the Total Environment, 612, pp. 950-956. https://doi.org/10.1016/j.scitotenv.2017.08.298

Nguyen, T.T., Bui, V.H., Lebarillier, S., Vu, T.K., Wong-Wah-Chung, P., Fauvelle, V., Malleret, L. (2024). Spatial and seasonal abundance and characteristics of microplastics along the Red River to the Gulf of Tonkin, Vietnam. Science of the Total Environment, 957. https://doi.org/10.1016/j.scitotenv.2024.177778

NOAA-Marine Debris Program (2009). Proceedings of the International Research Workshop on the Occurrence, Effects, and Fate of Microplastic Marine Debris. www.MarineDebris.noaa.gov

Obbard, R.W. (2018). Microplastics in Polar Regions: The role of long-range transport. In Current Opinion in Environmental Science and Health, Vol. 1, pp. 24-29. Elsevier B.V. https://doi.org/10.1016/j.coesh.2017.10.004

Ogata, Y., Takada, H., Mizukawa, K., Hirai, H., Iwasa, S., Endo, S., Mato, Y., Saha, M., Okuda, K., Nakashima, A., Murakami, M., Zurcher, N., Booyatumanondo, R., Zakaria, M. P., Dung, L. Q., Gordon, M., Miguez, C., Suzuki, S., Moore, C., Thompson, R.C. (2009). International Pellet Watch: Global monitoring of persistent organic pollutants (POPs) in coastal waters. 1. Initial phase data on PCBs, DDTs, and HCHs. Marine Pollution Bulletin, 58(10), 1437-1446. https://doi.org/10.1016/j.marpolbul.2009.06.014

Petersen, F., Hubbart, J.A. (2021). The occurrence and transport of microplastics: The state of the science. In Science of the Total Environment, Vol. 758. Elsevier B.V. https://doi.org/10.1016/j.scitotenv.2020.143936

Plastics Europe (2024). Plastics – The Fast Facts 2024. https://plasticseurope.org/knowledge-hub/plastics-the-fast-facts-2024/

Pojar, I., Kochleus, C., Dierkes, G., Ehlers, S.M., Reifferscheid, G., Stock, F. (2021a). Quantitative and qualitative evaluation of plastic particles in surface waters of the Western Black Sea. Environmental Pollution, 268. https://doi.org/10.1016/j.envpol.2020.115724

Pojar, I., Stănică, A., Stock, F., Kochleus, C., Schultz, M., Bradley, C. (2021b). Sedimentary microplastic concentrations from the Romanian Danube River to the Black Sea. Scientific Reports, 11(1). https://doi.org/10.1038/s41598-021-81724-4

Porter, A., Lyons, B.P., Galloway, T.S., Lewis, C. (2018). Role of Marine Snows in Microplastic Fate and Bioavailability. Environmental Science and Technology, 52(12), pp. 7111-7119. https://doi.org/10.1021/acs.est.8b01000

Revell, L.E., Kuma, P., Le Ru, E.C., Somerville, W.R.C., Gaw, S. (2021). Direct radiative effects of airborne microplastics. Nature, 598(7881), pp. 462-467. https://doi.org/10.1038/s41586-021-03864-x

Rios, L.M., Moore, C., Jones, P.R. (2007). Persistent organic pollutants carried by synthetic polymers in the ocean environment. Marine Pollution Bulletin, 54(8), pp. 1230-1237. https://doi.org/10.1016/j.marpolbul.2007.03.022

Rios, L.M., Jones, P.R., Moore, C., Narayan, U.V. (2010). Quantitation of persistent organic pollutants adsorbed on plastic debris from the Northern Pacific Gyre's "eastern garbage patch." Journal of Environmental Monitoring, 12(12), pp. 2226-2236. https://doi.org/10.1039/c0em00239a

Rocchia, M., Ruff, I., Vianello, A. (2017). Microplastic identification and characterization by Raman imaging spectroscopy.

Rodrigues, M.O., Abrantes, N., Gonçalves, F.J.M., Nogueira, H., Marques, J.C., Gonçalves, A.M.M. (2018). Spatial and temporal distribution of microplastics in water and sediments of a freshwater system (Antuã River, Portugal). Science of the Total Environment, 633, pp. 1549-1559. https://doi.org/10.1016/j.scitotenv.2018.03.233

Roy, P.K., Hakkarainen, M., Varma, I.K., Albertsson, A.C. (2011). Degradable polyethylene: Fantasy or reality. In Environmental Science and Technology, Vol. 45, Issue 10, pp. 4217-4227. https://doi.org/10.1021/es104042f

Shahira M. (2025). Plastic bank- Plastic pollution by country: latest statistics and insights. Https://Plasticbank.Com/Blog/Plastic-Pollution-by-Country/. Letöltve: 2025, March 26

Teuten, E.L., Saquing, J.M., Knappe, D.R.U., Barlaz, M.A., Jonsson, S., Björn, A., Rowland, S.J., Thompson, R.C., Galloway, T.S., Yamashita, R., Ochi, D., Watanuki, Y., Moore, C., Viet, P.H., Tana, T.S., Prudente, M., Boonyatumanond, R., Zakaria, M.P., Akkhavong, K., Takada, H. (2009). Transport and release of chemicals from plastics to the environment and wildlife. Philosophical Transactions of the Royal Society B: Biological Sciences, 364(1526), 2027-2045. https://doi.org/10.1098/rstb.2008.0284

Waldschläger, K., Lechthaler, S., Stauch, G., Schüttrumpf, H. (2020). The way of microplastic through the environment – Application of the source-pathway-receptor model (review). In Science of the Total Environment, Vol. 713. Elsevier B.V. https://doi.org/10.1016/j.scitotenv.2020.136584

Windsor, FM., Durance, I., Horton, A.A., Thompson, R.C., Tyler, C.R., Ormerod, S.J. (2019). A catchment-scale perspective of plastic pollution. In Global Change Biology, Vol. 25, Issue 4, pp. 1207-221). Blackwell Publishing Ltd. https://doi.org/10.1111/gcb.14572

Yang, L., Zhang, Y., Kang, S., Wang, Z., Wu, C. (2021). Microplastics in freshwater sediment: A review on methods, occurrence, and sources. In Science of the Total Environment, Vol. 754. Elsevier B.V. https://doi.org/10.1016/j.scitotenv.2020.141948

URL1: EU Strategy for the Danube Region (EUSDR) (2019). Plastic pollution of rivers in the Danube region. www.danube-region.eu

URL2: Plastic Overshoot Day 2025.Plastic… is… everywhere. https://Plasticovershoot.Earth/. Letöltve: 2025, April 1

URL3: Waste Direct 2025. Plastic Waste Statistics & Trends. https://Wastedirect.Co.Uk/Blog/Plastic-Waste-Statistics/. Letöltve: 2025, April 27

AUTHORS

PEGAH JAHANPEYMA received her bachelor's degree in project management engineering from Paramour University in Tehran in 2012, and her master's degree in Hydraulic Structures from Azad University in South Tehran in 2015. She is currently a doctoral student and research assistant at the Department of Hydraulic Engineering and Water Management of the Budapest University of Technology and Economics. Her doctoral research topic is "Analysis of Microplastic Transport in Rivers". Her research interests include the study of plastic pollution in rivers, flow conditions, and sediment migration using various field methods.

SÁNDOR BARANYA received his Civil Engineering degree from the Budapest University of Technology and Economics (BME) in 2003 and his PhD from the same university in 2010. He is currently the head of the Department of Hydraulic Engineering and Water Management at BME and an associate professor. His research interests include the study of riverbed morphology, flow dynamics, and sediment migration using field methods and computer modelling. He has been a member of the Hungarian Hydrological Society since 2003.

On the role of bank storage in attenuating lowland river floods

Gadadhara de Figueiredo FERRAZ[1,3], Tamás KRÁMER[2]

[1] Budapest University of Technology and Economics, Department of Hydraulic and Water Resources Engineering, Budapest, Hungary, 1521 Budapest, Pf. 91. (email: gadadhara.ferraz@emk.bme.hu)
[2] Budapest University of Technology and Economics, Department of Hydraulic and Water Resources Engineering, Budapest, Hungary, 1521 Budapest, Pf. 91. (email: kramer.tamas@emk.bme.hu)
[3] Corresponding author: gadadhara.ferraz@emk.bme.hu

DOI: 10.59258/hk.24054

Abstract
Overbank river floods generate a positive hydraulic gradient toward adjacent aquifers, while floodplain soils become saturated through vertical infiltration during the overbank phase of the flood. These processes contribute to temporary water storage and attenuate flood waves, yet their role in flood dynamics remains unrepresented or only partially represented in many models of river hydraulics. Here, we quantify river-aquifer exchange and evaluate the contribution of bank storage to flood attenuation at the scale of the Danube and Tisza Rivers in Hungary using a mechanistic model. We developed a coupled 1D surface water–2D groundwater model to simulate 100-year flood events in an idealised, prismatic geometry. Results, integrated over a 50 km reach, indicate that bank storage can account for 26–37% of the total (surface+bank) storage and can reduce peak flow by 0.7–0.8 percentage points in addition to the attenuation by surface storage. This translates to an average peak water level reduction of about 4 cm. The attenuation effect was most pronounced in systems with high soil hydraulic conductivity. Despite its role in mitigating flood risk, bank storage is frequently simplified to a conceptual level or omitted altogether in hydraulic river models. Since surface flow roughness parameters are routinely calibrated primarily against peak water levels, this omission is partially offset – even without identifying the source of error. However, compensating for the lack of groundwater storage within the timescale of surface storage is not only imperfect but also leads to inaccuracies when extrapolated to floods significantly larger than previously observed ones. Our findings underscore the benefits of integrating groundwater-surface water interactions into flood modelling to improve flood forecasts and risk assessments.

Keywords
Flood attenuation, bank storage, groundwater-surface water interaction, infiltration.

A felszín alatti tározódás szerepe a síkvidéki folyók árhullámainak csillapításában

Kivonat
Egy áradó folyó a nyomásgradiens révén szivárgást kelt a talajvíztartó irányába, és ezzel egy időben a partok szintjét meghaladó vízállások idején a hullámtér talaja a beszivárgás révén felülről is telítődik. A felszín alatti tározódás az árvizeknek a nagyvízi mederben való tározódásán felül érvényesül és ezáltal fokozza az árhullámok csillapítását, ennek ellenére leírása sok felszíni áramlástani modellből mégis hiányzik, vagy csak részleges. Jelen tanulmányban egy mechanisztikus modellel számszerűsítjük a folyó és a talajvíztartó közötti vízcserét a Duna és a Tisza hazai léptékében, valamint értékeljük a felszín alatti tározódás hozzájárulását az árvízcsillapításhoz. A szimulációkhoz egy egymással összekapcsolt 1D felszíni és 2D felszín alatti hidraulikai modellt fejlesztettünk ki, és 100 éves árvizek levonulását vizsgáltuk idealizált, prizmatikus geometriában. Egy 50 km hosszú folyószakaszra integrált eredményeink azt mutatják, hogy a felszín alatti tározódás a teljes (felszíni és felszín alatti) tározódásnak 26–37%-át teheti ki, és a felszíni tározódás által biztosított csillapításon felül további 0,7–0,8 százalékponttal csökkentheti a csúcsvízhozamot. Ez átlagosan körülbelül 4 cm-es csökkenést jelent a tetőző vízszintekben. A csillapító hatás a jó vízvezetőképességű talajok feltételezésével a legjelentősebb. Annak ellenére, hogy a felszín alatti tározódás számottevő szerepet játszik az árvízi kockázat mérséklésében, a felszíni áramlástani modellekben gyakran konceptuális szintre leegyszerűsítik vagy teljesen figyelmen kívül hagyják. Mivel a felszíni lefolyás simasági együtthatóit rutinszerűen elsősorban a folyó tetőző vízszintjein keresztül kalibrálják, ezért az elhanyagolás – a hibaforrás ismerete nélkül is – részben kompenzálódik. A talajvíz-tározódás hiányának a felszíni tározódás időskáláján való kompenzálása azonban nemcsak tökéletlen, de a múltbeli árvizeknél jóval nagyobbakra kiterjesztve pontatlan is. Eredményeink rávilágítanak arra, hogy az árvízi előrejelzések és kockázatértékelések javításához a modellezésbe érdemes bevonni a felszín alatti vizekkel való kölcsönhatást.

Kulcsszavak
Árhullám-csillapítás, parti tározás, felszín alatti és felszíni vizek kölcsönhatása, beszivárgás.

INTRODUCTION

River floodplains are essential for some hydrological and ecological processes, particularly during extreme flood events. They act as natural buffers, regulating runoff, storing excess water, and supporting essential biogeochemical cycles that mitigate nutrient and pollutant concentrations (*Krause et al. 2007*). Effective floodplain management requires understanding surface water–groundwater interactions and the connectivity between riverine and aquatic habitats, extending beyond in-channel processes to the active floodplain (*Sophocleous 2002*).

Direct field observations provide important insights into river–aquifer exchange processes during flood events. Observational studies have shown that groundwater levels in floodplain aquifers respond rapidly to changes in river stage, indicating strong hydraulic connectivity between rivers and adjacent aquifers. For example, *Li et al. (2017)* investigated groundwater dynamics in the floodplain wetlands of Poyang Lake, China, and found that floodplain groundwater is strongly influenced by lake water levels. Their results indicate that lake water recharges the floodplain aquifer during periods of high lake levels in spring and summer, whereas groundwater stored within the floodplain may discharge back to the lake during periods of low water levels, highlighting the bidirectional nature of lake–groundwater interactions. Similarly, *Ubell (1964)* analysed groundwater level profiles along a 30 km reach of the Danube in Hungary and estimated a mean infiltration of approximately 0.3 $m^3\ s^{-1}\ km^{-1}$ during a flood event with a peak discharge of 5500 $m^3\ s^{-1}$. However, direct measurements of river–aquifer interaction during extreme floods remain limited, and modelling approaches are therefore essential to quantify the magnitude and impacts of such exchanges (*Liang et al. 2018*).

Numerical modelling studies have therefore become an important tool to quantify river–aquifer interactions and their impact on flood dynamics. Early work by *Pinder and Sauer (1971)* and *Zitta and Wiggert (1971)* pioneered the coupling of one-dimensional (1D) unsteady open-channel flow with two-dimensional horizontal (2DH) groundwater flow to assess bank storage effects on the flood hydrograph. Subsequent modelling studies have further explored the dynamics of river–aquifer exchange and groundwater response to flood waves (*Weng et al. 2003, Vivoni et al. 2006, Derx et al. 2010, Liang et al. 2018*). More recently, integrated surface water–groundwater models have enabled the coupling of river hydraulics with variably saturated groundwater flow, allowing detailed simulation of infiltration processes and subsurface flow dynamics (*Shuai et al. 2017, Hong et al. 2020, Nguyen et al. 2025*). Integrating surface water–groundwater interactions into flood inundation models enhances river flow predictions and flood response assessments, leading to more reliable forecasts (*Szilagyi 2004, Saksena et al. 2019*). Process-based river models primarily rely on calibrated roughness coefficients to route flood waves. Operational flood forecasting systems and most 1D/2D hydraulic models omit explicit river–aquifer bank-storage exchange; although coupling to variably saturated groundwater models is technically feasible and has been demonstrated in several research studies (*Shuai et al. 2017, Hong et al. 2020, Nguyen et al. 2025*), it is still rarely implemented in operational forecasting models. The absence of a bank storage mechanism may be partly compensated for by modifying the roughness coefficients, but this often leads to significant inaccuracies in flood estimates, overpredicting river discharge during flood events (*Saksena et al. 2019*).

Several studies have combined field observations with numerical modelling to better constrain river–aquifer interactions during flood events. These studies typically use groundwater monitoring data to calibrate or validate numerical models of bank storage and groundwater response (*Vivoni et al. 2006, Liang et al. 2018*). Such combined approaches have demonstrated that rapid river stage fluctuations during large flood events can induce substantial water, sediment, and nutrient exchanges across the river–aquifer interface (*Bernard-Jannin et al. 2016*). *Bernard-Jannin et al. (2016)* combined field observations with numerical modelling to quantify both lateral riverbank infiltration and vertical infiltration across inundated floodplains during flood events. Their results indicate that overbank flow across the floodplain surface can dominate river–aquifer exchanges during long-duration floods, contributing up to 88% of total infiltration. However, many studies still focus primarily on lateral infiltration through riverbanks under in-bank flow conditions, while the contribution of vertical infiltration across inundated floodplains remains less explored.

These limitations highlight important knowledge gaps regarding the relative importance of horizontal riverbank infiltration and vertical infiltration across inundated floodplains, particularly for large lowland rivers during extreme floods. Addressing these gaps requires modelling approaches capable of isolating the influence of flood duration, river geometry, and soil hydraulic properties on river–aquifer exchange processes.

This study aims to investigate the relationships between key parameters – flood duration, channel geometry, and soil properties – and their influence on infiltration flows, bank storage, and flood attenuation. River–aquifer water exchange can be divided into (predominantly) horizontal and vertical infiltration, driven by variations in river stage. Horizontal infiltration across the riverbed induces the lateral propagation of a groundwater wave as surface water levels rise, while vertical infiltration penetrates into the unsaturated floodplain soil when floodwaters exceed bank elevations. To explore these mechanisms, we employ a coupled 1D surface water–2DH groundwater model for a fully penetrating river within an aquifer, using Darcy's law for exchange flow calculations (similar to the MODFLOW RIV package). Since the parameters determining the impact of infiltration vary from river to river, or from reach to reach, we focus here on the two largest rivers in Hungary, which have large, leveed floodplains of high aggregate flood risk. We apply this model to two idealised reaches: the lower reach of the Danube River and the middle reach of the Tisza River, the Danube's tributary, using a hypothetical 100-year return period flood hydrograph.

MATERIALS AND METHODS

A process-based model combining the 1D Saint-Venant equations with the 2DH groundwater flow equations derived from Darcy's law and mass conservation was used to simulate river flood propagation and its interaction with groundwater. Exchange fluxes from the river to the groundwater, driven by changes in river levels, are divided into horizontal and vertical components. In this study, we define vertical fluxes (f_V) as those occurring across the floodplain, while horizontal fluxes (f_H) are those that occur across the riverbed. Bank storage is also split according to the origin of the influx: BS_V represents the infiltrated volume from vertical fluxes, while BS_H represents the infiltrated volume from horizontal fluxes. When river water levels (h_R) rise above the riverbanks (H), water simultaneously flows into the aquifer vertically (f_V) through the floodplain and horizontally (f_H) through the riverbed. Consequently, the groundwater head (h_A) rises.

The geometry of the modelled reach is assumed to be prismatic, meaning that the cross-sectional shape and dimensions remain constant along the longitudinal direction, and the channel is characterized by a uniform bed slope. Under this assumption, no longitudinal variations in channel width, depth, or floodplain extent are considered within the modelled reach. The cross-section of the river is approximated as a combination of two rectangular sections: a main channel with width b and depth z, and an active floodplain of width b_{f_L} and b_{f_R} on the left and right banks, respectively, between the banks of the main channel and levees or higher terrain. *Figure 1* illustrates the generalised model configuration on which the physical processes are formulated.

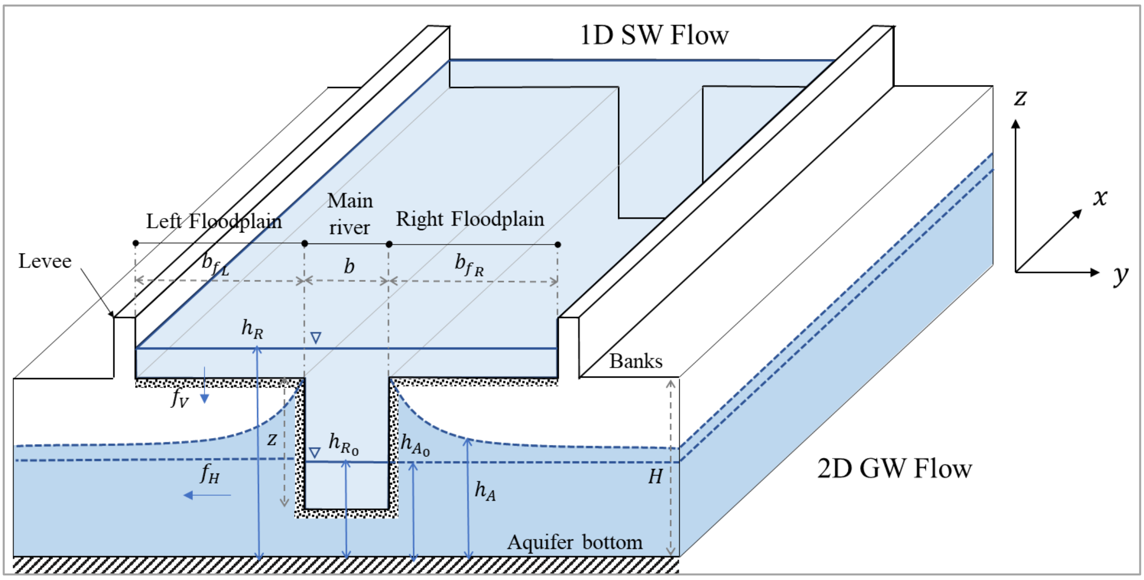

Figure 1. Model configuration in a cartesian coordinate system: 1D channel flow in the x direction, 2DH groundwater flow in the x–y direction, and 1D vertical infiltration

1. ábra. Modellfelépítés Descartes-i koordinátarendszerben: 1D felszíni lefolyás az x irányban, 2DH talajvízmozgás az x–y síkban és 1D függőleges beszivárgás

The groundwater module accounts for both confined and unconfined conditions depending on the position of the simulated groundwater head relative to the aquifer top. When the groundwater head is below the top of the aquifer, flow is treated as unconfined and storage is represented by the specific yield. When the groundwater head exceeds the aquifer top, the aquifer behaves as confined and storage is governed by the specific storage coefficient.

The model assumes a homogeneous and isotropic aquifer, hydraulically connected to the river, and an impermeable, horizontal base. The water level in the river and the piezometric head in the aquifer are measured from this base. The hydraulic connection between the river and the aquifer is represented through a riverbed and floodplain clogging layer with hydraulic properties distinct from those of the underlying aquifer, which controls the exchange flow between surface water and groundwater (*Brunner et al. 2009*).

The surface water domain boundaries were defined with sufficient extent to minimise any potential influence of downstream and lateral boundary conditions on flood attenuation or exchange flows within the analysed reach. The groundwater domain is bounded by no-flow conditions, except at the river-aquifer interface, where f_H (dimension: L/T) is imposed, governed by Darcy's law in proportion to the head difference between the river and the groundwater adjacent to the river. Similarly, f_V is imposed as a source term across the inundated floodplain and an equal-magnitude (but opposite) sink term in the groundwater domain. More specifically,

$$f_H = \frac{K_{rb}}{m_{rb}}(h_A - h_R), \qquad \text{and} \qquad f_V = \begin{cases} \frac{K_z}{m}[\max(h_A, H_b) - h_R] & \text{if } h_R > H_b \\ 0 & \text{otherwise,} \end{cases} \tag{1}$$

where K_{rb} and K_z are the hydraulic conductivities of the riverbed sediments and of the floodplain surface layer, respectively (dimension: L/T); h_R is the height of the river water surface above the aquifer bottom, calculated by the surface water model and uniform across the river section; h_A is the hydraulic head of the aquifer, calculated by the groundwater model and variable across the aquifer; m_{rb} and m are the thicknesses of the clogged interface layer in the riverbed and the floodplain, respectively (dimension: L); and H_b is the aquifer thickness (dimension: L).

Although natural aquifers may exhibit longitudinal hydraulic gradients parallel to the river, preliminary simulations were conducted using both a 1D and a fully 2D groundwater flow formulation to evaluate the influence of longitudinal groundwater flow. The results showed negligible differences between the two configurations, indicating that during flood events the dominant exchange processes are controlled by river–aquifer head gradients rather than regional longitudinal groundwater flow. Therefore, no-flow lateral boundaries were considered an appropriate simplification for the purposes of this study.

The methodology used here to calculate exchange flows is analogous to that used in the MODFLOW-2005 River Package (*Harbaugh 2005*). However, we developed our own finite-difference solver rather than using MODFLOW so that river flood propagation could be simulated more accurately with the full Saint-Venant equations, distinguishing between the Manning coefficient of the channel and that of the floodplain. The river domain is discretised into a sequence of equidistant cross-sections and the groundwater domain into a regular rectangular grid. The transverse gridlines of the groundwater domain overlap with the river cross-sections, but extend well beyond the levees. For each grid cell covering the active floodplain, a vertical flux is calculated.

Study area

We integrate bank storage and evaluate flood attenuation for two 50-km-long reaches, each approximating the mean geometry of the Lower Danube and the middle reach of the Tisza River in Hungary. At the inflow, a 100-year flood hydrograph was imposed, approximated separately for the two rivers. Soil hydraulic properties were kept constant over time.

The Lower Danube River in Hungary has a total floodplain width of approximately 1800 m, whereas the middle reach of the Tisza River features a slightly wider floodplain of about 2000 m. Both rivers have similar channel depths under banks (9.0 m for the Danube and 7.0 m for the Tisza), but the Danube's main channel is significantly wider (475 m compared to 180 m for the Tisza). Besides the geometry, the two rivers analysed also exhibit distinct flood hydrograph characteristics (*Figure 2*). The Danube has an overbank flood duration ($T_{overbank}$) of 15 days, reaching a peak discharge of 9850 m³/s on the 6th day after the start of overbank flood. The Tisza's flood extends for 80 days, with a peak flow of 2800 m³/s on day 40 after the beginning of the overbank flood.

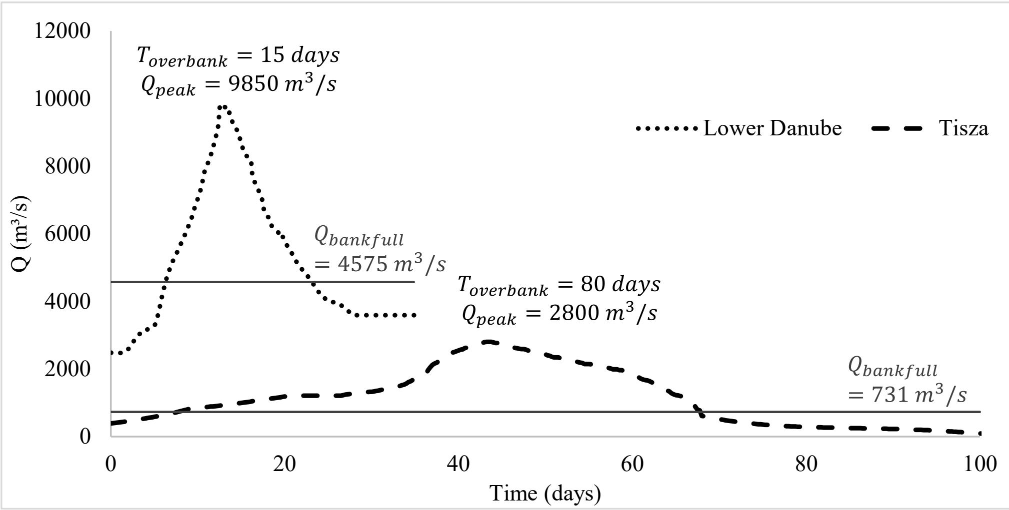

Figure 2. 100-year (HQ1%) flow hydrograph of the Lower Danube (dotted line) and the Tisza River (dashed line). Bankfull discharges are represented by solid lines for the Lower Danube and the Tisza. The vertical axis represents river flow Q (m³/s), while the horizontal axis shows time in days

2. ábra. A hazai Alsó-Duna (pontozott vonal) és a Közép-Tisza (szaggatott vonal) 100 éves visszatérési idejű (HQ1%) árhullámképe. A mederkitöltő vízhozamokat folytonos vonal jelöli az Alsó-Duna és a Tisza esetén. Függőleges tengely: Q vízhozam (m³/s), vízszintes tengely: idő (nap)

The hydraulic conductivity of the soil was varied by discretising the order of magnitude with three scenarios, SCN25 to SCN27 for the Danube River and SCN28 to SCN30 for the Tisza River, to address the spatial variability and uncertainty of soil hydraulic conductivity. The adopted conductivity values were not derived from direct field measurements within this study but were inferred from reported ranges in previous hydrogeological investigations of the region (*Ubell 1963, Kolencsik-Tóth and Kovács 2015, Murinkó and Bene 2017, Trásy et al. 2020, Wagner and Csoma 2022*). These studies describe the alluvial deposits surrounding the investigated rivers as predominantly sandy and gravelly aquifers. Based on these reported ranges, representative hydraulic conductivity values were selected and further adjusted during model calibration together with the Manning roughness coefficient.

Rather than representing a specific statistical distribution of measured values, the three scenarios were designed to capture plausible low-, medium-, and high-conductivity conditions within the range reported for similar alluvial environments. The upper conductivity scenario ($K_x = 500$ m/d; SCN27/30) represents a high-permeability gravel aquifer condition, characteristic of coarse alluvial deposits with strong river–aquifer connectivity, and was included to investigate the upper sensitivity range of infiltration and bank storage processes.

Table 1 summarises the data utilised in the model. For the Danube River, two reaches have been distinguished. The Lower Reach served for calibration and the analysis of the 100-year flood wave, whereas the Upper Reach was evaluated to validate the transferability of model parameters.

Table 1. Hydraulic parameters and their values used in the model for the analysed rivers.
1. táblázat. A vizsgált folyók modelljében használt hidraulikai paraméterek és értékeik

Parameter	Danube River (Lower Reach)	Danube River (Upper Reach)	Tisza River	Unit	Description
$\boldsymbol{b}$	475	574	180	m	Bottom width of the main channel
$\boldsymbol{z}$	9	7.5	7.0	m	Depth of the main channel
$\boldsymbol{S_0}$	7	7	2.5	cm/km	River slope
$\boldsymbol{n_m}$	0.033	0.033	0.03	s m$^{-1/3}$	Manning roughness of the main channel
$\boldsymbol{n_f}$	0.1	0.1	0.082	s m$^{-1/3}$	Manning roughness of the active floodplain
$\boldsymbol{b_f}$	1,800	240	2,000	m	Total width of the active floodplain
$\boldsymbol{K_{rb}/m_{rb}}$	0.15	0.15	0.15	d^{-1}	Riverbed leakance factor = ratio of riverbed hydraulic conductivity per thickness of the riverbed layer
$\boldsymbol{S_y}$	0.21	0.21	0.21	-	Specific yield for unconfined aquifer
$\boldsymbol{S_s}$	1×10^{-5}	1×10^{-5}	1×10^{-5}	m^{-1}	Specific storage when aquifer is fully saturated
$\boldsymbol{K_x = K_y}$	SCN25: 5 SCN26: 50 SCN27: 500	SCN25: 5 SCN26: 50 SCN27: 500	SCN28: 5 SCN29: 50 SCN30: 500	m d^{-1}	Horizontal hydraulic conductivity of the aquifer
$\boldsymbol{K_z/m}$	SCN25: 0.15 SCN26: 1.5 SCN27: 15	SCN25: 0.15 SCN26: 1.5 SCN27: 15	SCN28: 0.15 SCN29: 1.5 SCN30: 15	d^{-1}	Vertical leakance factor = ratio of floodplain vertical hydraulic conductivity per thickness of the floodplain surface layer
Q_{peak} (100-yr)	9,850	-	2,800	m^3 s^{-1}	Peak discharge during the 100-year flood hydrograph ($HQ_{1\%}$)
$T_{overbank}$ (100-yr)	16.75	-	60.25	d	Duration of overbank flooding during the 100-year event
Q_{peak} (2013)	9,080	9,346	-	m^3 s^{-1}	Peak discharge during the 2013 flood hydrograph
$T_{overbank}$ (2013)	16.0	15.5	-	d	Duration of overbank flooding during the 2013 event
$Q_{bankfull}$	4,575	4,522	731	m^3 s^{-1}	Bankfull discharge

The longitudinal slope was set to the mean slope of the actual river reaches.

Model calibration targeted three key variables: (1) the mean overbank depth (d), (2) the relative attenuation of peak discharge, expressed as $\Delta Q/Q_{peak} = \left[Q_{peak}(0) - Q_{peak}(L_x)\right]/Q_{peak}(0)$, where $Q_{peak}(0)$ is the river peak discharge at the inflow, and $Q_{peak}(L_x)$ is the river peak discharge at the longitudinal length from which attenuation is analysed, L_x, and (3) the average bank storage within the dry floodplain, defined as the area beyond the levees extending approximately 3 km inland. No groundwater data were available on the active floodplain (which is a routine limitation); therefore, calibration primarily focused on estimating bank storage within the dry floodplain (BS_{dry}).

The variables adjusted during calibration were the Manning roughness coefficient (n) of the river model and the vertical leakance factor, that is, the ratio of the floodplain vertical hydraulic conductivity of the soil to the thickness of the floodplain surface layer (K_z/m). The leakance factor of the riverbed was kept constant between scenarios because the observed variables were barely sensitive to it.

Uniform and river-specific Manning's n values were calibrated for the channel and floodplain using the 2013 flood of the Danube River over the 135 km Lower Danube reach between the river gauges of Dunaújváros and Mohács (rkm 1580-1446). The calibration targets were the mean overbank depth (d) and the relative attenuation of the peak discharge ($\Delta Q/Q_{peak}$). This approach was used to evaluate whether a simplified symmetric cross-section could represent the overall hydraulic behaviour of the actual irregular river sections, rather than to reproduce observations at individual gauge stations.

The floodplain geometry of this reach is highly variable, being relatively narrow along the upstream two-thirds and wider along the downstream third. Due to the nonlinear nature of the Saint–Venant equations, the prismatic model could not simultaneously reproduce both calibration indicators with exact agreement.

We validated the transferability of the model parameters to a distinct 47 km reach between the left-bank tributaries, the Váh (Vág) River and Hron (Garam) River, delimited by river gauges Iža and Esztergom (rkm 1764-1718.5), to which we refer here as the Upper Danube Reach. The reach was not extended beyond the tributaries to simplify the evaluation of flood peak attenuation. Except for the floodplain width, the character of the river and aquifer are similar to those of the Lower Danube Reach, so we transferred the Manning n values and the aquifer parameters unchanged and only updated the (still simplified) geometry of the river.

The floodplain in this reach is considerably narrower, which alters the relative contribution of vertical floodplain infiltration and horizontal riverbank infiltration processes. As a result, the simulated d and $\Delta Q/Q_{peak}$ show larger deviations from the reference values compared to the calibration reach. For the Lower Danube reach, simulated d ranges from 2.57 to 2.67 m compared to the target value of 3.0 m, while $\Delta Q/Q_{peak}$ ranges from 10.2% to 11.5% compared to the target value of 8.2%. For the Upper Danube reach, simulated $\Delta Q/Q_{peak}$ ranges from 0.9% to 1.1% compared to the reference value of 2.0% (*Table 2*). These differences indicate that the calibration compensates for the geometric variability of the Lower Danube floodplain and therefore performs less effectively when transferred to the more regular Upper Danube reach. However, because the objective of the model is to reproduce the order of magnitude of flood attenuation for idealised lowland river geometries rather than site-specific hydraulic conditions, we considered these deviations to be reasonable.

Table 2. Reference and simulated mean overbank depth (d) and flow attenuation ($\Delta Q/Q_{peak}$) over 135 km for the Lower Danube reach (used in the calibration), and over 47 km for the Upper Danube reach (used in the validation of parameter transferability), during the 2013 flood

2. táblázat. Referenciaként adott és szimulált átlagos hullámtéri vízmélység (d) és relatív vízhozam-csillapítás (ΔQ/Q_peak) a 2013-as árvíz idején; az Alsó-Duna 135 km-es szakaszán (kalibráció), valamint a Felső-Duna 47 km-es szakaszán (a paraméter-átvihetőség igazolása)

	Lower Danube (Calibration)				**Upper Danube (Validation)**			
	Target	**SCN25**	**SCN26**	**SCN27**	**Target**	**SCN25**	**SCN26**	**SCN27**
d (m)	**3.0**	2.67	2.66	2.57	**3**	4.43	4.41	4.41
$\boldsymbol{\Delta Q/Q_{peak}}$ (%)	**8.2**	10.3	10.2	11.5	**2.0**	0.9	1.1	1.0

For the groundwater model, the ratio of floodplain vertical hydraulic conductivity of the soil to the thickness of the floodplain surface layer was determined by targeting the bank storage under the dry floodplain (beyond the levees), as, for example, by *Ubell (1964).* Model results were compared with bank storage estimates derived from observed groundwater level data sourced from the General Water Directorate of Hungary.

Stations with a significant share of missing or erroneous data were excluded, resulting in a total of 21 valid groundwater stations on the left bank of the lower reach and 25 stations on the right bank of the upper reach for use in the final analysis. The wells are distributed along the study reaches at varying distances from the levee and river channel rather than along a single transect, and therefore represent groundwater responses across different locations of the dry floodplain.

These stations were all situated on the dry floodplain; the lack of data on the groundwater table or the saturation of the vadose zone under the active floodplain is the reason why total bank storage could not be estimated.

To evaluate groundwater response during the flood event from the measured gauge data, the maximum rise in groundwater level – from initial to peak stage – was plotted against the distance of each well from the levee (*Figure 3*). The levee serves as the boundary between the dry and wet floodplains. A logarithmic curve was fitted to the data, and a length-normalised bank storage under the dry floodplain (BS_{dry}) was estimated as the positive area under this lateral profile multiplied by a river length of 50 km.

For the Lower Danube Reach, the minimum distance between a groundwater well and the levee is 31 m, with an observed maximum groundwater rise of 2.86 m (average 0.65 m). For the Upper Danube Reach, these values are 54 m, 4.24 m, and 0.74 m, respectively. The distance over which the flood had a direct impact was about 2500 m in both reaches. The bank storage along the left dry floodplain was approximately 13 × 10^6 m^3 (16 × 10^6 m^3) over 50 km. For both reaches, we estimated that the total bank storage under the dry floodplain (BS_{dry}) was twice the one-sided value.

During calibration and validation, the numerical model was applied to the 2013 flood event of the Danube River, using three sets of hydraulic conductivity values representing plausible ranges for alluvial aquifers reported in the literature. Horizontal conductivities of 5, 50, and 500 m d^{-1} were tested, each paired with vertical leakance factors of 0.15, 1.5, and 15 d^{-1}, respectively. These parameter sets were used to explore the sensitivity of the simulated groundwater response and bank storage to hydraulic conductivity. The initial condition of the groundwater head was assumed to be in equilibrium with the surface water head.

As in the observational analysis, only the bank storage under the dry floodplain was calculated from the model results. *Table 3* presents both the observation-based bank storage estimates (derived from groundwater level data) and the simulated values. Considering that the modelled BS_{dry} varied by more than a factor of 16 between the bounding scenarios, BS_{dry} for the medium conductivity scenario (24×10^6 m^3) aligned well with the value derived from measurements (25×10^6 m^3). Model validation using the Upper Danube Reach yielded a measurement-based estimate of 32×10^6 m^3, compared to a result of 24×10^6 m^3 modelled with the medium K scenario. This is satisfactory evidence that the medium K scenario captures the order of magnitude of the mean conductivity for the Danube.

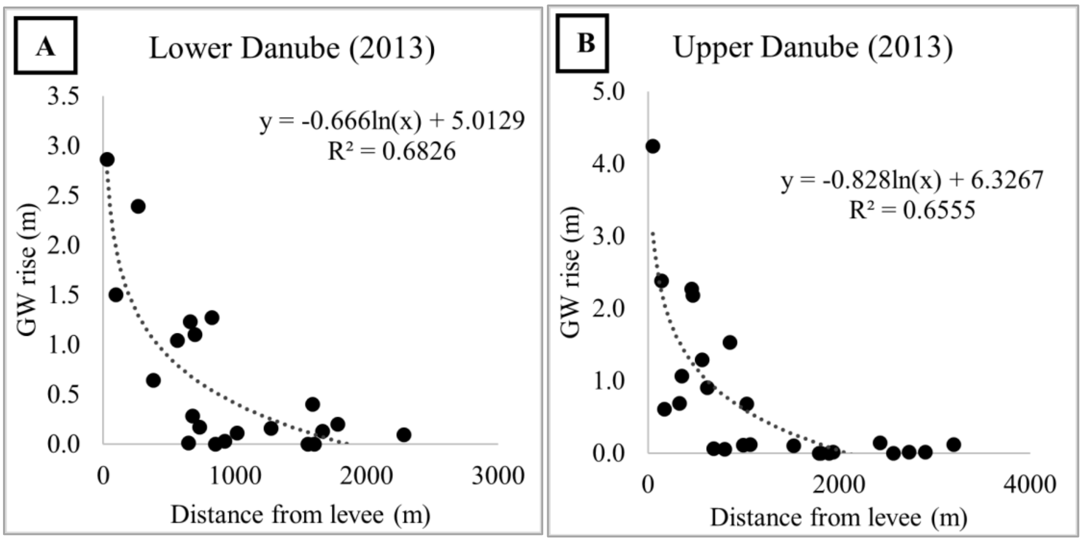

Figure 3. Observed maximum groundwater rise (y) during the 2013 Danube flood as a function of distance from the levee on the dry floodplain (x), for the lower (A) and the upper (B) Danube reach
(A logarithmic regression curve was fitted to the data)
3. ábra. Megfigyelt maximális talajvízszint-emelkedés (y) a 2013-as dunai árvíz idején a mentett oldali ártéren, az árvízvédelmi töltéstől mért távolság (x) függvényében, az alsó (A) és a felső (B) dunai szakaszra
(Az adatokra logaritmikus regressziós görbe lett illesztve)

Table 3. Simulated and measured bank storage under the dry floodplain (BS_{dry}, [10^6 m^3]) on the left (Lower Danube) and right (Upper Danube) banks, during the 2013 flood. "Measured" bank storage was estimated from observed groundwater level data
3. táblázat. A szimulált és a mért felszín alatti tározódás összehasonlítása a mentett oldali ártér alatt (BS_{dry}, [10^6 m^3]) a dunaszakaszok bal (Alsó-Duna) ill. jobb (Felső-Duna) partján, a 2013-as árvíz idején. A „mért" felszín alatti tározódást a megfigyelt talajvízszint-adatok alapján becsültük

Conductivity scenario	Lower Danube reach		Upper Danube reach	
	Numerical model	Measured	Numerical model	Measured
SCN25 (low K)	3	25	6	32
SCN26 (medium K)	24	25	24	32
SCN27 (high K)	80	25	43	32

The definition of the flood start introduces some uncertainty in the estimation of bank storage, particularly when antecedent water level variations precede the main flood wave. Since bank storage was estimated from the groundwater rise between the initial and peak stages, changes in the selected initial condition may influence the absolute storage values. However, the same flood period and initial conditions were used for both the observation-based estimates and the numerical simulations, ensuring consistency in the comparison between measured and modelled bank storage.

The Manning n values of the Tisza River were calibrated separately, as for the Lower Danube Reach, against maximum overbank depth and discharge peak attenuation. Results are not presented here. The hydraulic properties of the aquifer were transferred from the Danube River without recalibration or validation.

Groundwater calibration and validation were only performed for the Danube River. Although a dense groundwater monitoring network exists along the Middle Tisza River, preprocessing and interpretation of the groundwater time series were beyond the scope of the present study. Therefore, the Tisza results are presented as scenario-based sensitivity analyses, and no individual hydraulic conductivity scenario is interpreted as the best-fitting representation of field conditions.

In the following sections, we analyse how these characteristics influence exchange flows between rivers and aquifers, bank storage, and their contribution to flood attenuation for the Lower Danube Reach and the Tisza River, which differ markedly in flood magnitude, flood duration, and longitudinal slope. The Upper Danube Reach will not be analysed further.

RESULTS

To assess the effect of bank storage on the attenuation of flood peaks, we seek to determine the mean lateral exchange of water from the channel into adjacent aquifers (expressed as a volumetric flow per unit river length) and to evaluate how this exchange varies spatially over management-relevant scales. To this end, we averaged the instantaneous volumetric flow rates Q_V and Q_H at each model transect during the simulation period, excluding zero flows. Finally, to obtain a reach-scale metric, we averaged these volumetric flows over a 50 km reach.

This 50 km average length was chosen because it approximates typical levee-management units and is long enough to integrate cumulative attenuation effects while remaining short enough to align with operational planning. The resulting 50 km-averaged specific flow components, q_H and q_V, provide a meaningful indicator of bank-storage capacity that can be directly compared across the Hungarian reaches of the Danube River and Tisza River.

Regarding the bank storage volume, we first calculate the time evolution of the specific bank storage for each transect by integrating the specific infiltration flow rate over time for the entire duration of the flood hydrograph. For each transect, we then identify the maximum value of the specific bank storage, which we finally integrate over a 50 km reach, resulting in 50 km-averaged peak specific bank storage components BS_H and BS_V. Note that these capture bank storage under the entire floodplain, including the active and the dry floodplains.

Table 4 summarises the results for mean specific flow rates from the river and peak specific bank storage, both per river km, across the six different river scenarios analysed.

Table 4. Vertical and horizontal components, and total specific infiltration flow from the river into the aquifer (q_V, q_H, q_T), averaged over the simulation period of the 100-year flood. The associated maximum bank storage volumes (BS_V, BS_H, BS_T), for all scenarios. All variables are averaged/integrated over a 50 km river length

4. táblázat. A folyóból a talajvíztartóba irányuló fajlagos szivárgási vízhozam függőleges és vízszintes összetevői és ezek összege (q_V, q_H, q_T), a 100 éves árvíz szimulációs időszakára átlagolva. A táblázat tartalmazza a hozzájuk tartozó maximális felszín alatti tározott víztérfogatokat is (BS_V, BS_H, BS_T) minden változatra. Minden változó 50 km-es folyószakaszra átlagolva/integrálva értendő

Scenario	River	K_z/m [d^{-1}]	K_x [m/d]	Mean q_V [m³/s/km]	Mean q_H [m³/s/km]	Mean q_T [m³/s/km]	Max BS_V [10³ m³/km]	Max BS_H [10³ m³/km]	Max BS_T [10³ m³/km]
SCN25	Lower Danube	**0.15**	**5**	0.58 (87%)	0.09 (13%)	0.67	1,013 (90%)	111 (10%)	1,125
SCN26	Lower Danube	**1.5**	**50**	0.81 (84%)	0.16 (16%)	0.97	1,419 (89%)	181 (11%)	1,600
SCN27	Lower Danube	**15**	**500**	1.54 (88%)	0.22 (13%)	1.76	2,632 (91%)	249 (9%)	2,880
SCN28	Tisza	**0.15**	**5**	0.16 (84%)	0.03 (16%)	0.19	1,091 (90%)	126 (10%)	1,217
SCN29	Tisza	**1.5**	**50**	0.25 (86%)	0.04 (14%)	0.29	1,742 (91%)	173 (9%)	1,915
SCN30	Tisza	**15**	**500**	0.58 (89%)	0.07 (11%)	0.65	3,763 (93%)	285 (7%)	4,048

In both rivers, specific infiltration flows through the floodplain (q_V) were greater than those through the riverbed (q_H), contributing approximately 86% of the total specific infiltration flows, owing mainly to the large floodplain width. The bank storage volume originating from the vertical infiltration (BS_V) represents 91% of the total ($BS_V + BS_H$) for the Tisza River scenarios and 90% for the Danube River scenarios.

Exchange flows

River–aquifer exchange flows are driven by the hydraulic gradient between river water and groundwater levels, which is conceptually split into horizontal and vertical infiltration pathways. The total reach-integrated infiltration flow rate, obtained as the sum of vertical and horizontal flow rates ($Q_T = Q_H + Q_V$), has a sharper peak than the surface flow hydrograph.

Figure 4 presents the exchange flow hydrographs for the three hydraulic conductivity scenarios of the Danube River. As expected, higher hydraulic conduc-tivities result in greater infiltration flows throughout the flood event.

Q_H begins to develop as soon as river levels start to rise. It peaks early, approximately one day before the start of overbank flooding (t_1), with peak values ranging from 16 m³ s^{-1} in the low-conductivity scenario (SCN25) to 57 m³ s^{-1} in the high-conductivity scenario (SCN27). As the aquifer near the riverbed becomes saturated, Q_H declines due to a reduced hydraulic gradient.

In contrast, Q_V persists for longer and typically peaks during the rising limb of the flood, influenced by the timing and extent of overbank flooding. Q_V continues to enter the aquifer even beyond the flood peak, though with reduced magnitude, and ceases only as water recedes into the main channel. While the timing of the Q_V peak is moderately sensitive to soil hydraulic conductivity, occurring at approximately t_1 + 9 hours in the high-conductivity scenario and at t_1 + 5 days in the low-conductivity case, the duration of the vertical infiltration varies much more substantially between scenarios. Peak Q_V values span an order of magnitude, from 51 m³ s^{-1} (SCN25) to 502 m³ s^{-1} (SCN27).

Figure 5 presents the river-aquifer exchange flow hydrographs at the outlet section of the Tisza River for the three hydraulic conductivity scenarios.

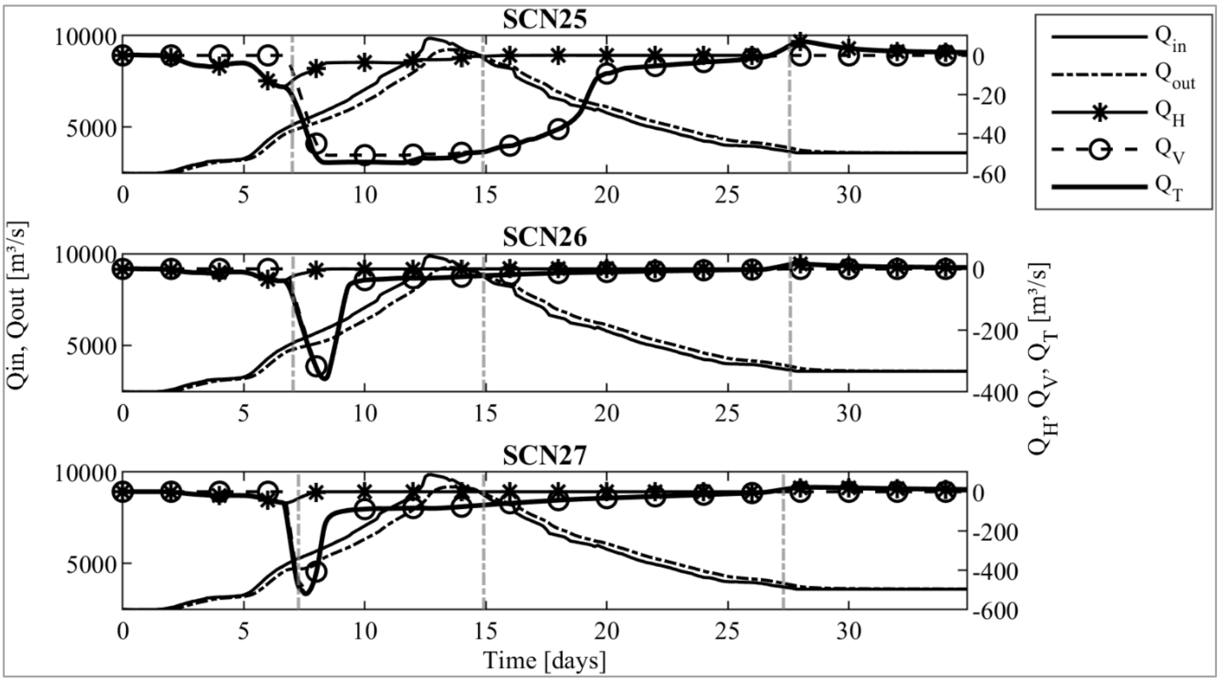

Figure 4. Reach-integrated exchange flow rates between river and aquifer (negative values: flow into the aquifer) for the Lower Danube reach under the conductivity scenarios (SCN25 – low; SCN26 – medium; SCN27 - high). Horizontal exchange flow rate (Q_H) is shown with asterisk markers, vertical exchange flow rate (Q_V) with open-circle markers, and total exchange flow rate ($Q_T = Q_V + Q_H$) with a solid thick line. River discharge at the inflow (Q_{in}) is represented by a solid black line and at the outflow (Q_{out}) by a dash-dot line (Results are shown for a 50 km river reach)

4. ábra. A folyó és a talajvíztartó közötti, az Alsó-Duna 50 km hosszú szakaszára integrált szivárgási vízhozamok (negatív érték: a víztartó felé irányuló áramlás) a különböző hidraulikai vezetőképességi változatok mellett (SCN25 – alacsony; SCN26 – közepes; SCN27 – magas). A vízszintes szivárgási hozamot (Q_H) csillag, a függőlegest (Q_V) üres kör szimbólum jelöli; a kettő összegét ($Q_T = Q_V + Q_H$) vastag folytonos vonal mutatja. A folyó belépő árhullámképét (Q_{in}) fekete folytonos vonal, a kilépőt (Q_{out}) pont-vonal jelzi

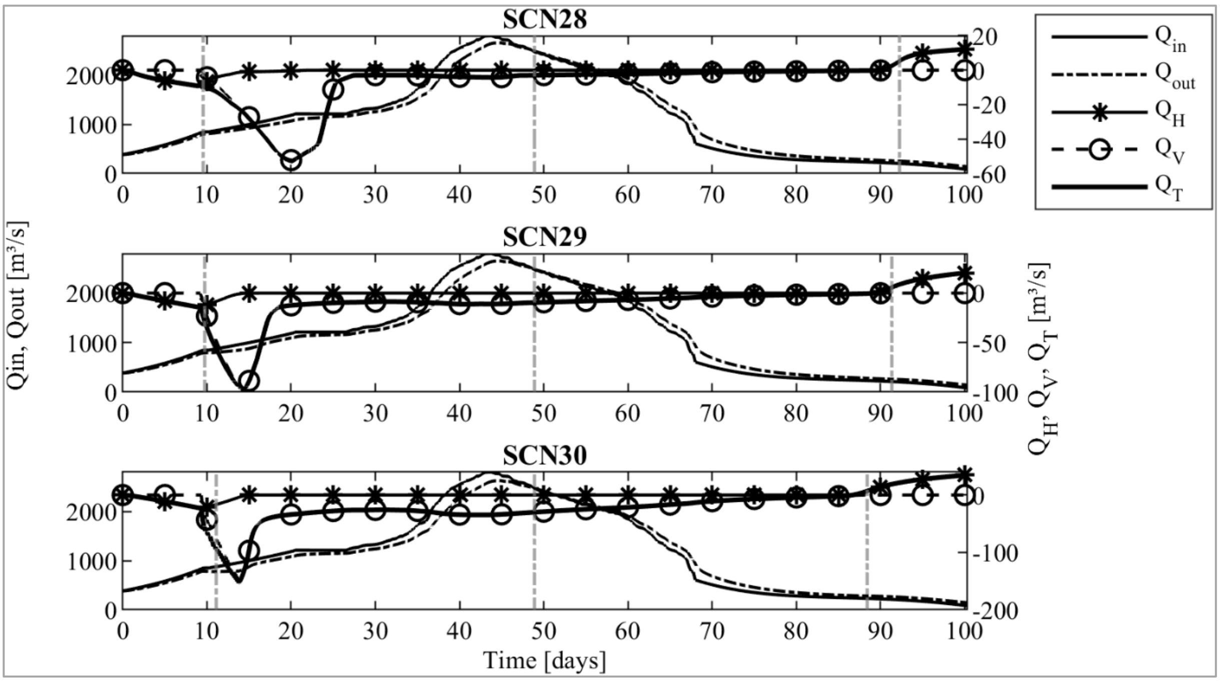

Figure 5. Reach-integrated exchange flow rates between river and aquifer (negative values: flow toward the aquifer) for the Tisza River under the conductivity scenarios (SCN28 – low; SCN29 – medium; SCN30 - high)

(Descriptions of the curves are presented in Figure 4)

5. ábra. A folyó és a víztartó közötti szakaszintegrált szivárgási vízhozamok (negatív érték: a víztartó felé irányuló áramlás) a Tisza folyón a különböző hidraulikai vezetőképességi változatok mellett (SCN28 – alacsony; SCN29 – közepes; SCN30 – magas)

(A görbék jelölése: lásd 4. ábra)

Q_H peaks approximately one day before the onset of overbank flooding (t_1), but the time to peak is sensitive to the hydraulic conductivity, ranging from 14 hours in the low-conductivity scenario (SCN28) to 2 days in the high-conductivity scenarios (SCN30). The peak values of Q_H range from 9 m³ s⁻¹ (SCN28) to 23 m³ s⁻¹ (SCN30).

This is followed by the peaking of Q_V, which occurs on average at t_1 + 6 days, although it varies depending on the scenario. In detail, Q_V peaks at t_1 + 11 days, t_1 + 5 days, and t_1 + 3 days in the low- (SCN28), medium- (SCN29), and high-conductivity (SCN30) scenarios. Peak Q_V values range from 52 m³ s⁻¹ (SCN28) to 150 m³ s⁻¹ (SCN30).

Flood attenuation

To investigate the modification of a flood hydrograph due to bank storage, the inflow hydrograph was routed through a long river reach and evaluated along the uppermost 50 km reach (not impacted by the outflow boundary condition), both with and without infiltration. In the first case, both horizontal and vertical infiltration were allowed through the riverbed and active floodplain, while in the second case, the channel and floodplain were treated as impermeable, preventing any infiltration. *Table 5* summarises the flow and river stage attenuation, as well as flood wave delay, for all simulated scenarios.

The impact of bank storage on flow attenuation is evident across the scenarios. In the Lower Danube simulations, incorporating bank storage resulted in a peak flow reduction of 6.2% (613 m³/s), an excess of +0.5 percentage points (+48 m³/s) compared to the case without infiltration, for the middle scenario (SCN26). Although no delay in peak discharge timing was observed, the inclusion of vertical and horizontal infiltration led to an average decrease in water depth of 3.1 cm in SCN26. In the Tisza River, bank storage reduced the peak flow by 6.2% (151 m³/s), a change of +0.6 percentage points (+16 m³/s) compared to the case without infiltration, for the middle scenario (SCN29). Water levels in the Tisza decreased by 2.8 cm in SCN29. A consistent trend emerges across both rivers: higher soil hydraulic conductivity corresponds with greater flow attenuation, underscoring the effect of permeable soils on the bank storage processes.

During flood events, surface water storage refers to the temporary retention of water within river channels and floodplains, naturally regulating flood wave propagation and peak attenuation. This surface storage was calculated by integrating the channel's wetted cross-sectional area at the local peak flood conditions over the entire modelled reach. When comparing bank storage to total storage (i.e., the sum of surface and bank storage), bank storage contributes a smaller, yet significant, proportion. Its contribution increases with soil permeability: for the Lower Danube, bank storage represents 12%, 16%, and 26% in the low (SCN25) to high (SCN27) conductivity scenarios, respectively. For the Tisza River, the corresponding values are higher: 14%, 21%, and 37% (SCN28 to SCN30).

Table 5. Flow attenuation factor ($\Delta Q/Q_{peak}$) with and without infiltration, river depth attenuation (Δh) with and without infiltration, and time to peak (Δt_{peak}) delay between inflow and outflow with and without infiltration, for all 100-year scenarios
5. táblázat. Relatív vízhozam-csillapítás ($\Delta Q/Q_{peak}$), vízszint-csillapítás (Δh), valamint a tetőzés időeltolása a belépő és kilépő szelvények között (Δt_{peak}) beszivárgással és beszivárgás nélkül, az összes 100 éves árvízi változatra vonatkozóan

Scenario	K_z/m (d⁻¹)	K_x (m/d)	$\Delta Q/Q_{peak}$ w/inf (%)	$\Delta Q/Q_{peak}$ w/out inf (%)	Δt_{peak} w/ inf (h)	Δt_{peak} w/out inf (h)	Δh w/inf (cm)	Δh w/out inf (cm)
Lower Danube	**0.15**	**5**	6.2%	5.7%	17.0	17.0	22.8	19.6
	0.5	**50**	6.2%	5.7%	17.0	17.0	22.7	19.6
	1.5	**500**	6.7%	5.7%	17.0	17.0	25.8	19.6
Tisza	**0.15**	**5**	5.2%	4.8%	25.0	25.0	14.0	12.4
	0.5	**50**	5.4%	4.8%	25.0	25.0	15.1	12.4
	1.5	**500**	6.3%	4.8%	26.0	25.0	18.8	12.4

DISCUSSION

The primary objective of this study was to investigate infiltration into the aquifer during extreme (100-year) flood events, with a focus on how different combinations of river, aquifer, and flood hydrograph characteristics affect river-aquifer exchange and contribute to flood attenuation. The analysis centred on the two major Hungarian rivers, the Danube River and the Tisza River, which represent two distinct river configurations with large levee-protected floodplains where accurate prediction of flood attenuation is critical.

A prismatic, symmetric river geometry was adopted and evaluated against observed flow rates and overbank depths derived from hydraulic modelling based on surface water gauge data. The transferability of the calibrated model parameters was then assessed by applying them to a different reach of the Danube River. This comparison showed that the simplified geometry provides a reasonable representation for scenario-based sensitivity analyses.

To assess the influence of soil hydraulic properties, multiple scenarios were tested for each river, varying both horizontal and vertical (floodplain surface layer) conductivity values. Calibration was performed using groundwater observations from the 2013 flood in the Lower Danube Reach. The modelled bank storage estimates aligned well with observational data under the medium-conductivity scenario, confirming the model's capability to realistically simulate infiltration-driven bank storage during major flood events.

For lowland rivers such as the Hungarian reaches of the Lower Danube and Tisza, both horizontal (Q_H) and vertical (Q_V) reach-integrated infiltration flow rates tended to peak during the rising limb of the flood. Q_H declined rapidly as the hydraulic gradient decreased and the floodplain became progressively saturated, whereas Q_V persisted longer, remaining active through much of the rising limb of the hydrograph.

The timing and magnitude of these peaks were strongly influenced by soil hydraulic conductivity: in high-conductivity scenarios, infiltration rates peaked quickly and reached higher values, while in low-conductivity scenarios, the peaks were lower but more sustained. This pattern is consistent with the findings of *Helton et al. (2014)* and *Doble et al. (2012)*, who reported that aquifer exchange is initially high as floodwaters spread across the floodplain and then diminishes as sediments saturate and the river stage increases.

Mean river–aquifer exchange flows were higher in the Lower Danube River, driven by steeper hydraulic gradients and rapid rates of overbank water level rise (~47 cm/day), compared to ~8 cm/day for the Tisza. However, the Tisza River exhibited much greater total bank storage volumes, attributed primarily to its longer inundation duration and secondarily to its wider floodplain. Vertical infiltration through the active floodplain dominated bank storage in both rivers: 90% in the Danube and 91% in the Tisza. These values are consistent with *Bernard-Jannin et al. (2016)*, who reported 88% floodplain infiltration in the Garonne River (Spain), reinforcing the importance of surface water–groundwater exchange through overbank flows in flood modelling.

Over a 50 km reach, the Lower Danube showed an average flow peak reduction of 6.4% (Tisza: 5.6%) and a peak water level decrease of 4 cm (Tisza: 6.4 cm). Our results show that bank storage contributed significantly to this attenuation, reducing flows and water levels in both systems and accounting for 12–26% of total storage in the Danube and 14–37% in the Tisza. The Danube River's rapid rise produced higher infiltration flow rates, aligning with findings by *Hou et al. (2021),* which noted that a rapid rise in flood depth enhances infiltration by inundating more land earlier in the flood event. *Ubell (1963)* similarly highlighted that infiltration is influenced not only by the hydraulic gradient but also by the intensity of river level fluctuations, with rapid surface water rises promoting higher infiltration rates. Yet, despite these elevated exchange flow rates in the Danube, the Tisza River's longer inundation and broader floodplain enabled more sustained infiltration and greater peak reduction. This shows that the duration and spatial extent of flooding can be more influential than the exchange flow rates alone.

While often underrepresented in flood models, bank storage has been shown in this study to play a substantial role in water retention and flood attenuation. To improve model accuracy and efficiency, especially in flood risk mapping and flood forecasting, incorporating infiltration and bank storage effects is essential (*Szilagyi 2004, Hou et al. 2021*). Even when the model's process description doesn't represent bank storage, the resulting errors are partly mitigated during the calibration of the flow resistance parameters (e.g., Manning's n), by matching peak river water levels, peak river discharges and flood propagation speed. However, this compensation remains imperfect because roughness and bank storage influence flood dynamics through different mechanisms. Roughness mainly affects momentum losses and flood-wave routing, whereas bank storage introduces temporary subsurface storage and delayed groundwater release, acting over longer timescales than surface storage processes. Consequently, calibration of roughness parameters cannot fully reproduce the temporal shift associated with groundwater storage and release.

This limitation becomes increasingly important when models are extrapolated beyond the flood events used for calibration. In the present study, neglecting infiltration reduced the average attenuation in the Danube from 6.4% to 5.7% for the analysed 100-year flood scenarios. For the Tisza River, attenuation decreased from 5.6% to 4.8%. Although the attenuation differences are comparable between both rivers, bank storage was considerably larger in the Tisza due to its wider floodplain and longer flood duration. In addition, the sensitivity to hydraulic conductivity was more pronounced in the Tisza, where the variation among permeability scenarios was approximately twice that observed for the Danube. These findings indicate that roughness calibration may reproduce observed flood levels within the calibration range, but may become less reliable when applied to flood events with different magnitudes, durations, or floodplain inundation extents, where infiltration and groundwater storage processes play a larger role.

Sedimentation can reduce soil permeability (as well as surface storage) over time. In particular, in the Middle and Lower Tisza River, sedimentation rates of 1.1 cm yr^{-1} and 0.8 cm yr^{-1}, respectively, have led to rising riverbed levels (*Murányi and Koncsos 2022*), which in turn reduce hydraulic conductivity and limit bank storage. These authors also explore the reconnection of deep floodplains along the Tisza to increase surface storage by up to 2400 million m^3. In addition to this storage, our study shows that, for a 100-year flood, subsurface storage may represent 14–37% of surface storage in the Middle Tisza River, increasing the relevance of adding river-aquifer interactions when studying alternative nature-based solutions for flood risk mitigation. It is worth noting that bank storage over a 50 km river reach is of the same order of magnitude as the storage capacity of existing or planned flood retention reservoirs on the middle reach of the Tisza River (Tiszaroffi: 97, Hanyi-Tiszasülyi: 247, Nagykunsági: 99 million m^3) (*Ungvári and Kis 2021*). Similarly, *Schweitzer (2015)* reported a trend of flood wave heights rising by 2–3 cm yr^{-1} along the Tisza River between 1970 and 2013 due to channel capacity deterioration.

In the present modelling framework, the riverbed leakance factor (K_{rb}/m_{rb}) was assumed constant across all scenarios in order to isolate the influence of aquifer hydraulic conductivity and floodplain vertical leakance on bank storage dynamics. However, sedimentation processes may modify the permeability of the riverbed and create clogging layers that reduce hydraulic connectivity between the river and aquifer. Future work could therefore explore the sensitivity of river-aquifer exchange flows to variations in riverbed leakance, particularly in systems where sediment accumulation progressively alters riverbed hydraulic properties.

Finally, our simulations reveal that in both the Lower Danube and Tisza rivers, bank storage extended well beyond the active floodplain in the medium- to high-conductivity scenarios, reaching a distance of 1–3 km from the levee. This has negative implications for flood control infrastructure, since prolonged flood waves have historically led to dike breaches on the Tisza (*Lóczy 2010*), especially when subsurface flow pressures build up. Hence, flood mitigation strategies should carefully balance structural measures with natural processes such as infiltration and groundwater recharge.

CONCLUSIONS

This study investigated river–aquifer interactions during extreme flood events in two lowland river reaches, approximating the Lower Danube River and the Middle Tisza River in Hungary, using a physically based modelling approach. By simulating a range of infiltration scenarios across varying soil hydraulic conductivities, we assessed the role of bank storage in flood dynamics.

Our results demonstrate that bank storage is a significant component of total floodwater storage, accounting for up to 26% in the Lower Danube and up to 37% in the Tisza, particularly assuming a highly conductive aquifer. While the Danube River exhibited higher mean infiltration flow rates, driven by a steep hydraulic gradient and rapid overbank rise, the Tisza River showed greater bank storage and stronger attenuation of the river flood wave. This is attributed primarily to its longer flood durations, which allow for more extensive and sustained infiltration.

These findings underscore the benefits of accounting for bank storage in flood modelling and flood risk assessment. Incorporating infiltration dynamics improves predictions of flood peak magnitudes and durations. From a management perspective, recognizing the contribution of subsurface storage can support nature-based flood mitigation strategies, such as floodplain reconnection, or dike relocation with better (increased) estimates of storage capacity.

ACKNOWLEDGEMENTS

This research was funded by the Ministry of Culture and Innovation and the National Research, Development and Innovation Office under Grant Nr. TKP2021-NVA-02. Furthermore, this work was carried out as part of the first author’s studies supported by the Stipendium Hungaricum Scholarship through the Hungarian Government’s initiative, administered via the Tempus Public Foundation; the author thanks the programme for the opportunity.

REFERENCES

Bernard-Jannin, L., Brito, D., Sun, X., Jauch, E., Neves, R., Sauvage, S., Sánchez-Pérez, J. M. (2016). Spatially distributed modelling of surface water-groundwater exchanges during overbank flood events-a case study at the Garonne River. Advances in Water Resources, 94, pp. 146-159. https://doi.org/10.1016/j.advwatres.2016.05.008

Brunner, P., Cook, P.G, Simmons, C.T. (2009). Hydrogeologic controls on disconnection between surface water and groundwater, Water Resour. Res., 45, W01422. https://doi.org/10.1029/2008WR006953

Derx, J., Blaschke, A.P., Blöschl, G. (2010). Three-dimensional flow patterns at the river-aquifer interface: A case study at the Danube. Advances in Water Resources, 33(11), pp. 1375-1387. https://doi.org/10.1016/j.advwatres.2010.04.013

Doble, R.C., Crosbie, R.S., Smerdon, B.D., Peeters, L., Cook, F.J. (2012). Groundwater recharge from overbank floods. Water Resources Research, 48(9), W09522. https://doi.org/10.1029/2011WR011441.

Harbaugh, A.W. (2005). MODFLOW-2005, the US Geological Survey modular ground-water model: the ground-water flow process (Vol. 6). Reston, VA, USA: US Department of the Interior, US Geological Survey. https://doi.org/10.3133/tm6A16

Helton, A.M., Poole, G.C., Payn, R.A., Izurieta, C., Stanford, J.A. (2014). Relative influences of the river channel, floodplain surface, and alluvial aquifer on simulated hydrologic residence time in a montane river floodplain. Geomorphology, 205, pp. 17-26. https://doi.org/10.1016/j.geomorph.2012.01.004

Hong, M., Mohanty, B.P., Sheng, Z. (2020). An explicit scheme to represent the bidirectional hydrologic exchanges between the vadose zone, phreatic aquifer, and river. Water Resources Research, 56(9), e2020WR027571. https://doi.org/10.1029/2020WR027571.

Hou, J., Zhang, Z., Zhang, D., Shi, B., Chen, G., Zhang, H. (2021). Study on the influence of infiltration on flood propagation with different peak shape coefficients and duration. Water Policy, 23(4), pp. 1059-1074. https://doi.org/10.2166/wp.2021.193

Kolencsik-Tóth, A., Kovács, B. (2015). Calibration process for groundwater flow model of a river influenced shallow aquifer. Central European Geology, 58(1-2), pp. 186-198. https://doi.org/10.1556/24.58.2015.1-2.12

Krause, S., Bronstert, A., Zehe, E. (2007). Groundwater-surface water interactions in a North German lowland floodplain: Implications for the river discharge dynamics and riparian water balance. Journal of Hydrology, 347(3-4), pp. 404-417. https://doi.org/10.1016/j.jhydrol.2007.09.028

Li, Y., Yao, J., Zhao, G., Zhang, Q. (2017). Evidences of hydraulic relationships between groundwater and lake water across the large floodplain wetland of Poyang Lake, China. Water Science and Technology: Water Supply, 18(2), pp. 698-712. https://doi.org/10.2166/ws.2017.150

Liang, X., Zhan, H., Schilling, K. (2018). Spatiotemporal responses of groundwater flow and aquifer-river exchanges to flood events. Water Resources Research, 54(3), pp. 1513-1532. https://doi.org/10.1002/2017WR022046.

Lóczy, D. (2010). Flood hazard in Hungary: A re-assessment. Central European Journal of Geosciences, 2, pp. 537-547.https://doi.org/10.2478/v10085-010-0029-0.

Murányi, G., Koncsos, L. (2022). Analysis of nature-based flood management in the Tisza River Valley, Hungary. Pollack Periodica.
https://doi.org/10.1556/606.2022.00456

Murinkó, G., Bene, K. (2017). Hydrologic modelling of the loess bluff in Dunaujvaros, Hungary. Pollack Periodica, 12(1), pp. 3-15.
https://doi.org/10.1556/606.2017.12.1.1

Nguyen, W.D., Datta, S., Knappett, P.S., Cardenas, M.B. (2025). The Effects of Tidal and Seasonal Scale Flooding and Soil Texture on Surface Water-Groundwater Interactions Along a Fluvio-Deltaic Floodplain: The Meghna River, Bangladesh. Water Resources Research, 61(10), e2025WR039919.
https://doi.org/10.1029/2025WR039919.

Pinder, G.F., Sauer, S. P. (1971). Numerical simulation of flood wave modification due to bank storage effects. Water Resources Research, 7(1), pp. 1-25. https://doi.org/10.1029/WR007i001p00063

Saksena, S., Merwade, V., Singhofen, P.J. (2019). Flood inundation modelling and mapping by integrating surface and subsurface hydrology with river hydrodynamics. Journal of Hydrology, 575, pp. 1155-1177. https://doi.org/10.1016/j.jhydrol.2019.06.024

Schweitzer, F. (2015). Strategy or disaster: New-style river regulation as an issue of national security. Hungarian Geographical Bulletin, 64(4), pp. 307-315. https://doi.org/10.15201/hungeobull.64.4.5

Shuai, P., Knappett, P.S., Hossain, S., Hosain, A., Rhodes, K., Ahmed, K.M., Cardenas, M.B. (2017). The impact of the degree of aquifer confinement and anisotropy on tidal pulse propagation. Groundwater, 55(4), pp. 519-531. https://doi.org/10.1111/gwat.12509

Sophocleous, M. (2002). Interactions between groundwater and surface water: the state of the science. Hydrogeology Journal, 10, pp. 52-67.
https://doi.org/10.1007/s10040-001-0170-8

Szilagyi, J. (2004). Accounting for stream-aquifer interactions in the state-space discretization of the Kalinin-Milyukov-Nash cascade for streamflow forecasting. Journal of Hydrologic Engineering, 9(2), pp. 135-143. https://doi.org/10.1061/(ASCE)1084-0699(2004)9:2(135)

Trásy, B., Magyar, N., Havril, T., Kovács, J., Garamhegyi, T. (2020). The Role of Environmental Background Processes in Determining Groundwater Level Variability-An Investigation of a Record Flood Event Using Dynamic Factor Analysis. Water, 12(9), 2336.
https://doi.org/10.3390/w12092336

Ubell, K. (1963). Surface-and groundwater relationships along the Hungarian reach of the Danube River. In Symposium surface waters held at the occasion of general assembly of Berkeley of IUGG, Vol. 19, No. 31.8.

Ubell K. (1964). A folyó és talajvíz összefüggése a Duna mentén [The relationship between the river and groundwater along the Danube]. Hidrológiai Közlöny, 44(5), pp. 193–200.

Ungvári, G., Kis, A. (2022). Reducing flood risk by effective use of flood-peak polders: A case study of the Tisza River. Journal of Flood Risk Management, 15(3), e12823. https://doi.org/10.1111/jfr3.12823

Vivoni, E.R., Bowman, R.S., Wyckoff, R.L., Jakubowski, R.T., Richards, K.E. (2006). Analysis of a monsoon flood event in an ephemeral tributary and its downstream hydrologic effects. Water Resources Research, 42(3). https://doi.org/10.1029/2005WR004036

Wagner F., Csoma R. (2022). A felszín alatti áramlás és árhullámok kapcsolatának vizsgálata változó folyami vízszintek esetében. Hidrológiai Közlöny, 102(3), pp. 50-60.

Weng, P., Sánchez-Pérez, J.M., Sauvage, S., Vervier, P., Giraud, F. (2003). Assessment of the quantitative and qualitative buffer function of an alluvial wetland: Hydrological modelling of a large floodplain (Garonne River, France). Hydrological Processes, 17(12), pp. 2375-2392. https://doi.org/10.1002/hyp.1248

Zitta, V.L., Wiggert, J.M. (1971). Flood routing in channels with bank seepage. Water Resources Research, 7(5), pp. 1341-1345.
https://doi.org/10.1029/WR007i005p01341.

AUTHORS

GADADHARA FERRAZ is a hydraulic engineer. She obtained her master's degree in Environmental technology and Water resources at the Federal University of Pernambuco, Brazil, in 2019. She is currently a Ph.D. candidate in Hydraulics and Water Resources at the Budapest University of Technology and Economics, Hungary. Her research focuses on river–aquifer interactions, and their role in flood dynamics.

TAMÁS KRÁMER obtained his Ph.D. in civil engineering in 2007, and is currently an associate professor at Budapest University of Technology and Economics (BME). His research is focused on the hydrodynamics of surface waters, with an emphasis on rivers, lakes and floodplains. He introduced methodological innovations and contributed to flood protection and flood forecasting, and his research results support major projects on the country's largest lakes. He has been a member of the Hungarian Hydrological Society since 2000.

Extreme precipitation amounts and dry periods in the Hungarian Great Plain (1980–2020): four urban stations

Dorottya SZÁM[1,2,5], Kíra Erika KÁVÁSSY[3], Ádám BERGER[3], Zsolt HETESI[3,4]

[1] Institute of Biology, Faculty of Sciences, University of Pécs,7624 Pécs, Hungary
[2] Department of Regional Water Management, Faculty of Water Sciences, Ludovika University of Public Service, 6500 Baja, Hungary
[3] Department of Water and Environmental Security, Faculty of Water Sciences, Ludovika University of Public Service, 6500 Baja, Hungary
[4] Institute of Mathematics and Informatics, Faculty of Natural Sciences,, University of Pécs, 7624, Pécs, Hungary
[5] Corresponding author: szam.dorottya.reka@gmail.com

DOI: 10.59258/hk.24056

Abstract
This study explores changes in the frequency and spatiotemporal distribution of precipitation-free periods in the Hungarian Great Plain (1980–2020), with a focus on agricultural challenges under climate change. During the study, we analysed the occurrence of dry periods lasting up to 16 days, their seasonal frequency, and their differences in four cities (Szolnok, Hódmezővásárhely, Nyíregyháza, Kalocsa). Based on the data, the frequency of dry periods increased slightly in certain locations; however, the statistical significance of the trend was inconclusive; F-tests mainly indicated increased variance. The two-sample Kolmogorov–Smirnov test revealed that the differences in distribution between cities were not significant, indicating that the hypothesis of regional divergence was not confirmed. The research also emphasizes the need for increased soil moisture retention capacity, especially in sandy and saline soils, which lose moisture more quickly due to a lack of precipitation, negatively affecting their agricultural productivity.

Keywords
Hungarian Great Plain, precipitation analysis, extreme weather events, climate change, water shortage.

Csapadékszélsőségek vizsgálata 1980–2019. között négy alföldi városban Magyarországon

Kivonat
A tanulmány célja, hogy feltárja a csapadékmentes periódusok gyakoriságának, időbeli és térbeli eloszlásának változásait a magyarországi Alföld térségében 1980–2020 között, különös tekintettel a klímaváltozás mezőgazdasági kihívásaira. A vizsgálat során elemeztük a 16 napot elérő száraz időszakok előfordulását, évszakos gyakoriságát, azok különbségeit négy alföldi város (Szolnok, Hódmezővásárhely, Nyíregyháza, Kalocsa) esetében. Az adatok alapján a száraz periódusok gyakorisága bizonyos helyeken enyhén növekedett, bár a tendencia statisztikai szignifikanciája nem volt egyértelmű, az F-próbák elsősorban szórásnövekedést jeleztek. A kétmintás Kolmogorov–Smirnov-próba azt mutatta, hogy a városok közötti eloszlásbeli eltérések nem szignifikánsak, így a térségi divergencia hipotézise nem igazolódott. A kutatás továbbá hangsúlyozza a megnövelt talajnedvesség-megtartó képesség szükségességét, különösen homokos és szikes talajok esetén, amelyek a csapadékhiány hatására gyorsabban veszítenek nedvességet, ami negatívan befolyásolja a mezőgazdasági termelékenységüket.

Kulcsszavak
Alföld, csapadékelemzés, extrém időjárási események, klímaváltozás, vízhiány.

INTRODUCTION

The Great Plain is one of the most important agricultural regions of Hungary, where the success of production directly depends on the physical properties of the soil, especially its water retention capacity. Its natural features – loose sedimentary rocks, horizontal or gently sloping surface, and the complexity of the surfaces and underground water network – dynamically interact to create a complex environment in which the interdependent processes of soil formation, water management, and land use take place (*Keveiné Bárány 1998, Pálmai 2005*). The climate of the Great Plain is temperate continental, shaped by the low altitude, the closed nature of the Carpathian Basin, and the dominance of continental influences. The average annual temperature in the region is typically 10-11 °C, and the number of hours of sunshine exceeds 2 000 per year, while the amount of precipitation is low in national terms: less than 550 mm (*HungaroMet 2022*).

According to the consensus of several studies (*Bartholy and Pongrácz 2007, Barcza et al. 2013, Mezősi et al. 2017, Fehér and Rakonczai 2019, Lakatos 2021*), the Great Plain is particularly exposed to the harmful effects of climate change: temperature increases, precipitation variability, and droughts (*Kis et al. 2025*). More recent regional analyses further confirm that the Great Plain belongs to the most climate-vulnerable areas of Hungary, especially with respect to drought frequency and water balance changes (*Kis et al. 2025*). Measurements in Hungary between 1901 and 2009 show that the annual and all-season mean temperatures have an increasing trend. The national annual mean temperature increased by 0.99 °C from the beginning of the last century to 2009 (*Barcza et al. 2013*). The change (+1.17 °C) is particularly noticeable in the summer (*Barcza et al. 2013*). The study by *Barcza et al.* (*2013*) examined the change in the seasonal mean temperature of five major Hungarian cities (Budapest, Debrecen, Szeged, Szombathely, Pécs) between 1980 and 2009. It was found that the two Great Plain cities (Debrecen: +2.08 °C, Szeged: +2.14 °C) had the highest average summer temperature increase. These tendencies are also reflected in more recent observational datasets and model-based assessments, indicating that warming during the summer half-year has continued in the Great Plain after 2009 (*Lakatos 2021*). Recent work by *Bihari and Szentes (2024),* based on 30-year climate normals and a forthcoming high-resolution climate atlas, confirms the continuation of these climate change trends, providing a detailed regional perspective for Hungary. Moreover, the HISTALP precipitation dataset for the Central European region, including Hungary, provides a homogenized, long-term record that allows for more accurate detection of regional precipitation trends, supporting observations of decreasing rainfall and increasing dry spells in the Great Plain (*Chimani et al. 2023*). Detailed analyses of recent drought events also provide important context for these trends, highlighting the increasing frequency and intensity of dry periods in Hungary (*Szentes 2023*). In addition, modern climate monitoring indices and real-time datasets provided by HungaroMet further support the assessment of regional temperature, precipitation, and drought trends (*Lakatos et al. 2024*).

The average annual precipitation in Hungary shows a decreasing trend. Wet years occurred more frequently in the first half of the last century; the decrease was 7% between 1901-2009 (*Barcza et al. 2013*). According to the unanimous conclusion of several studies, periods of low precipitation have become increasingly frequent, which in many cases also represents a significant change (*Bartholy et al. 2008*). This is especially true for spring. The largest decrease among the seasons between 1901-2009 occurred in spring, at almost 20% (*Barcza et al. 2013*). Recent analyses based on homogenized station data and grid-point datasets indicate that this long-term decrease is increasingly accompanied by pronounced interannual variability and longer dry spells, particularly in the central and eastern parts of the Great Plain (*Kis et al. 2025*).

More frequent low-rainfall periods adversely affect not only the overall water balance but also soil structure, porosity, and fertility. Evaporation increases, which further reduces soil moisture. The strengthening of evapotranspiration and the decrease in groundwater levels can already be observed, especially in the Danube–Tisza basin and in some parts of the Nyírség (*Keveiné Bárány 1998, Mezősi et al. 2020*). *Fehér and Rakonczai (2019)* also highlight that climate-induced groundwater decline has become a key driver of landscape sensitivity in several regions of the Great Plain, directly linking meteorological trends with soil degradation processes. The change in the water balance of the Great Plain affects not only the surface water system, but also directly affects the groundwater level. The decrease in water levels in the Danube–Tisza basin in recent decades has had serious consequences for both soil moisture and the state of vegetation. According to research by *Ladányi (2009),* in the Homokhátság, the groundwater has sunk by more than 5 meters in some places compared to the 1980s, which has already caused a significant transformation in the composition of the natural vegetation. Similar tendencies have been confirmed by recent drought-monitoring and impact assessment studies, which emphasize that groundwater-dependent ecosystems are among the most sensitive to ongoing climatic changes in the Great Plain (*Fiala et al. 2018*). The previously water-saturated saline and marsh habitats have dried up, and in their place have appeared steppe-like plant communities with lower water requirements. The physical and chemical characteristics of the soil have also changed: the salt and sodium content of the upper layer has decreased, while the humus concentration has increased, which indicates an improvement in the soil structure and a retreat of salinization. The deepening groundwater table has serious ecological and economic consequences: maintaining cultivation requires ever more irrigation water, withdrawn from the same dwindling supply. This self-perpetuating process is unsustainable in the long run (*Ladányi 2009*).

A problem is that precipitation often does not fall at an optimal time for plants. This highlights the great difficulty of the agricultural areas of the Great Plain that rely on natural precipitation (*Mezősi 2020*). A study examining the Danube–Tisza basin found that a decrease in the amount of precipitation resulted in a significant decrease in groundwater. On one hand, this causes significant damage to farming, and on the other hand, it causes the transformation of natural vegetation (*Makra et al. 1986, Nováky 1993, Ladányi 2009*). More recent regional climate impact studies confirm that this temporal mismatch between precipitation occurrence and crop water demand has intensified during the last decades, increasing production risks under rain-fed conditions (*Kis et al. 2025*).

It is worth noting, however, that the seemingly clear trends in national average precipitation amounts mask the actual regional variability. These are primarily influenced by distance from the sea, topography, land cover, land use, and micrometeorological conditions (*Makra et al. 1985, Konkolyné et al. 2008*). Regions closer to the Tisza, such as Szolnok, receive more precipitation on average than regions in the southern Great Plain, such as Hódmezővásárhely or Kalocsa. The difference can be as much as 50-100 mm per year (*Demeter 2016*). Behind the simplicity of the Great Plain's topography lie subtle structural and climatic differences, which directly influence the condition of the soils and their usability through different water management characteristics. Clayey, more cohesive sediments let water through more slowly, thus being able to store moisture for a longer period of time, while soils formed from loose sandy or loess bedrock dry out more quickly. This geological background partly explains why significant differences can occur in the effects of a lack of precipitation, even under identical meteorological conditions. Geological conditions are, therefore, not just passive background factors, but actively influence water management processes, thus indirectly, affecting the frequency, intensity and consequences of dry periods (*Molnár and Várallyai 1993*).

Despite regional variability, several regional studies in Hungary have shown a decreasing trend in precipitation. One study (*Marton and Szanyi 1997a, 1997b*) found that the increasing precipitation deficit makes Nyírség one of the most vulnerable regions of the Great Plain, which is not fed by surrounding precipitation flows. More recent investigations based on multimodel simulations suggest that these vulnerabilities are likely to persist or even intensify during the 21st century, particularly with respect to summer low-flow conditions and prolonged dry periods (*Kis et al. 2023*). Water shortages have been affecting the Debrecen region, as well as the stratigraphic and near-surface water bodies of the Hajdúság and Hortobágy regions, since the 1990s. A study examining the Upper Tisza region, based on multimodel simulations (*Kis et al. 2023*), projects that during the 21st century, the average daily water discharges are expected to decrease in the Tiszabecs section of the Upper Tisza compared to the annual averages. Furthermore, a significant decrease in the flow of the summer months is likely (especially in July and August), while a smaller increase can be expected for January and February. The number of cases exceeding the third flood protection readiness level is expected to be significantly lower by the middle and end of the 21st century, but these may occasionally be more severe in terms of flood volume than is currently usual. According to the study by *Kiss et al. (2019),* analysing more than 140 years of data, the average temperature in Mosonmagyaróvár (located in the Little Hungarian Plain, a region with slightly cooler and wetter conditions than the Great Plain) has increased significantly, and the precipitation distribution has become more extreme. While the trends observed in Mosonmagyaróvár illustrate long-term regional climate change, care should be taken when comparing them directly to the Great Plain, whose climate is generally warmer and drier, particularly in the central and southern areas. According to the study, precipitation does not show a significant decrease in the long term, but based on the results of GARCH modelling, the temporal distribution of precipitation is becoming increasingly unpredictable and the frequency of extreme precipitation events is increasing. A study conducted in the settlement of Nagybajom (*Szám et al. 2025a*) found that the frequency of periods without precipitation lasting at least 25 days increased significantly in the second half of the period studied (1965-2022). Another study conducted in the Szentes region (*Szám et al. 2025b*) examined the period between 1981 and 2020. It was found that the number of days with high rainfall increased by 19.3%, and the 201 number of days with extreme rainfall increased by 40.9%. Even larger increases were observed for the highest five-day rainfall totals (62.1%).

The decrease in average precipitation is in most cases accompanied by an increase in the frequency of extreme precipitation situations (*Bartholy and Pongrácz 2007*). A study analysing data series from 1901 to 2009 for the entire Great Plain (*Berényi et al. 2021*) draws attention to the increase in the daily precipitation intensity (SDII) index used to detect precipitation extremes. Recent local-scale studies further support this tendency, showing a simultaneous increase in both dry spell duration and short-term high-intensity precipitation events in several Great Plain settlements (*Szám et al. 2025a, Szám et al. 2025b*). The changes in the values of other indicators also indicate an increase in the frequency of precipitation extremes. An increase in the frequency of days with high precipitation (RR10) and extreme precipitation (RR20) can also be observed in several regions of the Great Plain. This poses a serious challenge for agriculture and environmental engineering interventions.

The results of the isotopic studies (conducted by *György Czuppon et al.* in collaboration with HungaroMet and CSFK) provide important new information on the origin of precipitation in Hungary (*Czuppon et al. 2021*). These findings add a new dimension to climate change assessments in the Great Plain, as changes in moisture source regions are expected to further enhance the variability and extremity of precipitation patterns in the future. Based on the analysis of the hydrogen and oxygen isotope composition (δD and $\delta^{18}O$) of the precipitation samples, it was determined that the majority of the precipitation falling on Hungary originates from the Mediterranean region. This source region has become dominant in recent years, overtaking the Atlantic, the North Sea region, and the local recycled moisture sources of the Carpathian Basin. This determination of the origin of precipitation was made using so-called backward atmospheric trajectories and isotopic signals (e.g., deuterium excess, d-excess). Based on the principal component analysis, it can be clearly shown that the warming of the Mediterranean Sea and the moisture from the Adriatic and Ionian regions play an increasingly decisive role in the formation of precipitation in Hungary. This trend is related to the warming of the Mediterranean region and the increased evaporation potential, which increases the moisture content of the airflows coming from there.

This change is significant from a meteorological and climatic perspective: on the one hand, it increases the probability of precipitation events of a shower and thunderstorm nature, and on the other hand, the unpredictability of the temporal and spatial distribution of precipitation. Based on the isotopic composition, therefore, not only the amount of precipitation but also its meteorological origin has changed, which contributes to the increase in the climate asymmetries of the region.

MATERIAL AND METHOD

The aim of our study was to determine the precipitation conditions for the period 1980-2020, for which we used the historical data series of the Hungarian National Meteorological Service (HungaroMet). Following the introduction of HungaroMet's open data policy in 2021, meteorological observation data became freely and openly accessible via the odp.met.hu server. In this study, synoptic precipitation data series originating from HungaroMet measuring stations were used. These data series come from an automatic measuring station network. The network is regularly maintained, and the instruments are calibrated. HungaroMet took care of the quality assurance (validation, data supplementation) of the data series we analyzed.

We have daily precipitation data from four Great Plain meteorological stations (Szolnok, Hódmezővásárhely, Nyíregyháza, Kalocsa) between 1980 and 2020. In our first study, we were interested in the cross-correlations of our precipitation data for the four settlements. We determined the Pearson correlation coefficients (R values) of the six pairs of settlements. The methodology of this practically differs from a conventional correlation study in that here we do not compare the measured data to an independent variable (e.g., location or time), but we compare the precipitation data of two cities with each other and look for a correlation between the two measured values.

In our second study, we examined the frequency changes of longer dry periods. We considered dry periods to be consecutive days when the daily precipitation did not exceed 1 mm. We included periods of at least 16 days but no more than 40 days in the evaluation. The only exceptionally long period, 44 days, was registered in Hódmezővásárhely in the autumn of 1983, but this falls outside the compared range. We used statistical tests to compare the daily precipitation amounts of the first and second halves of the period (1980-1999, 2000-2019). We used the F-test to examine the variation in the standard deviation of long dry periods. In order to compare the distribution of dry periods lasting at least 16 days, we used the two-sample Kolmogorov–Smirnov test. This nonparametric test is sensitive to changes in the distribution shape, such as shifts in the incidence rate of extremely long or short periods, and is therefore well suited to examining skewed distributions in natural systems (*Figure 1*). The two-sample Kolmogorov test works even if the theoretical distribution of the samples to be compared is unknown (*Gibbons and Chakraborti 2003*).

Our third study focused on the seasonal distribution of dry periods. The data source was the previously used daily precipitation dataset between 1980 and 2020. We considered a dry day to be any day on which the daily precipitation total did not reach 1 mm. The seasonal comparison of dry periods was performed by first calculating the mean and standard deviation of the length of dry periods for each city separately for each season (spring, summer, autumn, winter). Subsequently, we compared the seasonal means and standard deviations of the cities in pairs in order to explore whether there were systematic differences in the length of dry periods between settlements. This "pair-by-pair" approach allowed us to see not only the difference in absolute values but also the relative differences between cities. In this way, we could identify those locations where dry periods are consistently longer or shorter at a given time of year.

The aim of our fourth study was to detect significant differences in the distribution of the length of dry periods (≥16 days) between the four studied stations. To do this, we compared each pair of cities based on the period 2000-2019. We used a two-sample Kolmogorov–Smirnov test to determine whether the two samples (here: city pairs) come from the same distribution. Based on the p-value, we determined whether the difference was statistically significant ($p < 0.05$).

The aim of the fifth study was to analyse and evaluate soil moisture data. The data come from the monitoring network of the General Directorate of Water Management (OVF - Országos Vízügyi Főigazgatóság), which provides data measured at a depth of 10 cm in the studied regions. For spatial interpolation and temporal filling, we used the ERA5 (*Hersbach et al. 2023*) database from the global reanalysis data (ERA5 - ECMWF Reanalysis 5th Generation), which is developed by the European Centre for Medium-Range Weather Forecasts (ECMWF) within the framework of the European Union's Copernicus Climate Change Service (C3S). ERA5 provides meteorological and soil moisture variables on a regular latitude–longitude grid with a horizontal spatial resolution of 0.25° × 0.25° (approximately 31 km), which is suitable for regional-scale climatic and hydrological analyses. ERA5 is particularly valuable for research, as it integrates measurements from Hungarian meteorological stations (including those collected by HungaroMet) in addition to global model-based estimates, thus providing a reliable basis for drawing regional conclusions. In this study, ERA5 grid-point data corresponding to the vicinity of the monitoring stations were used primarily to support spatial consistency and temporal completeness of the in situ soil moisture records. While the applied spatial resolution may smooth small-scale variability associated with localized convective precipitation events, it provides a robust representation of large-scale and regional soil moisture dynamics relevant to multi-decadal analyses. As a complementary source, we also used remote sensing data from the European Union Copernicus satellites Sentinel-1 and Sentinel-2, which supported the spatial assessment of soil moisture, land cover, and vegetation status through their radar and optical channels. The Sentinel-1 mission is the first satellite mission of the European Union Copernicus programme, implemented jointly by the European Space Agency (ESA) and the European Commission. Sentinel-1 is a radar-based Earth observation system consisting of two sun-synchronous polar-orbiting satellites (Sentinel-1A and Sentinel-1B) with a 180° phase shift. This configuration allows for regular and rapid coverage of the Earth's surface, regardless of weather conditions or time of day. The system is based on the Sentinel family of satellites, equipped with different types of sensors, making them suitable for various purposes in the field of land, sea, and atmosphere observations. Their application areas include monitoring land surface deformations, flood observations, detection of sea ice and oil spills, and support for disaster response (*EU Copernicus Programme 2025*). The integration of datasets from multiple sources enables the comparison of short- and long-term variables and the identification of regional characteristics. The data analysis toolbox includes spatial interpolation and time series decomposition, which support the detailed interpretation of climatic and soil moisture patterns. The calculations were performed in a programming and GIS environment, which ensures the structured processing and visualization of large amounts of data.

RESULTS

The strongest correlation was found between the precipitation data of Szolnok and Hódmezővásárhely (R=0.90), followed by Kalocsa and Hódmezővásárhely (R=0.86), indicating that these stations are frequently affected by similar large-scale atmospheric situations. In contrast, Nyíregyháza shows considerably weaker correlations with the other Great Plain cities, especially with Kalocsa (R=0.55) and Hódmezővásárhely (R=0.61) (*Table 1*). This suggests that the northeastern part of the Great Plain is more often influenced by precipitation-generating mechanisms that differ from those dominating the central and southern regions.

Previous studies have shown that summer precipitation over the Great Plain is increasingly dominated by convective processes, which are highly localized and sensitive to mesoscale conditions such as surface heating, soil moisture feedbacks, and atmospheric instability (*Bartholy and Pongrácz 2007, Lakatos et al. 2021*). The lower inter-station correlation involving Nyíregyháza is therefore consistent with findings that the eastern and northeastern Great Plain are more frequently affected by isolated convective events, while the Danube–Tisza Interfluve and southern regions are more often influenced by spatially coherent precipitation associated with Mediterranean cyclones or frontal systems (*Mezősi et al. 2017*). Consequently, the observed correlation differences likely reflect regional contrasts in dominant precipitation regimes, particularly during the summer half-year.

Table 1. Pairwise comparison of precipitation patterns of the four examined Great Plain cities
1. táblázat. A négy vizsgált alföldi város csapadékmintázatainak páros összehasonlítása

Municipality 1	Municipality 2	Correlation coefficient (R)
Szolnok	Hódmezővásárhely	0.90
Szolnok	Nyíregyháza	0.66
Szolnok	Kalocsa	0.82
Hódmezővásárhely	Nyíregyháza	0.61
Hódmezővásárhely	Kalocsa	0.86
Nyíregyháza	Kalocsa	0.55

In the case of Szolnok, Hódmezővásárhely, and Nyíregyháza, the frequency of dry periods lasting 16-20, and 21-25 days increased significantly between 1980 and 2020. A decrease occurred only in the case of Kalocsa. The frequency of dry periods lasting 26 days or longer has developed differently in the four settlements (*Figure 1*).

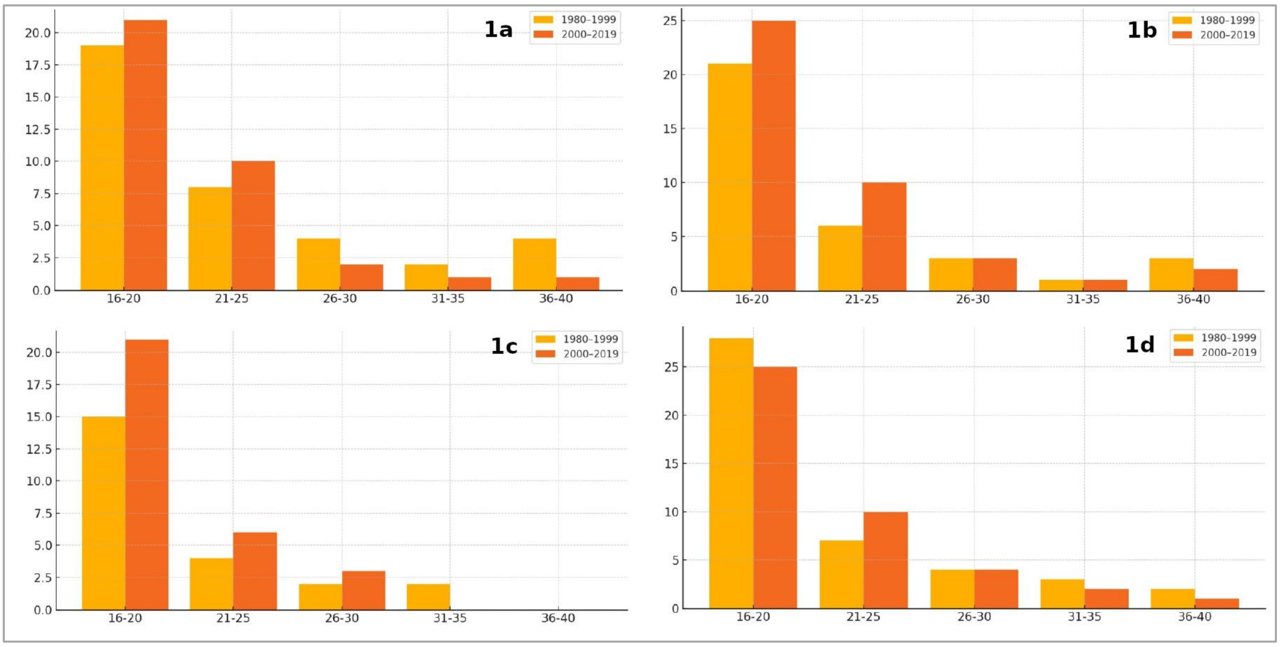

Figure 1. Distribution of the frequency of dry periods at the measuring stations of Szolnok (1a), Hódmezővásárhely (1b), Nyíregyháza (1c), Kalocsa (1d) in the periods 1980-1999 and 2000-2019 (Data source: HungaroMet)
1. ábra. A száraz időszakok gyakoriságának eloszlása a szolnoki (1a), hódmezővásárhelyi (1b), nyíregyházi (1c), kalocsai (1d) mérőállomásokon 1980–1999 és 2000–2019 időszakban. (Adatforrás: HungaroMet)

Based on the results, most long dry periods started in summer, but in Kalocsa and Nyíregyháza a significant number of events also occurred in autumn. The seasonal statistics of ≥16-day dry spells (*Table 2*) show that summer remains the dominant season for the onset of long dry periods in all four cities. A secondary maximum appears in autumn, especially in Kalocsa and Szolnok. Spring dry spells became more frequent in Hódmezővásárhely and Nyíregyháza after 2000, in line with the seasonal shift already noted in the main text. Winter dry periods are also common, but their mean length is similar to that of autumn, indicating year-round drought sensitivity in the Great Plain.

Comparing (*Table 3*) the two periods (1980-1999, 2000-2019), there is no clear shift at all stations, but in the case of Hódmezővásárhely and Nyíregyháza the frequency of spring dry periods increased after 2000.

Based on the results of the two-sample Kolmogorov-Smirnov test, the differences between cities between 2000 and 2019 were not statistically significant; i.e., the distribution of long dry periods did not differ significantly from one station to another (*Table 4*). This supports the observation that these regions of the Great Plain show a similar climatic pattern in terms of drought susceptibility.

Table 2. Seasonal mean length and standard deviation of ≥16-day dry periods in the four examined Great Plain cities (1980–2020) (The column "n" indicates the number of dry spells detected in the given season)
2. táblázat. A ≥16 napos száraz időszakok szezonális átlagos hossza és szórása a négy vizsgált alföldi városban (1980–2020) (Az „n" oszlop az adott évszakban észlelt száraz időszakok számát jelzi)

Location	Spring (mean / std / n)	Summer (mean / std / n)	Autumn (mean / std / n)	Winter (Mean / std / n)
Szolnok	20.36 / 3.72 / 11	19.67 / 2.65 / 9	22.44 / 6.78 / 32	22.76 / 7.46 / 25
Hódmezővásárhely	19.42 / 3.99 / 12	21.55 / 4.46 / 11	22.12 / 6.85 / 33	20.83 / 6.32 / 24
Nyíregyháza	19.36 / 3.41 / 11	19.00 / 4.24 / 4	20.04 / 4.48 / 23	20.00 / 5.05 / 17
Kalocsa	18.23 / 2.49 / 13	20.44 / 3.16 / 16	22.20 / 6.14 / 35	22.21 / 6.04 / 28

Table 3. F-test of the dry periods of the four examined Great Plain cities for the time intervals between 1980-1999 and 2000-2019
3. táblázat. A vizsgált négy alföldi város száraz időszakainak F-próbája az 1980-1999 és a 2000-2019 közötti időintervallumokban

Municipality/ Station	16-40 days periods (1980-1999)	16-40 days periods (2000-2019)	F-test value	F-test assessment	Longer than 35-days periods	Significant difference (F probe)
Szolnok	37	35	0.0713	Borderline case	5	Not significant
Hódmezővásárhely	34	41	0.4215	Not significant	6	Not significant
Nyíregyháza	23	30	0.0598	Borderline case	0	Not significant
Kalocsa	44	42	0.2345	Not significant	3	Not significant

Table 4. Results of the two-sample Kolmogorov-Smirnov test based on the number of dry periods for pairs of cities
4. táblázat. A kétmintás Kolmogorov-Szmirnov teszt eredményei a várospárok száraz időszakainak száma alapján

Municipalities	K-S stat	p value	Significance (p<0.05)
Szolnok - Hódmezővásárhely	0.0832	0.9284	Not
Szolnok - Nyíregyháza	0.1820	0.2225	Not
Szolnok - Kalocsa	0.1087	0.6777	Not
Hódmezővásárhely - Nyíregyháza	0.1103	0.7864	Not
Hódmezővásárhely - Kalocsa	0.0734	0.9632	Not
Nyíregyháza - Kalocsa	0.1837	0.1852	Not

We considered using a GARCH (Generalized Autoregressive Conditional Heteroskedasticity) model, which is suitable for time series with time-varying variance (*Korponai 2019*). However, the residuals of soil moisture data showed no such heteroskedastic behaviour, so a GARCH specification was not justified. Instead, a simple AR(1) model (first-order autoregressive) adequately described the temporal dynamics of soil moisture, reflecting the strong dependence of each day's values on those of the previous day.

The link between soil moisture and precipitation proved weaker than expected. Daily precipitation showed virtually no correlation with soil moisture. Aggregating rainfall over 7 days slightly improved the correlation, and over 30 days it was only marginally stronger. These results suggest that soil moisture is controlled not only by rainfall but also by evaporation, soil type, and groundwater conditions, which dilute the direct effect of precipitation.

The main findings can be summarized as follows:

- There is practically no correlation between daily precipitation and soil moisture in any city ($\rho \approx 0.01–0.02$).
- The 7-day precipitation total increases the correlation, but it still remains weak (Szolnok: $\rho \approx 0.029$).
- The relationship with the 30-day precipitation total is slightly stronger (Szolnok: $\rho \approx 0.036$), but it remains weak.
- The standard deviation of the residuals of the soil moisture AR(1) model is relatively stable in a 30-day time window, there is no strong heteroscedasticity in any city.
- Consequently, the application of the GARCH model is not justified for these data.

Figure 2 presents the 30-day rolling standard deviation of the AR(1) residuals of soil moisture. The variability remains within a moderate and physically plausible range throughout the examined period, and no systematic increase in residual variance is detected.

Following the analysis presented in *Figure 2*, it is evident that daily precipitation alone does not explain the variability of soil moisture in the four studied cities. The main findings indicate practically no correlation between daily precipitation and soil moisture ($\rho \approx 0.01–0.02$). Aggregating rainfall over 7 days slightly increases the correlation (e.g., Szolnok: $\rho \approx 0.029$), and over 30 days it becomes only marginally stronger (Szolnok: $\rho \approx 0.036$), but the relationship remains weak overall. The standard deviation of the AR(1) residuals remains relatively stable in a 30-day rolling window, showing no strong heteroskedasticity, confirming that a GARCH model is not justified for these data.

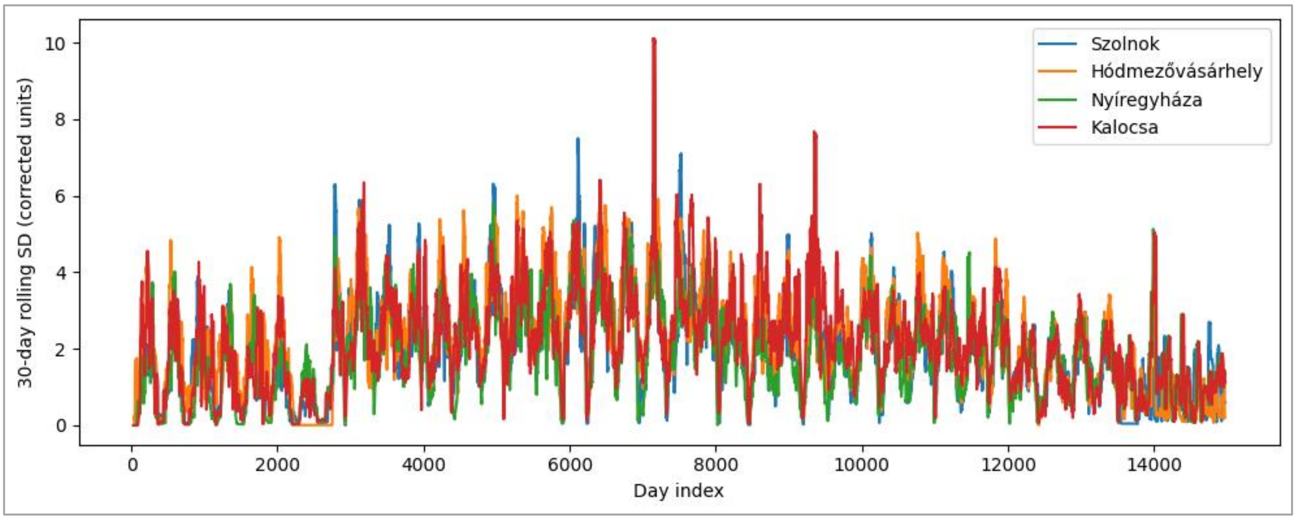

Figure 2. The 30-day rolling standard deviation of residuals of AR(1) models
2. ábra. Az AR(1) modellek reziduálisainak 30 napos gördülő szórása

These results suggest that other factors—including soil type, evapotranspiration, and groundwater conditions—strongly influence soil water content, which dilutes the direct effect of precipitation. The temporal persistence observed in the AR(1) models reflects the buffering capacity of different soils against short-term rainfall variability. Although the four cities show broadly similar drought susceptibility patterns, local differences in soil texture and hydrological properties likely lead to variations in moisture retention and drainage. Therefore, considering soil type-specific characteristics, infiltration, and evapotranspiration is essential for more precise predictions of soil water content, particularly for agricultural and hydrological applications.

Our findings are consistent with previous studies emphasizing the dominant role of soil properties and local hydrology in controlling soil moisture (*Fehér and Rakonczai 2019, Mezősi et al. 2020*). The observed weak correlations align with results from *Lakatos et al. (2021),* who also reported that soil moisture in the Great Plain is buffered against short-term precipitation variability. Furthermore, local variability in soil moisture response supports earlier findings by *Ladányi (2009)* and *Kis et al. (2025),* highlighting that groundwater-dependent ecosystems and soil water availability are sensitive to both climatic and pedological factors. Our results also reflect conclusions by *Szentes (2023)* and *Bihari and Szentes (2024)*, stressing that accurate assessment of soil moisture requires integration of precipitation, soil type, infiltration, and evapotranspiration rather than relying on rainfall alone.

Overall, these observations underscore that even within regions with broadly similar drought susceptibility patterns, soil and hydrological characteristics modulate soil water availability, emphasizing the importance of including these factors in regional climate and agricultural impact assessments.

CONCLUSIONS

Our results clearly show that the frequency, timing, and spatial distribution of prolonged precipitation-free periods in the Great Plain have changed substantially in recent decades. One of the most important consequences of climate change – in addition to the increase in average temperatures – is the increasing occurrence of these dry periods, which pose a challenge for agriculture, especially in the spring and summer periods.

The frequency of long dry periods exceeding 16 days varied between the periods examined. In the case of some cities – especially Hódmezővásárhely and Nyíregyháza – the number of dry periods increased slightly; however, the change was not statistically significant in all cases. Based on the F-tests, the results indicating an increase in the standard deviation can be interpreted as a trend rather than a generally valid change. During the examination of the seasonal distribution, it was observed that the beginning of the dry periods shifted towards the vegetation period in some locations – for example, in the Hódmezővásárhely area – especially in spring. At the same time, the summer periods remained dominant, so the seasonal shift was not clearly evident in all the study locations. Based on the analysis of the regional differences, it can be stated that there was no significant difference in the distribution of long dry periods between the four cities examined. The results of the Kolmogorov–Smirnov test showed that the differences between the pairs of cities cannot be considered statistically significant, so the hypothesis that regional differences increased was not supported. It should be noted here that in the case of longer time intervals (and the necessary longer time series), significant differences can be detected between earlier and later intervals in the same geographical location. *Szám et al. (2025*) showed that in the eastern part of the Great Plain, the number of dry periods increased significantly, approximately twice, compared to intervals of the same length, and periods of previously inexperienced length also appeared.

The results of the research highlight the need to increase the water retention capacity of the soil. The moisture content of the topsoil is particularly sensitive to longer periods without precipitation, especially in sandy and saline soils with weaker water retention capacities. In these soil types, a lack of precipitation reduces moisture content more quickly to below critical levels. Below critical levels, soil structure deteriorates, which negatively affects agricultural production efficiency.

Predicting and monitoring dry periods associated with climate change is key to developing future agricultural strategies. The Sentinel satellite program (especially the Sentinel-1 and Sentinel-2 systems) now provides high temporal and spatial resolution data for monitoring soil moisture, vegetation status, and land cover. Over the past decade, monitoring has also become available through the use of agricultural drones, which have enabled higher-resolution assessments. Further potential is offered by innovative solutions such as precision water distribution, the results of drought tolerance analyses of different plant varieties, and plant protection monitoring using soil and leaf moisture sensors. These can help us preserve the agricultural potential of the Great Plain sustainably in the future.

REFERENCES

Barcza Z., Bartholy J. (Ed.), Bihari Z., Lakatos M., Mészáros R., Pieczka I., Pongrácz R. (Ed.), Práger T., Radics K. (2013). Klímaváltozás. Eötvös Loránd Tudományegyetem, Természettudományi Kar. (In Hungarian)

Bartholy, J., Pongrácz, R. (2007). Regional analysis of extreme temperature and precipitation indices for the Carpathian Basin from 1946-2001. Global and Planetary Change, 57, pp. 83-95. https://doi.org/10.1016/j.gloplacha.2006.11.002

Bartholy, J., Pongrácz, R., Gelybó, Gy., Szabó, P. (2008). Analysis of expected climate change in the Carpathian basin using the PRUDENCE results. Időjárás, 112, pp. 249-264.

Berényi A., Pongrácz R., Bartholy J. (2021). Csapadékszélsőségek változása Európa déli alföldi régióiban az 1951-2019 időszakban. Modern Geográfia, 16(4), pp. 85-101. (In Hungarian)
https://www.doi.org/10.15170/MG.2021.16.04.05

Bihari Z., Szentes O. (2024). Megfigyelt éghajlatváltozás 30 éves klímanormálok és egy készülő éghajlati atlasz tükrében. Légkör, 69 K, pp. 12–17.
DOI:https//doi.org/10.56474/legkor.2024.K.2

Chimani, B., Bochníček, O., Brunetti, M., Ganekind, M., Holec, J., Izsák, B., Lakatos, M., Tadić, M.P., Manara, V., Maugeri, M., Šťastný, P., Szentes, O., Zardi, D. (2023). Revisiting HISTALP precipitation dataset. International Journal of Climatology, 43(15), pp. 7381–7411. https://www.doi.org/10.1002/joc.8270.

Czuppon, G., Bottyán, E., Kristóf, E. (2021). Stable isotope data of daily precipitation during the period of 2013-2017 from K-puszta (regional background monitoring station), Hungary. Data in Brief, 36(12), pp. 1-5. https://www.doi.org/10.1016/j.dib.2021.106962

Demeter Sz. (2016). Konvektív és rétegfelhőből hulló csapadék statisztikai vizsgálata állomási mérések alapján. Szakdolgozat, Eötvös Loránd Tudományegyetem, Budapest (Témavezetők: Dr. Pieczka Ildikó, Soósné Dr. Dezső Zsuzsanna), 49 p. (In Hungarian)

EU Copernicus Program (2025). SentiWiki. [Online] Available at: https://sentiwiki.copernicus.eu/web/s1-mission.

Fehér, Zs., Rakonczai, J. (2019). Analysing the sensitivity of Hungarian landscapes based on climate change in duced shallow groundwater fluctuation. Hungarian Geo graphical Bulletin, 68(4).
https://www.doi.org/10.15201/hungeobull.68.4.3

Fiala K., Barta, K., Benyhe, B., Fehérváry, I., Láng, I., Lábdy, J., Sipos, Gy., Győrffy, L. (2018). Development of an Operational Drought and Water Scarcity Monitoring System in Hungary. Global Water Partnership.

Gibbons, J.D., Chakraborti, S. (2003). Non-Parametric Statistical Inference. Chapman and Hall, New York. https://www.doi.org/10.1201/9781439896129

Hersbach, H., Bell, B., Berrisford, P., Biavati, G., Horányi, A., Muñoz Sabater, J., Nicolas, J., Peubey, C., Radu, R., Rozum, I., Schepers, D., Simmons, A., Soci, C., Dee, D., Thépaut, J-N. (2023). ERA5 hourly data on single levels from 1940 to present. Copernicus Climate Change Service (C3S) Climate Data Store (CDS), [Online] Available at: https://cds.climate.copernicus.eu/datasets/reanalysis-era5-single-levels?tab=overview.
https://www.doi.org/10.24381/cds.adbb2d47

HungaroMet (2022). Tanulmányok, Szárazság Magyarországon 2022-ben és a múltban. (In Hungarian)

Keveiné Bárány I. (1998). Talajföldrajz. Budapest: Nemzeti Tankönyvkiadó. (In Hungarian)

Kiss T., Hetesi, Zs., Füzi, T. (2019). Az átlaghőmérséklet és a csapadékmennyiség alakulása Mosonmagyaróváron. Statisztikai Szemle, 97(6), pp. 568-593. https://www.doi.org/10.20311/stat2019.6.hu0568 (in Hungarian)

Kis A., Pongrácz R., Bartholy J., Szabó J.A. (2023). Az éghajlatváltozás várható hatásának integrált, modell alapú becslése a Felső-Tisza vízjárására, a bizonytalanság számszerűsítésével. Hidrológiai Közlöny, 103(4). pp. 35-51. (In Hungarian)
https://www.doi.org/10.59258/hk.13172

Kis, A., Szabó, P., Pongrácz, R. (2025). Analysis of detected and future drought conditions - a case study for the Great Hungarian Plain. Theoretical and Applied Climatology, 156(6), 303 https://www.doi.org/10.1007/s00704-025-05510-2

Konkolyné Bihari Z., Lakatos M., Szalai S. (szerk.) (2008). Magyarország éghajlatáról: Változás, változékonyság térben és időben. OMSZ, Budapest. 23. p. (In Hungarian)

Korponai E. (2019). A volatilitás vizsgálata GARCH modellek segítségével., Debrecen: Debreceni Egyetem. (In Hungarian)

Ladányi Zs. (2009). Klímaváltozás hatása egy Duna-Tisza közi mintaterületen. In: Kiss, T. (Szerk.) 2009. Természetföldrajzi folyamatok és formák. Geográfus Doktoranduszok IX. Országos Konferenciájának Természetföldrajzos Tanulmányai, Szeged. ISBN: 978-963-482-923-2 (in Hungarian)

Lakatos M. (2021). Kiterjedt, gyors és egyre intenzívebb az éghajlatváltozás az IPCC 6. értékelő jelentése szerint. Légkör 66(3) p. 29. (In Hungarian)

Lakatos, M., Bokros, K., Szentes, O., Izsák, B., Bihari, Z. Marton, A. (2021). Regional soil moisture trends and buffering effects in the Great Plain of Hungary, International Journal of Climatology, 41(8), pp. 3921–3935.

Lakatos, M., Bokros, K., Szentes, O., Izsák, B., Bihari, Z. Marton, A., (2024). Climate monitoring information on the webpage of HungaroMet. Available at: https://meetingorganizer.copernicus.org/EMS2024/EMS2024-854.html [Accessed 31 Jan. 2026].

Makra, L., Kiss, Á., Palotás, J. (1985). The Spatial and Temporal Variability of Drought in the Southern Part of the Great Hungarian Plain. Acta Climatologica 18-20, 1-4, pp. 65-85.

Makra, L., Kiss, Á., Abonyiné Palotás, J. (1986). Az aszály klimatológiai és talajvízháztartási összetevői, valamint néhány mezőgazdasági vetülete a Dél-Alföldön. Alföldi tanulmányok, 10, pp. 99-111. (In Hungarian)

Marton J., Szanyi J. (1997a). Kelet-magyarországi pleisztocén üledékek geostatisztikai vizsgálata. 1. A transz misszivitás térképezése. Hidrológiai Közlöny. 77 évf. 5. szám. pp. 233-241. (In Hungarian)

Marton J., Szanyi J. (1997b). Kelet-magyarországi pleisztocén üledékek geostatisztikai vizsgálata. 2. A rétegek közötti átszivárgás területi meghatározása. Hidrológiai Közlöny. 77(5). pp. 241-248. (In Hungarian)

Mezősi G., Bata T., Blanka V., Ladányi Zs. (2017). A klímaváltozás hatása a környezeti veszélyekre az Alföldön. Földrajzi Közlemények 141(1) pp. 60-70. (In Hungarian)

Mezősi G., Blanka V., Ladányi Zs. (2020). Hőmérsékleti szélsőségekkel kapcsolatos természeti és társadalmi-gazdasági veszélyek. In: Farsang, A., Ladányi, Zs, Mucsi, L. (Ed.) Klímaváltozás okozta kihívások - Globálistól lokálisig. Szeged, Magyarország, Szegedi Tudományegyetem Természettudományi és Informatikai Kar Földrajzi és Földtudományi Intézet (2020) 216. p. pp. 23-33., 11. p. ISBN: 9789633067345 (In Hungarian)

Molnár E., Várallyai Gy. (1993). A magyar Alföld talajainak vízgazdálkodása és a térség mezőgazdasági termelése valamint környezetgazdálkodása közötti kapcsolat elemzése. In: Timár J., Baukó T., Duró A., Gurzó I, Velkey G (ed.) Az "alföldi út" kérdőjelei: Alföld-kongresszus, Békéscsaba, Magyarország, MTA Regionális Kutatások Központja (MTA RKK) 320 p. pp. 97-110., 14. p. (In Hungarian)

Nováky B. (1993). Az Alföld éghajlatának és vízháztartásának változása. Hidrológiai Közlöny, 73(1), pp. 20-23. (In Hungarian)

Pálmai O. (2005). Hazánk talajainak környezeti állapota. In: Német T. (szerk.) *A talaj vízgazdálkodása és a környezet.* Budapest: MTA Talajtani és Agrokémiai Kutatóintézet, pp. 161-169. (In Hungarian)

Szám, D., Hetesi, Zs., Bódi, T., Marosi Z.I. (2025a). Analysis of Precipitation Data Series in the TIVIZIG Operational Area (Hungary). Hidrológiai Közlöny, 105(1), pp. 46-54. https://www.doi.org/10.59258/hk.18331

Szám, D., Keve, G., Fekete, Á., Hetesi, Zs. (2025b). Changing rainfall patterns and their impact on cereal crops in the Szentes district. Időjárás - Quarterly Journal of the HungaroMet Hungarian Meteorological Service, 129(2), pp. 201-217.
https://www.doi.org/10.28974/idojaras.2025.2.6

Szentes, O. (2023). Szárazság Magyarországon 2022-ben és a múltban. Légkör, 68(1), pp. 9-19.
https://www.doi.org/10.56474/legkor.2023.1.2

AUTHORS

DOROTTYA SZÁM graduated as a plant scientist and agricultural engineer at the Hungarian University of Agricultural and Life Sciences (2022), and is currently a research assistant at the University of Pécs, and a student at the Doctoral School of Biology and Sports Biology. Her research area is the plant health impact of extreme weather events caused by climate change, with a special focus on plant pathogenic fungi that produce mycotoxins. She has been a member of the Hungarian Hydrological Society (MHT) since 2022.

KÍRA ERIKA KÁVÁSSY obtained a BSc degree in environmental engineering in 2025 from the Faculty of Water Sciences of the National University of Public Service. Her area of interest is the effects of climate change on precipitation and soil conditions in the Hungarian Great Plain.

ÁDÁM BERGER is a certified agricultural engineer and an assistant professor at the Department of Water and Environmental Safety, Faculty of Water Sciences, National University of Public Service. He obtained his PhD degree in 2025 from the Military Technical Doctoral School of the National University of Public Service. His research areas are disaster management and industrial safety.

ZSOLT HETESI holds a degree in physics and a PhD from the Faculty of Science of Eötvös Loránd University. He is currently a habilitated associate professor at the Faculty of Water Sciences of the National University of Public Service, and a senior research fellow at the Institute of Mathematics and Informatics of the University of Pécs. His research interests include sustainability and the modelling of stochastic processes in environmental science.

OxiTop microcosm model as a possible tool to study the effects of antibiotic exposure on the microbial community

Dongze JIANG[1], Yi YANG[1], Mátyás CSERHÁTI[2], Balázs KRISZT[1], Edit KASZAB[1,3]

[1] Department of Environmental Safety, Institute of Aquaculture and Environmental Safety, Hungarian University of Agriculture and Life Sciences, Páter Károly utca 1, H-2100 Gödöllő, Hungary

[2] Department of Molecular Ecology, Institute of Aquaculture and Environmental Safety, Hungarian University of Agriculture and Life Sciences, Páter Károly utca 1, H-2100 Gödöllő, Hungary

[3] Corresponding author: Kaszab.Edit@uni-mate.hu

DOI: 10.59258/hk.24058

Abstract

The bacterial community of surface waters is a key element of self-cleansing, but under antibiotic pressure, it should be closely monitored to evaluate the emergence of antimicrobial resistance. According to the World Health Organization (WHO), antibiotic resistance is one of the three most serious threats to human health. Antibiotic resistance can develop due to the selective pressure of antibiotics on the natural microbial ecosystem discharged through the effluents of wastewater treatment plants (WWTPs). This study aimed to find a link between sewage load and the biological activity of the bacterial community with and without antibiotic pressure. To reach this goal, an OxiTop microcosm experiment was set using surface water samples originating from a Hungarian site with and without sewage load. Samples were supplemented with different combinations of antibiotics relevant in human and veterinary therapy (colistin, florfenicol, imipenem, ceftazidime). During the incubation period, biological oxygen demand (BOD) was regularly measured and was paired with traditional cultivation and next-generation sequencing. Based on our results, the bacterial diversity decreased under antibiotic pressure, but the viable cell counts were not necessarily affected. The microbial community of surface water with sewage load had a higher level of adaptability to the antibiotics. The key taxa under antibiotic pressure that are possible hosts of multiple antibiotic resistance genes were *Cellvibrio*, *Aquabacterium,* and *Flavobacterium*.

Keywords

Antibiotics, antibiotic resistance, microbial community, OxiTop microcosm model, sewage, next generation sequencing, 16S rRNA.

OxiTop mikrokozmosz modell, mint lehetséges eszköz az antibiotikumok mikrobiális közösségre gyakorolt hatásainak vizsgálatára

Kivonat

A felszíni vizek bakteriális közössége kulcsfontosságú eleme a szennyvízbevezetések helyén zajló öntisztulásnak, azonban az antibiotikum rezisztencia kialakulása körükben is mind nagyobb figyelmet érdemel. Az Egészségügyi Világszervezet (WHO) szerint az antibiotikum-rezisztencia az emberi egészséget fenyegető három legsúlyosabb veszély egyike. Antibiotikum-rezisztencia kialakulhat a szennyvíztisztító telepek kibocsátásával a természetes mikrobiális ökoszisztémára gyakorolt szelektív nyomás következtében. A tanulmány célja, hogy kapcsolatot találjon a szennyvízterhelés és a bakteriális közösség biológiai aktivitása között antibiotikum terhelés mellett és anélkül, melynek érdekében OxiTop™ mikrokozmosz kísérletet állítottunk be egy magyarországi, szennyvízterhelés alatt álló víztestből származó minták felhasználásával. A mintákhoz humán és állatgyógyászati szempontból jelentős antibiotikumok különböző kombinációit adtuk (Kolisztin, Florfenikol, Imipenem, Ceftazidim). Az inkubációs időszak során folyamatosan mértük a minták mikrobaközösségének biológiai aktivitását, melyet hagyományos tenyésztési módszerekkel és újgenerációs szekvenálással egészítettünk ki. Eredményeink alapján az antibiotikum terhelés hatására csökkent a bakteriális diverzitás, de a bakteriális sejtszám nem. A szennyvízterheléssel érintett felszíni víz mikrobiális közössége nagyobb alkalmazkodóképességet mutatott az antibiotikumokkal szemben, mint a háttér minta. Eredményeink alapján az antibiotikumok hatására dominánssá váló taxonok – amelyek potenciális hordozói lehetnek többféle antibiotikum-rezisztencia génnek – a *Cellvibrio*, az *Aquabacterium* és a *Flavobacterium* voltak.

Kulcsszavak

Antibiotikumok, antibiotikum rezisztencia, mikrobiális közösség, OxiTop mikrokozmosz modell, szennyvíz, újgenerációs szekvenálás, 16S rRNS gén.

INTRODUCTION

The World Health Organization has listed antimicrobial resistance (AMR) as one of the top 10 threats to public health (*WHO 2023*). Due to the gradually growing pharmaceutical (*González Peña et al. 2021*) and antibiotic use all over the world (*Klein et al. 2018*), antibiotic-resistant bacteria (ARB) are distributed widely not only in healthcare institutes (*Serra-Burriel et al. 2020*) but in various environments, such as soil (*Bombaywala et al. 2021*) and freshwater systems (*Nnadozie and Odume 2019*). Wastewater treatment plants (WWTPs) are verified sources of antibiotic load (*Rodriguez-Mozaz et al. 2020*), resistant microorganisms (*Rodríguez-Molina et al. 2019*), and resistance genes (*Li et al. 2022*). Therefore, WWTPs are potential hotspots for ARB spread into the environment (*Rizzo et al. 2013*). At the same time, the available information on the effect of last-resort antibiotics, such as colistin (polymyxin E) (*El-Sayed et al. 2020*) and broad-spectrum antibiotics, like carbapenems *(Armstrong et al. 2021*) and florfenicol (*Zhang et al. 2020*) on the environmental microbiome is limited, despite the scientific evidence suggesting that wastewater effluent is frequently polluted with colistin (*Smyth et al. 2020*) and carbapenem-resistant bacteria (*Araújo et al. 2021*). In Hungary, the bacterial community structure of wastewater effluents (*Benedek et al. 2014*) and the effect of antibiotic pressure on the forming microbial community is poorly understood, and the impact of the simultaneous load of wastewater and antibiotics on the recipient surface water's microbiome and its activity has not been examined in detail.

Based on this background, this work aimed to compare two sections of a chosen surface water body located in Hungary, with and without sewage load, and to evaluate the effect of antibiotic pressure on the biological activity and composition of the cultivable and non-cultivable microbial communities. To reach this goal, a microcosm model was set using different treatments with four "Watch" and "Reserve" types of antibiotics (colistin, florfenicol, imipenem, ceftazidime) according to the WHO classification for evaluation and monitoring (*WHO 2019*). For antibiotic treatment, sewage-affected and background surface water samples were used. The initial hypothesis of this study was that the microbial communities of environmental samples affected by sewage inlets show a higher level of adaptability to antibiotics and a higher number of cultivable ARB.

MATERIALS AND METHODS

Sampling

The sampling strategy was to choose a surface water stream with and without the effect of urban sewage effluent. Our choice was the section of the Rákos stream localized between Gödöllő and Isaszeg, Hungary, receiving the effluent of Gödöllő WWTP (wastewater treatment plant), with a capacity of 50000 population equivalent (10000 m^3/day). As background, an unaffected area of the same stream was sampled 200 m upstream (see Figure 1). Samples were taken on the 30th of March 2021 aseptically into sterile 1 L volume bottles and immediately transported to the MATE - Institute of Aquaculture and Environmental Safety, Department of Environmental Safety laboratory for analysis. Antibiotic concentrations were not measured in the native samples.

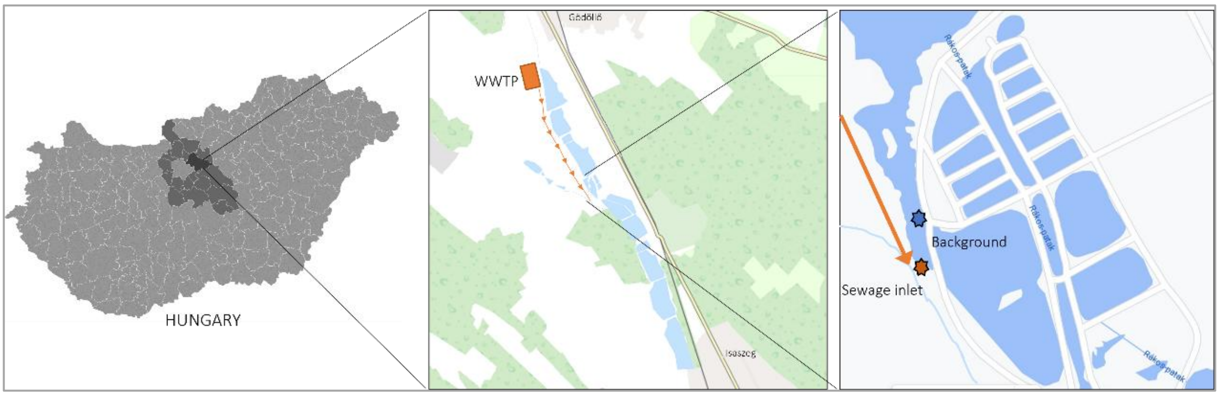

Figure 1. Location of the examined WWTP and the sampling site, Gödöllő, Hungary (©2023 Google Map, ©2000-2021 Michelin Travel Partner)

Notes: Blue mark – background (unaffected) area (GPS coordinates: 47°33'54.8"N 19°22'03.0"E); orange mark – WWTP effluent affected area (GPS coordinates: 47°33'53.6"N 19°22'02.9"E)

1. ábra. A vizsgált szennyvíztisztító telep és a mintavételi hely elhelyezkedése, Gödöllő, Magyarország (©2023 Google Térkép, ©2000–2021 Michelin Travel Partner)

Megjegyzés: Kék jelölés – háttér (nem érintett) terület (GPS koordináták: 47°33'54.8"N 19°22'03.0"E); narancssárga jelölés – a szennyvíztisztító telep kifolyása által érintett terület ((GPS koordináták: 47°33'53.6"N 19°22'02.9"E); narancssárga nyíl – a víz áramlásának iránya

Experimental settings

To reveal the effect of the chosen antibiotics and their combinations on the microbial community and biological activity of the examined (sewage-affected and background) samples, a laboratory experiment was set in three replicates using 0.5 L sterile bottles inoculated with 200 mL volume of native samples. At the beginning of the experiment, samples were treated with three different combinations of antibiotics using MAST disks (Mast Diagnostica, Germany) to reach a final 300 µg/L antibiotic concentration (*Table 1*). The chosen sub-lethal concentrations were higher than the previously detected concentrations of antibiotics in the environment (*Wang et al. 2025*), because we aimed to reach the inhibitory concentration of the sensitive organisms and therefore, to perform a persistent selective pressure on the microbial community.

Table 1. Sample types and antibiotic treatments in the experimental settings
1. táblázat. A kísérleti beállítások során használt mintatípusok és antibiotikum kezelések

Sample identifiers and sample types	Treatment
B (Background) SA (Sewage affected) surface waters	Native (non-treated)
B-COL (Background + Colistin) SA-COL (Sewage affected + Colistin)	Colistin (300 µg/L)
B-FLOR (Background + Florfenicol) SA-FLOR (Sewage affected + Florfenicol)	Florfenicol (300 µg/L)
B-MIX (Background + antibiotic mixture) SA-MIX (Sewage affected + antibiotic mixture)	Colistin (100 µg/L) Imipenem (100 µg/L) Ceftazidime (100 µg/L)

OxiTop^{TM} System to measure biological oxygen demand

To determine the biological oxygen demand (BOD) of the microbial community under the effect of antibiotics, a manometric method measuring pressure differences via piezoresistive electronic pressure sensors (Oxitop^{TM}, WTW, Weilheim, Germany) was used (*González Peña et al. 2021*). Samples were kept in a sealed container fitted with a pressure sensor. During the incubation, oxygen was consumed, and the biologically active microorganisms released carbon dioxide. The pressure decreased because sodium hydroxide pellets were added to a separate container above the sample level to absorb carbon dioxide.

The incubation temperature was 15°C, and the incubation time was 7 days (168 h) with continuous stirring using the platforms of the OxiTop^{TM} system. Negative pressure (that correlates with the microbial activity, i.e., BOD value of the sample) was measured automatically in every 30 minutes during the incubation period. At the end of our experiment, outlier bottles (with more than ±10 Pa deviation compared to the average of the replicates) were excluded from further data analysis in each setting (altogether 2 bottles in the whole experiment). Pressure curves of the remaining technical replicates with acceptable deviation in pressure values were averaged and further analyzed.

Cultivation-based methods

Traditional cultivation aimed to determine the colony-forming units (CFUs) of bacteria from the treated and non-treated environmental samples. A tenfold series of dilutions was prepared. and the diluted samples were used for the pour plate technique. Preliminary experiments were performed to evaluate the sufficient media for the cultivation and isolation of antibiotic-resistant microorganisms originating from environmental samples. Based on these preliminary tests, R2A (Agar, 15.0 g; Casein acid hydrolysate, 0.5 g; Dextrose, 0.5 g; Dipotassium phosphate, 0.3 g; Magnesium sulphate, 0.024 g; Proteose peptone, 0.5; Sodium pyruvate, 0.3 g; Starch (soluble), 0.5 g); Yeast ex-tract, 0.5 g, Distilled water, 1,000 ml) was the most chosen for cultivation (data not shown). After incubation at 28°C for 96h, colony-forming units (CFUs) of the tenfold dilu-tions were counted and averaged to calculate the CFU/ml values of the original (100%) samples.

Amplicon sequencing

For amplicon sequencing, at the end of the 7-day OxiTop^{TM} experiment, we averaged the technical replicate samples, and aseptically filtered 200-300 ml volume of each experimental setting using a 0.22 µm pore size, hydrophilic MCE membrane filter, 47 mm diameter, white, Triton-free (Millipore). We extracted community DNA from the filtrate using the DNeasy PowerSoil DNA extraction kit (Qiagen, Germany) according to the manufacturer's instructions.

During our experiment, we amplified bacteria domain-specific genetic elements from the community DNA. For paired-end 16S rRNA amplicon sequencing, the variable V3 and V4 regions of the 16S rRNA gene were amplified using primers containing overhang Illumina adapters. Paired-end fragment reads (2x250 bp read length) were generated on the Illumina MiSeq platform using MiSeq Reagent Kit v3 by Biomi Ltd., Hungary. Reads were trimmed according to their quality and length using the CLC Genomics Workbench Tool; the minimum required length of nucleotides was set to 50. Trimmed sequences were processed using mothur v 1.41.1 (*Schloss et al. 2009*), an open-source, platform-independent, community-supported software for describing and comparing microbial communities. Sequences were assorted based on their alignment using the SILVA 138.2 database (*Quast et al. 2013*) followed by the chimera detection and the removal of singleton reads. The standard 97% similarity threshold was used to determine operational taxonomic units (OTUs) as suggested by *Tindall et al. (2010)* for prokaryotic species delineation. After data processing, the mothur software summarized taxonomy and diversity results of the examined samples in data files. Data was exported to Excel for further analysis.

RESULTS AND DISCUSSION

Based on the examination of environmental samples with and without sewage load of the same geographical location (CW and SL samples) and their treatment with different types of antibiotics, we gained information about the composition and activity of the microbial community. Hereby we present results by cell counts (colony-forming units - CFU), BOD values, microbial community (amplicon sequencing).

Cell counts (colony-forming units) under antibiotic treatment

With traditional cultivation, colony-forming units were determined on R2A medium at the beginning and at the end of the 7-day (168h) long experiment. CFU values are summarized in *Figure 2*.

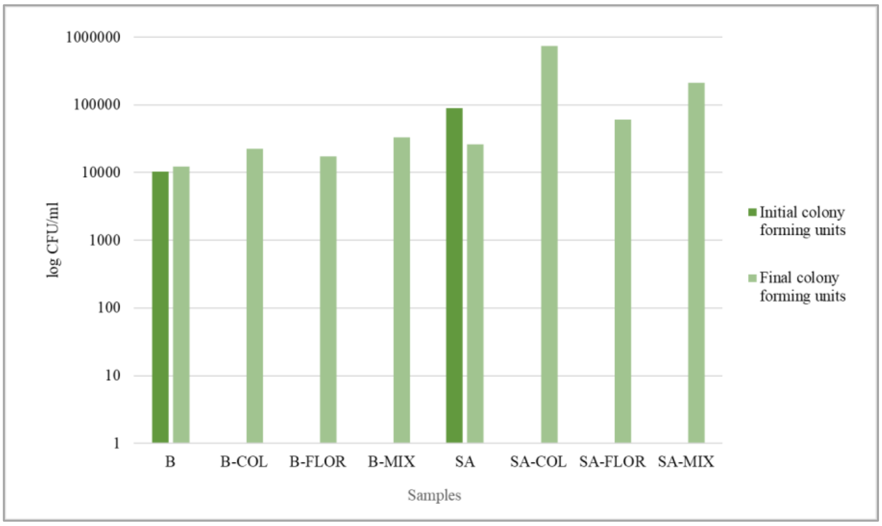

Figure 2. Log CFU values of the averaged samples of the experimental settings using background (B) and sewage affected (SA) surface waters with and without antibiotic supplementation on R2A agar.

Note: Initial colony forming units - 0h; Final colony forming units – 168h; COL – Colistin (300 µg/L); FLOR – Florfenicol (300 µg/L); MIX – Colistin, Imipenem, Ceftazidime mixture (100-100 µg/L)

2. ábra. A háttér (B) és a szennyvízzel terhelt (SA) felszíni vizek kísérleti beállításainak átlagolt mintáin mért log CFU értékek antibiotikum-kiegészítéssel és anélkül R2A agaron

Megjegyzés: Kiindulási CFU értékek – 0 óra; Záró CFU értékek – 168 óra; COL – Kolisztin (300 µg/L); FLOR – Florfenikol (300 µg/L); MIX – Kolisztin, Imipenem, Ceftazidim keverék (100–100 µg/L)

In *Figure 2,* the cell count of the background surface water sample (without sewage load) was stable; there were no significant increases or decreases in CFU values after 7 days of incubation in the OxiTop^{TM} system. At the same time, SA samples, especially with colistin treatment, increased their cultivable microbial numbers, which was an unexpected outcome of antibiotic treatment. The difference was higher in the case of sewage-affected surface water samples, which is in accordance with previous findings that in the sewage microbial community, the adaptability and resistance to antibiotics are higher (*Rizzo et al. 2013*). However, the stable or increasing cell counts were unexpected: we hypothesized that antibiotic treatment would reduce the number of cultivable microorganisms. A possible explanation is that with the effect of antibiotics, sensitive microorganisms were eradicated, and without the competition, resistant, fast-growing bacteria could easily proliferate till the 7-day-long experiment; consequently, the CFU values increased.

Microbiological activity under antibiotic treatments

During the 7-day-long experiment, we continuously measured the changes of negative pressure in each bottle to evaluate the microbial activity. The result of biological oxygen demands (BODs) of the eight different settings (B and SA samples, the other 6 samples treated by antibiotics and their combinations (B-/SA-COL, B-/SA-FLOR, B-/SA-MIX) during the incubation period are summarized in *Figure 3.* supplemented with the average value obtained by the replicate flasks (2-3 replicates/settings) after the exclusion of the outliers.

In *Figure 3,* the pressure goes down when the microbial community is consuming a significant amount of oxygen, which means that it is biologically active. If the curve is flat, it means there was only minimal biological activity because the microbial community was not consuming much oxygen. This graph showed that the lowest level of biological activity was in the untreated Background (B) surface water sample. The biological activity was also lower than the average value in the background (B) samples supplemented with colistin (B-COL), florfenicol (B-COL), and with the mixture of colistin, imipenem, and ceftazidime (B-MIX). According to the BOD values of the Background samples, we could conclude that the antibiotic treatment did not cause a significant change in the biological activity of the microbial community, which correlates with the stable CFU values of these samples.

Among the sewage affected (SA) sample types, the untreated sample (SA) had the lowest degree of biological activity and was the only one that stayed below the average value during the 168h incubation. The biological activity of the organisms in the sewage-affected samples supplemented with antibiotics was much higher than the average: florfenicol (SA-FLOR) and mixed (SA-MIX with colistin, imipenem, and ceftazidime) antibiotic treatment induced a similar, significant increase in BOD values, while colistin (SA-COL) sample had the highest biological activity among all sample types, with a significant BOD increase especially in the second half of our experiment. The extremely high biological oxygen demand of the SA-COL sample can be a result of the higher microbial cell counts verified by the plate counting technique.

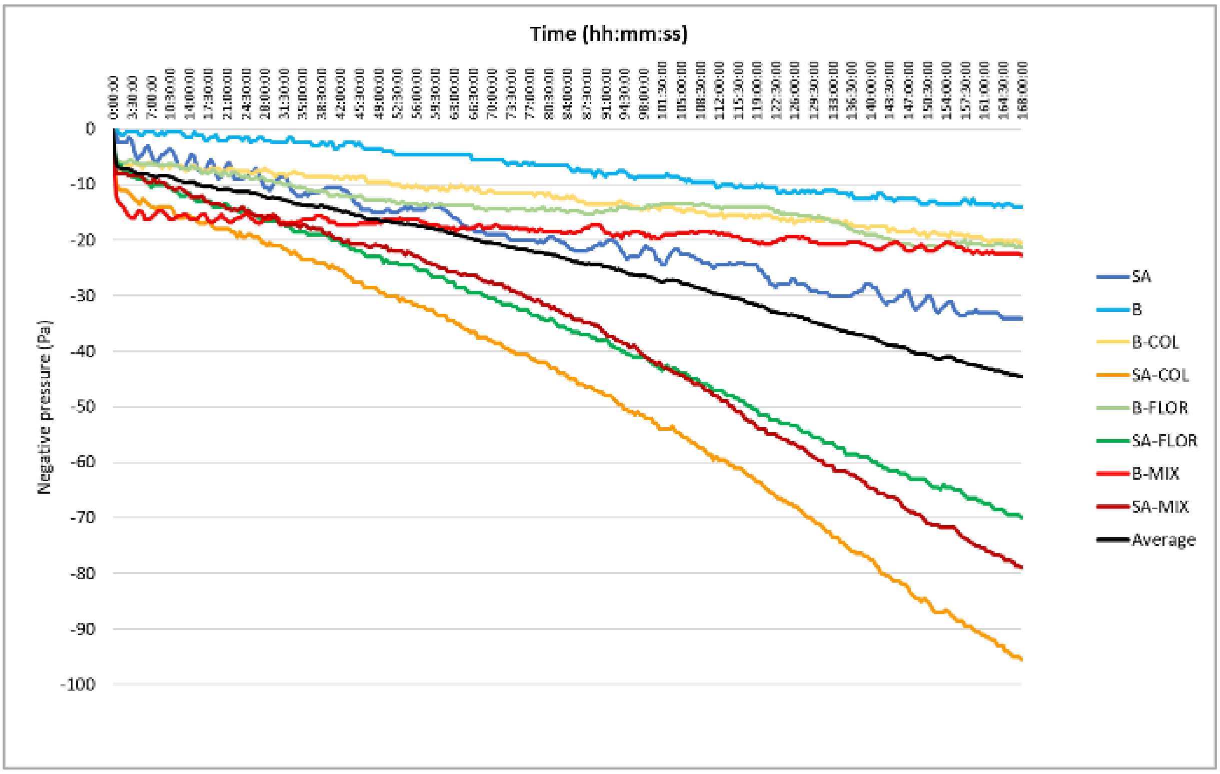

Figure 3. Microbiological activity of the examined samples expressed in negative pressure measured by OxiTop system
Note: SA-sewage affected, B-background, COL-Colistin; FLOR-Florfenicol; MIX-antibiotic mixture
3. ábra. Az OxiTop rendszerben vizsgált minták biológiai aktivitása negatív nyomás értékben kifejezve
Megjegyzés: SA-szennyvízterhelés alatt álló víz; B- háttér minta; COL - Kolisztin; FLOR - Florfenikol; MIX-antibiotikum keverék

In the background (B) water group, samples without antibiotic treatment had the lowest microbiological activities. When a solo or combined antibiotic treatment was used, the biological activity of the microorganisms is increased. The three combined antibiotics of colistin, imipenem, and ceftazidime had the greatest impact on microbial activity in the background sample during the incubation, but after 168h only minor differences could be detected between the different treatments.

Antibiotics have a significant impact on microbial activity, particularly in the case of colistin, but after the first 24h, stagnating biological activity, the determined effect was not inhibition. BOD is the measure of the amount of oxygen taken up by aerobic microorganisms that decompose organic waste matter in water. A high BOD indicates the presence of a large number of microorganisms, which suggests a high level of biodegradable organic matter, such as drug residues or other organic pollutants (*Ijoma 2010*).

Therefore, we can presume that the applied concentrations of antibiotics during a long-term incubation are not only environmental pollutants, but potentially carbon sources for fast-growing microorganisms and their presence does not necessarily decrease the biological activity or inhibit the bacterial growth.

Compared to scientific literature, there are only a few similar studies regarding the comparison of BOD values of microbial communities under different antibiotic treatments. Panta and Doerrler described colistin resistance as a complex and multifactorial phenomenon noting that colistin resistance can be linked to the pH and oxygen level of the medium (*Panta and Doerrler 2021*). Li and her coauthors mentioned that the relative abundances of antibiotic resistance genes (ARGs) were negatively correlated with temperature and BOD *(Li et al. 2020*). In our case, the temperature was constant during the incubation and pH was not measured; therefore, we could not draw similar conclusions. Based on the biodegradation rates of the examined antibiotics, carbapenems and colistin reach a significantly higher degradation rate in wastewater than in natural water; physicochemical factors such as temperature and pH greatly affect the degradation rates (*Sharma et al. 2023*). Consistent with this, we observed a higher biological activity in wastewater-affected samples, suggesting that antibiotic degradation rates in these environments are likely to be higher.

Diversity and taxonomy of water samples with and without antibiotic treatment

The bacterial diversity of the samples was determined by the Mothur algorithm using the Illumina next-generation sequencing data and was expressed with the commonly used Shannon diversity index that considers both the number and distribution of the detected species. Shannon diversity indices are summarized in *Figure 4*.

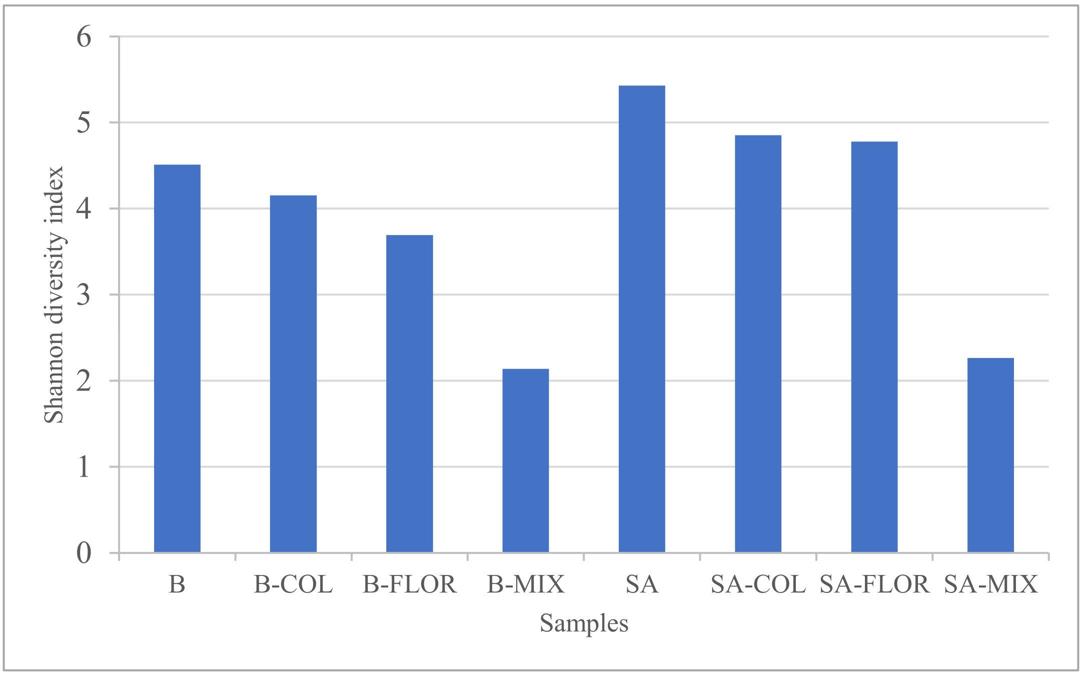

Figure 4. Shannon diversity index of the examined samples after 168h incubation with and without antibiotics
Note: SA-sewage affected, B-background, COL-Colistin; FLOR-Florfenicol; MIX-antibiotic mixture
4. ábra. A vizsgált minták Shannon diverzitás index értékei 168 órás inkubációt követően antibiotikum kiegészítéssel és anélkül
Megjegyzés: SA-szennyvízterhelés alatt álló víz; B- háttér minta; COL - Kolisztin; FLOR - Florfenikol; MIX-antibiotikum keverék

As *Figure 4* shows, after 7 days of incubation, the Background (B) samples had a lower level of microbial diversity, while the surface water sample with sewage load (SA) had the highest Shannon index. Compared to native (B and SA) samples, all antibiotic treatments led to a lower level of bacterial diversity: according to our results, the SA-COL setting had the highest, and B-MIX/SA-MIX samples had the lowest diversity of all antibiotic treatments. Compared to the determined CFU values of each sample (*Figure 2*), there is an inverse correlation between diversity and cell counts. According to this information, we could state that antibiotic treatment caused a decrease in the microbial diversity of the examined samples, while most of the time the microbial counts remained the same or increased. A possible explanation is that antibiotic treatment eradicated the sensitive microorganisms and opened a niche to the fast-growing, antibiotic-resistant species.

To determine the key members of the microbial community, at the end of the experiment, the genus-level composition of the bacterial community under different treatments was determined by next-generation sequencing. The composition of the top 20 identified bacterial genera of each sample is summarized in *Figure 5*, which shows that the Background (B) and Sewage affected (SA) samples had different microbial communities. B sample contained typical surface water-related taxa such as *Perlucidibaca* and *Aquabacterium*. *Aquabacterium* species such as *A. citratiphilum*, *A. commune* and *A. parvum* were previously isolated from biofilm from the Berlin drinking water system (*Pham et al. 2015*), while *A. fontiphilum* and *A. limnoticum* were found in freshwater springs in China (*Chen et al. 2012, Lin et al. 2009)*. Some potentially pathogenic species of the genus had the highest abundances in biofilm samples and were described as hosts harbouring many resistance genes (*Zhao et al. 2021*). The Gram-negative freshwater bacterial genus *Perlucidibaca* was described in 2008 (*Song et al. 2008*).Together with *Aquabacterium, Perlucidibaca* belong to the family *Moraxellaceae* and species; they presumably play a role in the early colonization of microplastics travelling in wastewater (*Martínez-Campos et al. 2021*). In contrast to the background (B) sample, the sewage-affected (SA) surface water contained many sewage-originating organisms, such as *Ferruginibacter* (*Kong et al. 2024*).

Antibiotic treatment induced significant changes in both sample types. With antibiotic treatment, the dominance of the *Nevskia* genus was suppressed in both B and SA samples. *Nevskia* species have a wide nutritional spectrum and can utilize sugars as growth substrates (*Gutierrez et al. 2012*), but based on the scientific literature, *Nevskia* species are not discussed in context with antibiotic resistance, which is supported by our results.

At the same time, the proportions of the *Perlucidibaca* and in the background samples, *Aquabacterium* and *Hydrogenophaga* species remained similar under COL and FLOR treatment; only the MIX antibiotic setting eradicated the members of these genera. The preponderance of some of these genera in COL samples is understandable, given that *Perlucidibaca, Hydrogenophaga* and *Aquabacterium* are members of the *Comamonadaceae* and *Moraxellaceae* families and are innately resistant to colistin. At the same time, we couldn't find any information about their florfenicol resistance, which should be investigated further in the future.

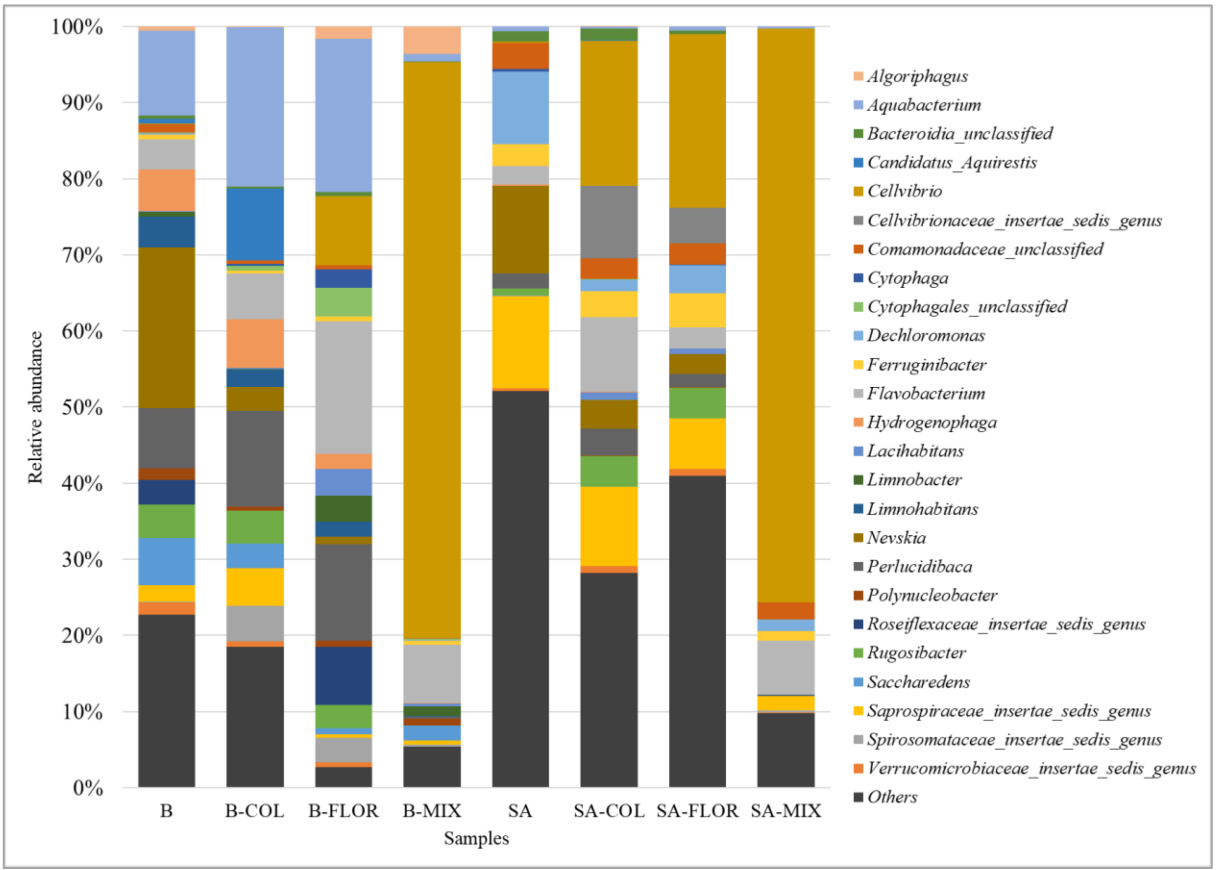

Figure 5 The composition of the top25 bacterial taxa with >1% abundance of the examined samples after 168h incubation with and without antibiotics

Note: SA-sewage affected, B-background, COL-Colistin; FLOR-Florfenicol; MIX-antibiotic mixture

5. ábra. A vizsgált mintabeállításokban 1%-nál nagyobb abundanciát elérő, baktériumnemzetségek top25 képviselője 168 óra inkubációt követően, antibiotikum kiegészítéssel és anélkül

Megjegyzés: SA-szennyvízterhelés alatt álló víz; B- háttér minta; COL - Kolisztin; FLOR - Florfenikol; MIX-antibiotikum keverék

Interestingly, *Cellvibrio* species, which had a negligible proportion in the native samples, reached an outstanding abundance in the B-MIX and SA-MIX samples, followed by B-FLOR, SA-FLOR and SA-COL treatment. They were only absent in the B-COL setting. This genus is involved in the breakdown of cellulose and its presence correlates with the frequency of antibiotic resistance genes - according to the results of Han and his co-workers, *Cellvibrio* species are possible hosts of ARGs in agricultural soils treated with different sources of animal manure, conferring resistance to aminoglycoside, tetracycline, and MLSB (Macrolide-lincosamide-streptogramin B) *(Han et al. 2018*). Recently, it was proven that the abundance of *Cellvibrio* species can grow under chronic antibiotic exposure in the gut microbiome of zebrafish (*Danio rerio*) as well, which correlates with our results (*Yang et al. 2024*).

Flavobacterium, which was the second most abundant genus in SA samples and also frequently detectable in B samples, reached at least 5% abundance in all examined settings, and it was the only genus that remained abundant in both sample types under all antibiotic treatment. The presence of *Flavobacterium* species was previously described to correlate with the presence of various ARGs, including aminoglycoside, tetracycline, MLSB, FCA (fluoroquinolone, quinolone, chloramphenicol, florfenicol and amphenicol) resistance genes, sulfonamide, β-lactam and multidrug resistance genes (*Zhang et al. 2022*). Moreover, *Flavobacterium* species were previously described as antibiotic degraders (*Ma et al. 2022*) that can explain their presence under antibiotic pressure.

Among the less abundant genera, *Ferruginibacter* and *Dechloromonas* were detectable in SA samples regardless of the antibiotic treatment; many of them were previously cultured from wastewater, activated sludge and granular activated carbon filters in water treatment (*Kong et al. 2024, Mulder and Deinema 2006, Magic-Knevez et al. 2009)*. In the Background samples, *Hydrogenophaga* species were the predominant bacteria in the B, B-COL, and B-FLOR samples and were the most abundant in the B-COL setting. The members of this genus have a significant nutritional versatility and capacity utilize various substrates (*Garrity et al. 2005, Magic-Knevez and van der Kooij 2006)*. *Hydrogenophaga* was described as a new host of ARGs in samples after O_3/Cl_2 disinfection (*Zhang et al. 2019*) and harboured Class 1 integrons that are playing a significant role in the worldwide problem of antibiotic resistance (*Gillings et al. 2008*).

CONCLUSIONS

Based on the OxiTop^{TM} microcosm experiment using surface water samples taken from the Rákos stream with and without sewage load, the diversity of the microbial community was correlated with the origin of the sample (background and sewage-affected section). Antibiotic treatments with clinically and veterinary relevant antibiotics (colistin, florfenicol, imipenem, ceftazidime) significantly influenced the biological activity, bacterial diversity, and composition. It was verified that antibiotic-resistant bacteria that are non-susceptible to the four examined antibiotics are present in the untreated surface water samples and easily proliferate when the selective pressure of antibiotics opens a niche for them. Sewage affected (SA) microbial community had a higher diversity, showed an increased level of adaptability to the antibiotic treatments, therefore reached a higher cell count and biological activity until the end of the 168h-long experiment due to the dominance of fast-growing microorganisms such as *Cellvibrio* species. Based on the overview of the scientific literature, many of the identified bacterial genera (such as *Flavobacterium, Cellvibrio and Aquabacterium*) have been proven to be antibiotic-resistant or to harbour antibiotic resistance genes. Since the sensitive bacteria have been eradicated by antibiotics, the growth rate of the resistant bacteria has accelerated due to reduced competition, increasing the number and biological activity of potentially antibiotic-resistant microorganisms.

The OxiTop^{TM} system has been adapted and optimized for the examination of antibiotic treatment using natural freshwater samples with and without sewage load. Under the controlled environment (temperature) provided by this microcosm model, the OxiTop^{TM} system can be optimal to evaluate the long-term effects of antibiotic exposure not only on the composition, diversity and cell count of a bacterial community, but to measure the biological activity of microorganisms.

In the future, the developed methodology can be further improved by measuring the effect of pH and other temperature settings, as these factors also affect the relative abundance of ARGs (*Panta and Doerrler 2021, Li et al. 2020*). Quantifying various antibiotic resistance genes using molecular methods, complemented by traditional cultivation and characterization of antibiotic-resistant bacteria, can provide valuable insights into the dissemination of antimicrobial resistance in sewage-affected surface waters and contribute to improved environmental safety.

ACKNOWLEDGEMENTS

This research was supported by the 2020-1.1.2-PIACI-KFI-2021-00239 provided by the Ministry of Innovation and Technology of Hungary from the National Research, Development and Innovation Fund, financed under the PIACI KFI funding scheme. The scientific work of E. Kaszab was supported by the János Bolyai Research Grant of the Hungarian Academy of Sciences (BO/00236/20/4), D. Jiang was supported by the Stipendium Hungaricum scholarship.

REFERENCES

Araújo, S., Sousa, M., Tacão, M., Baraúna, R.A., Silva, A., Ramos, R., Alves, A., Manaia, C.M., Henriques, I. (2021). Carbapenem-resistant bacteria over a wastewater treatment process: Carbapenem-resistant Enterobacteriaceae in untreated wastewater and intrinsically-resistant bacteria in final effluent. Science of The Total Environment, pp. 782. 146892. https://doi.org/10.1016/J.SCITOTENV.2021.146892

Armstrong, T., Fenn, S.J., Hardie, K.R. (2021). JMM Profile: Carbapenems: a broad-spectrum antibiotic. Journal of Medical Microbiology, 70(12), pp. 1462. https://doi.org/10.1099/JMM.0.001462

Benedek, T., Táncsics, A., Szilágyi, N., Tóth, I., Farkas, M., Szoboszlay, S., Krifaton, C., Hartman, M., Kriszt, B. (2014). Analysis of biofilm bacterial communities responsible for carbon removal through a reactor cascade treating wastewater. World Journal of Microbiology and Biotechnology, 30(3), pp. 977-987. https://doi.org/10.1007/S11274-013-1516-9/FIGURES/6

Bombaywala, S., Mandpe, A., Paliya, S., Kumar, S. (2021). Antibiotic resistance in the environment: a critical insight on its occurrence, fate, and eco-toxicity. Environmental Science and Pollution Research 2021 28(20), pp. 24889-24916. https://doi.org/10.1007/S11356-021-13143-X

Chen, W.M., Cho, N.T., Yang, S.H., Arun, A.B., Young, C.C., & Sheu, S.Y. (2012). Aquabacterium limnoticum sp. nov., isolated from a freshwater spring. International Journal of Systematic and Evolutionary Microbiology, 62(Pt_3), pp. 698-704. https://doi.org/10.1099/ijs.0.030635-0

El-Sayed Ahmed, M.A.E.G., Zhong, L.L., Shen, C., Yang, Y., Doi, Y., Tian, G.B. (2020). Colistin and its role in the Era of antibiotic resistance: an extended review (2000–2019). Emerging Microbes & Infections, 9(1), pp. 868. https://doi.org/10.1080/22221751.2020.1754133

Garrity, G.M., Brenner, D.J., Krieg, N.R., Staley, J.T. (2005). Bergey's Manual of Systematic Bacteriology, 2nd edition, Volume 2: The Proteobacteria. Springer-Verlag, US, 1106 p.

Gillings, M., Boucher, Y., Labbate, M., Holmes, A., Krishnan, S., Holley, M., Stokes, H.W. (2008). The Evolution of Class 1 Integrons and the Rise of Antibiotic Resistance. Journal of Bacteriology, 190(14), pp. 5095-5100. https://doi.org/10.1128/JB.00152-08

González Peña, O.I., López Zavala, M.Á., Cabral Ruelas, H. (2021). Pharmaceuticals Market, Consumption Trends and Disease Incidence Are Not Driving the Pharmaceutical Research on Water and Wastewater. International Journal of Environmental Research and Public Health, 18(5), pp. 1-37. https://doi.org/10.3390/IJERPH18052532

Gutierrez, T., Green, D.H., Whitman, W.B., Nichols, P.D., Semple, K.T., Aitken, M.D. (2012). Algiphilus aromaticivorans gen. nov., sp. nov., an aromatic hydrocarbon-degrading bacterium isolated from a culture of the marine dinoflagellate *Lingulodinium polyedrum*, and proposal of *Algiphilaceae fam. nov.* International Journal of Systematic and Evolutionary Microbiology, 62(Pt_11), pp. 2743-2749. https://doi.org/10.1099/ijs.0.033324-0

Han, X.M., Hu, H.W., Chen, Q.L., Yang, L.Y., Li, H.L., Zhu, Y.G., Li, X.Z., Ma, Y.B. (2018). Antibiotic resistance genes and associated bacterial communities in agricultural soils amended with different sources of animal manures. Soil Biology and Biochemistry, 126, pp. 91-102. https://doi.org/10.1016/j.soilbio.2018.08.018

Ijoma, G.N. (2010). Antibiotic resistance of coliform bacteria in the Rietspruit river. Dissertation. Vaal University of Technology, Vanderbijlpark, South Africa. 139 p.

Klein, E.Y., Van Boeckel, T.P., Martinez, E.M., Pant, S., Gandra, S., Levin, S.A., Goossens, H., Laxminarayan, R. (2018). Global increase and geographic convergence in antibiotic consumption between 2000 and 2015. Proceedings of the National Academy of Sciences of the United States of America, 115(15), pp. E3463–E3470. https://doi.org/10.1073/pnas.1717295115

Kong, W., Jalalah, M., Alsareii, S.A., Harraz, F.A., Almadiy, A.A., Thakur, N., Salama, E.S. (2024). Occurrence, characteristics, and microbial community of microplastics in anaerobic sludge of wastewater treatment plants. Environmental Pollution, pp. 344, 123370. https://doi.org/10.1016/j.envpol.2024.123370

Li, B.-B., Zhi, L.L., Peng, Z.Y., Ma, X.X., Li, J. (2020). Contrasting distribution of antibiotic resistance genes and microbial communities in suspended activated sludge versus attached biofilms in an integrated fixed film activated sludge (IFAS) system. Science of The Total Environment, 742, pp. 140481. https://doi.org/10.1016/j.scitotenv.2020.140481

Li, S., Ondon, B.S., Ho, S.H., Jiang, J., Li, F. (2022). Antibiotic resistant bacteria and genes in wastewater treatment plants: From occurrence to treatment strategies. Science of The Total Environment, 838, 156544. https://doi.org/10.1016/J.SCITOTENV.2022.156544

Lin, M.C., Jiang, S.R., Chou, J.H., Arun, A.B., Young, C.C., Chen, W.M. (2009). Aquabacterium fontiphilum sp. nov., isolated from spring water. International Journal of Systematic and Evolutionary Microbiology, 59(4), pp. 681-685. https://doi.org/10.1099/ijs.0.000745-0

Ma, J., Cui, Y., Li, A., Zou, X., Ma, C., Chen, Z. (2022). Antibiotics and antibiotic resistance genes from wastewater treated in constructed wetlands. Ecological Engineering, 177, pp. 106548. https://doi.org/10.1016/j.ecoleng.2022.106548

Magic-Knevez, A., van der Kooij, D. (2006). Nutritional versatility of two *Polaromonas* related bacteria isolated from biological granular activated carbon filters, pp. 303–311. In: *Gimbel R., Graham N.J.D., Collins M.R. (eds.)*, Recent progress in slow sand and alternative biofiltration processes. IWA Publishing, London, UK, 582 p.

Magic-Knevez, A., Wullings, B., Van der Kooij, D. (2009). Polaromonas and *Hydrogenophaga* species are the predominant bacteria cultured from granular activated carbon filters in water treatment. Journal of Applied Microbiology, 107(5), pp. 1457-1467. https://doi.org/10.1111/j.1365-2672.2009.04337.x

Martínez-Campos, S., González-Pleiter, M., Fernández-Piñas, F., Rosal, R., Leganés, F. (2021). Early and differential bacterial colonization on microplastics deployed into the effluents of wastewater treatment plants. Science of The Total Environment, 757, pp. 143832. https://doi.org/10.1016/j.scitotenv.2020.143832

Mulder, E.G., Deinema, M.H. (2006). The Genus *Haliscomenobacter* . In: Dworkin, M., Falkow, S., Rosenberg, E., Schleifer, KH., Stackebrandt, E. (eds.) The Prokaryotes. Springer, New York, NY. https://doi.org/10.1007/0-387-30747-8_22

Nnadozie, C.F., Odume, O.N. (2019). Freshwater environments as reservoirs of antibiotic-resistant bacteria and their role in the dissemination of antibiotic resistance genes. Environmental Pollution, pp. 254, 113067. https://doi.org/10.1016/J.ENVPOL.2019.113067

Panta, P.R., Doerrler, W.T. (2021). A link between pH homeostasis and colistin resistance in bacteria. *Scientific Reports*, *11*(1), 13230. https://doi.org/10.1038/s41598-021-92718-7

Pham, V.H.T., Jeong, S.W., Kim, J. (2015). Aquabacterium olei sp. nov., an oil-degrading bacterium isolated from oil-contaminated soil. International Journal of Systematic and Evolutionary Microbiology, 65(Pt_10), pp. 3597-3602. https://doi.org/10.1099/ijsem.0.000458

Quast, C., Pruesse, E., Yilmaz, P., Gerken, J., Schweer, T., Yarza, P., Peplies, J., Glöckner, F.O. (2013). The SILVA ribosomal RNA gene database project: improved data processing and web-based tools. Nucleic Acids Research, pp 41, D590–596. https://doi.org/10.1093/nar/gks1219

Rizzo, L., Manaia, C., Merlin, C., Schwartz, T., Dagot, C., Ploy, M.C., Michael, I., Fatta-Kassinos, D. (2013). Urban wastewater treatment plants as hotspots for antibiotic resistant bacteria and genes spread into the environment: a review. The Science of the Total Environment, 447, pp. 345-360. https://doi.org/10.1016/J.SCITOTENV.2013.01.032

Rodríguez-Molina, D., Mang, P., Schmitt, H., Chifiriuc, M.C., Radon, K., Wengenroth, L. (2019). Do wastewater treatment plants increase antibiotic resistant bacteria or genes in the environment? Protocol for a systematic review. Systematic Reviews, 8(1), pp. 1-8. https://doi.org/10.1186/S13643-019-1236-9

Rodriguez-Mozaz, S., Vaz-Moreira, I., Varela Della Giustina, S., Llorca, M., Barceló, D., Schubert, S., Berendonk, T.U., Michael-Kordatou, I., Fatta-Kassinos, D., Martinez, J.L., Elpers, C., Henriques, I., Jaeger, T., Schwartz, T., Paulshus, E., O'Sullivan, K., Pärnänen, K.M.M., Virta, M., Do, T.T., Manaia, C.M. (2020). Antibiotic residues in final effluents of European wastewater treatment plants and their impact on the aquatic environment. Environment International, pp. 140. 105733. https://doi.org/10.1016/J.ENVINT.2020.105733

Schloss, P.D., Westcott, S.L., Ryabin, T., Hall, J.R., Hartmann, M., Hollister, E.B., Lesniewski, R.A., Oakley, B.B., Parks, D.H., Robinson, C.J., Sahl, J.W., Stres, B., Thallinger, G.G., Van Horn, D.J., Weber, C.F. (2009). Introducing mothur: Open-Source, Platform-Independent, Community-Supported Software for Describing and Comparing Microbial Communities. Applied and Environmental Microbiology, 75(23), pp. 7537-7541. https://doi.org/10.1128/AEM.01541-09

Serra-Burriel, M., Keys, M., Campillo-Artero, C., Agodi, A., Barchitta, M., Gikas, A., Palos, C., López-Casasnovas, G. (2020). Impact of multi-drug-resistant bacteria on economic and clinical outcomes of healthcare-associated infections in adults: Systematic review and meta-analysis. PLOS ONE, 15(1), pp. e0227139. https://doi.org/10.1371/JOURNAL.PONE.0227139

Sharma, E., Kelso, C., Zhang, S., Guo, Y., Sivakumar, M., Jiang, G. (2023). Stability of Colistin and Carbapenems in Water and Wastewater. ACS ES&T Water, 3(11): 3496–3504. https://doi.org/10.1021/acsestwater.3c00219

Smyth, C., O'Flaherty, A., Walsh, F., Do, T.T. (2020). Antibiotic resistant and extended-spectrum β-lactamase producing faecal coliforms in wastewater treatment plant effluent. Environmental Pollution, 262, pp. 114244. https://doi.org/10.1016/J.ENVPOL.2020.114244

Song, J., Choo, Y.J., Cho, J.C. (2008). Perlucidibaca piscinae gen. nov., sp. nov., a freshwater bacterium belonging to the family *Moraxellaceae*. International Journal of Systematic and Evolutionary Microbiology, 58(1), pp. 97–102. https://doi.org/10.1099/ijs.0.65039-0

Tindall, B.J., Rosselló-Móra, R., Busse, H.J., Ludwig, W., Kämpfer, P. (2010). Notes on the characterization of prokaryote strains for taxonomic purposes. International Journal of Systematic and Evolutionary Microbiology, 60(1), pp. 249-266. https://doi.org/10.1099/ijs.0.016949-0

Wang, D., Li, M., Liao, C., Dong, K., Yao, Y. (2025). The occurrence characteristics and ecological risks of antibiotics in surface water and groundwater of the Huixian Wetland. Toxics, 13, pp. 460. https://doi.org/10.3390/toxics13060460

WHO (2019). The 2019 WHO AWaRe classification of antibiotics for evaluation and monitoring of use. Geneva: World Health Organization. (WHO/EMP/IAU/2019.11).

WHO (2023). Antimicrobial resistance. Retrieved January 18, 2023, from https://www.who.int/news-room/fact-sheets/detail/antimicrobial-resistance

Yang, J.H., Park, J.W., Kim, H.S., Lee, S., Yerke, A.M., Jaiswal, Y.S., Williams, L.L., Hwang, S., Moon, K.H (2024). Effects of antibiotic residues on fish gut microbiome dysbiosis and mucosal barrier-related pathogen susceptibility in zebrafish experimental model. *Antibiotics* (Basel). 13(1), pp. 82. https://doi.org/10.3390/antibiotics13010082

Zhang, H., Chang, F., Shi, P., Ye, L., Zhou, Q., Pan, Y., Li, A. (2019). Antibiotic resistome alteration by different disinfection strategies in a full-scale drinking water treatment plant deciphered by metagenomic assembly. Environmental Science & Technology, 53(4), pp. 2141-2150. https://doi.org/10.1021/acs.est.8b05907

Zhang, Z., Qu, Y., Li, S., Feng, K., Cai, W., Yin, H., Wang, S., Liu, W., Wang, A., Deng, Y. (2020). Florfenicol restructured the microbial interaction network for wastewater treatment by microbial electrolysis cells. Environmental Research, pp. 183. 109145. https://doi.org/10.1016/J.ENVRES.2020.109145

Zhang, K., Fan, Y., Chang, S., Fu, Q., Yang, G., Sun, X. (2022). Characterization of antibiotic resistance genes in drinking water sources of the Douhe Reservoir, Tangshan, northern China: the correlation with bacterial communities and environmental factors. Environmental Science Europe, 34, pp. 56. https://doi.org/10.1186/s12302-022-00635-x

Zhao, Y., Gao, J., Wang, Z., Dai, H., Wang, Y. (2021). Responses of bacterial communities and resistance genes on microplastics to antibiotics and heavy metals in sewage environment. Journal of Hazardous Materials, 402, pp. 123550. https://doi.org/10.1016/j.jhazmat.2020.123550

AUTHORS

DONGZE JIANG completed his bachelor's degree in environmental engineering at Óbuda University, Hungary, in 2018, and his master's degree in the same field at the Hungarian University of Agriculture and Life Sciences in 2020. His continuous and specialized academic training has provided him with solid expertise and extensive skill in environmental engineering, along with strong laboratory and experimental skills. In 2020, he began his PhD studies, focusing on research in microbial contamination and antibiotic resistance.

YI YANG graduated in environmental engineering at the Hungarian University of Agriculture and Life Sciences, Gödöllő, Hungary, then she continued her studies at Wageningen University's Master of Environmental Sciences. In 2023, she won a special award at the 36th Hungarian Scientific Student Conference in the Agricultural Science section, Environmental Management division.

MÁTYÁS CSERHÁTI obtained his PhD in 2013 and is currently an Associate Professor at the Institute of Aquaculture and Environmental Safety, MATE. His research interests include the biodegradation of mycotoxins by bacteria and the study of microbial populations affecting soil fertility, utilizing metagenomic and bioinformatic approaches. He also contributes to BSc and MSc education and serves as secretary for international students in the Environmental Sciences Doctoral School since 2014.

BALÁZS KRISZT associate professor is the Director of the Institute of Aquaculture and Environmental Safety at MATE. His expertise lies in environmental microbiology, biodegradation, microbial ecotoxicology, and molecular ecology. He leads research initiatives focusing on environmental safety and microbial interactions in aquatic systems.

EDIT KASZAB earned her PhD in 2011 and serves as Head of the Department of Environmental Safety and Associate Professor at the Institute of Aquaculture and Environmental Safety, Hungarian University of Agriculture and Life Sciences (MATE). Her research focuses on environmental microbiology, including the detection of opportunistic pathogens, antibiotic resistance, and microbial community analysis in various ecosystems. She is actively involved in environmental safety assessments and remediation processes.

Peacebuilding through water cooperation? Institutional design and peace-relevant functions in the Indus and Nile Basins

Ferenc Miklós SULLIVAN

University of Public Service, Faculty of Water Sciences, Budapest, Hungary (email: ferenc.sullivan@gmail.com)

DOI: 10.59258/hk.24061

Abstract

Transboundary water cooperation is often promoted as a pathway to peace, but empirical evidence remains uneven and conceptually underspecified. This article advances a mechanism-oriented approach that links institutional design to peace-relevant functions and applies it to two high-salience basins characterized by power asymmetry, infrastructure expansion, and recurring political shocks: the Indus (Permanent Indus Commission, under the 1960 Indus Waters Treaty) and the Nile (Nile Basin Initiative, launched in 1999, currently transitioning toward a permanent commission following the Cooperative Framework Agreement's (CFA) entry into force in 2024). Using structured, focused comparison and process tracing across emblematic episodes (Indus hydropower disputes and third-party adjudication; Nile programmatic cooperation, early warning, and the political processes surrounding the Grand Ethiopian Renaissance Dam [GERD] and the CFA), the analysis identifies a pattern of form-function complementarity. Legalized bilateralism in the Indus Basin is comparatively strong at producing "negative peace" functions: stabilizing expectations, reducing misperception through the routine of data exchange and channelling disputes into precisely defined technical-legal forums. Programmatic multilateralism in the Nile Basin is comparatively strong at cultivating foundations of "positive peace" by building shared knowledge, professional networks, and cooperative benefits that broaden society's demand for stability. Neither form is sufficient on its own: legalized regimes can become brittle without adaptive and participatory capacities, while programmatic platforms struggle to contain high-stakes distributive conflicts without credible legalization and mechanisms of dispute settlement. The article concludes that the benefits of peace depend on the success of combining rule-based stability with bounded flexibility, along transparent knowledge systems and legitimacy-enhancing participation, while simultaneously maintaining harmony between the support provided by external stakeholders and the role of the riparian states without undermining ownership.

Keywords

Environmental peacebuilding, water diplomacy, transboundary water governance, Indus Waters Treaty, Permanent Indus Commission, Nile Basin Initiative, hydro-hegemony, dispute settlement, institutional design.

Békeépítés vízügyi együttműködésen keresztül? Intézményi tervezés és békével kapcsolatos funkciók az Indus és a Nílus vízgyűjtőjén

Kivonat

A határokon átnyúló vízügyi együttműködést gyakran a béke felé vezető útként írják le, azonban ezen feltételezés empirikus bizonyítékai egyenetlenek, és az elméleti megalapozottsága is hiányos. A jelen tanulmányban kidolgozott mechanizmusorientált megközelítés az intézményi kialakítást a békéhez kapcsolódó funkciókkal köti össze, és ezt két kiemelt jelentőségű vízgyűjtő területen alkalmazza, amelyekre hatalmi aszimmetria, infrastrukturális bővülés és visszatérő politikai sokkok jellemzők. Ezek az Indus (az 1960-as Indus Vízegyezmény által felállított Állandó Indus Bizottság) és a Nílus (az 1999-ben alapított Nílus-medence Kezdeményezés, amely jelenleg egy állandó bizottság létrehozása felé halad a Kooperatív Keretmegállapodás [CFA] 2024-es hatálybalépését követően) vízgyűjtői. Az elemzés strukturált, fókuszált összehasonlítás és folyamatkövetés segítségével, jellegzetes eseteken keresztül (Indus-vízerőművitás és harmadik fél általi döntőbíráskodás; Nílus menti programalapú együttműködés, korai előrejelzés és a Nagy Etióp Reneszánsz Gát [GERD] körüli politikai folyamatok, valamint a CFA), egy forma–funkció komplementaritási mintázatot azonosít. Az Indus-medencében a jogilag szabályozott bilaterális együttműködés viszonylag erős a „negatív béke" funkcióinak megteremtésében: stabilizálja az elvárásokat, rutinszerű adatcsere révén csökkenti a félreértések lehetőségét és a vitákat jól körülhatárolt technikai-jogi fórumok keretei közé tereli. A Nílus-medencében a programalapú multilateralizmus viszonylag erős a „pozitív béke" alapjainak kiépítésében azáltal, hogy közös tudást, szakmai hálózatokat és együttműködési előnyöket hoz létre, amelyek kiszélesítik a stabilitás iránti társadalmi bázist. Egyik forma sem elegendő önmagában: a jogilag szabályozott rendszerek rugalmatlanná válhatnak adaptív és részvételi kapacitások nélkül, míg a programalapú platformok nehezen kezelik a nagy téttel bíró elosztási konfliktusokat hiteles jogi szabályozás és vitarendezési mechanizmusok nélkül.

A tanulmány arra a következtetésre jut, hogy a békéből származó előnyök attól függenek, hogy sikerül-e ötvözni a szabályalapú stabilitást a korlátozott rugalmassággal, az átlátható tudásrendszerekkel és a legitimációt erősítő részvétellel, mindezt úgy, hogy a külső szereplők támogatása összhangban marad a folyóparti államok tulajdonosi szerepével, anélkül, hogy aláásná azt.

Kulcsszavak

Környezeti béketeremtés, vízdiplomácia, határon átnyúló vízkormányzás, Indus-vízegyezmény, Állandó Indus Bizottság, Nílus-medence Kezdeményezés, hidrohegemónia, vitarendezés, intézményi tervezés.

INTRODUCTION

Freshwater basins frequently cut across political borders, turning water into a collective-action problem in which upstream decisions often generate downstream externalities and uncertainty. In policy discourse, this interdependence is regularly framed as an opportunity: negotiated rules and joint institutions can create predictability, reduce conflict risks, and secure cross-sector benefits (*Conca and Dabelko 2002, Sadoff and Grey 2002*). Yet, the "water for peace" narrative sits alongside two persistent doubts. First, cooperation is common, but peace outcomes are not automatic; many river basins have agreements while still experiencing intense securitized bargaining. Second, cooperation can coexist with, or even legitimize, durable inequalities, especially where power is asymmetric and knowledge is politicized (*Zeitoun and Warner 2006, Mirumachi 2015*).

This article addresses these doubts by reframing the research problem from "Does cooperation create peace?" to "Which institutional functions plausibly contribute to peace, through what mechanisms, and under what conditions?" The argument is that peacebuilding effects depend less on whether states cooperate in general and more on the specific institutional pathways that cooperation creates. These include monitoring and transparency regimes; regularized communication; credible compliance management; adaptive operating rules; and participation and accountability arrangements that shape perceived legitimacy (*Giordano et al. 2014, Pahl-Wostl 2015*). These pathways can produce two analytically distinct, though related, forms of peacebuilding:

- Negative peace functions: preventing escalation and containing disputes (*Galtung 1969*).
- Positive peace functions: building legitimate, inclusive and resilient governance that can accommodate change and distributional claims (*Pahl-Wostl 2015, Richmond 2014).*

The study applies a comparative empirical strategy. The Permanent Indus Commission (PIC) and the Nile Basin Initiative (NBI) are prominent and unusually well-documented institutions that embody contrasting design philosophies. The PIC is a treaty-mandated bilateral commission embedded in a dense legal-technical rule system and a formal dispute-settlement ladder. The NBI is a multi-riparian, transitional platform centred on programme delivery, shared knowledge and capacity building, historically underpinned by substantial donor financing and only recently moving toward a more formal legal-institutional order via the Nile Cooperative Framework Agreement (CFA). Both institutions operate under pronounced power asymmetries and high hydropolitical salience, making them suitable "stress tests" for institutional performance under rivalry.

This article argues that the peacebuilding potential of transboundary water cooperation depends not primarily on the existence of institutions, but on the specific functions those institutions perform. It identifies five institutional functions – transparency, predictability, compliance management, adaptive learning and legitimacy – that mediate the relationship between cooperation and peace outcomes. Through a structured comparison of the Indus and Nile basins, it shows that different institutional designs produce distinct bundles of these functions. Durable peacebuilding is most likely when these functions are combined rather than treated as substitutes.

ENVIRONMENTAL PEACEBUILDING AND INSTITUTIONAL DESIGN: CONCEPTS AND EXPECTATIONS

Environmental peacebuilding and the "contingency" problem

Environmental peacebuilding examines how environmental interdependence can be leveraged to mitigate conflict risks and promote cooperative relations (*Conca and Dabelko 2002, Ide 2018*). Early environmental security debates often assumed a direct link between resource scarcity and violent conflict. Subsequent research has largely rejected deterministic claims, instead emphasizing that scarcity and variability operate as risk multipliers filtered through institutions, governance capacity and political contestation.

The central theoretical challenge is contingency: institutions can enable cooperation but can also fail or succeed in narrow ways that do not translate into broader peace. Liberal institutionalist accounts emphasize how legalization (precision, monitoring, adjudication) reduces transaction costs and creates credible commitments (*Keohane 1984, Abbott et al. 2000*). Adaptive governance scholarship highlights that rigid rules can become maladaptive under climatic uncertainty and socio-technical change; institutions must therefore combine predictability with bounded flexibility and learning (*Cosens et al. 2014, Pahl-Wostl 2015*). Political ecology and hydro-hegemony critiques argue that cooperation may reflect and reproduce power, shaping "whose knowledge counts" and how costs and benefits are distributed (*Zeitoun and Warner 2006, Cascão 2009*). From this perspective, peacebuilding hinges on legitimacy: whether affected actors perceive outcomes as fair and procedures as accountable.

Water diplomacy, institutions and peace-relevant functions

Water diplomacy refers to the use of negotiation and institutional design to prevent, manage and resolve disputes over shared waters while enabling equitable and sustainable use (*Sadoff and Grey 2002*). With regard to peacebuilding, the relevant question is not merely whether institutions exist, but which functions they reliably deliver. This article focuses on five peace-relevant institutional functions, each linked to observable mechanisms:

(1) Transparency and shared facts: joint monitoring, standardized datasets and information-sharing routines reduce uncertainty and rumour-driven escalation (*Giordano et al. 2014*).

(2) Predictability and expectation management: clear rights and obligations, time-bound procedures and regular meetings stabilize behaviour even when trust is low (*Abbott et al. 2000*).

(3) Credible compliance management: escalation ladders and third-party processes provide authoritative interpretations and reduce incentives to "test" the other side through unilateral action (*Brochmann and Hensel 2009*).

(4) Bounded flexibility and learning: review clauses, standing technical groups and iterative joint studies allow adaptation to shocks without compromising predictability (*Cosens et al. 2014*).

(5) Legitimacy and inclusion: participation, public transparency and attention to distributional fairness reduce contestation and strengthen domestic buy-in for cooperation (*Derman and Ferguson 2003*).

These functions map imperfectly onto negative and positive peace. Transparency, predictability, and compliance management are most directly linked to negative peace (containment). Learning, inclusion, and fairness are central to positive peace (legitimacy and resilience), though they also reduce escalation risks by lowering grievance intensity.

The following diagram (*Figure 1*) summarizes the article's conceptual framework, linking institutional design to peace-relevant functions and outcomes:

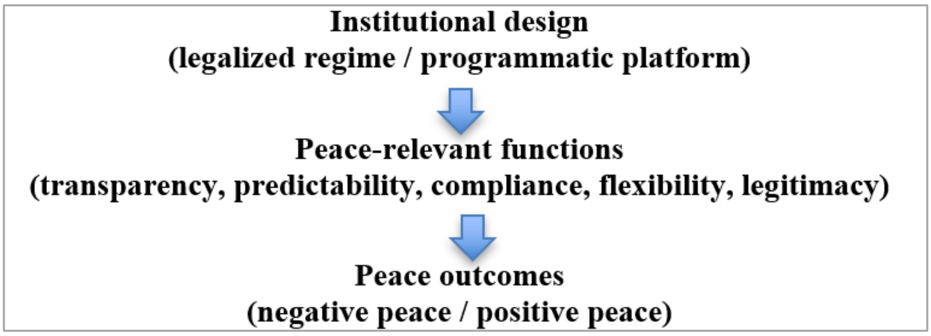

Figure 1. Conceptual framework (own work)
1. ábra. Fogalmi keretrendszer (saját szerkesztés)

Testable expectations

The framework yields four hypotheses, treated as probabilistic rather than deterministic factors:

- H1 (Transparency–stability): credible monitoring and accessible information correlate with fewer/shorter crises over water operations (*Giordano et al. 2014*).
- H2 (Flexibility–resilience): institutions that combine clear rules with bounded flexibility sustain cooperation better during climatic or political shocks (*Cosens et al. 2014*).
- H3 (Inclusion–legitimacy): formal mechanisms for stakeholder participation and accountability increase perceived fairness and reduce contestation (*Derman and Ferguson 2003, Pahl-Wostl 2015*).
- H4 (External support–durability): aligned external finance and facilitation strengthen institutions when embedded in local ownership and sensitive to sovereignty (*Paisley and Henshaw 2020*).

METHODS AND COMPARATIVE FRAMEWORK

Research design and evidence base

The analysis employs a qualitative, structured, and focused comparison (*George and Bennett 2005*). It combines (i) document analysis of treaty texts, institutional reports, and third-party records; (ii) indicator-based assessment to structure cross-case comparison; and (iii) process tracing of selected episodes to identify causal mechanisms linking institutional practices to peace-relevant outcomes (*Beach and Pedersen 2013*).

The unit of analysis is the institutional regime at the basin scale: the Indus Waters Treaty/Permanent Indus Commission regime and the Nile Basin Initiative regime, including its current transition towards a permanent commission under the Cooperative Framework Agreement (CFA). The empirical focus is primarily on the period since the late 1990s, when both basins faced intensified infrastructure development and climate-related variability.

The Indus and Nile cases constitute a most-different institutional design comparison. The Indus regime represents a highly legalized bilateral treaty with detailed rules and a formalized dispute-resolution ladder. The Nile Basin Initiative represents a programmatic multilateral platform emphasizing joint projects, knowledge production, and gradual institutionalization. Despite these institutional differences, both basins exhibit similar structural challenges – power asymmetry, infrastructure expansion, and recurrent political tension – making them suitable comparative stress tests for assessing how institutional design conditions peace-relevant functions.

Comparative indicators

To compare different institutional forms, the framework operationalizes peace-relevant performance across the following dimensions:

A. Cooperation capacity: precision and adaptability of rules, operational coordination, data exchange, and monitoring.

B. Conflict management: early-warning and shock-response protocols, dispute-settlement design and use, and crisis performance.

C. Participation and accountability: stakeholder voice, transparency, and distributional fairness signals.

D. External influences: donor engagement, geopolitics, and third-party facilitation.

Indicators are scored on an ordinal 0–3 scale (absent to strong/embedded) based on observable evidence. The purpose is not to produce a definitive ranking but to provide a comparison, highlight consistent strengths and gaps, and guide process tracing toward mechanisms rather than outcomes alone.

HISTORICAL, TECHNICAL AND WATER-RELATED CONFLICT DIMENSIONS OF THE INDUS AND NILE BASINS

The preceding framework links institutional design to peace-relevant functions. That link becomes clearer if the Indus and Nile cases are presented as historically layered and technically specific water conflicts instead of merely generic examples of cooperation under scarcity. In both basins, disputes over institutional form are inseparable from earlier state-building projects, inherited legal claims, contested hydraulic infrastructures, and uncertainty over future hydrology. This chapter, therefore, supplements the comparative analysis by specifying the historical, technical, and water-related dimensions that activate the five institutional functions identified above.

The analytical point is that historical narratives shape what riparian states regard as legitimate, while technical design choices determine how much discretion infrastructure operators possess and how easily suspicions can lead to concerns over national security. Water-related risks such as floods, droughts, storage operations, sedimentation, environmental flows, and seasonal variability then determine whether institutions merely process paperwork or provide useful risk-reduction capacity. The chapter thus treats the two basins as hydropolitical systems characterized by the interaction of legal rules, engineering choices, and political attitudes.

Indus: partitioned hydraulic space and low-trust engineering

The Indus conflict is rooted in the abrupt political partition of an already integrated irrigation system. Colonial Punjab had been transformed through canals, barrages, and command areas, the logic of which followed gradients, soils, and headworks rather than later international borders. The 1947 partition divided this system between India and Pakistan, leaving several important headworks upstream in India while major canal-dependent command areas lay downstream in Pakistan. The resulting 1948 canal-water crisis converted a technical problem of irrigation continuity into an existential concern for the new Pakistani state (*Alam 2002*, *Zawahri 2009*).

The 1960 Indus Waters Treaty stabilized this conflict by replacing joint basin development with a territorialized allocation of rivers. India obtained use of the Eastern Rivers (Ravi, Beas, and Sutlej), while Pakistan obtained the main use of the Western Rivers (Indus, Jhelum and Chenab), subject to limited Indian non-consumptive, agricultural, and run-of-river hydropower uses under the Treaty and its annexures (*UNTS 1960*). The bargain worked because it reduced day-to-day bargaining over volumes, but it also locked the parties into a compartmentalized form of cooperation. It can be described as peace-preserving arrangement rather than a basin-planning arrangement.

The political setting made this design especially significant. The headwaters and several hydropower sites lie in or near Jammu and Kashmir, a territory central to the India-Pakistan rivalry. Water disputes, therefore, become easily entangled with sovereignty, territorial security, and national identity. Even when disagreements are of a technical nature, they are rarely interpreted as pure technicalities in domestic debate. This explains why the PIC can keep communication open without necessarily improving broader political trust. It also explains why India's April 2025 decision to hold the Treaty "in abeyance" had hydropolitical significance beyond its immediate hydrological effects; the move signalled that the water regime itself could become an instrument of political pressure during security crises (*Singh and Shahid* 2025, *von Lossow 2025*).

Technically, contemporary Indus disputes concentrate on the design and operation of Indian run-of-the-river hydropower projects on the Western Rivers. The central question is not simply whether India may build such projects – the Treaty permits them within limits – but how design features affect the possibility of flow manipulation. Spillway gates, low-level outlets, pondage, drawdown flushing, sediment management, intake elevations, and dead storage are, therefore, politically sensitive engineering parameters. They define the margin between legitimate hydropower generation and perceived upstream control.

The Baglihar proceedings, closed in 2007, illustrate this pattern. Pakistan challenged design features of the Baglihar plant on the Chenab, especially matters linked to gated spillways, pondage, power intake levels, and flood design. The Neutral Expert accepted some of India's engineering arguments but required modifications and emphasized that Treaty interpretation had to take account of contemporary engineering standards as well as the Treaty text (*Salman 2008*). The episode demonstrates that technical modernization can be incorporated through adjudication, but also that in the absence of agreed updating mechanisms, each new project can reopen questions embedded in the 1960 design logic.

The Kishenganga arbitration of 2013 added an ecological and diversion dimension. The Court of Arbitration allowed India to proceed with a hydropower diversion but required a minimum flow in the Kishenganga/Neelum River and clarified limits on drawdown flushing (*PCA 2013*). The award is important because it shows how water-related conflict has expanded from allocation to the interaction of hydropower efficiency, environmental flows, sediment management, and downstream livelihoods. In this sense, the Indus regime increasingly manages technical externalities that were not central to the original partition bargain.

Hydrologically, the Indus Basin is exposed to seasonal and climatic uncertainty. Upper Indus flows depend on snowmelt, glacier melt, and monsoon rainfall, with substantial sub-basin variation. Glacier and snow processes buffer flows during dry periods, but climate change may alter the timing, variability, and reliability of that buffering effect (*Lutz et al. 2014, Biemans et al. 2019*). This matters for conflict because a delayed monsoon, extreme flood, rapid melt event, or low-flow season can turn routine dam operations into evidence for hostile narratives. The peace-relevant value of the PIC's data exchange and inspection routines therefore lies not only in legal compliance but in reducing misperceptions during hydrological stress.

The Indus case thus has a distinctive conflict structure. It is historically rooted existential dependence, technically precise but contested hydropower rules, and water-related risks intensified by climatic variability. This combination explains why the PIC is strong at negative peace. It converts a dispute about possible upstream coercion into a reviewable claim about design criteria, data, and procedure. However, the same structure also shows the limits of this form. Without a legitimate pathway for updating technical standards, sediment rules, environmental flow practices, and extreme-event protocols, the Treaty may increasingly rely on litigation-like processes to solve adaptive problems. The basin-specific supplement to the article's findings is, therefore, that Indus peacebuilding requires not only preserving the IWT's dispute ladder but also modernizing its technical interface with climate, sediment, and ecological realities.

Nile: historical rights, upstream development and reservoir coordination

The Nile conflict is historically different from the Indus because it did not originate in a single territorial partition of infrastructure. Instead, it developed from a long legal and diplomatic history in which downstream control and prior-use claims were privileged. In the past two centuries, a total of ten water-related agreements were concluded in the Nile basin, all of which favoured Egypt and failed to resolve conflict between countries *(Azizi and Leandro 2025).* The 1929 arrangements and the 1959 Agreement between Egypt and Sudan entrenched downstream allocations and administrative understandings without the consent of most upstream riparian states. The latter agreement allocated 55.5 billion cubic metres annually to Egypt and 18.5 billion cubic metres to Sudan, measured at Aswan, while no quantitative share was allocated to Ethiopia or the equatorial riparian states (*UAR and Sudan 1959, Waterbury 2002*).

This historical settlement became a legitimacy problem as upstream states gained capacity and sought space for development. Ethiopia, whose highlands contribute most of the Blue Nile flow, rejected the idea that colonial or bilateral agreements could permanently constrain its development options. The Nile Basin Initiative, launched in 1999, attempted to move beyond this legal deadlock by emphasizing a shared vision, technical studies, and cooperative investment preparation. Yet the underlying disagreement over historical rights versus equitable and reasonable utilization remained unresolved (*Cascão 2009, Salman 2013*).

The Cooperative Framework Agreement (CFA) represents an effort to transform that disagreement into a basin-wide legal framework. Its entry into force in October 2024 among ratifying parties is therefore a major institutional development. However, it is also a partial one because Egypt and Sudan have refused to join the settlement. The transition from the NBI to a permanent Nile River Basin Commission thus occurs under a paradox: legal institutionalization is progressing, but not yet inclusively enough to settle the most sensitive downstream-upstream disputes (*NBI 2024*).

Technically, the Nile dispute is centred on large reservoir operation rather than on the detailed design criteria of many small or medium projects. The Grand Ethiopian Renaissance Dam (GERD) is the key infrastructural facility. Located on the Blue Nile near the Sudanese border, it has a reservoir volume of approximately 74 cubic kilometres, roughly equivalent to more than one annual Blue Nile flow at key downstream gauges, depending on the hydrological baseline used (*IHA n.d.).* The dam is designed primarily for hydropower generation, not consumptive irrigation. Nevertheless, the timing of filling, drought-year releases, and coordination with Sudanese dams and Egypt's High Aswan Dam have major distributional consequences.

The technical disagreement is therefore not reducible to whether Ethiopia may generate hydropower. It concerns who bears hydrological risk during filling, prolonged drought, and multi-reservoir operation. From Ethiopia's perspective, faster filling and flexible operation improve energy security and sovereign development. From Egypt's perspective, however, the crucial issue is the reliability of downstream supply during low-flow sequences. Sudan's position has been more ambivalent because the GERD can offer flood regulation, sediment reduction, and electricity benefits, while also creating operational risks if information and coordination are insufficient (*Waterbury* 2002, *Wheeler et al. 2020*).

The water-related dimension is amplified by the Nile's variability. The Blue Nile is highly seasonal, with the Ethiopian highlands providing a large share of annual flow during a concentrated wet season. Climate variability affects both flood and drought risks, and future climate change may increase uncertainty around the frequency and severity of extremes (*Conway 2005, Swain 2011*). Under these conditions, a technically rational dam operation from one national perspective may be interpreted as threatening from another if data, rules, and communication are inadequate. The peace-relevant challenge is, therefore, to transform hydrological uncertainty into jointly managed risk rather than politically exploitable suspicion.

Sediment and flood management also complicate the picture. The GERD can trap sediment and regulate flood peaks, creating benefits for hydropower operation and downstream infrastructure, but these benefits depend on coordinated reservoir rules, reliable seasonal forecasts, and a shared understanding of risk thresholds. Quantitative modelling shows that coordinated operation and transparent drought-management rules can reduce risks for multiple parties, whereas unilateral operation increases the probability of extreme hydrological conditions becoming political crises (*Wheeler et al. 2020*).

The Nile case has a conflict structure built around contested legal history, a rebalancing of upstream development capacity, and a technical need for multi-reservoir coordination under uncertainty. This explains why the NBI is strong at positive peace foundations but weaker at acute conflict containment. Shared tools, professional networks, and joint studies are valuable, but they do not themselves specify how much risk each party will bear during a prolonged drought or how release decisions will be verified. The basin-specific supplement to the article's findings is, therefore, that Nile peacebuilding requires the programmatic gains of the NBI to be translated into modular, credible and inclusive operating rules for data exchange, drought triggers, emergency coordination, and long-term reservoir management.

Comparative conflict profile

Table 1. Historical, technical, and water-related conflict profile (own work)
1. táblázat. A konfliktus történeti, műszaki és vízügyi profilja (saját szerkesztés)

Dimension	Indus Basin	Nile Basin
Historical conflict driver	Partition of an integrated irrigation system; Kashmir-linked security rivalry; downstream dependence after upstream headworks remained in India.	Colonial and bilateral downstream legal claims; upstream exclusion from earlier allocation arrangements; changing regional power balances.
Primary technical object	Run-of-river hydropower design on Western Rivers: spillways, pondage, outlets, intake levels, sediment and diversion impacts.	Large-reservoir filling and operation: GERD coordination with Sudanese dams and High Aswan Dam, drought releases and flood regulation.
Water-related risk	Low-flow periods, monsoon floods, glacier/snowmelt variability, project-specific flow manipulation fears and ecological flow impacts.	Multi-year drought, high seasonal variability, flood-risk management, sediment trapping and distribution of storage benefits and risks.
Peace-relevant institutional need	Protect routine data exchange and dispute procedures while adding adaptive protocols for modern hydropower, sediment, environmental flows and extremes.	Preserve NBI knowledge systems while developing credible operating rules for data sharing, drought triggers, coordinated releases and inclusive CFA/NRBC transition.

Cross-case implications for the analysis and conclusions

Three cross-case implications can be drawn from the above. First, historical path dependence heavily influences the legitimacy of institutions. In the Indus, legitimacy rests on the Treaty as a substitute for trust after partition; in the Nile, legitimacy is contested because the inherited allocation order excluded many upstream riparian states. This means that similar institutional functions can have different political meanings. A dispute-settlement procedure in the Indus may be viewed as protecting a hard-won bargain, while a legal framework in the Nile may be viewed by non-parties as either a corrective to historical exclusion or as a new source of bloc politics.

Second, technical specificity shapes the kind of peacebuilding that is possible. Indus disputes are often project-specific and can be translated into design criteria, measurements, and adjudicative questions. This favours legal-technical containment. Nile disputes are more system-wide because GERD operation interacts with downstream reservoirs and drought management across the basin. This favours joint modelling, scenario planning, and operating rules, but also requires political agreement on risk sharing. The comparison, therefore, confirms that institutions do not perform peace functions in the abstract; they perform them through the technical objects they are able to govern.

Third, water-related risks are temporal. Conflict is not only about average annual allocation but also about timing: when water is stored, released, withheld, diverted, or forecast. Both basins show that peace-relevant institutions must be designed for hydrological sequences rather than static entitlements. In the Indus, project notifications and inspections must remain reliable during floods, droughts, and security crises. In the Nile, drought-year rules, seasonal forecasts, and reservoir-operation transparency are more important for crisis prevention than general declarations of cooperation.

The practical implication is a modular reform agenda. For the Indus, priority modules would include updated technical guidance on contemporary hydropower design, sediment management, environmental flows, extreme-event data exchange, and non-politicization of Commission contacts. For the Nile, priority modules would include real-time GERD data exchange, agreed drought triggers, coordinated operation protocols, independent joint fact-finding, and pathways for non-parties to participate in technical cooperation even where legal accession remains politically difficult. In both basins, peacebuilding through water cooperation depends on making historical grievances discussable, technical claims verifiable, and hydrological risks jointly manageable.

CASE I: PERMANENT INDUS COMMISSION UNDER THE INDUS WATERS TREATY

Institutional origins and design logic

The Indus Waters Treaty of 1960, negotiated with World Bank involvement (*UNTS 1960*), is often cited as a durable example of water diplomacy between adversarial neighbours. Its central bargain is a geographical partition of rivers, coupled with a detailed operational-technical rule system. The Permanent Indus Commission was established as the routine bilateral mechanism for treaty implementation in the Indus River basin. *(See Figure 2 for map.)* It is mandated to exchange data, review planned measures, undertake inspections, and serve as the first forum for questions under the treaty.

The IWT's core bargain was a geographic partition of rivers: India received rights over the "Eastern Rivers" (Ravi, Beas, Sutlej), while Pakistan received rights over the "Western Rivers" (Indus, Jhelum, Chenab), subject to limited Indian "non-consumptive uses" (e.g., run-of-river hydropower) and agrarian transition on the Eastern system (*UNTS 1960, Arts. II–III*). To enable Pakistan to replace irrigation supplies lost from the Eastern Rivers, the parties concluded, alongside the Treaty, the Indus Basin Development Fund Agreement (IBDF), mobilizing an unprecedented international financing package administered by the World Bank and contributed by Australia, Canada, Germany, New Zealand, the United Kingdom, the United States, India (via Treaty payments), and the Bank itself (*IBDF 1960, WB 1960–1975*).

The IWT's design reflects a "low-trust engineering" logic: instead of relying on broad principles and flexible bargaining, it encodes specific entitlements and constraints and provides procedures to test compliance. This is visible in its annexes governing hydropower and storage design parameters and in its graduated dispute-settlement ladder: the PIC addresses questions first; certain "differences" can proceed to a Neutral Expert; and specified "disputes" can proceed to a Court of Arbitration. The design aims to (I) reduce uncertainty, (ii) limit discretionary space, and (iii) ensure that disagreements are handled within bounded procedures rather than through coercive signalling.

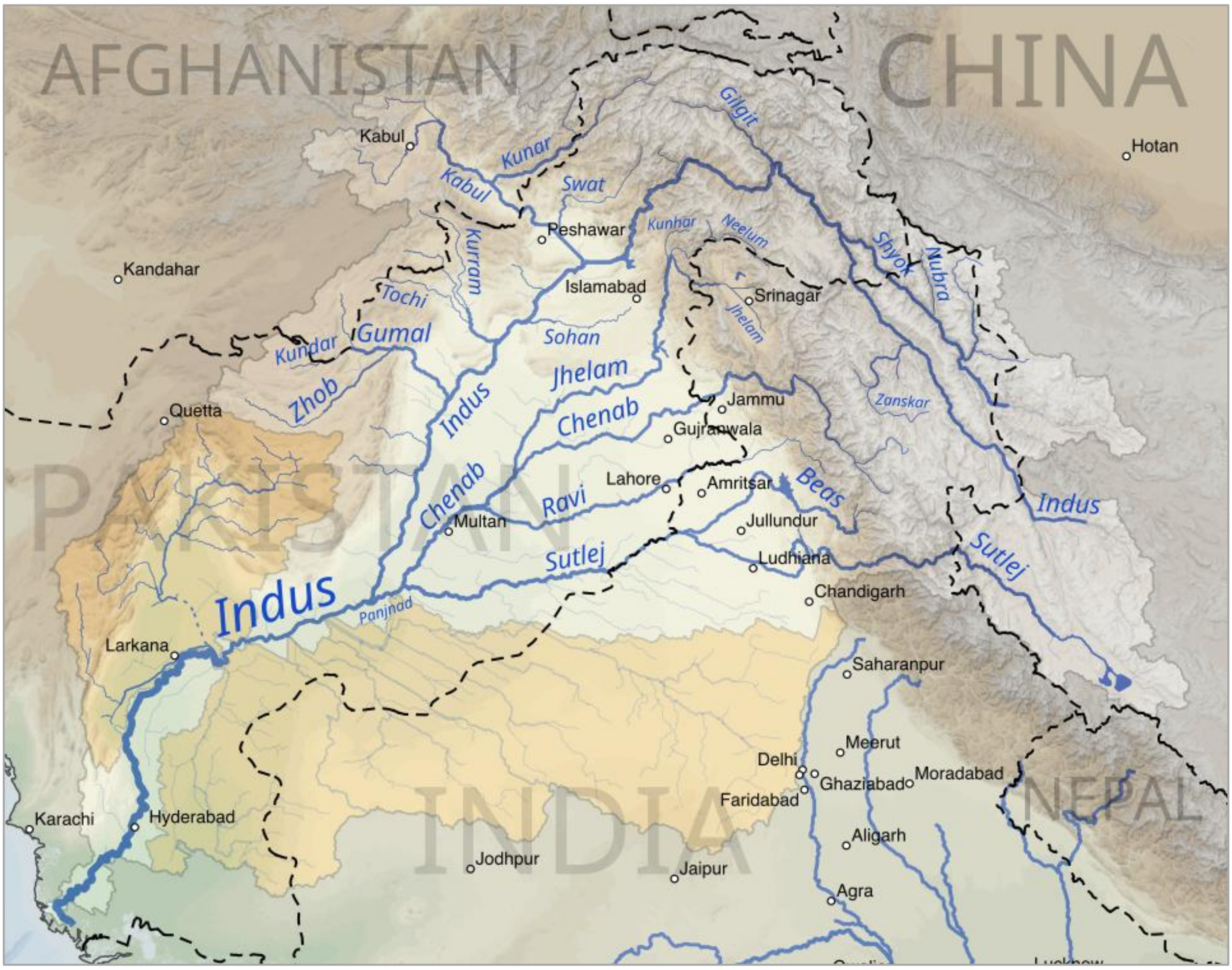

Figure 2. Map of the Indus River basin (URL1)
2. ábra. Az Indus folyó vízgyűjtője (URL1)

Peace-relevant practices: communication, data and bounded adjudication

The Pick's peace-relevant contributions arise from what can be described as routine-based, technical diplomacy. Regular meetings, systematic data exchange, and the possibility of joint inspections create repeated interaction even when political relations deteriorate. This interaction does not eliminate rivalry, but it provides a predictable channel through which concerns can be expressed and clarified.

The dispute-settlement ladder is central to compliance management. It lowers the temptation to respond to contested infrastructure with retaliatory measures by providing a forum in which claims can be assessed against treaty criteria and technical evidence. Two widely discussed episodes illustrate the mechanism.

Baglihar (Neutral Expert, 2005–2007): Pakistan challenged aspects of an Indian hydropower project's design on a western river, arguing that certain features could enable manipulation of flows. The Neutral Expert's decision allowed particular design choices while requiring modifications, balancing treaty constraints with contemporary engineering considerations (*Salman 2008*). The peace-relevant mechanism lies in procedural containment. Rather than triggering retaliatory infrastructure development or broader diplomatic escalation, the Baglihar dispute was translated into a technical-legal process governed by the treaty's dispute-settlement ladder. (The treaty established three-tiered dispute resolution system [PIC → Neutral Expert → Court of Arbitration] with specific technical annexures detailing design and operational parameters for Indian projects on the Western Rivers (*UNTS 1960, Arts. VII–IX; Annexures D–G*). The Treaty has often been cited as a "gold standard" for hydro-diplomacy because it has survived multiple wars [1965, 1971, 1999], territorial crises, and prolonged diplomatic freezes while providing a continual venue for notification, data exchange, site inspections, and disagreement management (*Zawahri 2009*). The Neutral Expert's decision clarified design parameters and required specific engineering modifications, allowing project construction to proceed while addressing Pakistan's concerns. The episode demonstrates how legalized procedures can transform potentially escalatory infrastructure disputes into bounded technical disagreements subject to authoritative determination.

Kishenganga *(PCA 2013*): Pakistan initiated arbitration concerning a hydropower diversion project. The tribunal permitted India to proceed with the diversion for hydropower but required a minimum environmental flow and placed limits on certain storage practices, thereby clarifying contested interpretations (*PCA 2013*). Again, even though both sides criticized aspects of the award, the process produced an authoritative reference point that enabled project continuation under constraints, reducing the likelihood of unilateral escalation.

These episodes support the claim that legalized precision, combined with third-party procedures, can convert disputes into "bounded" technical-legal disagreements. This tends to contribute to negative peace by containing escalation and by maintaining communication under stress.

Institutionalized routines as a channel of negative peace

The PIC's everyday work is mundane by design: exchanging hydrological and operational data, reviewing planned measures, organizing inspections, and producing annual reports. Yet this routine-based process is precisely what can matter for negative peace. In crises, the greatest escalation risks often arise from uncertainty and worst-case assumptions, for example, fears that an upstream actor may be withholding water, manipulating reservoir releases, or using infrastructure as a coercive tool. Data exchange at regular intervals and the possibility of verification through inspections reduce the plausibility of such claims and provide decision-makers with an alternative to public accusation.

The durability of these routines is often emphasized in studies on the Indus regime because the treaty and commission persisted through major interstate crises and wars. This persistence should not be overstated as evidence of "friendship", but it does indicate that both states historically perceived continued technical engagement as instrumentally valuable, even when political relations collapsed. From a peacebuilding perspective, the PIC therefore functions as an institutional "firebreak": it does not resolve conflict, but it reduces the likelihood that water issues become accelerants during broader confrontations.

Limits: brittleness, narrow scope and legitimacy constraints

The PIC's strengths are also its constraints. The IWT prioritizes allocation stability and dispute containment but provides limited scope for joint basin planning, benefit, sharing or ecological governance. Environmental considerations are weakly embedded: participation is largely confined to state water bureaucracies; and transparency to the public is limited, often mediated through national political narratives. From a positive peace perspective, the institutional model produces a "thin" form of cooperation whose legitimacy depends on state acceptance and performance rather than on broader societal accountability.

A second limit is adaptability. The treaty's detailed engineering provisions were designed for mid-twentieth-century conditions. As infrastructure technologies evolve and climatic variability intensifies, these precise rules can become focal points of contestation rather than stabilizers. Adjudication can substitute for explicit flexibility to a point, but repeated litigation-like processes increase transaction costs and can politicize technical disagreements.

A third limit is the vulnerability of procedure to politics. Legalization only supports peacebuilding if parties continue to recognize the legitimacy of the process. When political leaders seek to renegotiate, suspend, or reinterpret commitments, or when parallel legal tracks create the possibility of conflicting outcomes, the very architecture meant to contain disputes can become a fault line. This highlights a general peacebuilding lesson: institutions that rely on procedure must be insulated from geopolitical shocks to preserve their stabilizing functions.

Third parties and the politics of procedural credibility

Third-party roles are unusually prominent in the Indus regime and help explain its resilience. The World Bank's involvement in the treaty's formation and in the financing package that enabled Pakistan's post-partition "replacement works" created reputational and material stakes in maintaining the agreement. More importantly for contemporary peacebuilding, the treaty assigns external appointment functions in the Neutral Expert and arbitration procedures. These functions are narrow, but they matter because they sustain a credible pathway when bilateral political relations stall. In institutional terms, third parties increase the credibility of commitments by lowering the risk that one party can unilaterally block dispute settlement.

As a sign of severely deteriorating relations between the two countries, India announced the immediate unilateral suspension of the IWT in April 2025 following a terrorist attack in Kashmir that claimed the lives of multiple civilians. While deliberately falling short of formal withdrawal, the move reflected the growing inclination to use the IWT, and treaties in general, as instruments of political pressure (*Zehra 2025*). One year after India's decision, it remains unclear whether it was a genuine break in cooperation or rather an episode of prolonged tactical manoeuvring.

CASE II: NILE BASIN INITIATIVE AND THE CFA TRANSITION

Institutional logic: shared vision, program delivery and gradual legalization

The Nile Basin Initiative, launched in 1999, was designed as a transitional platform to move the basin from fragmented arrangements toward cooperative, basin-wide planning in the Nile River basin (*Figure 3*). Its institutional architecture includes a council of ministers (Nile-COM), a technical advisory committee (Nile-TAC), and a secretariat (Nile-SEC), alongside sub-basin implementation centres in the Eastern Nile and the Nile Equatorial Lakes. Unlike the IWT, the NBI did not begin with a binding basin-wide allocation treaty. Its core instruments were programmatic: joint studies, capacity building, shared information systems, and cooperative investment preparation. Obviously, Egypt and Sudan would have strongly objected to an IWT-like treaty as they insist on historical rights and their bilateral water-sharing agreement from 1959, which distributed the entire flow volume between the two countries.

The NBI's "shared vision" approach reflects a different cooperation theory. In politically contested basins, sustained joint work on information and projects can build trust, professional networks, and shared problem definitions that later support legalization. This approach has been supported by extensive donor engagement, including trust-fund financing and the involvement of development banks, which enabled data systems and investment pipelines that many riparian states could not fund alone (*NBI n.d.*)

Programmatic cooperation and the production of cooperative constituencies

The NBI's comparative strength lies in its capacity to generate what might be termed "cooperative constituencies." When basin initiatives produce tangible outputs – such as improved flood forecasting systems, regional power interconnections, or jointly prepared investment projects – state agencies, utilities and regional planners acquire practical interests in maintaining cooperation. These actors can act as stabilizing forces within national policy debates, advocating continued engagement with basin institutions even when interstate rhetoric becomes confrontational (*Sadoff and Grey 2002*).

In practice, such constituencies are uneven across the Nile. They are strongest in the Nile Equatorial Lakes region, where cooperative power and infrastructure projects can be linked to regional integration agendas. They are weaker in the Eastern Nile, where dam operations and drought risk distribution dominate security narratives and where benefits and risks are perceived as concentrated. The NBI's peacebuilding effects are therefore spatially differentiated: it can contribute to stabilization and integration in some sub-basins while remaining peripheral to the most securitized disputes in others.

Peace-relevant practices: knowledge systems, early warning, and cooperative benefits

The NBI's peace-relevant contributions are most evident in mechanisms that reduce uncertainty and generate cooperative benefits. Basin-wide decision-support tools and scenario analysis strengthen the epistemic basis for planning and can reduce factual contestation. Flood forecasting and early warning in parts of the basin provide an applied form of risk management that can save lives and strengthen the perceived utility of cooperation. In the Nile Equatorial Lakes region, cooperative hydropower and electricity network interconnection projects create material incentives for collaboration: shared infrastructure and cross-border power trade can broaden constituencies that benefit from stability.

These practices align closely with the foundations of positive peace. They foster social learning and professionalize interaction among riparian agencies; they can improve administrative capacity; and they can make cooperation visible through tangible outputs. The NBI's participatory architecture, though uneven, is also generally more developed than the PIC's state-centric model: consultations and stakeholder forums are used in several programmes to engage line ministries, utilities, and, at times, civil society and local actors (*Paisley and Henshaw 2020*).

Figure 3. Map of the Nile River basin (URL2)

3. ábra. A Nílus vízgyűjtője (URL2)

Limits: high-stakes distributive politics and the challenge of non-participation

The NBI's principal limitation is that programmatic cooperation does not necessarily resolve high-stakes distributive conflicts where sovereignty and national identity are salient. The construction and staged filling of the GERD on the Blue Nile and the unresolved negotiations over long-term drought management and coordinated operations illustrate this limitation. While the NBI has facilitated basin-wide dialogue and technical work, the most politically charged bargaining has often been handled in separate forums under the auspices of the African Union or through ad hoc negotiations. Where trust deficits are high and perceived risks are existential, cooperative projects and knowledge products may be insufficient to prevent securitized escalation narratives unless paired with credible legal commitments. Quantitative risk-modelling work suggests that coordinated reservoir operation and transparent rules could reduce drought-management risks for multiple parties (*Wheeler et al. 2020*).

A second limitation is fragmentation through non-participation. Egypt and Sudan have remained outside the Cooperative Framework Agreement and contest aspects of its approach to "water security." This constrains the prospect of a truly basin-wide legal-institutional settlement and raises transition risks: the movement from a transitional initiative (NBI) to a permanent commission (Nile River Basin Commission, NRBC) must preserve existing knowledge systems and cooperation routines while creating incentives for non-parties to engage. The NBI experience therefore illustrates an important institutional dilemma: inclusiveness in membership may be necessary for legitimacy, but achieving inclusive legalization can be politically difficult, and partial legalization may harden bloc politics if not managed carefully.

The 2024 CFA entry into force: opportunity and stress test

The CFA's entry into force in October 2024 represents a significant step towards formalizing basin-wide cooperation among ratifying parties. In principle, it enables a shift from donor-dependent programme delivery to a more permanent governance structure with clearer mandates. At the same time, because major downstream actors remain outside, the CFA's institutionalization is also a stress test for whether partial legalization can coexist with basin-wide functional cooperation. If the transition is perceived as exclusionary, it may reduce the NBI's capacity to serve as a neutral platform; if it is managed as a flexible, open-ended framework that preserves technical cooperation and offers pathways for accession, it can strengthen both negative and positive peace functions over time (*Muhumuza 2024*).

At the same time, third-party involvement also creates vulnerability in terms of legitimacy. When parties contest the competence of a tribunal or accuse external actors of bias, procedural credibility can erode, and water disputes can re-enter the arena of geopolitical signalling. The Indus experience therefore suggests that third-party roles must be carefully designed: they should be predictable, limited to clearly defined functions, and embedded in mutually accepted rules that reduce the scope for politicized contestation.

Financing, capacity and the donor-state bargain in the Nile

External support has been central to the NBI's institutional development. Donor financing enabled the creation and maintenance of the NBI's three-centre architecture (secretariat and sub-basin offices), supported basin-wide knowledge systems, and underwrote the preparation of cooperative investments. This support can be interpreted as a "donor-state bargain": donors provided resources to a cooperative platform that promised regional benefits, while riparian states retained sovereignty by emphasizing that the NBI is not a supranational authority but an intergovernmental partnership.

The bargain has clear benefits for peacebuilding: it makes cooperation materially feasible, sustains regular interaction, and enables the production of visible cooperative goods. Yet it also generates a well-known risk: when core budgets and programme pipelines depend heavily on external finance, perceptions of donor-driven agendas may undermine ownership. The NBI's trajectory therefore underscores H4's caveat: external support strengthens durability when it is aligned with basin priorities, transparent in accountability, and paired with gradual increases in member-state financing and political commitment (*NBI 2020*).

The CFA transition as institutional evolution

The CFA's entry into force offers a window into institutional evolution, e.g. how basins attempt to move from functional cooperation to a more formal legal order. This is of prime importance because different tasks incur different political costs. Data sharing, joint training and early warning can often be agreed upon earlier than allocation rules; project-based cooperation can proceed under flexible understandings even when legal status is contested. Over time, successful delivery can create a climate within public opinion and professional networks that makes legalization more feasible.

However, the order or ranking of the various measures can also fail. If legalization is pursued without sufficient political inclusion, it may create institutional fragmentation; if functional cooperation is pursued without a credible pathway to address distributive disputes, it may be dismissed as technocratic "window dressing." The NBI illustrates both possibilities. Its knowledge and project work have created cooperative capacity, but the most contentious allocation and dam-operation issues have not been settled within its framework. The CFA may strengthen the legal pathway for some riparian states, but its peacebuilding value will depend on whether it can remain open, preserve basin-wide technical cooperation, and create incentives for eventual broader participation (*Mohammed 2025*).

COMPARATIVE FINDINGS: HOW INSTITUTIONAL FORM INFLUENCES PEACE-RELEVANT FUNCTIONS

The following table provides a comparison of the peace-relevant functions of both river basin regimes.

Three core claims can be drawn from the comparison:

- Legalized regimes are comparatively strong at negative peace functions.

The PIC's core design choice-detailed legalization combined with a dispute-settlement ladder-makes it well-suited for containing disputes under low trust. Transparency is embedded through routine data exchange and notification; predictability arises from clear entitlements and time-bound procedures; and compliance management is supported by third-party adjudication. The Baglihar and Kishenganga episodes show how contentious infrastructure disputes were processed into implementable technical-legal outcomes rather than driving open-ended escalation. This pattern is consistent with findings that legalization and institutionalized river claims management correlate with a reduced risk of military conflict (*Brochmann and Hensel 2009, Wolf et al. 2003*).

- Programmatic platforms are comparatively strong at positive peace foundations.

The NBI's design – centred on shared knowledge, capacity building, and cooperative projects – is well suited for building professional networks, reducing factual uncertainty, and producing visible cooperative gains. These mechanisms contribute to legitimacy and resilience by creating constituencies for cooperation and by improving the problem-solving capacity of basin institutions. The NBI's participation practices, though uneven, generally exceed those of the PIC and better align with positive peace claims about inclusion and accountability (*Pahl-Wostl 2015, Paisley and Henshaw 2020*).

- The two forms are complementary rather than substitutable.

The Indus case shows that legalization can stabilize cooperation without delivering broad legitimacy or adaptive capacity. The Nile case shows that programmatic cooperation can build knowledge and benefits without being able to contain acute distributive disputes among pivotal actors. In other words, each form covers a different subset of peace-relevant functions. The implication is "functional pluralism": robust peacebuilding architectures combine rule-based containment with adaptive learning and legitimacy-building participation.

Table 2. Peace-relevant institutional profile (diagnostic summary)
2. táblázat. A békével kapcsolatos intézményi profil (diagnosztikai összefoglaló)

Function / design feature	PIC (Indus)	NBI (Nile)
Rule precision and predictability	Strong: detailed treaty annexes constrain discretion	Moderate: guidance and programmes, limited binding allocation rules
Routine communication	Strong: mandated commissioner channel and regular meetings	Moderate: ministerial/technical forums, intensity varies by sub-basin
Transparency and verification	Moderate-strong internally; limited public transparency	Moderate: growing data tools, uneven openness and coverage
Dispute settlement / compliance	Strong: Neutral Expert and arbitration ladder	Weak-moderate: political forums and ad hoc negotiation, limited adjudication
Flexibility and learning	Moderate: adaptation mainly via adjudication	Strong: iterative studies, tools and programme learning
Participation and accountability	Weak: state-centric technocratic model	Moderate: stakeholder forums, consultations, uneven but more developed
Material cooperative benefits	Limited: treaty stabilizes entitlements, few joint projects	Stronger in some sub-basins: joint investments and capacity building
Exposure to geopolitics	High; procedures can buffer rivalry but are vulnerable to politicization	High; programmatic cooperation persists but struggles in mega-project politics

Evidence relative to expectations (H1–H4)

H1 (Transparency–stability) is broadly supported. In the Indus, transparency mechanisms are reinforced by adjudication, which makes information credible and actionable. In the Nile, transparency through shared tools and early warnings contributes to routine risk management, but its stabilizing effect is more contingent because it lacks an accepted basin-wide adjudicative backstop.

H2 (Flexibility–resilience) is partially supported and design-dependent. The NBI's programmatic approach institutionalizes learning and can respond iteratively to new information and shocks. The Indus regime adapts to new challenges more slowly because its flexibility is largely "imported" through dispute settlement rather than through explicit review clauses or adaptive operating rules. Where political commitment to procedures weakens, this pathway becomes fragile.

H3 (Inclusiveness–legitimacy) is asymmetrically supported. The NBI's stakeholder engagement practices more plausibly contribute to legitimacy and compliance, particularly in project-based cooperation. The PIC's state-centric design provides efficiency but limits societal voice; legitimacy is therefore more vulnerable to domestic politicization and nationalist framing, especially during crises.

H4 (External support–durability) is supported with caveats. In both basins, third parties have been catalytic: they provided resources, convening power, and, in the Indus, procedural roles that strengthened credible commitments. However, external engagement also carries risks: donor agendas can distort priorities, and perceived intrusion into sovereignty can trigger backlash. The durable support of peacebuilding therefore requires alignment with basin-defined priorities and transparent accountability arrangements.

Conflict mitigation versus conflict resolution

A central lesson from both basins is the analytical difference between mitigating disputes and resolving underlying conflicts. The PIC is optimized for mitigation: it provides a routine for communication, predictable procedures for "planned measures," and a legal-technical ladder that can translate disagreements into decisions. This helps prevent water issues from becoming triggers in a wider security rivalry. Yet the PIC is not designed to resolve deeper distributive grievances, identity conflicts, or territorial disputes that shape India–Pakistan relations. Its contribution is therefore best described as a stabilizing "buffer" around a vital resource rather than a pathway to political reconciliation.

The NBI illustrates the inverse pattern. Its programmatic portfolio can contribute to conflict transformation in limited ways by building habits of cooperation, establishing linkages between technical communities and society at large, and generating cross-border benefits. However, when core questions of entitlement and risk distribution are securitized – as in debates over large dam operations and drought management – programmatic cooperation has limited leverage. In those moments, conflict resolution requires a political settlement on rules, not only projects and studies. The implication is that claims to peacebuilding must be specified: institutions can generate negative peace (containment) without resolving political conflict, and they can generate positive peace foundations without guaranteeing settlement on allocation.

Power asymmetry, hydro-hegemony, and the politics of knowledge

Both cases also show that institutional design interacts with power. In the Indus, India's upstream position on several tributaries and its larger economic and military capacity create bargaining advantages; Pakistan's downstream dependence and security concerns encourage a defensive posture. The IWT's precise rules and third-party procedures can be interpreted as "soft equalizers": they narrow discretion and provide Pakistan with a procedurally legitimate channel to contest designs. At the same time, the treaty's partition logic also reflects historical power and bargaining constraints; it stabilizes expectations but does not create a joint developmental vision.

In the Nile, historical hydro-hegemony has been associated with downstream influence, particularly by Egypt, anchored in diplomatic leverage and legacy agreements. Over the last decades, upstream states have increasingly mobilized finance, technology, and coalition-building to pursue hydropower and irrigation development, reshaping the dynamics of bargaining (*Cascão 2009*). The NBI's shared-vision approach partly sought to depoliticize these contests by building a common knowledge base. Yet the politics of knowledge remains central: whose models are accepted, which scenarios are emphasized, and how uncertainty is communicated can all affect perceived legitimacy. In this sense, transparency is not only about releasing data but also about establishing trusted processes for joint fact-finding and interpretation. Institutions that neglect this risk seeing technical debates re-securitized in the public sphere.

A mechanism typology for peace-relevant water institutions

Synthesizing across the two cases, the following mechanisms appear especially important for negative peace and for positive peace, respectively.

Negative peace mechanisms:

(1) Proceduralized communication: predictable meetings and notification routines keep channels open and reduce misperceptions during crises.

(2) Verifiable transparency: data exchange tied to monitoring standards and inspections provides a shared evidentiary base.

(3) Bounded adjudication: time-bound escalation ladders and third-party determinations reduce incentives for unilateral escalation.

Positive peace mechanisms:

(4) Social learning and epistemic community building: joint tools, models and studies generate shared problem definitions and professional norms.

(5) Legitimization through inclusion and benefit visibility: participation and tangible cooperative outputs broaden constituencies that value stability.

The PIC strongly instantiates (1)-(3) and only weakly (4)-(5). The NBI strongly instantiates (4) and, in part, (5), while (1)-(3) depend more on political conditions and remain uneven at the basin scale. The key theoretical implication is that different institutional forms can be functionally plural: they can deliver different bundles of peace-relevant mechanisms. This helps explain why empirical claims about "water cooperation" often appear inconsistent; what matters is which mechanisms are present and credible in a given institutional setting.

Detailed case scores and justifications can be found in the *Annex* to this study.

Limitations and scope conditions

Two limitations constrain the findings. First, peacebuilding outcomes such as trust and legitimacy are difficult to measure directly; the analysis therefore relies on observable proxies (institutional routines, dispute trajectories, transparency practices, and participation architectures). Second, the study focuses on interstate institutions and thus only indirectly captures subnational impacts. In both basins, domestic politics, centre–province relations, and national development narratives can override institutional incentives. These factors do not negate institutional effects, but they shape their scope conditions: even well-designed institutions cannot substitute for political willingness to cooperate, and poorly designed domestic governance can erode transboundary legitimacy.

Future research can strengthen causal inference by combining comparative institutional analysis with micro-level evidence on how affected communities perceive fairness and how national bureaucracies internalize transboundary commitments. It can also examine how "modular" cooperation (data, forecasting, emergency rules, joint investments) may accumulate into more comprehensive legal settlements over time.

Comparative profile in brief

The indicator-based assessment can be summarized as a diagnostic profile rather than a scorecard. The PIC is strongest where legalization, verification, and escalation procedures matter, and weakest where legitimacy-building transparency and inclusion are imperative. The NBI is strongest where knowledge production, project delivery, and stakeholder engagement matter, and weakest where binding basin-wide rules and enforcement would be required to contain distributional disputes.

This profile helps clarify what it means to "strengthen cooperation." For the Indus, strengthening is less about adding more rules and more about modernizing and legitimizing existing ones. For the Nile, strengthening is less about producing additional studies and more about translating knowledge and programme experience into credible, inclusive rule systems for risk sharing-while keeping non-parties engaged.

CONCLUSION

Comparative evidence suggests that peacebuilding through water cooperation is most plausible when institutions deliver a balanced portfolio of functions. The following implications can be drawn from the analysis:

1. Pair legal precision with bounded flexibility.

Precise rights and obligations reduce uncertainty, but rigidity increases friction under change. Institutions should include review clauses, emergency operating rules, and standing technical groups that can update procedures without reopening fundamental bargains (*Cosens et al. 2014*). Where full treaty revision is politically infeasible, side protocols can specify drought/flood coordination, data standards, and technical design updates.

2. Treat knowledge systems as peace infrastructure.

Shared models, interoperable datasets, and transparent forecasting reduce factual contestation and can de-escalate rumours during crises (*Giordano et al. 2014*). Investments in data systems should include tiered public access to strengthen legitimacy while protecting sensitive security information.

3. Maintain a credible, time-bound dispute pathway.

Dispute ladders contribute to negative peace by offering authoritative decisions and limiting forum shopping. Their credibility depends on clear rules of ranking, predictable timelines, and recognized gatekeeping. Where adjudication is politically contested, advisory joint fact-finding or third-party technical panels can still lower uncertainty and provide face-saving options.

4. Expand participation to strengthen domestic buy-in.

Transboundary institutions depend on domestic politics. Structured engagement with subnational authorities, user associations and affected communities can strengthen legitimacy and reduce contestation (*Derman and Ferguson 2003*). Participation should be designed to be meaningful rather than symbolic consultations; e.g. feedback loops for consultations should be included.

5. Focus on distributional legitimacy and risk-sharing.

Peace dividends are fragile when benefits and risks are perceived as imbalanced. Institutions should prioritize joint scenarios that make distributional effects explicit (especially under drought) and develop compensatory or benefit-sharing arrangements where feasible (*Sadoff and Grey 2002*).

6. Align external support with ownership and accountability.

External finance and facilitation are most valuable when they enable long-term capacity building and reinforce local priorities (*Paisley and Henshaw 2020*). Donors should avoid designs that substitute for political commitment; instead, they can support monitoring infrastructure, joint training, and the institutionalization of transparent budgeting and evaluation.

7. Insulate technical cooperation from geopolitical shocks.

Where political relations deteriorate, technical channels and data exchange become even more valuable. Crisis-communication protocols, protected working-level contacts, and jointly agreed non-politicization norms can preserve cooperation during shocks.

Basin-specific implications: Indus

For the Indus, the key priority is to protect and modernize the containment functions that have historically reduced escalation risks. This implies safeguarding routine data exchange and meetings even when broader diplomacy deteriorates, because these routines are the institution's core asset in terms of peacebuilding. Technical modernization should focus on reducing recurring design disputes by clarifying, through agreed technical protocols or updated annex guidance, how contemporary hydropower and sediment-management practices can remain consistent with treaty objectives. An explicit, jointly agreed "shock protocol" – for example, for extreme floods, drought years, or major infrastructure incidents – would provide bounded flexibility without reopening the treaty's fundamental bargain.

At the same time, strengthening legitimacy requires moving beyond a purely state-centric model. Without transforming the PIC into a broad stakeholder forum, incremental steps are feasible: more systematic publication of non-sensitive meeting summaries, clearer public communication of dispute procedures, and structured interfaces with affected subnational authorities and expert communities. Such measures can reduce rumour-driven politicization and help maintain domestic support for continued procedural engagement.

Basin-specific implications: Nile

For the Nile, the central challenge is to preserve the NBI's functional cooperation while transitioning toward a more formal legal order. The impending creation of a permanent commission should not disrupt the knowledge systems, technical staffing, and project pipelines that the NBI has accumulated. A practical approach is to treat these systems as shared "basin public goods" and insulate them from political contestation over legal status.

Because the most securitized disputes relate to dam operations and drought risk-sharing, modular agreements can provide a bridge where comprehensive settlement is politically infeasible. For example, riparian states could negotiate technical rules for data sharing on reservoir levels and planned releases, joint drought triggers, and principles for coordinated emergency response, without requiring immediate agreement on permanent allocations. Independent joint fact-finding panels – potentially supported by regional organizations or mutually acceptable third parties – can help establish trusted baselines for negotiation and reduce the incentives for public escalation.

Cross-basin lesson: design for complementarity

Across basins, institutional reform agendas should avoid copying a single "model." Instead, reforms should diagnose which peace-relevant functions are missing and add design elements accordingly. Where legalization exists but is brittle, invest in adaptive capacity, participation, and trusted knowledge production. Where programmatic cooperation exists without credible conflict containment, develop time-bound procedures for dispute management and modular legal commitments that can gradually expand.

A checklist for practitioners

Across both basins, the following questions provide a quick diagnostic for whether a cooperation arrangement is likely to generate peace-relevant effects:

- Can parties verify key claims (flows, storage, operations) through shared monitoring and agreed data standards?
- Are there predictable meeting and notification routines that persist during political downturns?
- Does the framework provide a credible and time-bound pathway for moving disagreements from technical consultation to a binding or authoritative resolution?
- Do operating rules specify how risks are shared during extremes (droughts, floods) and how rules are reviewed?
- Are affected stakeholders able to contest and inform decisions through structured participation, and are non-sensitive outputs publicly communicated?
- Are cooperative benefits visible enough to create domestic constituencies that value stability?
- Is external support aligned with basin priorities and designed to reinforce, not replace, ownership?

If several answers are "no," cooperation may still exist, but its claims of contributing to peacebuilding should be treated cautiously.

The comparison of the PIC and the NBI shows that water cooperation can contribute to peacebuilding, but not automatically and not uniformly. Effects emerge when design features, practices, and context align to generate transparency, predictability, reciprocity, learning, and legitimate risk sharing. In an era of climatic variability and infrastructure expansion, durable cooperation is more likely when stability-oriented legal procedures are coupled with adaptive and inclusive programmatic capacities, supported by external actors in ways that reinforce rather than replace basin ownership. The comparison suggests that peacebuilding through water cooperation should be understood as contingent institutionalism: institutions contribute to peace not by their mere existence but by the specific functions they perform. In practice, stable cooperation emerges when rule-based containment mechanisms are complemented by institutions that generate shared knowledge, adaptive capacity, and broader constituencies for cooperation.

The APPENDIX (attached in a separate file: *Évf. 106 szám EN1 (2026) | Hidrológiai Közlöny*) documents the indicator codebook, scoring rules, and case-specific justifications used in the thesis's comparative analysis. It is designed to maximize transparency and replicability. The framework contains four dimensions (A–D), each with three indicators (1–3). Each indicator is scored on a 0–3 scale. Scores are justified for both cases: the Permanent Indus Commission (PIC, Indus Basin) and the Nile Basin Initiative / Nile River Basin Commission (NBI/NRBC, Nile Basin). Three worked examples per basin illustrate the coding procedure and evidence trace

REFERENCES

Abbott, K.W., Keohane, R.O., Moravcsik, A., Slaughter, A.-M., Snidal, D. (2000). The Concept of Legalization. International Organization, 54(3), pp. 401-419. https://doi.org/10.1162/002081800551271

Alam, U.Z. (2002). Questioning the Water Wars Rationale: A Case Study of the Indus Waters Treaty. The Geographical Journal, 168(4), pp. 341-353. https://doi.org/10.1111/j.0016-7398.2002.00060.x

Azizi, M.A., Leandro J. (2025). Factors Affecting Transboundary Water Disputes: Nile, Indus, and Euphrates–Tigris River Basins. Water 2025, Vol. 17, Issue 4, Number 525. https://doi.org/10.3390/w17040525

Beach, D., Pedersen, R.B. (2013). Process-Tracing Methods: Foundations and Guidelines. Ann Arbor, MI: University of Michigan Press. https://doi.org/10.3998/mpub.2556282

Biemans, H., Siderius, C., Lutz, A.F., Nepal, S., Ahmad, B., Hassan, T., von Bloh, W., Wijngaard, R.R., Wester, P., Shrestha, A.B., Immerzeel, W.W. (2019). Importance of snow and glacier meltwater for agriculture on the Indo-Gangetic Plain. Nature Sustainability, 2, pp. 594-601. https://doi.org/10.1038/s41893-019-0305-3

Brochmann, M., Hensel, P.R. (2009). Peaceful Management of International River Claims. International Negotiation, 14(2), pp. 393-418. https://doi.org/10.1163/157180609X432879

Cascão, A.E. (2009). Changing Power Relations in the Nile River Basin: Unilateralism vs. Cooperation? Water Alternatives, 2(2), pp. pp. 245-268.

Conca, K., Dabelko, G.D. (Eds.). (2002). Environmental Peacemaking. Washington, D. C., Woodrow Wilson Center Press. https://doi.org/10.56021/9780801871924

Conway, D. (2005). From headwater tributaries to international river: observing and adapting to climate variability and change in the Nile basin. Global Environmental Change, 15(2), pp. 99-114. https://doi.org/10.1016/j.gloenvcha.2005.01.003

Cosens, B.A., Gunderson, L., Chaffin, B.C. (2014). The Adaptive Water Governance Project: Assessing Law, Resilience and Governance in Regional Socio-Ecological Water Systems Facing a Changing Climate. Idaho Law Review, 51, pp. 1-27.

Derman, B., Ferguson, A. (2003). The Value of Water: Political Ecology and Water Reform in Southern Africa. Human Organization, 62(3), pp. 277-288. https://doi.org/10.17730/humo.62.3.4um4hl7m2mtjagc0

Galtung, J. (1969). Violence, Peace, and Peace Research. Journal of Peace Research, 6(3), pp. 167-191. https://doi.org/10.1177/002234336900600301

George, A.L., Bennett, A. (2005). Case Studies and Theory Development in the Social Sciences. Cambridge, MA: MIT Press.

Giordano, M.F., Giordano, M.A., Wolf, A.T. (2014). International Resource Conflict and Mitigation. Journal of Peace Research, 49(1), pp. 29-42. https://doi.org/10.1177/0022343305049666

IBDF (1960). Indus Basin Development Fund Agreement, September 19, 1960. World Bank Depository. https://documents1.worldbank.org/curated/en/239781468100481033/pdf/Loan-0266-Pakistan-Indus-Basin-Project-Development-Fund-Agreement.pdf. [Accessed: March 15, 2026]

Ide, T. (2018). The impact of environmental cooperation on peacebuilding: Definitions, mechanisms, and empirical evidence. International Studies Review, 20(3), pp. 495-512. https://doi.org/10.1093/isr/viy014

IHA (n.d.). Ethiopia – Grand Ethiopian Renaissance Dam (GERD). International Hydropower Association. https://www.hydropower.org/sediment-management-case-studies/ethiopia-grand-ethiopian-renaissance-dam-gerd [Accessed: June 6, 2026]

Keohane, R.O. (1984). After Hegemony: Cooperation and Discord in the World Political Economy. Princeton, NJ., Princeton University Press.

Lutz, A.F., Immerzeel, W.W., Shrestha, A.B., Bierkens, M.F.P. (2014). Consistent increase in High Asia's runoff due to increasing glacier melt and precipitation. Nature Climate Change, 4, pp. 587-592. https://doi.org/10.1038/nclimate2237

Mirumachi, N. (2015). Transboundary Water Politics in the Developing World. Routledge. https://doi.org/10.4324/9780203068380

Mohammed, Y. A. (2025). Journey of the Nile River Basin Toward a Permanent Institution. International Journal of Water Management and Diplomacy, 1(8), 21–31. https://doi.org/10.2139/ssrn.5109210.

Muhumuza, R. (2024). Nile basin nations say water-sharing accord has come into force without Egypt's backing. Associated Press, October 14, 2024. https://apnews.com/article/nile-river-accord-egypt-ethiopia-water-sharing-e245661a016bb75d9337d3e45a7753f7 [Accessed June 6, 2026]

NBI (n.d.). NBI Strategy 2017–2027. Abridged version. https://faolex.fao.org/docs/pdf/mul-211416.pdf [Accessed June 6, 2026]

NBI (2020). State of the River Nile Basin. Water Security in the Nile Basin 2021. https://adelphi.de/system/files/document/State%20of%20Basin%202021.pdf [Accessed June 6, 2026]

NBI (2024). Announcement by the Nile Basin States of the Entry into Force of the Nile River Basin Cooperative Framework Agreement. Nile Basin Initiative, October 13, 2024. https://nilebasin.org/sites/default/files/2024-10/Announcement%20of%20the%20Entry%20into%20force%20of%20the%20CFA%20%20on%2013%20October%202024.pdf [Accessed: June 6, 2026]

Pahl-Wostl, C. (2015). Water Governance in the Face of Global Change. Berlin: Springer. https://doi.org/10.1007/978-3-319-21855-7

Paisley R.K., Henshaw, T. (2020). Transboundary Governance of the Nile River Basin: Past, Present and Future. Water International, 45(3), pp. 214-229.

PCA (2013). Permanent Court of Arbitration, Award in the Arbitration regarding the Indus Waters Kishenganga (Pakistan v. India). Permanent Court of Arbitration, February 18, 2013.

Richmond, O.P. (2014). Failed Statebuilding. Cambridge, MA: Yale University Press. https://doi.org/10.12987/yale/9780300175318.001.0001

Sadoff, C.W., Grey, D. (2002). Beyond the River: The Benefits of Cooperation on International Rivers. Water Policy, 4(5), pp. 389-403. https://doi.org/10.1016/S1366-7017(02)00035-1

Salman, S.M.A. (2008). The Baglihar Difference and its Resolution Process: A Triumph for the Indus Waters Treaty? Water Policy, 10(2), pp. 105-117. https://doi.org/10.2166/wp.2008.060b

Singh, S.C., Shahid, A. (2025). What is the Indus Waters Treaty between India and Pakistan? Reuters, May 16, 2025. https://www.reuters.com/world/asia-pacific/what-is-indus-waters-treaty-between-india-pakistan-2025-04-24/ [Accessed: June 6, 2026]

Swain, A. (2011). Challenges for water sharing in the Nile basin: changing geo-politics and changing climate. Hydrological Sciences Journal, 56(4), pp. 687-702. https://doi.org/10.1080/02626667.2011.577037

UAR and Sudan (1959). Agreement (with annexes) for the full utilization of the Nile Waters. https://treaties.un.org/doc/Publication/UNTS/Volume%20453/volume-453-I-6519-English.pdf [Accessed: June 6, 2026]

UNTS (1960). The Indus Waters Treaty 1960 (with annexures). United Nations Treaty Series, vol. 419, I-6032.

von Lossow, T. (2025). Indus Water Treaty 2025: A pause of cooperation, not an end. Clingendael Alert, July 18, 2025. https://www.clingendael.org/publication/indus-water-treaty-2025-pause-cooperation-not-end [Accessed: June 6, 2026]

Waterbury, J. (2002). The Nile Basin: National Determinants of Collective Action. Cambridge, MA: Yale University Press.

WB (1960-1975). World Bank Archives 1960–1975

Wheeler, K.G., Jeuland, M., Hall, J.W., Zagona, E., Whittington, D. (2020). Understanding and managing new risks on the Nile with the Grand Ethiopian Renaissance Dam. Nature Communications, 11:5222, pp. 1-9. https://doi.org/10.1038/s41467-020-19089-x

Wolf, A.T., Yoffe, S., Giordano, M. (2003). International Waters: Identifying Basins at Risk. Water Policy, 5(1), pp. 29-60. https://doi.org/10.2166/wp.2003.0002

Zawahri, N.A. (2009). India, Pakistan and Cooperation Along the Indus River System. Water Policy, 11(1), pp. 1-20. https://doi.org/10.2166/wp.2009.010

Zehra, I. (2025). The Indus Treaty verdict: When water outlasts war. July 4, 2025. https://www.lowyinstitute.org/the-interpreter/indus-treaty-verdict-when-water-outlasts-war(Accessed: March 15, 2026)

Zeitoun, M., Warner, J. (2006). Hydro-hegemony: A Framework for Analysis of Trans- boundary Water Conflicts. Water Policy, 8(5), pp. 435-460. https://doi.org/10.2166/wp.2006.054

URL1. https://en.wikipedia.org/wiki/Indus_Basin#/media/File:Indus_River_basin_map.svg

URL2. https://en.wikipedia.org/wiki/Nile_Basin#/media/File:Nile_basin_map.png

AUTHOR

FERENC SULLIVAN (Budapest, 1990) holds Master’s degrees in International Relations (Corvinus University of Budapest, 2015), History (Pázmány Péter Catholic University, 2023) and International Water Governance and Water Diplomacy (University of Public Service, 2026). His research interests include geopolitics, the water-security nexus, Central European history and politics, and Hungarian minorities abroad. He is currently pursuing his PhD studies at the Doctoral School of Public Administration Sciences at the University of Public Service, Budapest, Hungary.

The Water-Energy-Food Nexus in Madagascar: Interdependencies, Cascading Failures, and an Integrated Governance Framework

Rovatiana Salema ANDRIANASOLOMAHEFA

Faculty of Public Governance and International Studies, Doctoral School of Public Administration, National University of Public Service, Budapest, Hungary (email: andrianasolomahefa.rovatiana.salema@stud.uni-nke.hu; rovatiana.salena@gmail.com)

DOI: 10.59258/hk.24124

Abstract
Madagascar's concurrent crises of energy poverty (33.7% electrification), acute food insecurity (1.63 million people in Integrated Food Security Phase Classification (IPC) Phase 3+ in 2024), and watershed degradation (4.85 million hectares of forest lost since 2000) are structurally interdependent, yet are governed in institutional silos with no cross-sectoral coordination mechanism. This paper maps the Water-Energy-Food (WEF) nexus dynamics of Madagascar, tests the hypothesis that institutional fragmentation – not physical resource scarcity – is the binding constraint on nexus performance, and proposes an evidence-based integrated governance framework. A sequential mixed-methods design integrates systematic secondary data synthesis with qualitative institutional analysis following a governance audit framework and the FAO three-systems nexus model. Five quantified nexus feedback loops are identified, the most critical being a biomass-deforestation-hydropower cascade that simultaneously impairs energy supply, watershed function, and food system productivity. Despite the per capita renewable freshwater endowments of ~12,000 m³/year due to climatic heterogeneity, this resource is distributed unevenly across the country; while this is double the Sub-Saharan African average, only 14% of the population accesses safely managed water, and 85% of primary energy derives from biomass. A 96% agricultural water withdrawal share, 47% child stunting rate, and projected temperature increases of 3–5 °C by 2100 compound these structural deficits. Madagascar's nexus failures are governance failures. To address the identified governance and resource management challenges, this study proposes three high-leverage policy measures. First, establish a National Water-Energy-Food (WEF) Nexus Coordination Secretariat to strengthen a cross-sectorial coordination and policy coherence. Second, implement nexus-aware investment screening anchored in the 2024 ECA-WFP geospatial initiative to ensure that public and private investments account for WEF interdependencies. Third, expand off-grid renewable energy, like solar deployment linked to productive agricultural use requirements, to improve energy access while enhancing agricultural productivity and water-use efficiency.

Keywords
Water-Energy-Food (WEF) Nexus, Madagascar, Food Security, Governance, Hydropower, Sustainable Development.

A víz-energia-élelmiszer összefüggés Madagaszkáron: Kölcsönös függőségek, kaszkádszerű kudarcok és egy integrált irányítási keretrendszer

Kivonat
Madagaszkár egyidejű válságai, mint például az energiaszegénység (33,7%-os villamosítás), az akut élelmiszer-bizonytalanság (1,63 millió ember az Integrált Élelmiszerbiztonsági Fázisbesorolás (IPC) 3+ fázisába került 2024-ben) és a vízgyűjtők degradációja (4,85 millió hektár erdő veszett el 2000 óta) strukturálisan egymástól függenek, mégis intézményi silókban, ágazatközi koordinációs mechanizmus nélkül irányítják őket. Ez a tanulmány feltérképezi Madagaszkár víz-energia-élelmiszer (WEF) nexus dinamikáját, teszteli azt a hipotézist, hogy az intézményi fragmentáció – nem a fizikai erőforrások szűkössége – korlátozza a nexus teljesítményét, majd bizonyítékokon alapuló integrált irányítási keretet javasol. A szekvenciális vegyes módszerű tervezés integrálja a szisztematikus másodlagos adatszintézist a kvalitatív intézményi elemzéssel, egy irányítási audit keretrendszert és a FAO háromosztatú nexus modelljét követve. Öt számszerűsített nexus visszacsatolási hurkot azonosít, amelyek közül a legkritikusabb a biomassza-erdőirtás-vízenergia kaszkád, amely egyszerre rontja az energiaellátást, a vízgyűjtő működését és az élelmiszerrendszer termelékenységét. Annak ellenére, hogy az egy főre jutó megújuló édesvízkészlet ~12 000 m³/év – ami a szubszaharai afrikai átlag kétszerese –, a lakosságnak csak 14%-a fér hozzá biztonságosan kezelt vízhez, és az elsődleges energia 85%-a biomasszából származik. A mezőgazdasági vízkivétel 96%-os aránya, a gyermekkori fejlődés elmaradásának 47%-os, valamint a 2100-ra előrejelzett 3–5 °C-os hőmérséklet-emelkedés súlyosbítja ezeket a strukturális hiányosságokat. Madagaszkár nexus hibái kormányzási hibák. Először is létre kell hozni egy Nemzeti Víz–Energia–Élelmiszer (WEF) Összefüggés-koordinációs Titkárságot a szektorok közötti koordináció és a politikai koherencia erősítése érdekében. Másodszor, a 2024-es ECA–WFP térinformatikai kezdeményezésen alapuló, a nexust figyelembe vevő beruházásszűrést kell bevezetni annak biztosítására, hogy az állami és magánberuházások figyelembe vegyék a víz, az energia és az élelmiszer közötti kölcsönös függőségeket. Harmadszor, ki kell bővíteni a hálózaton kívüli megújuló energiaforrások, például a napenergia felhasználását, összekapcsolva azt a termelői mezőgazdasági igényekkel, az energiaellátás javítása mellett a mezőgazdasági termelékenység és a vízfelhasználás hatékonyságának növelése érdekében.

Kulcsszavak
Víz-Energia-Élelmiszer (WEF) nexus, Madagaszkár, élelmiszerbiztonság, irányítás, vízenergia, fenntartható fejlődés.

INTRODUCTION

Madagascar presents a paradox that challenges conventional resource-scarcity narratives: it possesses extraordinary natural capital–337 billion m³ of renewable freshwater, 7,800 MW of unexploited hydropower potential, and solar irradiation averaging 5.5 kWh/m²/day–yet consistently records among the worst water, energy, and food security outcomes globally. As of 2024, only 33.7% of Malagasy citizens had access to electricity (*World Bank 2023*); 1.63 million people faced IPC Phase 3 or worse food insecurity conditions (*IPC 2024*); and 4.85 million hectares of forest cover had been lost since 2000, releasing an estimated 2.52 $GtCO_2e$ (*Andriamparany et al. 2023*). This configuration – abundant resources, catastrophic outcomes – is the defining problem that motivates the present analysis.

These aggregate figures, however, obscure a spatial asymmetry that is analytically decisive for the Water-Energy-Food (WEF) nexus. Madagascar's orographic structure concentrates the large majority of annual precipitation on the steep eastern escarpment (*Figure 1*), where short, high-gradient rivers discharge into the Indian Ocean before any significant water capture is possible. The same eastern corridor that generates the 7 800 MW hydropower potential –the energy pillar of the nexus – is thus hydrologically decoupled from the arid south and west, where food insecurity is most acute and where annual rainfall can fall below 400 mm. The result is that the three nexus dimensions are not merely underperforming in parallel: they are spatially misaligned at the outset, so that expanding hydropower on eastern rivers does not automatically relieve water or food stress in the regions that need it most. Understanding this structural disconnection is a precondition for interpreting both the governance failures and the policy interventions analysed in the sections that follow.

Existing research on Madagascar's development challenges addresses these sectors largely in isolation. Agricultural studies focus on productivity constraints (*Minten and Barrett, 2008*); energy studies address electrification gaps (*Nematchoua 2020*); climate studies examine adaptive behavior among smallholder farmers (*Barrett et al. 2025, Davies et al. 2024*). The Water-Energy-Food (WEF) nexus, as applied by *Nkiaka et al. (2023)* across 54 African nations using the WEF Nexus Index, demonstrates that suboptimal performance in all three dimensions simultaneously is the norm in Sub-Saharan Africa, and that the dominant constraint is institutional rather than physical. Yet Madagascar receives no country-specific nexus treatment in this or any comparable analysis. This is the research gap this paper addresses.

The underperformance of Madagascar's WEF nexus is primarily attributable to institutional fragmentation and governance failures, not to physical resource scarcity, and an integrated cross-sectoral governance framework would produce measurably superior outcomes across all three nexus dimensions.

This hypothesis raises the following four interrelated Research Questions (RQ):

- RQ1: What is the current state of Madagascar's water, energy, and food systems relative to regional benchmarks, and where do the most acute deficits lie?
- RQ2: What are the principal WEF nexus feedback mechanisms, what are their quantified magnitudes, and which feedback loops are most damaging?
- RQ3: How does observed and projected climate change modulate the nexus interdependencies, and which pathways are most critical for policy attention?
- RQ4: What governance architecture would most effectively address Madagascar's identified nexus failure modes, and what evidence-based institutional reforms are recommended?

LITERATURE REVIEW AND THEORETICAL FRAMEWORK

The WEF nexus concept, introduced by *Hoff (2011)* at the Bonn 2011 Conference, posits that water, energy, and food are governed as separate systems despite exhibiting deep physical interdependencies. Food and Agriculture Organization of the United Nations (*FAO 2014*) elaborated this insight into a three-pillar planning model emphasizing resource trade-offs and co-management synergies. *Bizikova et al. (2013)* extended this into a practical investment risk framework showing that siloed sectoral investments regularly generate negative externalities across nexus boundaries.

Leck et al. (2015) identified a translation deficit between nexus theory and actionable governance: the framework diagnoses interdependencies well but rarely produces institutional prescriptions. *Rasul (2016)* addressed this in a South Asian context, demonstrating that nexus performance is mediated by trade regimes, fiscal architecture, and institutional coordination capacity. *Herrera-Franco et al. (2024)*, in a systematic review linking the WEF nexus to clean energy transitions, found that renewable energy deployment consistently generates cross-system co-benefits when planned with nexus – awareness – a finding directly relevant to Madagascar's off-grid solar opportunity.

Nkiaka et al. (2023) applied the WEF Nexus Index to all 54 African nations, finding that sub-Saharan countries cluster around a pattern of simultaneous water-energy-food insecurity in which governance capacity, not physical endowment, predicts performance variation. *Authier et al. (2024)*, in the most methodologically proximate study to the present paper, applied a combined Geographic Information System (GIS) and optimization model to the Water-Energy-Food (WEF) nexus of Réunion Island – a comparable small island in the Indian Ocean context – demonstrating that land use competition between food, water, and energy systems can be quantified and mitigated through integrated spatial planning. Their finding that dietary behaviours are closely interlinked with land use competition is directly applicable to Madagascar's tavy-rice culture.

(Tavy is the Malagasy term for slash-and-burn agriculture – the practice of clearing forest by fire to create temporary cultivation plots, predominantly for upland rice. The tavy-rice manner thus refers to the structural interdependence between this deforestation-driven cultivation system and Madagascar's broader food, water, and energy dynamics: tavy provides subsistence food security to millions of smallholders while simultaneously driving the deforestation, watershed degradation, and soil erosion that undermine long-term agricultural and hydropower viability.) *Chagwiza et al. (2025)*, in a global systematic review of 117 empirical nexus studies, found that the most recent research direction extends the WEF nexus to incorporate soil and biodiversity resources whose degradation in Madagascar directly drives nexus failure.

For Madagascar specifically, *Barrett et al. (2025)* documented that annual precipitation declined at 14 of 15 long-term weather stations between 1961 and 2017, with temperatures projected to rise 3-5 °C by 2100, directly threatening rice productivity and river discharge for hydropower. *Davies et al. (2024)* found that gendered-related constraints on agricultural adaptation-lower asset ownership and, less extension access-disproportionately expose female smallholders to climate-nexus shocks. The International Monetary Fund (*IMF 2023*) integrated the Water-Energy-Food (WEF) nexus explicitly into Madagascar's macroeconomic framework, identifying the energy-water-food triad as the primary structural constraint on growth.

This paper positions itself within the governance-focused strand of nexus literature, building on the methodological approach of *Authier et al. (2024)* and the continental analytical framework of *Nkiaka et al. (2023)* to provide the first comprehensive Water-Energy-Food (WEF) nexus analysis for Madagascar at a national scale.

METHODS

Research Design

A sequential mixed-methods design was employed in four analytical stages: (i) systematic resource characterization, (ii) quantified nexus interdependency mapping, (iii) climate stress modulation analysis, and (iv) governance assessment and recommendation synthesis. The design follows *Bizikova et al. (2013)* for practical nexus planning and *Leck et al.'s (2015)* governance audit framework for the institutional dimension.

Data Collection

Secondary data were systematically retrieved from eight institutional databases, prioritizing 2018-2024 records: *FAO AQUASTAT (2022)* (water withdrawals, irrigation coverage), *World Bank 2023* (electrification, poverty, arable land), International Energy Agency (*IEA 2023*) (energy mix, renewable potential), International Renewable Energy Agency (*IRENA 2023a*), Integrated Food Security Phase Classification (*IPC 2024*) (food insecurity phase classifications), United Nations International Children's Emergency Fund (*UNICEF and WHO 2023*), Water, Sanitation and Hygiene (WASH) indicators, Global Forest Watch (*GWF 2024*), *Andriamparany et al. (2023)* (Landsat analysis-deforestation), Sustainable Energy for All (United Nations initiative) (*SE4All 2024*) (geospatial energy access), and United Nations Economic Commission for Africa and World Food Programme (*ECA and WFP 2024*) (nexus policy initiatives). Peer-reviewed literature was identified through searches in Web of Science, Scopus, and PubMed using the Boolean string: ('water-energy-food nexus' OR 'Water-Energy-Food (WEF) nexus') AND ('Madagascar' OR 'island developing' OR 'Sub-Saharan Africa') AND ('governance' OR 'food security' OR 'hydropower'). From 214 initial results, 40 studies met full inclusion criteria (empirical nexus or Madagascar-specific focus; published 2011–2025; Web of Science/Scopus indexed).

Analytical Approach

Water-Energy-Food characterization benchmarks Madagascar's indicators against Sub-Saharan African averages and Sustainable Development Goal (SDG) 2030 targets (*Table 1*). Nexus interdependency analysis constructs and quantifies five principal feedback pathways by triangulating magnitude data from multiple sources (*Table 2*). Climate stress analysis integrates Intergovernmental Panel on Climate Change (*IPCC 2022*) regional projections with station-level precipitation trend data from *Barrett et al. (2025)*. Governance assessment applies *Leck et al.'s (2015)* five-dimension audit (coordination, capacity, data, finance, accountability) to each sector and at the cross-sectoral level. Limitations include subnational WEF data available primarily for the Grand Sud and major river basins; no primary data collection; and the dynamic policy context post-2024 may not be fully captured.

Figure 1 positions Madagascar within the full cross-national distribution of the 54 Sub-Saharan African (SSA) nations covered by the WEF Nexus Index of *Nkiaka et al. (2023)*: each data point is a single SSA country-level observation for one of the three nexus dimensions (water access, energy access, food security), drawn from the same institutional databases listed above. Madagascar's values are distinguished to show where the country sits relative to the regional spread. This methodological choice is not incidental. The paper's central hypothesis – that Madagascar's nexus failures reflect institutional dysfunction rather than physical resource scarcity – can only be tested against a comparator group that shares broadly similar physical endowment levels. Plotting Madagascar within the SSA distribution allows the reader to verify directly whether its underperformance is a regional outlier or a structurally predictable outcome; if similarly endowed SSA peers achieve substantially better nexus scores, the institutional explanation gains empirical support. The figure therefore serves an evidentiary rather than illustrative function, and the data points are neither sub-national observations nor separate studies about Madagascar alone.

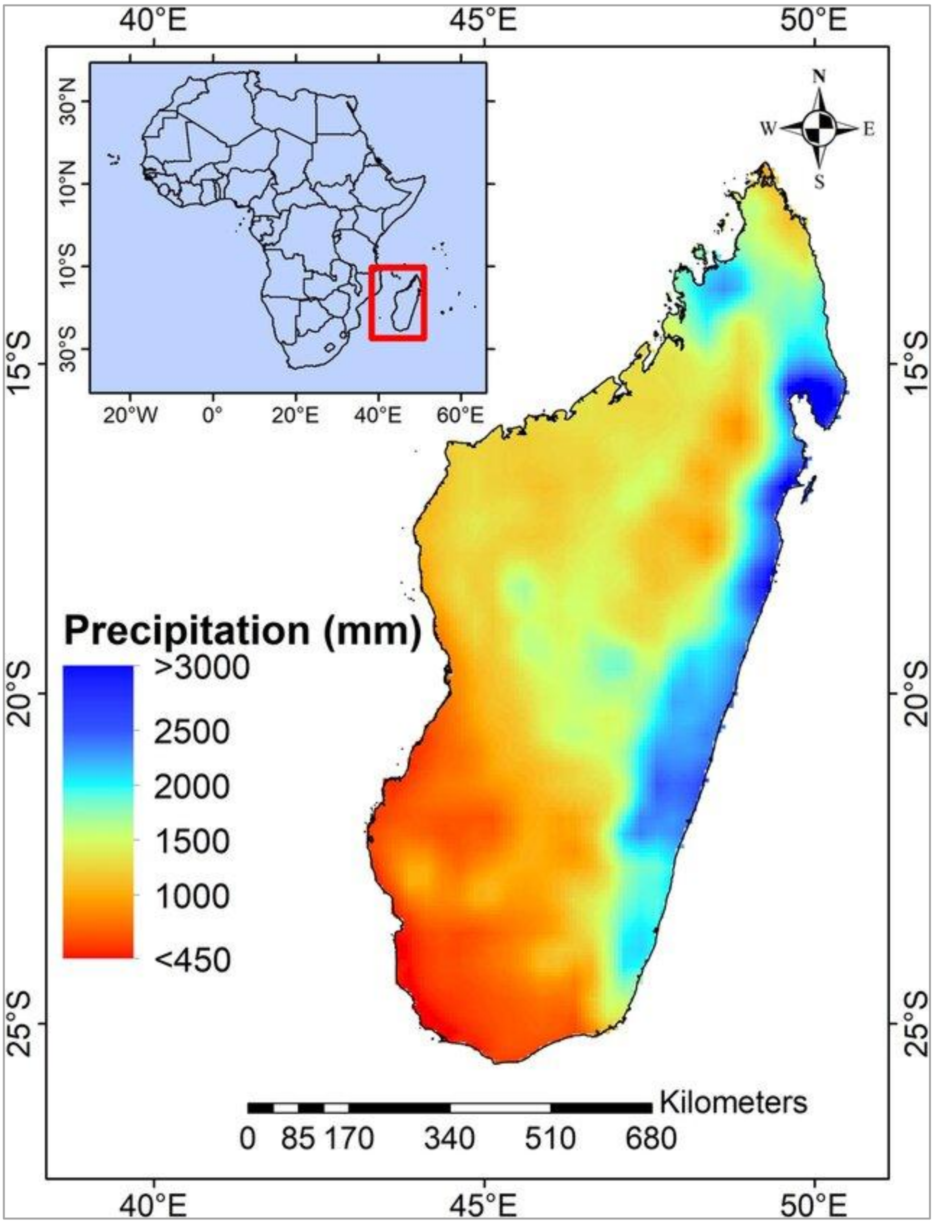

Figure 1. Spatial distribution of rainfall in Madagascar (Rabezanahary et al. 2025)
1. ábra. A csapadék területi eloszlása Madagaszkáron (Rabezanahary és társai 2025)

RESULTS

Water-Energy-Food Composite Stress Profile

Table 1 presents Madagascar's position across 12 WEF indicators benchmarked against Sub-Saharan African (SSA) averages and SDG 2030 targets. The data reveal a consistent pattern: despite national-level hydrological abundance (12,000 m³ per capita more, than double the SSA average of 5,800 m³), access as well as management performance are systematically below regional norms. Only 14% of the pop-ulation has access to safely managed drinking water com-pared with the Sub-Saharan African average of 28%; agri-cultural water withdrawals account for 96% of total fresh-water use, substantially exceeding the regional average of approximately 70%, indicating limited water availability for domestic and industrial uses. While the SSA average, in-cludes countries with markedly different socioeconomic and water management contexts, including South Africa, Mada-gascar remains among the region's poorest-performing countries on both indicators. The electrification deficit is equally stark: at 33.7% national and 6–10% rural rates, Madagascar trails the SSA average (48.4%) despite pos-sessing 7,800 MW of hydropower potential, of which only 162 MW 2.1% is currently exploited. Biomass constitutes approximately 85% of primary energy, versus an SSA aver-age of 68%, confirming Madagascar as a high-end outlier on traditional energy dependence. In the food dimension, 1.63 million people (15% of the population analysed) faced IPC Phase 3 or above food insecurity between September and December 2024, with 48,000 in Emergency (Phase 4); child stunting stands at 47% one of the five highest rates globally and post-harvest rice losses of 20-30% compound production deficits. Critically, the resource endowment col-umns (freshwater per capita, solar irradiation, hydropower potential) indicate that these outcomes are governance and infrastructure failures – not scarcity failures a finding that directly supports the central hypothesis.

Table 1. WEF Composite Stress Profile: Madagascar vs. SSA Benchmarks and SDG 2030 Targets (author' compilation based on cited databases)
1. táblázat. Víz-Energia-Élelmiszer (WEF) összetett stresszprofil: Madagaszkár vs. Szubszaharai Afrikára vonatkozó referenciaértékek és a 2030-as fenntartható fejlődési célok (a szerző szerkesztése a hivatkozott adatbázisok alapján)

Indicator	Madagascar	SSA Average	Target 2030	Source
Freshwater per capita (m³/yr)	11,072 – 13,179	~5,800	-	*FAO AQUASTAT (2022)*
Basic drinking water access (%)	53 – 55.8	70	100	*UNICEF and WHO (2023)*
Safely managed water (%)	22	28	100	*UNICEF and WHO (2023)*
Agricultural water share (%)	96	70	<85	*FAO AQUASTAT (2022)*
National electrification rate (%)	36	48.4	70	*ADB and World Bank (2023)*
Rural electrification rate (%)	5 - 7	28	70	*ADB and IEA (2023)*
Traditional biomass share (primary energy) (%)	80 ~ 90	~68	<50	*IEA (2023)*
Hydropower exploited / potential	162 MW/7,800 MW	n/a	≥2,000 MW	*IRENA (2023b)*
IPC Phase 3+ (Sep–Dec 2024)	1.63 M (15%)	Variable	< 5%	*IPC (2024)*
Child stunting (<5 yrs)	39 - 42 %	~35%	<10%	*WBG and WFP (2024)*
Post-harvest food losses (rice)	11,4 %	15–20%	<10%	*APHLIS and USAID (2020)*
Tree cover lost since 2000	4.85 Mha (25%)	Varies	Net zero loss	*Andriamparany et al. (2023)*

Nexus Interdependency Analysis

Table 2 quantifies five principal nexus feedback pathways identified through data triangulation. The dominant cascade is the biomass-deforestation-hydropower loop: charcoal and fuelwood demand (85% of primary energy) drives forest clearance at approximately 260 000 ha/year (*GFW 2024*), stripping riparian catchment cover, elevating erosion rates, and increasing sediment loads in rivers that feed Madagascar's hydropower infrastructure. The Betsiboka River now carries sediment concentrations, which are among the highest recorded globally. In drought years, this sedimentation-weakened system faces additional stress: dry-season river discharge in western and central catchments can decline 70–80% from wet-season peaks, reducing hydropower output and triggering load-shedding events of 12+ hours/day in Antananarivo, disabling the irrigation pumps, cold storage systems, and milling equipment that food security depends upon.

Table 2. Quantified Water-Energy-Food (WEF) nexus feedback pathways in Madagascar (author' compilation based on cited references)
2. táblázat. Mennyiségileg meghatározott víz-energia-élelmiszer (WEF) nexus visszacsatolási útvonalak Madagaszkáron (a szerző szerkesztése a hivatkozott hivatkozások alapján)

Nexus Pathway	Mechanism	Quantified Impact (Madagascar)	Key Reference
Deforestation → Hydropower	Sedimentation degrades reservoir capacity & turbine efficiency. But it also increases mean runoff at the same time	~260 kha natural forest lost/yr; dry-season load-shedding ≥12 h/day in drought years	*GFW (2024)* *Andriamparany et al. (2023)* *Moran et al. (2018)*
Energy deficit → post-harvest loss	No cold chain, no mechanical drying; rice sold at harvest-trough prices	20-30% rice post-harvest loss; 25-40% reducible with village electrification	*USAID (2020)* *IEA (2023)*
Deforestation + Drought → Hydropower → Food cascade	Deforestation increases runoff and flow variability while reducing dry-season baseflow; combined with recurrent drought, dry season discharge ↓70–80%; energy shortfall → pump failure → irrigation collapse	1.94 M people projected IPC ≥3 in lean season 2025; Grand Sud rainfall –5 to –10% by 2100	*IPC (2024)* *Barrett et al. (2025)*
Water-smart irrigation → Food security	Irrigated rice yields 3–4× rainfed; SRI (System of Rice Intensification) can increase yields 50–100%	60% of 1.5 Mha rice under irrigation; Lac Alaotra basin = 15% of national rice output	*FAO AQUASTAT (2022)* *FAO (2021)*
Biomass demand → Deforestation → Water	Charcoal harvesting strips riparian vegetation; accelerates erosion and sedimentation	85% primary energy from biomass; Betsiboka River sediment loads among highest globally	*IEA (2023)* *Scales (2012)*

The second critical pathway is the energy-to-food value chain gap. Post-harvest losses of 20-30% of rice production result directly from the absence of mechanical drying, milling, and cold storage, all of which require reliable electricity. *IEA (2023)* evidence from comparable Sub-Saharan contexts suggests that village-level electrification reduces such losses by 25-40%, implying that the energy deficit is effectively destroying between 375 000 and 750 000 tons of rice-equivalent output per year. The third pathway, smart irrigation represents the most tractable synergy: irrigated rice yields 3-4 times those of rain-fed cultivation, yet the Lac Alaotra basin, supplying 15% of national rice output, is experiencing documented reservoir capacity decline from sediment accumulation (*Scales 2012*), and much of the south receives fewer than 400 mm of annual rainfall, making irrigation infrastructure – not water per se – the binding constraint.

A gender dimension intersects all pathways. *Davies et al. (2024)* documented those female smallholders in Madagascar face systematically lower adaptation capacity than male counterparts due to asset constraints, limited extension access, and higher labour burdens in water and biomass collection. Since women manage approximately 70% of smallholder food production, these gender-nexus interactions have first-order food security implications that uniform policy instruments will not adequately address.

Climate Change Amplification

Madagascar's climate trajectory compounds all five nexus pathways. *Barrett et al. (2025)* documented precipitation declines at 14 of 15 long-term weather stations between 1961 and 2017, with temperature increases observed at all locations. Northeast Madagascar a key agricultural zone faces projected annual rainfall declines of 5–10% and temperature increases of 3–5 °C by 2100 under RCP (Representative Concentration Pathway) 4.5 and RCP 8.5 scenarios, respectively. These trends will alter the distribution of forested areas and reduce rice yields across the island's primary growing zones. For the Grand Sud, three consecutive years of below-average rainfall (2020-2023) produced the worst drought in 40 years, pushing 1.71 million people to IPC Phase 3+ at its peak and prompting UN agencies to describe it as a climate-attribution famine event-the first of its kind globally (*FAO and WFP 2022*).

Cyclonic events constitute a second climate-nexus amplifier operating at an event scale. Cyclone Gamane (in 2024) affected approximately 535,000 people in 33 flooded communes in northeast Madagascar, damaged approximately 1,700 hectares of rice cultivation, and disrupted both energy infrastructure and water supply systems simultaneously (*CRI 2024*). This simultaneous cross-system disruption illustrates how climate shocks propagate through nexus linkages: crop loss increases food insecurity; infrastructure damage disables pumping and cold storage; and post-event recovery deforestation accelerates sediment loads. The *IPCC (2022)* projects increased frequency and intensity of southern Indian Ocean tropical cyclones under higher emissions scenarios, meaning this event-scale nexus disruption will become more frequent.

Evaluation of the Central Hypothesis

As a result, Madagascar's per capita renewable freshwater endowment exceeds the global scarcity threshold by a factor of seven, yet safely managed water access stands at 14% – evidence that water poverty is a governance, infrastructure, and finance failure, not a supply failure. Hydropower potential of 7 800 MW dwarfs current installed capacity of 162 MW; the binding constraint is not hydrology but investment, regulatory capacity, and catchment management. Food production is constrained not by cultivable land area (3.0 million hectares of arable land exist) but by the combined failures of irrigation infrastructure, post-harvest energy, and transport connectivity, all of which are institutional. *Nkiaka et al. (2023)* reached an analogous conclusion for Sub-Saharan Africa broadly, finding governance capacity to be the dominant predictor of WEF nexus performance variation; the Madagascar-specific data presented here provide a quantified case study confirming this pattern at national level.

DISCUSSION

Comparison with Island Nexus Literature

Authier et al.'s (2024) GIS-optimization study of Réunion Island-geographically comparable to Madagascar (both Indian Ocean islands, with similar rainfall asymmetry between windward and leeward coasts) – found that WEF nexus land-use competition on small islands can be significantly reduced through integrated spatial planning that aligns renewable energy infrastructure locations with watershed protection and food production zones. Madagascar shares the structural feature of concentrated resource pressure on a limited land area but operates at 15 times Réunion's population scale with a fraction of its institutional capacity. The transferable insight is methodological: geospatial optimization at the commune level, as currently being developed through the *ECA and WFP (2024)* initiative, offers a tractable pathway to the kind of evidence-based nexus planning that *Authier et al. (2024)* demonstrate is feasible even in resource-limited island contexts.

The Biomass Trap as a Policy Priority

The biomass-deforestation-hydropower cascade identified in *Table 2* is the highest-priority nexus intervention target because it is simultaneously the dominant energy pathway, the primary deforestation driver, the main source of hydrological degradation, and a major contributor to food security failures through irrigation and cold-chain impairment. *Herrera-Franco et al. (2024)* demonstrated, in a systematic review linking the WEF nexus to clean energy transitions, that off-grid solar deployment consistently produces nexus co-benefits beyond the direct energy access effect: by substituting for biomass cooking, it reduces deforestation pressure; by enabling agricultural productive use, it improves irrigation efficiency and reduces post-harvest losses; and by reducing the labour burden of biomass collection (which falls primarily on women), it improves food production capacity. The Sahofika (205 MW) and Volobe (120 MW) hydropower projects, while transformative for grid electricity supply, do not address the biomass trap for the 66.3% of the population without electricity access. Off-grid solar, as *SE4All (2024)* confirmed through Madagascar's Integrated Energy Access Planning (IAP) process, is the cost-effective pathway for rural areas, but only if paired with productive use incentives and cold-chain subsidies.

Governance Architecture: What the Evidence Supports

Three governance reforms are directly supported by the evidence. First, the *ECA and WFP (2024)* initiative demonstrates that cross-ministerial nexus coordination is feasible: the joint engagement of the Ministries of Agriculture, Energy, and Hydrocarbons, and the National Mapping Agency under a shared geospatial analytical framework constitutes a de facto nexus planning platform that requires only formalization and resourcing to become a standing coordination mechanism. Second, the Forest Carbon Partnership Programme *FCPF (2024)* targeting a 40% deforestation reduction with an 11.8 $MtCO_2e$ emissions baseline and USD 50 million results-based payment provides an existing financial mechanism whose performance metrics could be expanded to capture downstream water and food security co-benefits, creating a results-based nexus finance instrument. Third, the *World Bank (2024)* (LEAD Project) model providing concessional household electricity connections at a 30% cost reduction demonstrates that innovative access pricing can overcome the affordability barrier in urban and peri-urban areas, a model ADER could adapt for rural mini-grids with agricultural productive-use requirements embedded in concession design.

CONCLUSION

This paper has provided the first comprehensive, data-grounded WEF nexus analysis of Madagascar, structured around an interrelated problem statement, testable hypothesis, and four research questions. The central hypothesis – that institutional fragmentation, not physical resource scarcity, is the binding constraint on Madagascar's WEF nexus performance is strongly supported by the evidence. Mad-agascar's water abundance (12 000 m³ per capita/ year) co-exists with 14% safely managed water access; its 7 800 MW hydropower potential coexists with 66.3% energy poverty; and 3.0 million hectares of arable land coexist with a 47% child stunting rate.

The five identified nexus feedback loops reveal that the biomass-deforestation-hydropower cascade is the systemic linchpin: disrupting it through off-grid solar deployment, upstream catchment restoration paired with the Sahofika and Volobe hydropower investments, and formalization of the ECA-WFP cross-sectoral coordination platform would simultaneously improve energy access, hydrological stability, irrigation reliability, and post-harvest food chain performance. Climate change is accelerating all five feedback loops and concentrating the costs on the most food-insecure and climate-exposed communities in the Grand Sud.

Three recommendations are directly evidence-supported: (i) formalize the *ECA and WFP (2024)* geospatial nexus initiative as a standing National Water-Energy-Food (WEF) Coordination Secretariat; (ii) embed nexus co-benefit metrics into the FCPF deforestation payment framework to create an integrated water-food-energy finance instrument; and (iii) adopt productive-use requirements in ADER rural electrification concessions to ensure off-grid solar deployment, which in turn generates food security and water management co-benefits at scale. Future research should prioritize commune-level nexus mapping using the SE4All geospatial platform, longitudinal evaluation of the Sahofika and Volobe projects as natural experiments, and gendered disaggregation of nexus outcomes.

REFERENCES

Andriamparany, J.N., Razafindramanana, J., Ralimanana, H. (2023). Status of deforestation in Madagascar (2001–2021): Landsat time-series analysis. Biological Conservation, 278, 109907. https://doi.org/10.1016/j.biocon.2023.109907

Authier, R., Pillot, B., Guimbretière, G., Corral-Broto, P., Gervet, C. (2024). Towards sustainable land management in small islands: A Water-Energy-Food nexus approach. PLOS ONE, 19(11), e0310632. https://doi.org/10.1371/journal.pone.0310632

Barrett, T.M., Soarimalala, V., Pender, M., Kramer, R.A., Nunn, C. L. (2025). Climate change perceptions and adaptive behavior among smallholder farmers in northeast Madagascar. PLOS Climate, 4(3), e0000501. https://doi.org/10.1371/journal.pclm.0000501

Bizikova, L., Roy, D., Swanson, D., Venema, H.D., McCandless, M. (2013). The water–energy–food security nexus: Towards a practical planning and decision-support framework for landscape investment and risk management. IISD. ISBN: 978-1-894784-42-2.

Chagwiza, C., Murandu, T., Mutambara, S. (2025). A global systematic review of resource nexus and nature-positive sustainable development. Sustainability Science, 20(2), pp. 1-18. https://doi.org/10.1080/27658511.2025.2554480

CRI (2024). Impacts of climate change and hazards on key sectors in Madagascar. Crisis and Resilience Institute. https://cri-world.com/publications/qed_dp_4626.pdf

Davies, B., Randrianasolo, H., Rajaonarison, M. (2024). Gendered implications for climate change adaptation among farmers in Madagascar. Climate and Development, 16(4), pp. 297-314. https://doi.org/10.1080/17565529.2024.2363377

ECA and WFP (2024). ECA, WFP explore renewable energy solutions for enhanced food security in Madagascar. 2024. March 15. UN Economic Commission for Africa. https://www.uneca.org/stories/eca,-wfp-explore-renewable-energy-solutions-for-enhanced-food-security-in-madagascar

FAO (2014). The water-energy-food nexus: A new approach in support of food security and sustainable agriculture. Food and Agriculture Organization of the United Nations. https://www.fao.org/3/bl581e/bl581e.pdf

FAO (2021). Madagascar: Country brief on nutrition. Food and Agriculture Organization. https://www.fao.org/countryprofiles/index/en/?iso3=MDG

FAO AQUASTAT. (2022). AQUASTAT country profile: Madagascar. FAO. https://www.fao.org/aquastat/en/countries-and-basins/country-profiles/country/MDG

FAO and WFP (2022). Crop and food supply assessment mission to southern Madagascar. FAO/WFP. https://www.wfp.org/publications/southern-madagascar-cfsam-2022

FCPF (2024). Madagascar country profile. Forest Carbon Partnership Facility, World Bank. https://www.forestcarbonpartnership.org/sites/default/files/documents/madagascar_country_profile_fcpf.pdf

GFW (2024). Madagascar deforestation rates and statistics. Global Forest Watch. https://www.globalforestwatch.org/dashboards/country/MDG/

Herrera-Franco, G., Bravo-Montero, L., Caicedo-Potosí, J., Carrión-Mero, P. (2024). A sustainability approach between the Water-Energy-Food nexus and clean energy. Water, 16(7), 1017. https://doi.org/10.3390/w16071017

Hoff, H. (2011). Understanding the nexus. Background paper for the Bonn 2011 Conference: The water, energy and food security nexus. Stockholm Environment Institute. https://www.sei.org/publications/understanding-the-nexus/

IEA (2023). Africa energy outlook 2023. International Energy Agency. https://www.iea.org/reports/africa-energy-outlook-2023

IMF (2023). Food insecurity and climate shocks in Madagascar (Selected Issues Papers, Vol. 2023, Issue 037). IMF. https://doi.org/10.5089/9798400236464.018

IPC (2024). Madagascar: Acute food insecurity situation for September–December 2024 and projections for January–August 2025. Integrated Food Security Phase Classification. https://www.ipcinfo.org/ipc-country-analysis/en/?country=MDG

IPCC (2022). Climate change 2022: Impacts, adaptation and vulnerability (H.-O. Pörtner et al., Eds.). Cambridge University Press. https://doi.org/10.1017/9781009325844

IRENA (2023a). Renewable energy statistics 2023. International Renewable Energy Agency. ISBN: 978-92-9260-584-8.

IRENA (2023b). Energy profile: Madagascar. IRENA. https://www.irena.org/-/media/Files/IRENA/Agency/Statistics/Statistical_Profiles/Africa/Madagascar_Africa_RE_SP.pdf

Leck, H., Conway, D., Bradshaw, M., Rees, J. (2015). Tracing the water-energy-food nexus: Description, theory and practice. Geography Compass, 9(8), pp. 445–460. https://doi.org/10.1111/gec3.12222

Minten, B., Barrett, C.B. (2008). Agricultural technology, productivity, and poverty in Madagascar. World Development, 36(5), pp. 797-822. https://doi.org/10.1016/j.worlddev.2007.05.004

Moran, E.F., Lopez, M.C., Moore, N., Müller, N., Hyndman, D.W. (2018). Sustainable hydropower in the 21st century. Proceedings of the National Academy of Sciences, 115(47), pp. 11891-11898. https://doi.org/10.1073/pnas.1809426115

Nematchoua, M.K. (2020). A study of climate change and energy consumption in Madagascar island. Health and Environment, 1(1), pp. 1-12. https://doi.org/10.25082/HE.2019.01.002

Nkiaka, E., Bryant, R.G., Manda, S., Okumah, M. (2023). An African perspective on the Water-Energy-Food nexus. Scientific Reports, 13(1), 16781. https://doi.org/10.1038/s41598-023-43606-9

Rabezanahary, T., Jun, Z., Andrianarimanana, M. (2025). Evaluation of the Performance of HighResMIP CMIP6 in Simulating Extreme Precipitation in Madagascar. International Journal of Climatology. V45. DO - 10.1002/joc.70011. https://doi.org/10.1002/joc.70011

Rasul, G. (2016). Managing the food, water, and energy nexus for achieving the Sustainable Development Goals in South Asia. Environmental Development, 18, pp. 14–25. https://doi.org/10.1016/j.envdev.2015.12.001

Scales, I.R. (2012). Lost in translation: Conflicting views of deforestation, land use and identity in western Madagascar. The Geographical Journal, 178(1), pp. 67-79. https://doi.org/10.1111/j.1475-4959.2011.00432.x

SE4All (2024). Madagascar integrated energy access planning: Clean cooking report. Sustainable Energy for All. https://www.seforall.org/system/files/2024-07/report-madagascar-iep_cleancooking-en.pdf

UNICEF and WHO (2023). Progress on household drinking water, sanitation and hygiene 2000–2022. WHO/UNICEF JMP. https://www.who.int/publications/i/item/9789240060272

USAID (2020). Madagascar feed the future country plan. USAID. https://www.usaid.gov/madagascar/food-assistance

WFP (2024). Madagascar country strategic plan 2022–2025. World Food Programme. https://www.wfp.org/operations/mg02-madagascar-country-strategic-plan-2022-2025

World Bank (2023). Madagascar climate and development report. World Bank Group. https://openknowledge.worldbank.org/handle/10986/madagascar-ccdr

World Bank. (2024) Energy access in Madagascar: LEAD Project brief. World Bank Group. https://www.worldbank.org/en/news/video/2024/09/19/energy-access-in-afe-madagascar

AUTHOR

ROVATIANA SALEMA ANDRIANASOLOMAHEFA has been a PhD student at the Doctoral School of Public Administration Sciences, Faculty of Public Governance and International Studies, Ludovika University of Public Service (LUPS), Budapest, Hungary, since 2024. He holds a Master's degree in Applied Geophysics from the University of Antananarivo, Madagascar, and a Master's degree from the National School of Administration (ENAM), Madagascar. Before joining LUPS, he worked for the Ministry of Water, Sanitation and Hygiene of Madagascar as a hydrogeological and water resources specialist and later served in the Ministry of National Education in public procurement and project management. His research focuses on water governance, Integrated Water Resources Management (IWRM), the Water–Energy–Food (WEF) Nexus, institutional reform, and climate-resilient water governance in Madagascar.

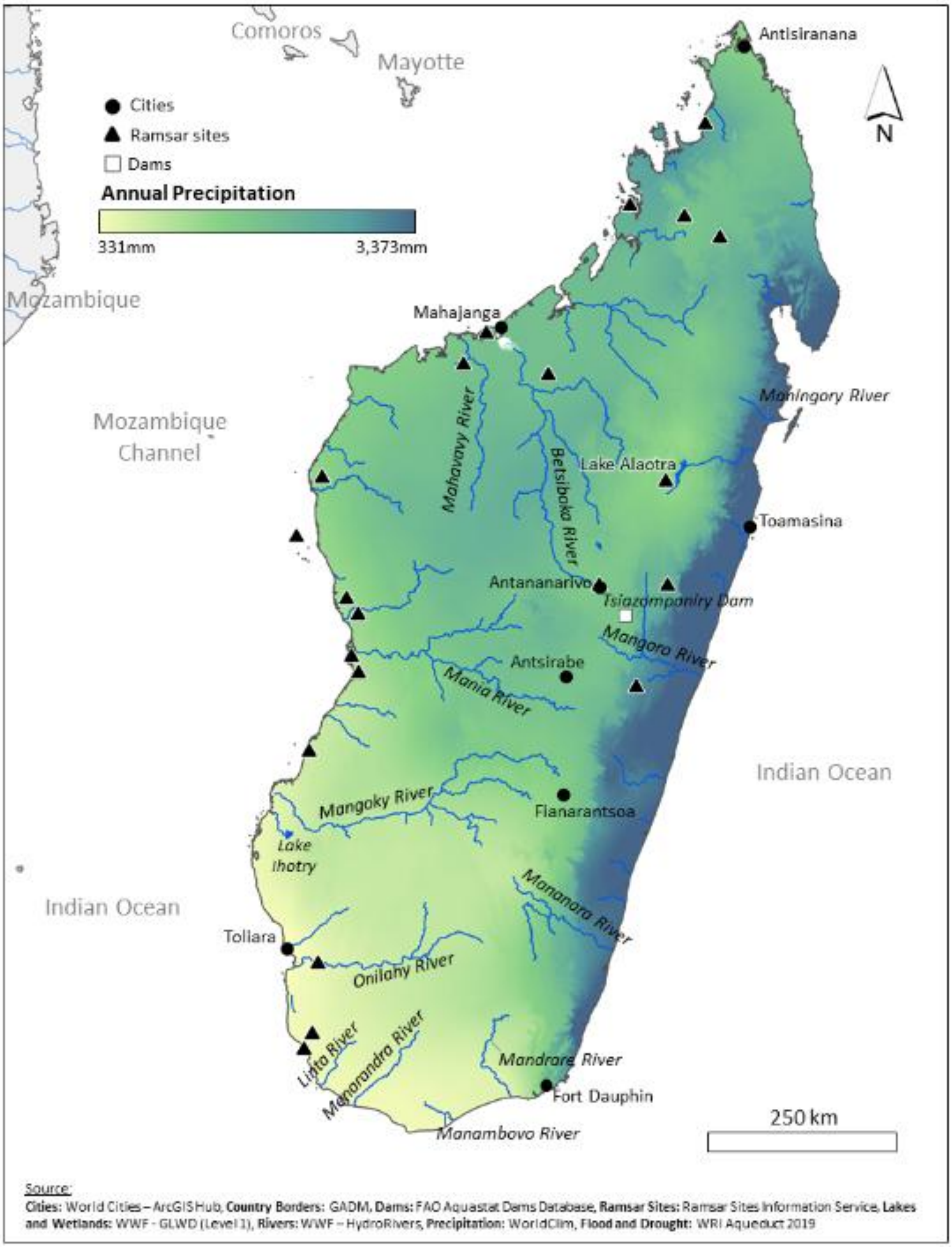

Madagascar's water resources (https://winrock.org/wp-content/uploads/2021/08/Madagascar_Country_Profile-Final.pdf)
Madagaszkár vízkészletei (https://winrock.org/wp-content/uploads/2021/08/Madagascar_Country_Profile-Final.pdf)

Youth Corner

The Hungarian Journal of Hydrology is committed to fostering the next generation of professionals. As part of this mission, the Youth Corner's pages provide high school students with the opportunity to present their research. We encourage our readers to welcome and support their studies with respect. This study was prepared for the Hungarian competition of the Stockholm Junior Water Prize in 2026.

Water chestnut (*Trapa natans*): a food of ancient times or a bioindicator of the modern world

Hanna HÁDA[1,3], Gábor KONCZ[1], Katalin JÁMBRIK[1], Csaba BERTA[2]

[1] György Bessenyei Secondary Grammar School, Iskola square 2, 4600 Kisvárda, Hungary (email: adahanna2008@gmail.com)

[2] Department of Hydrobiology, University of Debrecen (MÉK), Böszörményi Street 138, 4032 Debrecen, Hungary (email: berta.csaba@science.unideb.hu)

[3] Corresponding author: adahanna2008@gmail.com

DOI: 10.59258/hk.24063

Abstract

This study investigates the bioaccumulation of metals in Water chestnut seed samples collected from different locations of Lake Tisza, Hungary. Aquatic macrophytes can absorb and accumulate pollutants from water and sediments, making them useful indicators of environmental contamination. The aim of this research is to measure the concentrations of selected metals in the collected seeds. By analyzing the differences between sampling sites, the study also evaluates the distribution of metals within the lake ecosystem and the potential of aquatic plants as indicators of environmental pollution.

Keywords

Trapa natans, water chestnut, heavy metals, metals, bioaccumulation, Lake Tisza, ICP-MS.

Sulyom (*Trapa natans*): az ókor tápláléka vagy a modern világ bioindikátora

Kivonat

A tanulmány a nehézfémek bioakkumulációját vizsgálja a Tisza-tó különböző helyszíneiről gyűjtött sulyom (*Trapa natans*) magjának mintáiban. A vízi makrofiták képesek abszorbeálni és felhalmozni a vízből és az üledékből származó szennyezőanyagokat, így hasznos indikátorai lehetnek a környezeti szennyezésnek. A kutatás célja a vizsgált fémek koncentrációjának mérése a gyűjtött sulyom magjában. A mintavételi helyek közötti különbségek elemzésével a tanulmány a nehézfémek eloszlását a tó ökoszisztémáján belül, valamint a vízinövények potenciálját a környezeti szennyezés indikátoraként is értékeli.

Kulcsszavak

Sulyom (Trapa natans), nehézfémek, fémek, bioakkumuláció, Tisza-tó, ICP–MS.

INTRODUCTION

Lake Tisza

Lake Tisza is the second-largest lake in Hungary and is located in the eastern part of the country along the Tisza River. The lake is an artificial reservoir created in 1973 after the construction of the Kisköre Dam and hydropower plant. Its primary purposes include water level regulation, flood control, irrigation support, and hydroelectric power generation. The lake covers an area of approximately 127 km². Lake Tisza consists of a highly diverse mosaic of habitats. In addition to open water surfaces, the area contains extensive reed beds, marshes, oxbow-like channels, and shallow wetlands, which provide suitable habitats for numerous plant and animal species. A large part of the lake belongs to the Hortobágy National Park, making it an internationally significant wetland area.

The lake is well known for its rich aquatic vegetation, including several macrophyte species such as water chestnut (*Trapa natans*). These plants play an essential role in the functioning of the ecosystem, as they contribute to nutrient cycling, provide habitats for aquatic organisms, and support natural water purification processes. Besides its ecological importance, Lake Tisza is also a valuable research site. Studies focusing on water, sediment, and aquatic vegetation can provide important information about environmental conditions and the distribution of pollutants such as metals.

Trapa natans

Water chestnut (*Trapa natans*) is a floating-leaved aquatic plant widely distributed in freshwater habitats across Europe and Asia (*Hummel and Kiviat 2004*). In Hungary, it commonly occurs in slow-flowing rivers, lakes, oxbow lakes, and reservoirs. The plant forms a characteristic floating rosette of leaves on the water surface, while its roots are anchored in the sediment. In many water bodies, the species can grow very densely, forming large stands that may hinder water use and navigation. For this reason, the plant is often mechanically removed or mowed, and the collected biomass is typically not utilized but treated as waste.

However, the seeds of *Trapa natans* have considerable nutritional value. The white seed inside the hard shell is rich in starch and is naturally gluten-free, which makes it suitable for producing flour. In several Asian countries, water chestnut flour has traditionally been used to prepare different foods such as bread, cakes, and noodles. Therefore, the plant could represent a potential raw material for producing gluten-free food products (*Jain et al. 2025*).

Bioaccumulation of Metals in Water Chestnut (*Trapa natans*)

Aquatic plants play an important role in indicating and reducing environmental pollution in aquatic ecosystems. Macrophytes are significant because they are capable of accumulating various metals in their tissues. Water chestnut (*Trapa natans*) is an aquatic plant that, according to numerous studies, can absorb and store considerable amounts of metal ions. Therefore, it may serve as a useful indicator of pollution in aquatic environments and can also be applied for phytoremediation purposes.

Metals such as cadmium, lead, copper, zinc, and manganese can enter aquatic ecosystems through both natural and anthropogenic sources. Agricultural activities, industrial discharges, and municipal wastewater significantly increase the concentration of these elements in water and sediments. Aquatic plants are able to absorb these elements through their root systems and tissues, where they may accumulate in different plant organs.

Several studies have investigated the metal accumulation capacity of *Trapa natans*. For example, an Indian study measured the concentrations of six heavy metals (Cd, Cr, Cu, Fe, Mn, and Zn) in pond water, sludge, and different parts of *Trapa natans*. The results showed that the highest concentrations of metals were found in the roots, followed by the shoots, while the lowest concentrations were detected in the edible seeds. The order of metal accumulation in the plant was reported as follows: Cd < Cr < Cu < Zn < Mn < Fe (*Rai and Sinha 2001*).

Another study examined the role of aquatic plants in the purification of contaminated water. During phytoremediation experiments using municipal wastewater, *Trapa natans* significantly reduced several pollution parameters of the water, including biochemical oxygen demand and dissolved salts, as well as the concentrations of several metals. The results indicated that cadmium, copper, iron, manganese, and zinc were mainly accumulated in the leaves, while chromium and lead were predominantly concentrated in the roots (*Kumar and Chopra 2018*).

The accumulation of metals in macrophytes is influenced by several factors, such as the chemical composition of the water, the properties of the sediment, and the level of pollution in the habitat. A study conducted in a wetland ecosystem demonstrated that the concentration of metals may also vary seasonally. The highest concentrations in water and sediment were observed during the winter season, whereas the plants accumulated the largest amounts of metals during summer (*Taher at al. 2023*).

Water chestnut is therefore not only an ecologically important species but also plays a significant role in environmental research. The plant can accumulate different metals while often maintaining lower concentrations in its edible parts. This is particularly important in regions where the plant is consumed as food.

Based on the results of various studies, *Trapa natans* can be considered an effective indicator of metal pollution in aquatic environments (*Elbagory et al. 2026*). The examination of this plant provides valuable information about the condition of water and sediment, as well as the extent of environmental contamination. Consequently, the study of water chestnut may play an important role in the monitoring of aquatic ecosystems and environmental pollution.

Hypothesis

Our hypothesis is that in water bodies with higher environmental load or pollution, the concentration of metals in the seeds will be higher. This assumption is based on the idea that plants can absorb different metals from the water and the sediment, which may accumulate in their tissues, particularly in the seeds.

Objective

The aim of the research is to carry out an elemental analytical investigation of samples found in the different basins of Lake Tisza that have varying levels of environmental load. The study focuses on the Tiszavalk, Sarud, Poroszló, and Abádszalók basins, as these areas of the lake are characterized by different degrees of pollution and human impact. During the analysis, we aim to determine the concentration of various metals present in the samples, especially in the seeds. The results of this research may help determine whether the plant can be safely used for human consumption or whether it could rather play a role in phytoremediation, meaning the natural purification of polluted water bodies by plants.

MATERIAL AND METHODS

The sampling on which the study is based was carried out in August 2024 in different basins of Lake Tisza (*Figure 1*). The samples were collected by boat from areas where at least a 5 m^3 continuous water chestnut (*Trapa natans*) population was present (*Figure 2*). Within each plant patch, samples were taken from three randomly selected points. In total, samples were collected from 12 sampling sites.

The collected seeds were first dried in the laboratory at 70 °C until constant weight was reached. After drying, the samples were ground into a fine powder. This grinding step is important because inclusions and different parts of the plant tissues may accumulate metals differently; therefore, homogenization ensures more accurate and reliable analytical results. The elemental analysis of the samples was performed using ICP–MS (Inductively Coupled Plasma Mass Spectrometry), which allows the detection and precise quantification of metals even at very low concentrations.

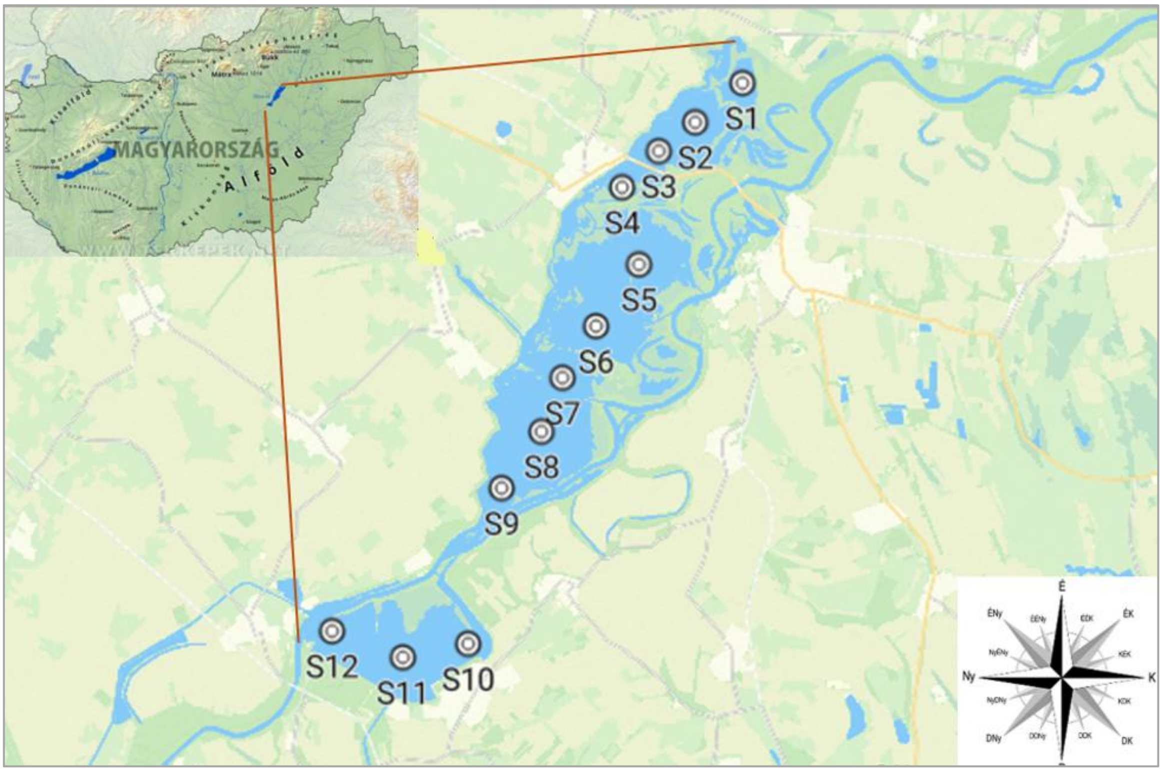

Figure 1. Sampling locations along Lake Tisza. S1-S12 represent the exact sampling points
1. ábra: Mintavételi helyszínek a Tisza-tó mentén. Az S1–S12 jelöli a pontos mintavételi pontokat

Figure 2. Trapa natans fruit
2. ábra. A Trapa natans termése

As part of the research, inorganic plant nutrient analysis from water samples is also carried out in order to determine the amount of dissolved nutrients in the water that are available for plant uptake.

In addition, the study aims to monitor abiotic and biotic changes in the environment, meaning both the physical–chemical environmental factors and the changes related to living organisms.

It is important to note that during the 2024 sampling, when the seeds were collected, sediment sampling was not carried out (*3. Figure*). However, in the following years of the research, sediment samples will also be collected. These samples will be taken using a core-type sampling method, and the collected sediment will be dried and ground before further analysis. For the sediment samples, the organic matter content and calcium carbonate content will be determined using the loss-on-ignition method. In this procedure, a measured amount of the sample is placed into a muffle furnace. In the first step, the sample is heated to 550 °C, during which volatile organic materials are removed. The resulting mass loss allows the determination of the organic matter content. In the second step, the sample is reheated to 950 °C, where carbonate compounds decompose. The additional mass loss observed at this stage is used to determine the calcium carbonate content.

RESULTS

Results of the one-way ANOVA analysis

The results indicate that there is a significant difference between the group means. Based on the results of the one-way analysis of variance, the group effect was very strong: $F(30,341) = 291.7$, $p < 0.001$ indicating that the null hypothesis, that the group means are equal can be rejected. The effect size was also extremely large: ($\omega^2 = 0.959$), suggesting that most of the total variance is explained by differences between the groups (*Table 1*).

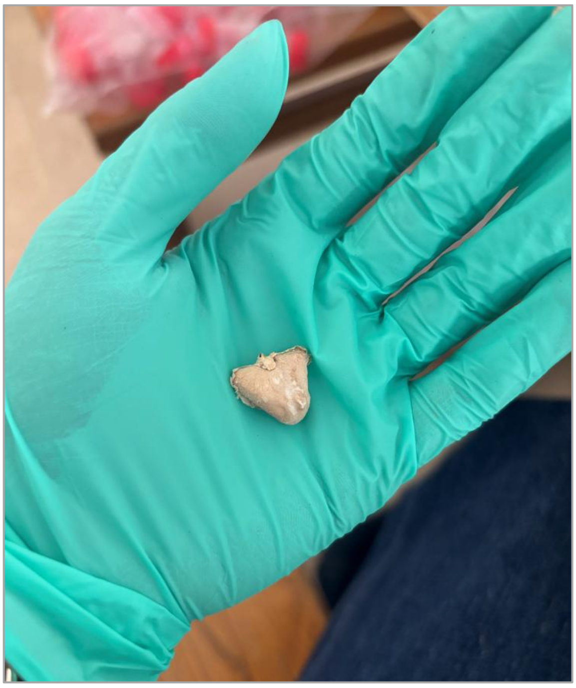

Figure 3. The seed of Trapa natans without the seed coat
3. ábra. A Trapa natans maghéj nélküli magja

Table 1. Test for equal means
1. táblázat. Az egyenlő átlagok vizsgálata

	Sum of sqrs	df	Mean square	F	p (sample)	Critical F (p=0,05)
Between groups	1.53072E06	30	51023.9	291.7	1,636E-223	1.143
Within groups	59645.5	341	174.914	Permutation p (n=99999)		
Total	1.59036E06	371	1,00E-05			

Since Levene's test yielded a significant result, the assumption of homogeneity of variances was violated; therefore, the results of the Welch test are also relevant. This procedure likewise showed a significant difference between the groups: $F(30, 117.8) = 827.4$, $p < 0.001$, confirming that the group means are not equal even when variances differ.

The Bayes factor is also extremely large, providing decisive evidence in favour of differences between the group means. Overall, the results indicate that there are statistically and practically significant differences among the examined groups.

The Kruskal–Wallis test also revealed a significant difference in the medians of the examined groups: $H(\chi^2) = 358.3$, $p < 0.001$. This suggests that at least one group's distribution differs from the others, and that the central tendencies of the groups are not identical.

Standardized Data Evaluation

The dataset was standardized prior to analysis, resulting in normalized values (z-scores) with a mean of zero and a standard deviation of one. This transformation allows for direct comparison between elements with different original scales and highlights relative differences between samples.

Based on the standardized values, clear patterns can be observed across the samples. Positive values indicate above-average concentrations, while negative values represent below-average levels for a given element.

Sample TN_12 shows consistently high positive values across multiple elements, including Ni, Mn, Pb, Cr, Ba, Fe, and Al. This indicates that TN_12 is one of the most enriched samples in the dataset. Similarly, TN_6 also exhibits elevated values for several elements, particularly Ni, Mn, Cr, Ba, and Fe, suggesting a relatively high overall elemental concentration.

In contrast, sample TN_11 displays strongly negative values across nearly all elements, indicating consistently low concentrations compared to the dataset average. This makes TN_11 the most depleted sample.

Sample TN_7 also shows predominantly negative values, although less extreme than TN_11, suggesting generally lower-than-average concentrations.

Several samples, such as TN_5 and TN_9, show mixed behaviour, with both positive and negative deviations, indicating more balanced or moderate compositions.

The standardized dataset also reveals potential covariation patterns between elements. For instance, Ni, Mn, Cr, and Ba tend to increase together in samples such as TN_6 and TN_12, suggesting a possible common source or similar geochemical behaviour. Conversely, samples with low values in these elements tend to show consistently negative deviations across multiple variables.

The Maucha diagram constructed from these standardized values allows for a clear visual comparison of the samples. Samples such as TN_12 and TN_6 would exhibit large, outward-extending shapes, reflecting high relative concentrations, while TN_11 would appear as a compressed shape near the centre, indicating low values across most elements.

Overall, the standardized data confirm strong heterogeneity among the samples and highlight distinct compositional groups, with enriched, depleted, and intermediate samples clearly distinguishable.

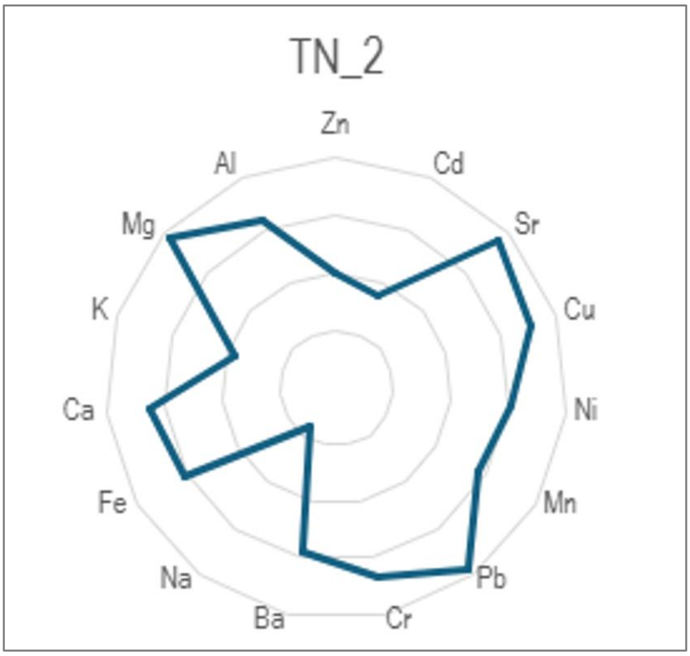

Figure 4. Maucha-diagramm of the samples-TN_2
4. ábra. A TN_2 minták Maucha diagramja

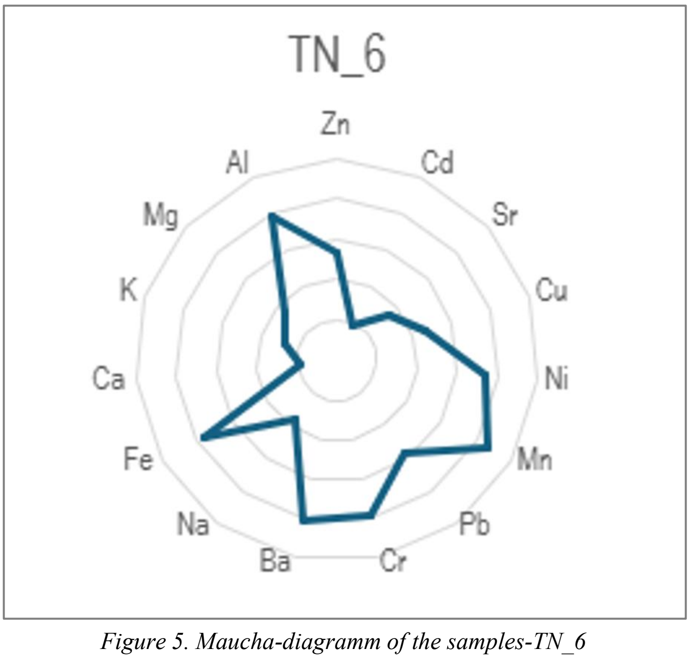

Figure 5. Maucha-diagramm of the samples-TN_6
5. ábra. A TN_6 minták Maucha diagramja

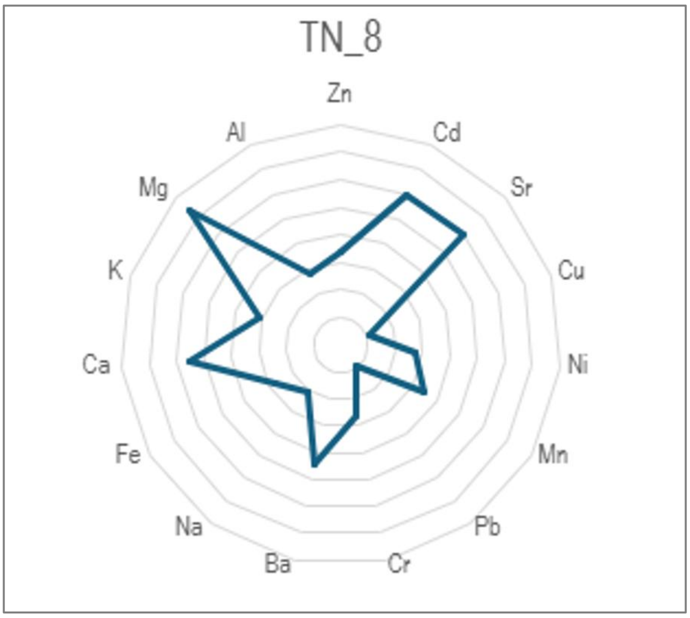

Figure 6. Maucha-diagramm of the samples-TN_8
6. ábra. A TN_8 minták Maucha diagramja

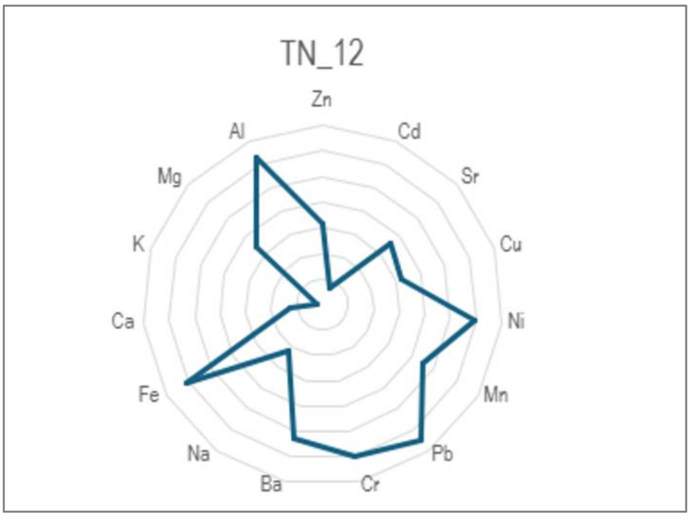

Figure 7. Maucha-diagramm of the samples-TN_12
7. ábra. A TN_11 minták Maucha diagramja

Metal and heavy metal content analysis

In this study, the elemental composition of 12 samples (TN_1–TN_12) was analysed based on the concentrations of 15 elements (Zn, Cd, Sr, Cu, Ni, Mn, Pb, Cr, Ba, Na, Fe, Ca, K, Mg, Al). The two provided tables contain the same data in different formats: one is element-oriented (elements in rows), while the other is sample-oriented (*Figure 6, Figure 7*).

Based on the data, substantial differences can be observed in the concentrations of the elements and their distribution across the samples. Some elements show relatively low variability; for example, cadmium (Cd) ranges between 0.006 and 0.011 across all samples, indicating minimal variation. In contrast, several elements exhibit considerable differences.

Sodium (Na) shows particularly high variability, with values ranging from 7.38 to 60.08. Sample TN_11 has an exceptionally high Na concentration (60.08), which clearly stands out from the rest. Similarly, iron (Fe) displays a wide range (4.57-59.28), with TN_12 having the highest value and TN_7 the lowest.

Calcium (Ca) concentrations also vary significantly, ranging between 131.84 and 313.65. Sample TN_4 shows an outstandingly high Ca value (313.65), clearly distinguishing it from the other samples.

Manganese (Mn) exhibits moderate variability (0.772-2.375), while potassium (K), magnesium (Mg), and aluminum (Al) also show noticeable differences among the samples. Aluminum, in particular, spans a wide range (2.69-37.9), indicating substantial variation.

Among the heavy metals, lead (Pb) includes one negative value (TN_4: -0.011), which may indicate measurement uncertainty or an extremely low concentration. The remaining Pb values are positive and fall within a relatively narrow range.

Table 2. Measured concentration of metalloids and heavy metals from the seed of Trapa natans
2. táblázat. A Trapa natans magjában mért félfém- és nehézfém-koncentrációk

	TN_1	TN_2	TN_3	TN_4	TN_5	TN_6	TN_7	TN_8	TN_9	TN_10	TN_11	TN_12
	(mg/100 g seed dry matter)											
Zn	0.413	0.357	0.396	1.061	0.254	0.523	0.516	0.398	0.285	0.511	0.287	0.501
Cd	0.007	0.007	0.007	0.008	0.006	0.009	0.01	0,011	0.008	0.01	0.007	0.008
Sr	0.393	0.344	0.431	0.615	0.352	0.6	0.447	0.448	0.299	0.417	0.384	0.425
Cu	0.172	0.112	0.169	0.207	0.153	0.172	0.203	0.188	0.123	0.622	0.133	0.177
Ni	0,082	0,03	0,05	0,049	0.029	0.062	0.029	0.066	0.055	0.079	0.056	0.111
Mn	2.176	1.061	1.499	1.352	0.772	1.797	0.772	1.486	1.338	1.737	1.713	2.375
Pb	0.024	0.011	0.02	-0.011	0.02	0.015	0.01	0.022	0.027	0.028	0.027	0.041
Cr	0.049	0.012	0.031	0.025	0.014	0.038	0.006	0.037	0.031	0.045	0.026	0.078
Ba	0.279	0.172	0.203	0.228	0.132	0.251	0.16	0.253	0.188	0.267	0.205	0.333
Na	9.28	7.38	16.34	13.63	12.72	13.98	13.08	10.82	12.41	15.11	60.08	25.43
Fe	40.36	9.71	21.22	19.99	12.5	30.01	4.57	27.23	27.51	34.37	20.64	5.28
Ca	180.99	136.06	191.72	313.65	152.64	260.1	213.1	212.09	131.84	201.29	144.27	169.84
K	29.99	17.24	37.99	35.99	32.66	35.27	40.47	33.37	29.56	36.04	25.74	24.99
Mg	45.61	38.37	41.61	48.06	27.37	57.61	47.55	45.1	34.45	44.73	34.19	46.01
Al	25.71	5.69	13.38	12.54	7.42	19.82	2.69	17.71	15.7	22.67	11.88	37.9

By comparing the samples, it can be observed that certain samples consistently show higher concentrations across multiple elements. For instance, TN_4, TN_6, TN_10, and TN_12 belong to the higher-value group for several components (*Figure 5*). In contrast, TN_2, TN_5, and TN_7 tend to have lower concentrations across multiple elements (*Figure 4*).

Based on the observed patterns, potential covariations between elements can be identified. Calcium (Ca), magnesium (Mg), and potassium (K) often follow similar trends across samples, while iron (Fe) and aluminum (Al) also tend to be high or low together. In contrast, sodium (Na) often behaves differently from the other elements (*Table 2*).

Overall, the tables indicate that the elemental composition of the samples varies considerably, with concentrations spanning wide ranges. This suggests a heterogeneous system in which clear differences can be observed between the samples.

Results of the Principal component analysis (PCA)

Figure 8 presents a PCA biplot, which simultaneously displays the sampling sites and the measured variables. The arrows represent the variables, and their direction and length indicate their contribution to the principal components. Several elements, such as Fe, Mn, Cr, and Ni, point in similar directions, suggesting a common pattern or co-variation, while others (e.g., Na) show different orientations, indicating distinct behaviour. The sampling sites are clearly separated along the components, with TN_12 and TN_6 positioned on the positive side, indicating higher relative concentrations, whereas TN_11 is located on the opposite side, reflecting lower overall values.

Results of the non-metrical multidimensional scaling (NMDS)

The *Figure 9* shows an ordination plot illustrating the relative similarity between the sampling sites. The distances between points represent differences in their multivariate composition: sites that are closer together are more similar, while those farther apart are more distinct. For example, TN_2, TN_5, and TN_9 appear relatively close to each other, suggesting similar characteristics, whereas TN_11 is clearly separated from the others, indicating a distinct composition. This visualization supports the presence of heterogeneity among the sampling sites.

DISCUSSION

The results of the present study are partly consistent with previous findings reported in the literature, while also revealing several notable differences.

According to earlier studies, *Trapa natans* is capable of accumulating significant amounts of metals, with the highest concentrations typically found in the roots, followed by the shoots, and the lowest levels detected in the edible parts of the plant (*Rai and Sinha 2001*). In the current research, only the seeds were analysed, and the results showed relatively low concentrations of heavy metals with limited variability, particularly in the case of cadmium (Cd: 0.006-0.011 mg/100 g seed dry matter). This observation supports the literature, suggesting that the edible parts of the plant tend to accumulate lower levels of heavy metals.

However, in contrast to some previous findings, the present study did not reveal consistently high accumulation levels across all examined elements in the seeds. This difference may be explained by the fact that heavy metals are primarily stored in other plant organs, such as roots and leaves, rather than in the seeds.

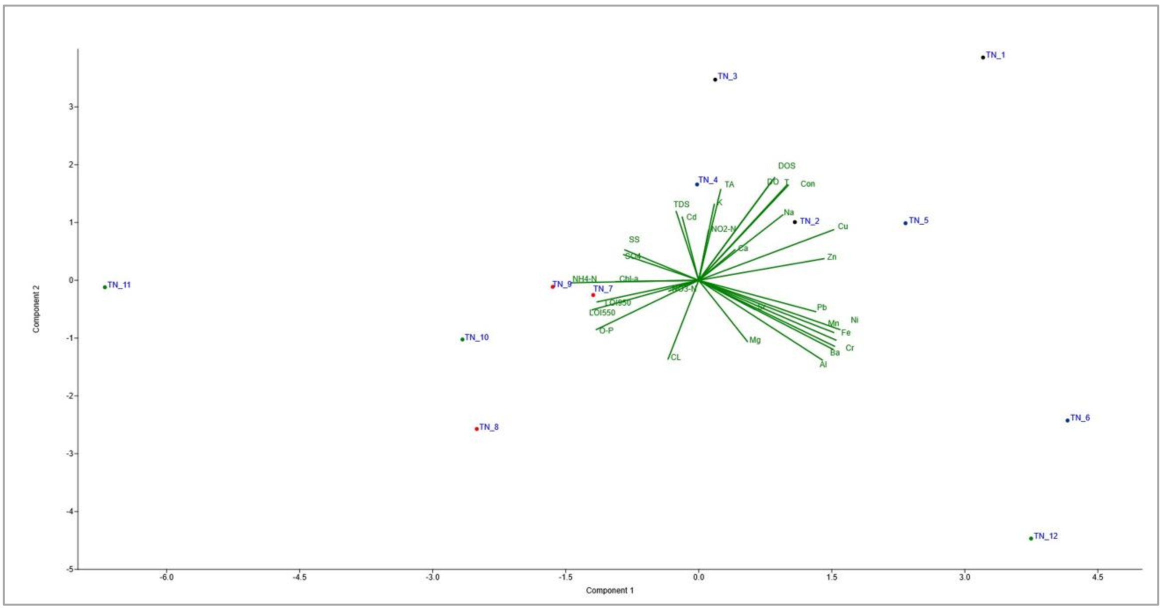

Figure 8. PCA biplot of the sampling sites and the measured variables
8. ábra. A mintavételi helyszínek és a mért változók PCA-biplotja

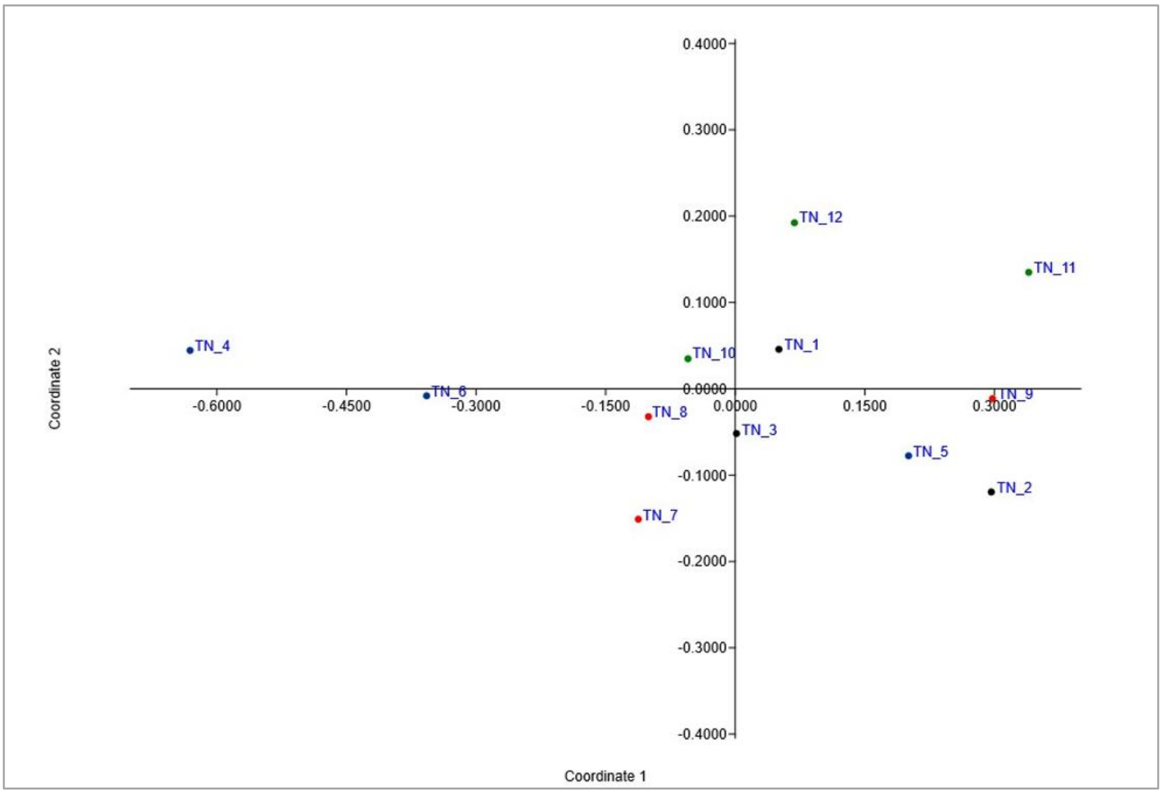

Figure 9. Similarity between sampling sites on an NMDS
9. ábra. A mintavételi helyszínek hasonlósága NMDS elemzés alapján

The results are also in agreement with the findings of *Kumar and Chopra (2018)*, who reported that certain elements (e.g., Cd, Cu, Fe, Mn, and Zn) are mainly accumulated in the leaves, while others (e.g., Cr and Pb) are predominantly concentrated in the roots. The relatively moderate concentrations measured in the seeds in this study indirectly support this distribution pattern within the plant.

Seasonal variation, as described by *Taher et al. (2023)*, may also play an important role in explaining the observed results. Considerable differences were observed among the samples, indicating that local environmental conditions—such as water chemistry, sediment characteristics, and pollution sources—have a strong influence on metal accumulation.

One of the most important findings of this study is the pronounced heterogeneity among the samples. Statistical analyses, including one-way ANOVA and the Kruskal–Wallis test, confirmed highly significant differences between the sampling sites ($p < 0.001$). This result is consistent with previous studies, which emphasize that the distribution of heavy metals in aquatic ecosystems is strongly influenced by spatial variability and environmental factors.

Certain samples (e.g., TN_12 and TN_6) exhibited elevated concentrations across multiple elements, while others (e.g., TN_11) showed consistently lower values. This pattern suggests that some areas of the lake may be subject to a higher environmental load, partially supporting the initial hypothesis.

However, the hypothesis was only partially confirmed. Although some samples showed higher metal concentrations, a clear and consistent relationship between the presumed pollution level and the metal content of the seeds could not be established. This indicates that metal accumulation is a complex process influenced not only by external environmental conditions but also by internal plant physiological mechanisms, including element transport and storage.

Overall, the findings of this study confirm that *Trapa natans* can serve as a useful bioindicator of heavy metal pollution in aquatic ecosystems. At the same time, the results highlight that analyzing only the seeds provides limited insight into the full extent of metal accumulation. Therefore, future studies should include the examination of roots, leaves, and sediments in order to obtain a more comprehensive understanding of the accumulation processes.

CONCLUSION

The present study aimed to investigate in detail the elemental composition and metal accumulation patterns of *Trapa natans* seeds collected from multiple basins of Lake Tisza. The analysis revealed a considerable degree of variability among the examined samples, clearly indicating that the distribution of elements within the lake ecosystem is not uniform but rather spatially heterogeneous. This heterogeneity suggests that localized environmental factors play a crucial role in shaping the chemical profile of aquatic plants.

The statistical evaluation of the data further supported these observations, as significant differences were detected between the various sampling sites. These differences were found to be highly significant, emphasizing that site-specific environmental conditions – such as water chemistry, sediment composition, and potential pollution sources – strongly influence the accumulation of elements in *Trapa natans*. Among the samples, certain ones (notably TN_12 and TN_6) consistently exhibited elevated concentrations across multiple elements, while others, such as TN_11, showed distinctly lower values. This pattern highlights the uneven exposure of different lake regions to environmental stressors.

The results partially confirm the initial hypothesis of the study. In some cases, samples originating from areas presumed to have higher environmental loads or pollution levels did indeed show increased concentrations of metals. However, this relationship was not consistent across all samples, indicating that the accumulation of metals in *Trapa natans* seeds cannot be explained solely by external contamination levels. Instead, the uptake, translocation, and storage of these elements appear to be governed by a complex interplay of environmental conditions and intrinsic plant physiological mechanisms, including selective absorption and detoxification processes.

Consistent with findings reported in previous studies, the current results suggest that the edible parts of the plant (specifically the seeds) generally contain lower concentrations of metals compared to other plant organs, such as roots or leaves. This observation is particularly important from a food safety perspective, as it indicates a potentially lower risk associated with the consumption of *Trapa natans* seeds. Nevertheless, despite these encouraging findings, further comprehensive investigations are required to fully evaluate possible health risks, especially under conditions of prolonged exposure or in more heavily contaminated environments.

Overall, *Trapa natans* demonstrated considerable potential as a bioindicator species for assessing environmental conditions in aquatic ecosystems. Its ability to reflect variations in elemental composition makes it a valuable tool for monitoring pollution. At the same time, the study also highlights an important limitation: the analysis of seeds alone provides only a partial understanding of metal accumulation processes. For a more complete and accurate assessment, future research should incorporate the examination of additional components, including roots, leaves, surrounding water, and sediment samples. Such an integrated approach would enable a more comprehensive evaluation of pollutant dynamics and pathways within the ecosystem.

In conclusion, the findings of this study contribute to a deeper understanding of the role of aquatic macrophytes in environmental monitoring. They also emphasize the importance of adopting multidisciplinary and integrative methodologies when assessing ecosystem health and pollution levels, thereby supporting more effective environmental management and conservation strategies.

In the next phase of the research, the investigations will also include water and sediment pollution of Lake Tisza.

REFERENCES

Elbagory, M., Altihani, F.A., El-Mesery, H.S., Mahdi, A.A., EL-Shafeey, S.E.E., El-Nahrawy, S., Mohamed, I., Siric, I., Pankaj Kumar, P. (2026). Accumulation of eight heavy metals in water chestnut (*Trapa natans* L.) of four major water bodies of Jammu and Kashmir, India. Sci Rep 16, 7383. https://doi.org/10.1038/s41598-026-39522-3

Hummel, M., Kiviat, E. (2004). Review of World literature on Water Chestnut with implications for management in North America. Journal of Aquatic Plant Management. Journal of Aquatic Plant Management. Vol. 42. pp. 17-27.

Jain, M., Jain, P., Singh, M. (2025). Gluten-free applications of water chestnut flour in bakery, snacks and traditional foods: A review. International Journal of Advanced Biochemistry Research SP-9(12). pp. 268-271. https://www.doi.org/10.33545/26174693.2025.v9.i12Sd.6506

Kumar, V., Chopra, A.K. (2018). Phytoremediation potential of water caltrop (Trapa natans L.) using municipal wastewater of the activated sludge process-based municipal wastewater treatment plant. Environ. Technol. 39, pp. 12-23. https://doi.org/10.1080/09593330.2017.1293165

Rai, U.N., Sinha, S. (2001). Distribution of Metals in Aquatic Edible Plants: Trapa Natans (Roxb.) Makino and Ipomoea Aquatica Forsk. Environ. Monit. Assess. 70, pp. 241-252. https://doi.org/10.1023/a:1010727325662

Taher, M.A., Zouidi, F., Kumar, P., Fayssal, S.A., Adelodun, B., Goala, M., Kumar, V., Andabaka, Ž., Širić, I., Eid, E.M. (2023). Impact of Irrigation with Contaminated Water on Heavy Metal Bioaccumulation in Water Chestnut (Trapa natans L.). Horticulturae 9, 190. https://doi.org/10.3390/horticulturae9020190

AUTHORS

Hanna HÁDA is an 11th-grade student at Bessenyei György Secondary Grammar School and Dormitory in Kisvárda, Hungary. She plans to continue her studies at the University of Veterinary Medicine Budapest. She participated in the Stockholm Junior Water Prize competition, where she was awarded a special prize for her research achievements.

Gábor KONCZ graduated from the University of Debrecen as a biologist-ecologist in 2007 and as a teacher of biology and environmental sciences in 2008. He completed his PhD studies in Environmental Sciences at the University of Debrecen and obtained his PhD degree in 2013. Since 2009, he has been working as a biology teacher at Bessenyei György Grammar School and Dormitory in Kisvárda. He is actively involved in talent development, science education, curriculum and textbook development, and environmental research. Since 2015, he has been a member of the Soil Biology Working Committee of the Hungarian Academy of Sciences.

Katalin JÁMBRIK PhD graduated from the University of Debrecen as a biologist-ecologist in 2007 and as a secondary school teacher of biology and environmental sciences in 2008. She completed her PhD studies in Biological Sciences at the University of Debrecen and obtained her PhD degree in 2011. From 2004, she was actively involved in research and teaching activities at the Department of Botany, focusing on the effects of cyanobacterial toxins on aquatic plants and plant stress responses. Since 2006, she has been a member of the Botanical Section of the Hungarian Biological Society and has authored and co-authored several international scientific publications in the fields of plant physiology, aquatic ecology, and environmental biology. Since 2014, she has been working as a biology teacher at Bessenyei György Grammar School and Dormitory in Kisvárda.

CSABA BERTA graduated from the University of Debrecen with a degree in Hydrobiology in 2015. In 2020, he obtained a PhD in Environmental Science at the UD. Since 2023, he has been an assistant professor at the Department of Hydrobiology. His main research interests are hydrobiology, zooplankton, macroinvertebrates, and macrophytes, mainly focusing on the environmental patterns in natural water bodies and the utilisation of species as bioindicators.